Extraction de composés énergétiques à partir de microalgues par application conjuguée d'impulsions de champ électrique et de sollicitations mécaniques dans un système microfluidique.

Sakina Bensalem

université PARIS-SACLAY

NNT : 2019SACLN007

Thèse de doctorat

école normale supérieure paris-saclay

CentraleSupélec

Extraction de composés énergétiques à partir de microalgues par application conjuguée d'impulsions de champ électrique et de sollicitations mécaniques dans un système microfluidique.

Thèse de doctorat de l'Université Paris-Saclay
préparée à L'Ecole normale supérieure Paris-Saclay et l'Ecole CentraleSupélec Paris-Saclay

École doctorale n°575 : electrical, optical, bio : physics and engineering (EOBE)
Spécialité de doctorat : Physique

Thèse présentée et soutenue à Cachan, le 24 Janvier 2019, par

Sakina Bensalem

Composition du Jury :

Mme Rosaria Ferrigno Professeur des Universités, UCBL/INL (UMR 5270)	Présidente du Jury
Mme Marie-Pierre Rols Directrice de recherche, CNRS/IPBS (UMR 5089)	Rapportrice
Gilles Peltier Directeur de recherche, CNRS/CEA/BIAM (UMR 7265)	Rapporteur
Bruno Le Pioufle Professeur des Universités, ENS Paris-Saclay/SATIE (UMR 8029)	Directeur de thèse
Filipa Lopes Maître de conférences, CentraleSupélec/LGPM (EA 4038)	Co-Directrice de thèse
Olivier Français Professeur, ESIEE Paris	Co-Directeur de thèse
Dominique Pareau Professeur émérite, CentraleSupélec/LGPM (EA 4038)	Invitée

French thesis summary - *Résumé de la thèse en français*

Introduction

L'exploitation du pétrole en tant que principale source d'énergie fossile est aujourd'hui associée à des forts enjeux environnementaux, économiques et géopolitiques. Parmi les impacts les plus pesants figurent l'augmentation des émissions de polluants dans l'atmosphère tel que les gaz à effet de serre (GES), les changements climatiques mais également l'épuisement progressif des ressources naturelles fossiles. Par ailleurs, la croissance démographique mondiale conduit à une augmentation de la demande énergétique mondiale. Ce contexte a suscité un grand intérêt pour le développement des énergies renouvelables.

Les énergies renouvelables sont ainsi vues comme la meilleure solution alternative aux énergies fossiles, permettant de subvenir à la forte demande énergétique qui ne cesse de croître, tout en préservant l'environnement. Parmi les ressources renouvelables, les microalgues sont considérées comme une source d'énergie. En effet, certaines espèces, sous des conditions de stress (azoté, lumière, etc), sont capables d'accumuler des quantités importantes de triglycérides qui peuvent ensuite être convertis en biocarburants. Les microalgues sont des micro-organismes unicellulaires photosynthétiques qui convertissent de l'énergie lumineuse en énergie chimique, tout en consommant du dioxyde de carbone. Elles présentent de nombreux avantages pour un grand nombre de secteurs économiques tels que la santé et la cosmétique (molécules à haute valeur ajoutée), l'agroalimentaire (pigments et protéines), et l'énergie.

Les principales étapes de production de microalgues sont la culture des cellules (souvent dans des bassins ouverts appelés « raceway », ou des photobioréacteurs), la récolte de la biomasse qui est parfois suivie d'une étape de séchage, et l'extraction et purification des molécules d'intérêt. La production de microalgues à des fins commerciales a commencé il y a environ une cinquantaine d'années, donnant des produits tel que le bêta-carotène, les oméga 3 EPA (acide eicosapentaénoïque) et DHA (acide docosahexaénoïque) en tant que compléments alimentaires (Anlit, DSM, Frutarom Health BU…) et l'antioxydant astaxanthine (Cyanotech…). Néanmoins, malgré ce vif intérêt industriel, il reste des verrous scientifiques et technologiques à lever afin d'optimiser les systèmes de production, notamment dans le secteur de la production de biocarburants, afin de les rendre économiquement plus compétitives et durables.

En particulier, l'extraction de molécules nécessite généralement l'utilisation de solvants, souvent toxiques (tels que l'hexane ou des mélanges de chloroforme et méthanol) ; elle est souvent couplée à une étape de prétraitement de la biomasse pour améliorer l'efficacité de celle-ci et qui vise à fragiliser les barrières cellulaires (paroi et membrane). Cependant, ces prétraitements tels que le broyage à billes et l'homogénéisation à haute pression, sont souvent très énergivores, alourdissant le coût environnemental et économique du procédé.

Des procédés de prétraitement alternatifs s'appuyant sur des méthodes mécaniques/physiques telles que l'ultrasonication, les micro-ondes et les chocs osmotiques, ou des méthodes biochimiques par l'utilisation d'enzymes sont utilisées à l'échelle du laboratoire et, pour certains, à l'échelle industrielle.

L'utilisation du traitement électrique par champs pulsés (PEF - Pulse Electric Fields) semble être également une solution alternative prometteuse. Il s'agit d'une augmentation de la perméabilité des membranes cellulaires (électroporation, électroperméabilisation) par l'application d'impulsions électriques de courte/longue durée et/ou intensité, en modifiant la structure des membranes et en favorisant la formation de pores.

Des publications récentes ont montré le fort potentiel de l'électro-perméabilisation en tant que prétraitement pour l'extraction de composés intracellulaires. Par exemple, il a été démontré que ce traitement sur une cyanobactérie facilitait l'extraction de molécules de lipides par le solvant isopropanol. Par ailleurs, cette technique semble prometteuse pour la réduction des coûts environnementaux et économiques de l'extraction de lipides. De plus, elle offre l'avantage d'induire une augmentation de perméabilité membranaire tout en préservant la viabilité de la cellule (dans le cas d'une électroporation dite « réversible », c'est-à-dire qui conduit à une ouverture de pore temporaire, permettant à la membrane de se refermer). Enfin, les autres avantages de cette méthode sont sa simplicité d'application, sa rapidité, sa reproductibilité et son efficacité d'extraction élevée.

Ces techniques alternatives de prétraitement permettent d'extraire des composés d'intérêt, dont les lipides, à partir d'une biomasse humide et ainsi d'ôter l'étape de séchage, extrêmement coûteuse, de la chaîne de production. Il faut cependant souligner qu'elles sont actuellement davantage étudiées à l'échelle du laboratoire que dans le cadre d'une production à l'échelle industrielle. De plus, les effets de ces prétraitements sur la cellule restent mal compris et peu maitrisés. Une étude approfondie de l'impact de ces prétraitements sur l'algue d'étude (sa physiologie, sa structure…), est ainsi primordiale dans le développement, l'optimisation et la maitrise des procédés d'extraction de molécules d'intérêt à partir de microalgues.

Ainsi, dans le cadre de cette thèse, une nouvelle approche est proposée, basée sur l'utilisation de prétraitements électriques (champs électriques pulsés) et/ou mécaniques pour l'extraction de lipides produits par la microalgue verte, *Chlamydomonas reinhardtii*. Nous avons ainsi conçu et réalisé des outils originaux, notamment des microsystèmes dédiés (*Lab-on-chip*) couplés à l'imagerie qui ont permis d'évaluer la réponse de la cellule aux différentes sollicitations appliquées et d'identifier les phénomènes mis en jeu à l'échelle microscopique. Ce travail a été réalisé dans le cadre d'une collaboration entre les laboratoires SATIE de l'ENS Paris-Saclay et le LGPM de CentraleSupélec.

Chlamydomonas reinhardtii a été ici utilisée comme modèle d'étude. En effet, cette microalgue est largement étudiée depuis plus d'une cinquantaine d'années dans le domaine de la biologie végétale (notamment du fait de la bonne connaissance de son génome). Depuis quelques années, c'est aussi devenu un modèle émergeant dans le domaine de la production de biocarburants.

D'autre part, cette microalgue offre l'avantage d'avoir une souche mutante, qui diffère de la souche dite « sauvage » (Wild type) par l'absence de la paroi cellulaire. C'est une particularité intéressante qui a pu être exploitée au cours de ce projet de thèse afin d'étudier le rôle de la paroi cellulaire dans l'extraction de molécules d'intérêt à partir de microalgues. En effet, la paroi cellulaire des microalgues peut représenter une épaisseur, une résistance plus ou moins importante selon l'espèce étudiée, et être ainsi un obstacle à l'extraction de composés intracellulaires.

Enfin, dans le cadre d'une application de champs électriques pulsés, deux paramètres doivent être prises en compte : la conductivité du milieu de culture (elle doit être faible afin de minimiser l'effet

Joule) et la taille de la cellule (Selon l'équation de Schwan, le rayon cellulaire a un lien direct avec la sensibilité de la cellule au champ électrique). *C. reinhardtii* est une microalgue d'eau douce et présente un diamètre d'environ 7 µm lorsqu'elle est en phase de croissance et d'environ 10 µm lorsqu'elle est soumise à une accumulation de lipides. C'est ainsi pour toutes ces raisons mentionnées précédemment, que *C. reinhardtii* a été retenue comme modèle dans notre étude.

Méthodologies adoptées

Dans le cadre de ce travail de thèse, *C. reinhardtii* (souche sauvage et mutante) a été cultivée dans des conditions de culture optimales (milieu TAP, température maintenue constante à 25 °C, un apport en CO_2 à 1.5 % (v/v), une intensité de lumière à 20 $\mu mol \cdot m^{-2} \cdot s^{-1}$ et une agitation continue de 100 rpm), avant d'être soumise à des conditions de stress azoté afin d'induire l'accumulation de lipides. Ces conditions de stress impliquaient : un milieu TAP dépourvu en azote, une intensité de lumière plus élevée (150 $\mu mol \cdot m^{-2} \cdot s^{-1}$), et un apport en CO_2 à 0.004 % (CO_2 atmosphérique).

Une nouvelle approche est proposée pour le prétraitement des cellules en vue d'une extraction de lipides par l'utilisation de solvants. Elle implique l'utilisation combinée de sollicitations impulsionnelles en champ électrique (électro-perméabilisation) et de sollicitations mécaniques sur les microalgues. Plusieurs solvants organiques, présentant différentes propriétés (hydrophobicité, solubilité, taille), ont été étudiés dans le cadre de cette étude dont l'hexane, le décane, ainsi que des mélanges de décane et dichlorométhane ou hexane et éthanol.

Afin d'appliquer le prétraitement PEF sur les cellules, ces dernières ont été introduites dans une cuvette d'électroporation (cuvettes Bio-Rad), comportant des électrodes distantes de 1 mm (volume échantillon = 130 µL). Un générateur d'impulsions haute tension bipolaire a été utilisé (ELECTRO cell B10 HVLV) pour l'application des champs électriques impulsionnels sur les cellules. Il permet d'appliquer des tensions dans une plage comprise entre -1000 V et + 1000 V et des durées de pulse allant de 5 µs à 50 000 µs. Afin d'évaluer l'impact des champs électriques pulsés sur *Chlamydomonas reinhardtii* (sauvage et mutante), plusieurs intensités de champ électrique et de durées d'impulsion ont été testés.

Un système microfluidique dédié couplée à l'imagerie (microscopie optique ou confocale), permettant l'observation *in situ* et en temps réel des cellules (section …), a été conçu et fabriqué pour l'application de contraintes mécaniques sur les microalgues. Ce dispositif est composé d'un réseau de capillaires dont le diamètre (5µm) est inférieur à la taille de la cellule (d'un diamètre en moyenne de 10 µm). Une force mécanique est appliquée quand la cellule passe de façon répétitive dans des canaux.

La fabrication de notre dispositif microfluidique comporte deux grandes étapes : la fabrication du « moule » contenant le design des canaux microfluidiques puis la réplication de ce design dans un matériau polymère (PDMS, PolyDiMéthylSiloxane) et l'assemblage (packaging) de cette membrane contenant le réseau microfluidique :

- Fabrication du moule : nous utilisons un substrat (ou wafer) de silicium de 4 pouces de diamètre, sur lequel on dépose une couche de résine SU8 photosensible avec une épaisseur de cinq micromètres par enduction centrifuge (ou « spin coating », en anglais). L'épaisseur de la résine déposée va dépendre de plusieurs paramètres tels que la vitesse angulaire, la durée de l'opération, et la résine utilisée. Le moule est ensuite finalisé à partir d'un masque sur lequel est dessiné (à

l'aide du logiciel L-Edit) le réseau de canaux microfluidiques souhaité. Le réseau de canaux est gravé sur le moule par photolithographie. La résine étant négative, la partie exposée à la lumière est réticulée et la partie non exposée reste soluble. Cette dernière est ensuite rincée par un solvant, pour obtenir le moule final. La géométrie du moule est définie de façon à produire les restrictions fluidiques qui permettent de générer les contraintes mécaniques sur la cellule. L'opération est répétée sur une seconde couche de SU8 (de 25 µm), superposée et alignée sur la première, pour aménager les accès fluidiques de la puce.

- Moulage et packaging du réseau microfluidique : lors de cette seconde étape, le réseau microfluidique reproduit en PDMS (cet élastomère peut être solidifié par réaction thermique lorsqu'il est mélangé avec un réticulant) le moule en résine SU8 préalablement fabriqué. La membrane PDMS ainsi structurée et assemblée de manière covalente sur une lame de verre, par plasma oxygène.

Le dispositif microfluidique a été fabriqué en salle blanche (pour la fabrication du moule) et dans la plateforme microfluidique (pour la fabrication du réseau microfluidique) à l'Institut d'Alembert de l'ENS Paris Saclay.

Suite à la conception et à la mise en place des dispositifs expérimentaux permettant l'application des deux prétraitements, le développement et l'optimisation de différentes techniques d'analyse fût nécessaire.

Afin d'évaluer l'impact des sollicitations électriques et mécaniques sur *C. reinhardtii*, des mesures de concentration cellulaire (notamment pour évaluer la lyse cellulaire produite par les prétraitements), viabilité et perméabilité cellulaires, et le contenu en lipides ont été réalisées à l'aide de la cytométrie en flux (Cytomètre Guava easyCyte, Millipore). Cette technique a été choisie pour les nombreux avantages qu'elle offre : analyse de faibles volumes d'échantillons cellulaires (500 µL – 1000 µL), analyse précise de plusieurs propriétés cellulaires à la fois, possibilité de trier les cellules (différentes populations cellulaires, par exemple dans le cas d'une contamination par bactéries), sensibilité de détection élevée et analyse rapide et simple.

Plusieurs méthodes ont été développées et optimisées : un modèle d'analyse corrélant la concentration cellulaire indiquée par le cytomètre avec un comptage cellulaire par cellule de Malassez pour la quantification de la concentration cellulaire, la viabilité cellulaire en utilisant le diacétate de fluorescéine (FDA), un marqueur fluorescent qui permet de détecter l'activité de l'enzyme estérase, la perméabilité cellulaire en utilisant l'Iodure de Propidium (PI) ou le Sytox Green (SG), deux marqueurs fluorescents de l'acide nucléique (ils pénètrent la cellule uniquement lorsque sa membrane est perméable) et enfin le contenu lipidique des cellules en utilisant le marqueur fluorescent Bodipy 505/515 qui est spécifique pour les lipides neutres. Pour chaque marqueur fluorescent, un modèle d'analyse au cytomètre a été développé et optimisé à travers notamment la détermination d'un temps d'incubation et d'une concentration de marqueur optimaux.

Afin d'évaluer l'efficacité d'extraction des lipides, une méthode spectrophotométrique, connue sous le nom de la méthode Sulpho-Phospho-Vanilline (SPV), a été étudiée et optimisée. Cette technique simple, rapide et reproductible, permet une analyse quantitative des lipides totaux des microalgues.

Pour évaluer l'impact du stress azoté sur la physiologie des cellules de microalgues, et en particulier leur profil protéique (tailles des protéines présentes), une méthode d'électrophorèse en gel de polyacrylamide en présence de dodécylsulfate de sodium, aussi connue sous le nom de la méthode SDS-PAGE, a été appliquée. Cette étude a été effectuée en collaboration avec la Faculté de pharmacie de Chatenay-Malabry, UFR Pharmacie, de l'Université Paris-Sud.

Afin de mieux comprendre l'effet des conditions de stress azoté, des prétraitements (champs électriques pulsés et sollicitations mécaniques) **et du traitement chimique** (application de différents solvants), **sur la cellule microalgale** (structure et physiologie), plusieurs outils d'imagerie ont été appliqués. Des composés intracellulaires tels que les gouttelettes lipidiques et la chlorophylle ainsi que la paroi cellulaire ont été détectés avec des marqueurs spécifiques et observées par microscopie confocale laser (marqueur Bodipy 505/515 pour les lipides, lectine Concanavaline A associée au conjugué fluorescent tétraméthylrhodamine pour la paroi et auto-fluorescence de la chlorophylle).

La structure (paroi, membrane, composants intracellulaires) et la morphologie de la cellule de *Chlamydomonas reinhardtii* ont été également évaluées par microscopie électronique en transmission (MET) en collaboration avec l'Institut de Biologie Intégrative de la Cellule (I2BC), UMR, (CEA, CNRS, Université Paris Sud).

Pour caractériser la taille des pores crées sur la membrane cellulaire après l'application des sollicitations électriques et mécaniques, une méthode innovante d'imagerie et traitement d'image a été développée et mise en place. Pour cela l'entrée des molécules de dextran de différents poids moléculaires, associées à l'isothiocyanate de fluorescéine (FITC), a été évaluée à l'aide de la microscopie confocale laser.

Résultats principaux

L'objectif principal de ce travail de thèse était de développer et optimiser une méthode novatrice pour l'extraction de molécules d'intérêt à partir de microalgues, et en particulier des composés lipidiques à des fins de production de biocarburants. Pour cela nous avons évalué l'efficacité de deux prétraitements et de leur combinaison : l'application de champs électriques impulsionnels, et l'application de contraintes mécaniques cycliques dans l'extraction par solvant organique.

Dans une première étude, nous avons montré que le couplage de prétraitements permettait d'augmenter l'efficacité d'extraction des lipides de *C. reinhardtii* par le solvant hexane. Plusieurs configurations de prétraitements ont été testées : des champs électriques impulsionnels seuls, des compressions mécaniques seules, la combinaison des champs électriques impulsionnels suivis d'une compression mécanique et une compression mécanique suivie des champs électriques impulsionnels. Nous avons montré une amélioration significative de l'extraction de lipides lorsqu'un prétraitement électrique (avec une intensité de champ de 5,5 kV/cm et une durée de pulse de 5 µm), suivi d'une compression mécanique était effectué. Une augmentation de 25% de lipides extraits par rapport au solvant seul a été observée. Le couplage de ces prétraitements est donc prometteur pour l'extraction de lipides issus des microalgues.

Afin de mieux comprendre l'impact de ces prétraitements sur la cellule et d'identifier les mécanismes d'extraction impliqués, très peu décrits dans la littérature, plusieurs paramètres ont été quantifiés dont la perméabilité et la lyse cellulaire.

Nos résultats ont montré que : 1) tous les prétraitements conduisent à une augmentation de la perméabilité cellulaire plus ou moins importante selon la technologie appliquée, sans pour autant conduire à la lyse cellulaire. L'augmentation la plus importante a été observée pour le couplage de technologies ; 2) la lyse cellulaire est nécessaire pour l'extraction de lipides de *C. reinhardtii* par l'hexane. Une augmentation significative de celle-ci a été mise en évidence pour le couplage de technologies par rapport au solvant seul ; ce qui est en accord avec l'amélioration de l'extraction observée. Ces résultats suggèrent l'impact majeur de la paroi cellulaire en tant que barrière pour l'extraction de molécules d'intérêt de *C. reinhardtii*.

Afin confirmer cette hypothèse, les souches sauvage et mutante de *C. reinhardtii* (dépourvue de paroi cellulaire) ont été exposées à divers solvants et en particulier au mélange décane et dichlorométhane. L'extraction de lipides n'a été possible que pour la souche mutante lysée, le mélange étant inefficace sur la souche sauvage.

D'autre part, nous avons confirmé, en utilisant l'imagerie confocale, que des gouttelettes lipidiques étaient bloquées dans la paroi même en présence de différents solvants. L'ensemble de ces résultats ont clairement confirmé que l'extraction de lipides de *C. reinhardtii* n'est possible que si la cellule est lysée et confirment que la paroi joue un rôle de barrière à l'action du solvant.

Les résultats de cette étude nous ont enfin permis de proposer un mécanisme original, à l'échelle microscopique, pour la suite des prétraitements (PEF suivie par sollicitation mécanique) couplée à l'extraction avec l'hexane : les barrières cellulaires (paroi et membrane) sont significativement fragilisées par le couplage de technologies rendant plus facile l'action du solvant par la suite.

Par ailleurs, nous avons évalué l'impact des différents prétraitements sur la viabilité cellulaire. Cela pourra être intéressant dans le cadre du développement d'un procédé qui permettrait la réutilisation des cellules à la suite d'une extraction de composés d'intérêt. Les deux prétraitements ont montré un effet sur la viabilité cellulaire : la compression mécanique a conduit à une diminution de viabilité de 15%, alors que dans le cas de l'électroporation seule, elle a diminué jusqu'à 67,5 % et 46,4 % pour le couplage de technologies. Une expérience complémentaire a été effectuée afin d'évaluer la capacité de ces cellules restantes à se diviser. Le résultat était positif pour tous les prétraitements.

Les résultats de cette étude sont présentés en deux articles : « *Understanding the mechanisms of lipid extraction from microalga Chlamydomonas reinhardtii after electrical field solicitations and mechanical stress within a microfluidic device* » (Bioresource Technology) et « *Structural changes of Chlamydomonas reinhardtii cells during lipid enrichment and after solvent exposure* » (Data in Brief).

Nous avons dans un second temps cherché à identifier les conditions opératoires d'électroporation permettant d'obtenir une ouverture réversible ou irréversible des pores sur la membrane plasmique de *C. reinhardtii*. De plus, on a pu montrer que la consommation énergétique par le traitement peut être optimisé en variant les paramètres d'amplitude et de durée d'impulsion. En effet, pour un même degré de perméabilité cellulaire, la consommation énergétique la plus faible a été obtenu pour la durée d'impulsion la plus courte (5 µs) et l'intensité du champ électrique la plus élevée (4,5 $kV \cdot cm^{-1}$ dans le cas d'une électroporation réversible et 7 $kV \cdot cm^{-1}$ dans le cas d'une électroporation irréversible).

Afin d'approfondir cette étude et mieux appréhender les mécanismes d'électroporation, des expériences ont été réalisées dans le but de caractériser la taille des pores crées par différentes

conditions d'électroporation et l'effet de la durée d'impulsion (de 5 µs à 500 µs) sur la perméabilité de la membrane. Différentes molécules de dextran-FITC de poids moléculaires variées ont été utilisés comme indicateurs de la taille des pores crées sur la membrane : 3 kDa (0,77 nm), 10 kDa (1,59 nm), 40 kDa (3,66 nm) et 70 kDa (5,11 nm).

On a pu en conclure que l'électroporation réversible ou irréversible, avec une durée de pulse de 5 µs engendrait des pores capables de laisser passer que le dextran 3 kDa. Les pores dans ces conditions ont une taille estimée entre 0,7 nm et 1,6 nm. Une augmentation de la taille des pores a été remarquée quand les cellules étaient soumises au couplage de prétraitements. De plus, nous avons constaté qu'une durée d'impulsion plus longue, pour une même intensité de champ, permettait de créer des pores plus larges sur la membrane. Dans notre cas, la durée de pulse de 10 µs a permis de laisser passer le dextran 10 kDa, 40 kDa et 70 kDa dans la microalgue. Ainsi, cette durée de pulse engendre des pores d'au moins 5 nm. Les effets des prétraitements sur la structure de la cellule ont par ailleurs été également observés au TEM (par exemple les pores membranaires créés par l'électroporation, et la déstructuration de la paroi induite par ces traitements).

Il convient enfin de souligner que cette étude présente, pour la première fois, une estimation des pores engendrés sur la membrane cytoplasmique d'une cellule algale par l'application d'un traitement électrique.

Ces expériences ont conduit à la soumission des deux articles suivants : « *Inducing reversible or irreversible pores in Chlamydomonas reinhardtii with electroporation: impact of treatment parameters* » (Algal Research, 2018) et « *Chlamydomonas reinhardtii's structural response to stress conditions, Pulsed Electric Fields and mechanical compressions for an efficient and controlled compound extraction »* (Bioresource Technology).

Nous nous sommes également intéressés à l'impact de la durée du stress azoté sur la structure de la cellule de *C.reinhardtii*. En effet, nos résultats ont démontré que plus la durée de stress sur la cellule était importante, plus l'extraction de lipides était efficace et cela malgré un épaississement de la paroi de la cellule (constituée de 7 couches) avec la durée. Ce résultat original suggère une évolution des propriétés physiques et/ou chimiques de la paroi dans le temps avec des conséquences sur l'extraction de molécules d'intérêt des microalgues. Cette étude est décrite en « *Chlamydomonas reinhardtii's structural response to stress conditions, Pulsed Electric Fields and mechanical compressions for an efficient and controlled compound extraction* » (Bioresource Technology).

Ces derniers résultats ont clairement montré le besoin d'approfondir nos connaissances sur la structure, en particulier la paroi, et la physiologie de *C.reinhardtii*. Nos images de microscopie de transmission montrent clairement que la paroi est différente selon la durée de stress, et plus la cellule est stressée plus la paroi perd en densité (ce qui se traduit par une plus faible opacité au TEM des couches composant cette paroi qui par ailleurs semble s'éloigner les unes des autres). Cette observation au TEM est complémentaire de celle faite en microscopie confocale, et nous a permis de comprendre que la paroi devient moins compacte et peut-être plus perméable avec la durée de stress.

Enfin, une étude complémentaire du contenu en protéines de *C. reinhardtii* a permis de mettre en évidence la dégradation progressive des protéines de grands poids moléculaires en fragments peptidiques (protéiques) de faibles poids moléculaires (de l'ordre de 10 KDa). Ceci peut être corrélé à notre étude de la taille des pores crées par l'électroporation afin de déterminer le type de protéines ou pigments pouvant être extraits dans ces conditions. L'ensemble de ces travaux a permis de mieux

comprendre l'impact de la durée du stress azoté sur la physiologie et la structure de la cellule de *C. reinhardtii*

Conclusions et perspectives

Ce travail de thèse a permis de montrer le potentiel de notre approche de couplage de prétraitements (champs électriques pulsés suivis d'une compression mécanique répétées) à une extraction par solvant pour la récupération de composés lipidiques de *C. reinhardtii*. Une amélioration significative l'efficacité d'extraction des lipides par l'hexane a été démontré.

Les expériences effectuées ont permis d'étudier, à l'échelle de la cellule, l'effet des contraintes électriques et mécaniques sur les microalgues afin d'en extraire les molécules d'intérêt. Elles nous ont également permis d'apporter des connaissances nouvelles sur les phénomènes mis en jeu lors d'une extraction de lipides par solvant et lorsque les microalgues sont soumises à des conditions de stress azoté engendrant leur accumulation en lipides.

La structure et la morphologie de *C. reinhardtii* et ses éventuelles modifications suite aux conditions de stress, aux prétraitements électriques et mécaniques et aux traitements par solvants ont été étudiés à l'aide des outils d'imagerie développés et mis en place.

Nos résultats ont démontré que la lyse cellulaire, et la fragilisation de la paroi et membrane sont nécessaires pour une extraction efficace de lipides. Les champs électriques impulsionnels ont, comme attendu, un effet sur la membrane. Cela a été caractérisé en déterminant la taille de pores ainsi qu'à travers des observations microscopiques (microscopie confocale et MET). Nous avons démontré qu'avec une intensité de champ électrique égale à 7 $kV \cdot cm^{-1}$ et une durée de pulse de 10 µs (correspondant à des conditions de consommation énergétique faible), il était possible de créer des pores d'au moins 5 nm (correspondant au FITC-dextran de 70 kDa) sur la membrane de *C. reinhardtii*. En termes de suite, des expériences pourraient être effectuées sur des molécules de FITC-dextran plus grosses afin de déterminer la taille de pore maximale dans ces conditions d'électroporation.

Nous avons confirmé le rôle de la paroi de la microalgue en tant que barrière à l'efficacité d'extraction. La paroi cellulaire de *C. reinhardtii* a montré une évolution au niveau de sa structure en fonction de la durée de stress à laquelle elle est exposée. Nous avons aussi montré que ce changement de structure impacte l'efficacité d'extraction des lipides par le solvant. Par ailleurs ceci a été également démontré lors des expériences utilisant la microscopie confocale et les molécules de FITC-dextran. En effet, la cellule est perméable au FITC-dextran de 40 kDa après 20 jours de stress alors qu'elle ne l'était pas à 7 jours de stress. Il est donc clair qu'il y a un lien entre la structure de la paroi avec l'efficacité d'extraction. Pour des expériences futures, il serait donc intéressant d'analyser de plus près la composition de la paroi cellulaire au cours du stress afin de définir de manière optimale l'instant de récolte permettant de maximiser l'extraction du composé ciblé.

Le schéma de procédé d'extraction proposé dans ce projet de thèse pourrait être utilisé pour évaluer l'effet de ces prétraitements sur différentes espèces de microalgues, selon les molécules d'intérêt ciblées.

Enfin, notre procédé d'extraction impliquant une électroporation réversible, et ainsi des niveaux de consommation énergétique faibles, avec une sollicitation mécanique, peut être envisagé dans le cadre d'une extraction successive de plusieurs molécules d'intérêt.

Dans le cas des lipides, de futures investigations pourraient être conduites afin de déterminer un mélange de solvant biocompatible/toxique efficace avec les prétraitements utilisés pour une extraction de lipides respectueuse de l'environnement et avec un faible coût énergétique et économique.

Acknowledgements - *Remerciements*

Ma thèse s'est déroulée au sein de deux laboratoires : le laboratoire Génie des Procédés et Matériaux (LGPM) de Centrale Supélec et le laboratoire Systèmes et Applications des Technologies de l'Information et de l'énergie (SATIE) de l'ENS Paris-Saclay. J'ai donc eu le plaisir de travailler avec deux équipes différentes, échanger avec les autres équipes au sein du même laboratoire et ainsi de rencontrer un grand nombre de chercheurs. Je dois la réussite de cette thèse à la participation de toutes les personnes que j'ai pu rencontrer dans les différents organismes de recherche.

Je remercie Patrick Perré, Directeur du laboratoire LGPM et Pascal Larzabal, Directeur du laboratoire SATIE, pour l'accueil chaleureux et les très bonnes conditions de travail mises à ma disposition.

J'adresse mes sincères remerciements à Magali Dupuy, Cyril Breton, Thierry Martin, Hélène Santigny, Mathilde Charters, Joël Casalinho, Jean Trubuil, Touhami Smaoui, Jamila El Bekri, Arnaud Buch et Corinne Roussel du côté du LGPM, ainsi que Rasta Ghasemi, Bertrand Cinquin, Jean-Pierre Lefevre, Gwenaël Robin, Hervé Leh, Eugène William, David POLIZZI, Nacima Abidi, Jeff Audibert, Frédéric Subra, Patrick Tauc, Martine Lefort et Gladys Mbemba du côté de l'IDA ainsi que tous les professeurs et autres permanents qui ont su se rendre disponible pour m'aider à avancer rapidement mes recherches. Je remercie toutes ces personnes qui ont accepté de répondre à mes questions durant mes recherches ainsi que pour leurs écrits, leurs conseils et leurs critiques qui ont guidé mes réflexions.

Cyril Breton et Bertrand Cinquin, merci à vous pour les expériences, toujours dans la bonne humeur, au microscope confocal. Ces expériences ont toujours été un plaisir pour moi pour découvrir beaucoup de belles choses ainsi que des images drôles que je garde précieusement.

Merci également à Rasta Ghasemi pour tous les moments passés ensemble, que ce soit pour le travail ou pour les discussions autour d'un déjeuner ou un café ! Je n'oublierais jamais ma première fabrication de moule, un moment riche en émotions ! Merci à toi pour ces beaux souvenirs.

Je remercie sincèrement le corps administratif des deux laboratoires LGPM et SATIE qui ont toujours su répondre à nos besoins et nous aider à alléger les démarches administratives, inévitables pendant les trois années de thèse. Catherine Kruch, Carole Bernard, Sandra Julien Anchier et Eugénie Gonçalves du laboratoire LGPM et Sophie Abriet, Béatrice Bacquet, Aurore Gracia et Dorothée Kouevi-Akoe du laboratoire SATIE, un grand merci pour leur aide et leur accueil toujours souriant ! Merci également aussi au service RH de l'ENS Paris Saclay pour leur disponibilité et leur aide.

Je remercie également Éric Cassan, le Directeur de l'école doctorale EOBE ainsi que le corps administratif qui m'ont suivi tout au long de cette thèse et qui, avec leur investissement en énergie et temps pour leurs doctorants, nous permettent de progresser dans les meilleures conditions. J'ai également apprécié faire partie des représentants des doctorants de cette école.

Par ailleurs, ce travail n'aurait pu être mené à bien sans les contributeurs financiers qui, au travers de leur soutien matériel, ont reconnu mon travail et m'ont fait confiance : le financement de l'ENS Paris Saclay et l'école doctorale EOBE (MESR – CD UPSAY 2015) et de LabeX LaSIPS (ANR-10-LABX-0040-LaSIPS).

Ayant un sujet pluridisciplinaire, j'ai également eu le plaisir de rencontrer d'autres équipes avec lesquelles j'ai discuté de mes travaux ou avec lesquelles j'ai travaillé pour une partie de mes travaux : le laboratoire LBPA (IDA, ENS Paris-Saclay) qui, suite au déménagement d'un des laboratoires où j'effectuais mes manips, m'a permis de poursuivre ma recherche en me donnant un espace et le matériel nécessaire pour mettre en place mon banc expérimentale et le laboratoire LPQM (IDA, ENS Paris-Saclay).

Je remercie Éric Deprez, Directeur de l'institut d'Alembert dans lequel se trouve plusieurs unités de recherche dont les laboratoires LBPA, LPQM et SATIE, de m'y avoir accueilli et de m'avoir permis d'avancer sur mes travaux de thèse dans les meilleures conditions. Je le remercie également de la confiance qu'il m'a accordée pour présenter mes travaux de recherche à la ministre actuelle de l'Enseignement supérieur, de la Recherche, et de l'innovation, Frédérique Vidal, et ses collaborateurs. Merci aussi au département de la direction de l'IDA pour leur aide et accueil chaleureux : Véronique Mathet, Brigitte Dudon et Valérie GUINAUD. Brigitte et Valérie merci beaucoup pour leur présence le jour de ma soutenance et leur aide pour les questions d'organisation et de préparation. Je remercie Yann Ferrandez de m'avoir aidé pour l'installation de l'équipement qui ont permis un bon déroulement de ma présentation.

Je remercie aussi l'i2bc, et tout particulièrement Claire Boulogne, Cynthia Gilles et Cynthia Dupas pour votre participation dans mes expériences TEM. Ce fut un réel plaisir de partager ces expériences et discussions scientifiques avec elles.

Merci aussi à Iulian Popa, professeure à la faculté de pharmacie d'avoir accepté de participer à ce travail.

Mes remerciements s'adressent également à Philippe Marmottant et toute son équipe du laboratoire Liphy de Grenoble, pour leur accueil chaleureux, leur disponibilité et les discussions et échanges scientifiques que nous avons pu avoir sur le domaine de l'acoustofluidique et des microalgues.

J'ai également eu le plaisir de rencontrer et de découvrir d'autres aspects du métier d'enseignant chercheur en faisant de l'enseignement à l'UPEC et dans le département EEA de l'ENS Paris-Saclay, en participant aux associations tels que l'association des doctorants de Centrale Supélec ou le bureau des jeunes chercheurs Ile de France avec RESPORE. Ces participations m'ont permis entre autres d'apprécier l'aspect communication de la recherche en organisant par exemple des journées rencontres entre chercheurs et industriels ou entre chercheurs et grand public.

Je souhaite remercier tout particulièrement mes quatre encadrants de thèse pour leur contribution scientifique sans faille ainsi que leurs qualités humaines qui m'ont permis d'apprécier ce travail. Leurs qualités pédagogiques et leur compétences scientifiques, d'un niveau d'excellence, m'ont permis de développer mes compétences scientifiques et pédagogiques dans des conditions exceptionnelles mais aussi d'approfondir ma passion pour le métier d'enseignant-chercheur. Votre participation infaillible ne m'a laissé aucun choix que de donner le maximum pour mener à terme et réussir ce travail de recherche. Merci à vous !

Mes sincères remerciements vont à mon Directeur de thèse, Bruno Le Pioufle, pour la qualité scientifique et humaine de son encadrement remarquable qui m'a permis de réaliser ce travail de recherche dans de très bonnes conditions. Je le remercie pour sa disponibilité, ses conseils endigués

tout au long de cette thèse. J'espère pouvoir en faire autant si je dois un jour diriger des thèses de doctorat. L'encadrement assuré par Bruno est pour moi un exemple à suivre.

Merci à Olivier Français, mon co-encadrant de cette thèse. Ce fut un honneur et un vrai plaisir de t'avoir en tant qu'encadrant. Il m'a souvent montré un autre point de vue pendant la réalisation de cette thèse et je l'en remercie.

J'adresse mes remerciements à Filipa Lopes, ma codirectrice de thèse, pour son investissement admirable pour le bon déroulement de ce travail. Je la remercie sincèrement pour sa présence, son soutien et ses qualités humaines qui m'ont toujours donné envie d'aller encore plus loin. Ses compétences, sa rigueur scientifique et sa clairvoyance m'ont beaucoup aidé. Ils ont été et resteront mes moteurs pour la conduite de mes travaux de recherche ultérieurs.

J'adresse de chaleureux remerciements à Dominique Pareau, d'avoir accepté d'encadrer ma thèse et pour toutes ses qualités scientifiques et humaines. Ça été un honneur de l'avoir en tant qu'encadrante. Merci pour tous ses précieux conseils scientifiques qui m'ont été très utiles pour avancer dans la bonne direction.

Marie-Pierre Rols et Gilles Peltier, rapporteurs de ma thèse, ont accepté de me consacrer leur temps. J'en suis honorée et je leur exprime toute ma profonde reconnaissance.

Mes remerciements vont également à Rosario Ferrigno, présidente du jury de la thèse, qui a accepté d'examiner et de présider le jury de cette thèse.

Merci à Pierre pour tous les moments qu'on a pu partager tout au long de notre thèse. Merci pour son soutien, pour les moments de joie et pour les discussions scientifiques qu'on a pu avoir. Grâce à ses qualités humaines, nous avons eu le privilège de faire de la science dans la joie et la bonne humeur. C'est tout ce qu'un doctorant peut espérer pour le déroulement de sa thèse.

Armelle Paule, Jordan Seira et Cédric Absalon merci pour leur soutien, leurs conseils et pour toutes les discussions et moments qu'on a pu partager. Les discussions que j'ai pu avoir avec eux resteront gravées pour toujours dans ma mémoire.

Je remercie aussi Marietta Morisson, Moustapha Diallo, Timothée Labouret, Li Gong, Jérôme Grenier, Arnaud Challansonnex, Vita Hou, Amélie Bécar, Sahar Azami Hassani et Sirine Ben Ghzaiel du côté du LGPM ainsi que Jean Roman, Yu-Sheng Lin, Sung Tsang, Abdellatif El Fellahi, Manon Boul, Tieying Xu, Thao Phuong, Pamela Didier, Alexiane Pasquier, Mehdi Ferhat et tous les autres post-docs, doctorants et stagiaires du laboratoire LGPM et du laboratoire SATIE avec qui j'ai pu partager également des moments de joie et d'échanges scientifiques dans la bonne humeur. Ça été un plaisir de les avoir rencontrés et j'espère que nous aurons l'occasion de se recroiser un jour !

Un grand merci tout particulier aux Biomis Kids qui se reconnaitront ! J'espère que nous continuerons à se voir et à découvrir nos différentes cultures à travers ce qu'on aime, la nourriture !

A tous mes amis, je les remercie sincèrement pour leur amitié, leur soutien inconditionnel et leur encouragement tout au long de ces années de thèse.

Ces remerciements ne peuvent s'achever, sans une pensée pour ma famille que j'aime tant et que je remercie pour son soutien indéfectible. Je remercie du fond du cœur mes très chers parents qui m'ont toujours soutenu et encouragé tout au long de ma vie, les années de thèse sans exception. Leur

présence et leurs encouragements sont pour moi les piliers fondateurs de ce que je suis et de ce que je fais.

Enfin, Olivier, mon ami, mon confident, devenu aussi mon mari au cours de cette thèse, merci pour son soutien inconditionnel et sa patience tout au long de ces dernières années. Merci d'avoir vécu cette aventure à mes côtés.

General description

Microalgae are sunlight-driven miniature factories that convert carbon dioxide into valuable molecules (i.e. lipids, proteins, carbohydrates, vitamins and pigments) for a broad range of industrial applications such as health, food and feed additives, cosmetics and energy production. They offer many advantages such as a rapid growth rate, a greenhouse gas fixation ability and high biomass and lipid productivities. Microalgae oil is therefore considered as a promising alternative energy source to fossil fuels.

However, despite these advantages, several scientific, technological and economical bottlenecks must be overcome before large-scale production of algae-based biofuels becomes feasible. In the particular case of lipid extraction, which is generally performed using toxic organic solvents, significant improvements are needed to enhance lipid recovery and ultimately develop a sustainable and economically viable process.

In this context, this work investigates the potential of using mechanical and non-mechanical pretreatments to improve lipid recovery from microalgae by affecting the cell barriers: plasma membrane and cell wall. The considered pretreatments, mechanical compressions and Pulsed Electric Fields (PEFs), are currently widely studied. However, their possible effects on the cells remain poorly understood and controlled, although it is of utmost importance in the context of developing and optimizing sustainable extraction processes.

In this study, the effect of electrical, mechanical and chemical (solvent) solicitations on the extraction of *Chlamydomonas reinhardtii*'s neutral lipids, cell permeability, morphology and structure (plasma membrane, cell wall and inner components such as the accumulated lipid droplets) are assessed. Several methods are used involving cytometric analysis and specifically designed microsystem devices coupled to microscopic tools. The effect of nutrient stress (nitrogen starvation) on *C. reinhardtii* cells is also investigated.

Chapter 1 of this work presents a literature review on microalgae and their current use as feedstock for industrial productions. The first part concerns the context and potential of microalgae as feedstock, followed by an introduction to microalgae and subsequently the description of the microalga chosen as our study model, *Chlamydomonas reinhardtii*. The literature review then describes the current production methods, in particular for a biodiesel application and concludes with the aim and objectives of this project.

Chapter 2 describes all methods and experimental setup developed and used during this study, including the investigated solicitations (PEFs, cyclic mechanical compressions through microfluidic constrictions and solvent extraction) and the analytical methods used to characterize and assess the impact of those solicitations and stress conditions on the microalga *C. reinhardtii*.

Finally, the results of this study are described in the last two chapters. **Chapter 3** focuses on lipid extraction including the study of the mechanisms involved in solvent extraction and role of the pretreatments PEFs and cyclic mechanical compressions on lipid extraction enhancement.

Chapter 4 more precisely investigates the effects of various pretreatments on the microalga *C. reinhardtii* structure. It includes the study of the impact of PEFs on the reversibility and irreversibility

of the pores created on the cell membrane as well as a characterization of the pore's size. It also presents a study on the impact of the pretreatments (alone or combined) and the nitrogen stress conditions on the microalgae cells' structure and morphology, in particular the cell wall.

These last two chapters include the following four articles with complementary results:

- Bensalem, S., Lopes, F., Bodénès, P., Pareau, D., Français, O., & Le Pioufle, B. (2018 a), "**Understanding the mechanisms of lipid extraction from microalga *Chlamydomonas reinhardtii* after electrical field solicitations and mechanical stress within a microfluidic device**". Bioresource Technology 257: 129-136.

- Bensalem, S., Lopes, F., Bodénès, P., Pareau, D., Français, O., & Le Pioufle, B. (2018 b), "**Structural changes of *Chlamydomonas reinhardtii* cells during lipid enrichment and after solvent exposure**". Data in Brief, 17, 1283-1287.

- Bodénès, P., Bensalem, S., Français, O., Pareau, D., Le Pioufle, B., Lopes, F. (2018), "**Inducing reversible or irreversible pores in *Chlamydomonas reinhardtii* with electroporation: impact of the treatment parameters**". Algal Research, 37, 124-132.

- Bensalem, S., Pareau, D., Cinquin, B., Français, O., Le Pioufle, B & Lopes, F., "***Chlamydomonas reinhardtii*'s structural response to stress conditions, Pulsed Electric Fields and mechanical compressions for an efficient and controlled compound extraction**". (Bioresource Technology-submitted article).

The content of those articles remains unchanged, even if the numbering and layout was adapted to the manuscript.

CHAPTER I - Introduction and literature review

Table of contents

References

1. The promising future of microalgae

1.1 An overview of the current world energy situation

1.1.1 Global energy demand and consumption

The world is currently facing important challenges due to the energy crisis generated by an overwhelming growth of human population and technological advancements. Today, the world population reached 7.6 billion and is expected to continue growing up to 8.6 million in 2030, 9.8 million in 2050 and 11.2 billion in 2100 (United Nations report 2017). In addition, the United Nations Department of Economic and Social Affairs has recently published a report guiding nations towards achieving the new Sustainable Development goals.

In respect with the Oil Market Report of 2016 (IEA, 2017), the world consumption of oil represents 35 billion barrels of oil every year. Scientists throughout the various energy agencies estimate that we've currently consumed 40% of the world's oil and that in 50 years, we will run out of oil and gas and in a century of coal. This abundant use of fossil fuels and dependency is perceived as highly dangerous for our future as it promises three non-negligible risks: a depletion of fossil fuel reserves, a worldwide competition for the "rare" remaining resources which could lead to a geopolitical conflict, and a damaging increase in atmospheric CO_2 (Figure 1) causing global warming (Rittmann, 2008).

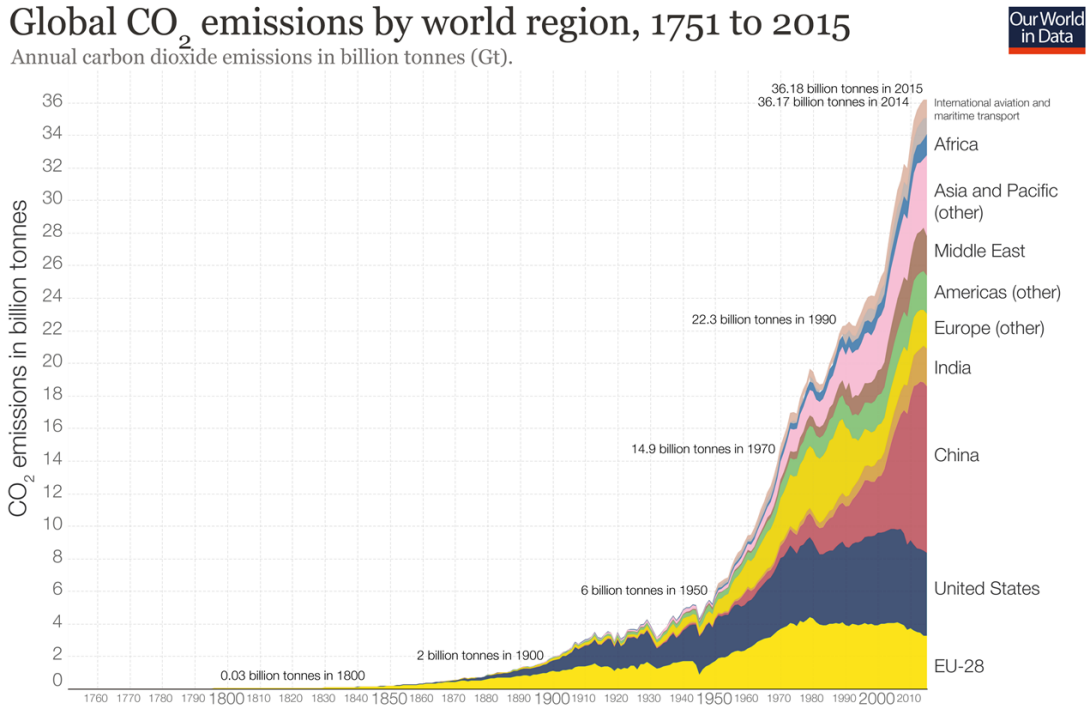

Figure 1: CO_2 emissions at the global scale from 1751 to 2015 (Data source: Carbon Dioxide Information Analysis Center (CDIAC)-Our World in Data).

According to the present estimates from the International Energy Outlook 2017 (IEO, 2017), the world energy consumption will grow by 28% from 2015 to 2040.

The Organization for Economic Co-operation and Development was created in 1961, connecting 18 European countries with the United States and Canada carrying a common aim

of stimulating economic progress and world trade. Today, it represents 36-member countries including most of the developed economies as well as emerging countries such as Mexico.

Currently the developed countries in OECD and non-OECD Europe and Eurasia are the ones who consume most of the total energy. However, estimates show that this majority will shift towards the non-OECD countries in Asia, the Middle East, Africa and South America such as China, India and Brazil; these countries are expected to consume the highest percentage of energy.

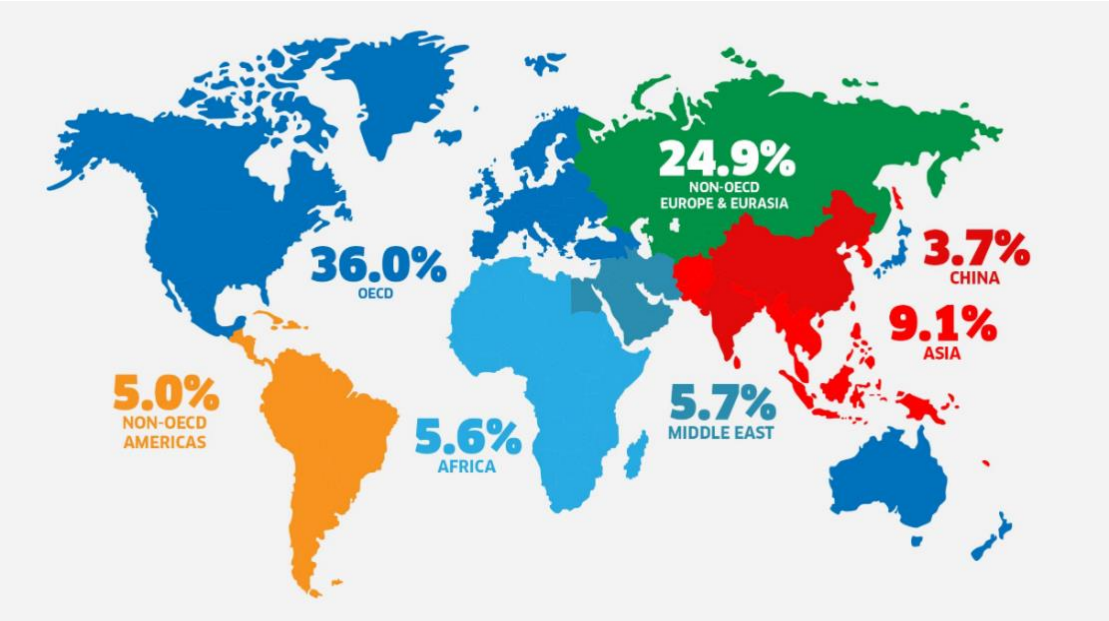

Figure 2: Map showing the distribution of total energy consumption across the world. Developed countries in the OECD and non-OECD Europe and Eurasia consume the highest percentage of total energy, while developing countries consume less (figure from energy mix (New Zealand) and data from Key World Energy Statistics 2015-International Energy Agency (IEA)).

The urge for finding alternative solutions is therefore highly justified.

In this context a preliminary comprehension of the way global energy is used by our society is of prime importance. One of the most familiar elements are electricity and liquid fuels. Electric energy is used to power elements such as lighting, elevators, computers, businesses and manufacturing as well as electric cars; liquid fuels are used in almost all forms of transportation. The adequate energy resource must take into consideration efficiency and energy transportation around the world.

To maximize efficiency their production must be placed in a strategic location to facilitate the worldwide transport, but this comes at a very high price. The infrastructure for transporting energy will therefore need to change drastically. Solar energy (sun), hydroelectric (water), geothermal (earth), wind, and biofuels (biomass) are all renewable energy sources that we hope to use as an alternative to fossil fuels.

1.1.2 Renewable energy resources, current state

Renewable energies are defined as energy produced from sources that are inexhaustible or can be replenished within a human's life time. Most of them derive directly or indirectly from the sun. The most common renewables are **solar energy** (direct use for heating and lighting, electricity, solar cooling…), **wind energy** (indirectly generated by the sun's heat), **hydropower** (indirectly generated by the sun's heat and the wind), **bioenergy** (biomass is used, also dependent on the sunlight to grow), **biofuels** (i.e. bioethanol, biodiesel, biohydrogen…), **geothermal energy** (generates from the earth's internal heat) and **ocean energy**.

Renewable energies are gaining a tremendous attention today. Numerous conferences are organized to discuss and share ideas and solutions for renewable energy sources to ultimately replace fossil fuels. The development of the renewable energy sector is highly investigated also because it can lead to new job opportunities. The International Renewable Energy Agency (IRENA, 2018) stated this year some key numbers such as:

- Global renewable energy employment represented 10.3 million jobs in 2017, which represents an increase of 5.3 % compared to 2016. It remains however highly concentrated in a small part of the nations worldwide. The following countries are at the top of the ranking: China, Brazil, the United States, India, Germany and Japan.

- There is an increasing number of countries that use renewable energy for their socioeconomic benefits.

- China alone represents 43 % of all renewable energy jobs. It is mainly shared between the following renewables: solar heating and cooling (83 %), solar photovoltaic (PV) sector (66 %) and wind power (44 %).

Renewable energies market growth rate is higher compared to fossil fuels and are expected to continue growing at exponential rates in the future. Fossil fuels however maintain a dominant share of the overall energy consumption and are expected to account for 77% of energy use in 2040, led by natural gas.

In 2016, the overall energy consumption was dominated by fossil fuels (85% of global energy consumption): the leader was oil with a third of global energy consumption, then came coal with 28% of global consumption, then natural gas with 24%. Renewables such as wind, solar, geothermal, and biomass represented 3% of the share and nuclear 5%. Renewables and hydropower together contributed to 10 % of primary energy consumption. The global primary energy consumption increased by 17 % in a decade. For reference, in 2010, renewables only represented 1.3 % and while the fossil fuels share was 86.9 %.

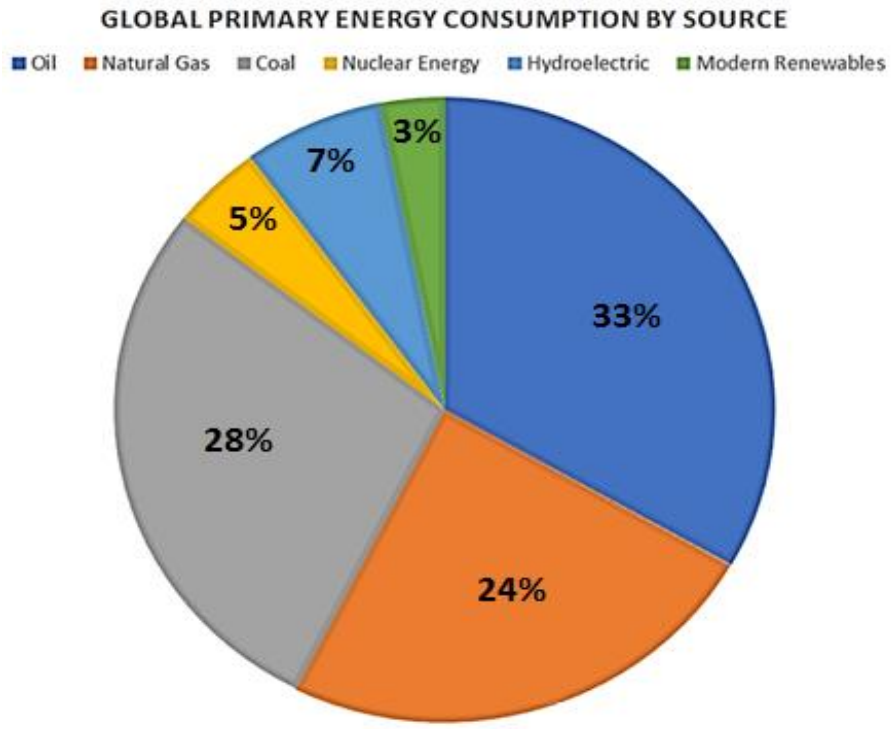

Figure 3: Primary energy consumption by source (modified from Papier, 2017 and data from BP Statistical Review of World Energy 2017).

By 2040, renewables are projected to become the world's fastest growing energy source, with a consumption increase of 2.3 % per year. Nuclear power is currently in the second position of the fastest growing energy source with a consumption increase of 1.5 %. The global energy consumption is projected to grow by 28% between 2015 and 2040 (Figure 4).

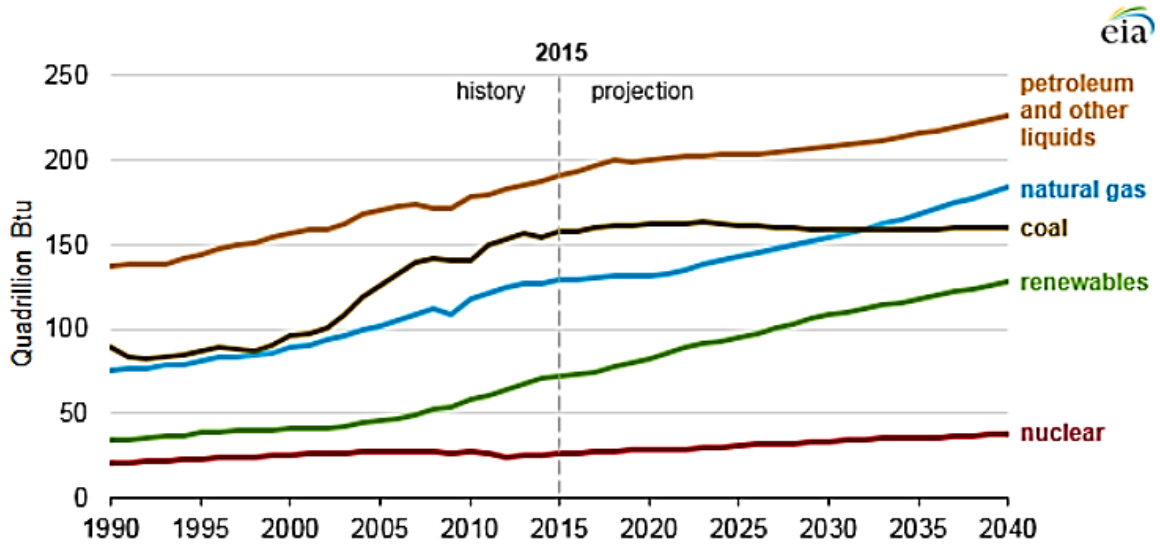

Figure 4: World energy consumption by energy source from 1990 to 2040 (U.S. Energy Information Administration, International Energy Outlook 2017)

1.2 Biofuels as a promising renewable energy resource

Biofuels have a tremendous potential in replacing fossil fuels. They can be described as a gas, a solid or a liquid that are produced from living organisms that contain energy from geologically recent carbon fixation. Biofuels can be created from biodegradable and renewable materials such as algal wastes, vegetable oils, animal fat or recycled cooking greases. Palm oil, rapeseed oil and soybean are the main sources of biofuel; palm oil is the most produced vegetable oil in the world and is largely promoted to produce biofuel.

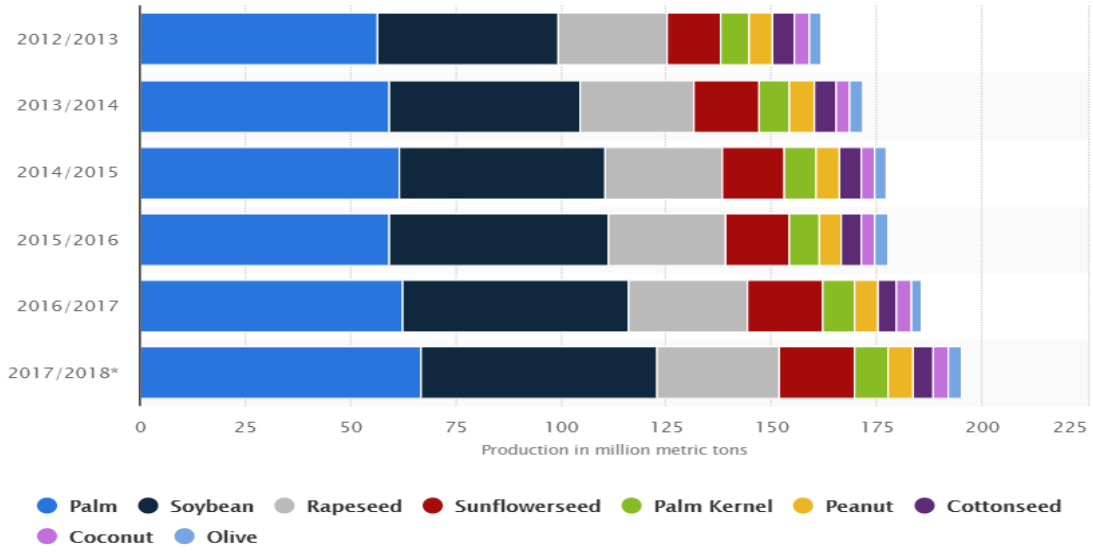

Figure 5: Production (million metric tons) of major vegetable oils worldwide from 2012/2013 to 2017/2018 (figure from Statista).

The feedstock used for its production defines the category in which the biofuel belongs to. Biofuels are categorized into four different generation biofuels (Figure 6).

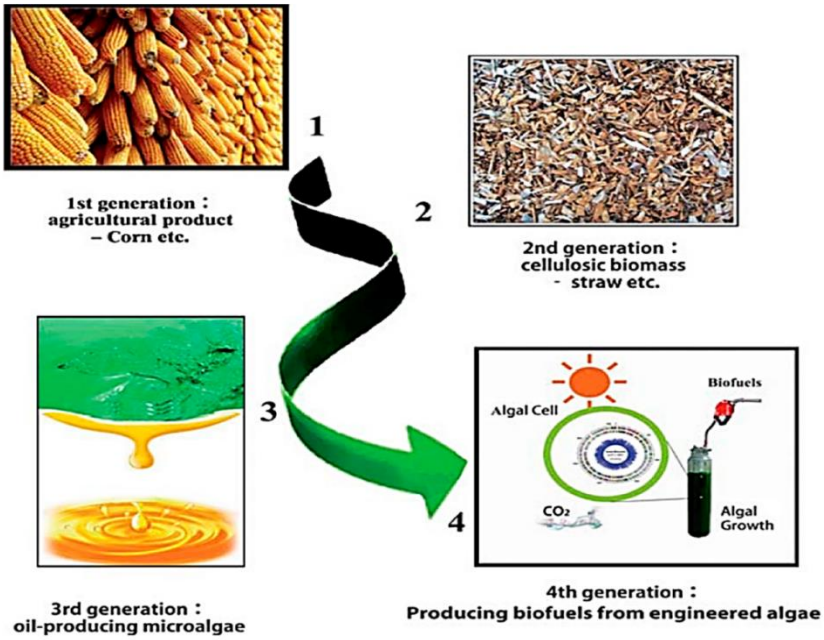

Figure 6: The four generations of biofuel production (Ravindran et al., 2016).

The **first generation of biofuels**, also known as "conventional biofuels" are produced from sugars and vegetable oils that are found in crops.

Several limitations were observed, generating new challenges such as: competition with food crops which led to an increase in food prices, inability to meet all promising environmental benefits, acceleration of deforestation and competition with water resources in some regions where water is highly limited.

The **second generation of biofuels**, also known as "advanced biofuels" differ from the first generation by the fact that they don't include food crops, unless the food crops have already been used as food and are no longer fit for human consumption. They refer to agricultural lignocellulosic waste therefore non-edible plant parts. They were therefore seen as a solution to the problems associated with 1st-generation biofuels since they are produced from waste products that are generated from other processes.

However, in the case of 1st and 2nd-generation biofuels, challenges such as land occupation leading to a clear competition between food and fuel remain. This is a major drawback in a context where the population grows along with the need for food, especially in developing nations.

Third generation biofuels refer to microalgae production. Indeed, microalgae are believed to be a promising resource for 3rd-generation biofuel as it offers tremendous advantages such as: a rapid growth rate and a high production capacity of lipids which are easily converted into biodiesel through thermochemical and metabolic processes.

As per estimates 50 000-140 000 liters of algae oil can be produced per hectare which is 10-30 times higher than oil crops such as palm oil.

Feedstock source	Oil content (% oil by wt. in biomass)	Oil yield (oil in litres/ha/year)	Biodiesel productivity (kg biodiesel/ha/year)
Oil palm	36	5366	4747
Maize	44	172	152
Physic nut	41-59	741	656
Caster	48	1307	1156
Microalgae with low oil content	30	58 700	51 927
Microalgae with medium oil content	50	97 800	86 515
Microalgae with high oil content	70	136 900	121 104

Table 1: Oil content, biodiesel productivity of microalgae and second-generation feedstock (Medipally et al., 2014).

Algae are also far from the competition between food and fuel since they can grow using land and water that are unsuitable for food production (i.e. non-arable land or saline water) which also helps with the issue of depleting water from sensitive regions. Furthermore, microalgal biomass can be converted into different kind of fuels such as diesel, petrol and jet fuel.

The **fourth generation of biofuels** includes the use of methods such as genetical modifications or metabolic engineering on living organisms, mainly microalgae, with the aim of creating a sustainable energy through an optimization of the photosynthetic ability of the algal cell as well as capturing and storing CO_2. In this strategy, CO_2 is captured, compressed then transported to a specific storage location where it will be injected beneath the earth's surface in for example deep aquifers or depleted oil and gas fields. This way, the carbon dioxide is isolated from the atmosphere for a long time. By capturing more carbon than it produces, this 4th generation of biofuels production has the potential of being carbon negative instead of carbon neutral (Mansor *et al.*, 2015).

1.3 Industrial and biotechnological applications of microalgae

1.3.1 Biochemical composition: useful substances present in algae and their applications

Besides biofuels, microalgae (and cyanobacteria) are considered as a promising sustainable source of various products for a broad range of industrial applications including food and non-food applications. These microorganisms, under specific conditions, can produce a large variety of compounds of interest such as **lipids** (up to 70 % of their dry cell (Chisti, 2007; Hu *et al.*, 2008; Zhu, Li and Hiltunen, 2016)), **proteins** (up to 60 % DCW (Becker, 2007)), **pigments** (for example astaxanthin, up to 7 % from *H. pluvialis*; β-carotene, up to 12 % from *D. salina*; phycocyanin, up to 17.5 % from *Arthrospira platensis (Spirulina)* (Kang *et al.*, 2005; Patel *et al.*, 2005; Del Campo, García-González and Guerrero, 2007)), **carbohydrates** (up to 60 % DCW (Choi, Nguyen and Sim, 2010; Pruvost *et al.*, 2011; Bondioli *et al.*, 2012; Chen *et al.*, 2013), and other **high-value products** such as EPA (around 39% of total fatty acids from *Phaeodactylum tricornutum*) and DHA (around 45 % from *Crypthecodinium cohnii*), both high value polyunsaturated fatty acids (PUFAs) (Cohen *et al.*, 1993; Benedetti *et al.*, 2004).

Major microalgal pigments

Algal pigments draw increasing attention for their high market values and are even perceived as the most promising products from algae that have the highest potential for commercial success (Koller, Muhr and Braunegg, 2014; Eriksen, 2016). The major part of algal pigments is associated with light occurrence, they are responsible for light harvesting (used for photosynthesis) and they protect the cells from the damage that could be caused by excessive illumination. They are also responsible for the macroscopic coloration of the algae culture. The major pigments found in microalgae are the following: **chlorophylls** (primary photosynthetic compound, responsible for green coloration), **carotenoids** (including carotenes, responsible for orange coloration, and xantophylls, yellowish coloration), and **phycobilins** (red or blue coloration).

Chlorophylls are one of the most important pigments found in nature. They selectively absorb light in the blue and red regions, which gives the green coloration and they are the most predominant algal pigments; chlorophyll a, one of the main types of chlorophyll with chlorophyll b, is an omnipresent pigment in all microalgae.

Chlorophylls have a potential in various applications. They are generally employed as food additive for coloration responding to the market demands of using natural coloring agents in food products. They are also, with their derivatives, used in other applications such as therapeutic and pharmaceutical applications due to their anti-cancer activity (Díaz, Li and Dashwood, 2003) and their ability to stimulate tissue growth which makes them attractive for the treatment of ulcers, oral sepsis or in proctology in the context of rectal surgery (Halim *et al.*, 2010). They help increase the rate of tissue healing. Finally, they are also associated to an antibacterial property and a high deodorant capacity; they are therefore used to remove odors from the wound and as ingredients in personal hygiene products (deodorants…).

Carotenoids (carotenes and xantophylls), known as secondary light harvesting pigments, also have a major potential for various applications in market: as colorant in food (Shahidi and Brown, 1998; Eriksen, 2016) and cosmetics (Igielska-Kalwat, Wawrzyńczak and Nowak, 2012), for functional food products and cancer prevention due to their anti-oxidant activity (which also enables them to protect cells from the negative effects of excessive solar radiation). These pigments absorb light energy at wave lengths ranging from 400 nm to 500 nm (spectral ranges where chlorophylls can't absorb energy).

β-carotene, also named vitamin A, is employed for nutritional purposes (vitamin supplement) but also human health for its major role in human metabolism to prevent negatives effects caused by free radicals. This pigment is often associated to the microalga *Dunaliella salina*; this microalga is mainly cultivated in Israel and Australia and can produce up to 14 % of its DCW (Paniagua-Michel, 2015).

Astaxanthin, another prominent pigment of the carotenoid group, is often associated to the microalga *Haematococcus pluvialis* (up to 3 % DCW) (Lorenz and Cysewski, 2000; Olaizola, 2000). This pigment is considered as the most powerful natural anti-oxydant and is therefore used for applications such as the protection of the skin from UV-induced photo-oxidation, antibody production, cancer prevention, anti-tumor therapy and age-related diseases (Koller, Muhr and Braunegg, 2014).

Other carotenoids are used for food coloration, cosmetics or human health such as: bixin (food additive E160b, cosmetics), violaxanthin (food additive E161e, anti-cancer), lutein (food additive E161b; feed additive, pigmentation of animal tissues, anti-macular degeneration, anti-colon cancer, coloration in cosmetics) and zeaxanthin (food additive E161h, animal feed, anti-colon cancer, eye health).

Phycobilins are unique photosynthetic pigments due to their particularity of binding to certain water-soluble proteins forming phycobiliproteins. They are responsible for transferring the harvested light energy to chlorophylls for photosynthesis. They are therefore also known as secondary light harvesting pigments. The major phycobiliproteins are phycoerythrin (PE, 540 - 570 nm), phycocyanin (PC, 610 - 620 nm) and allophycocyanin (APC, 650 - 655 nm) (Parmar *et al.*, 2011).

Phycobilins are used as chemical tags (phycobiliproteins bind to antibodies), food colorants and in cosmetics (Koller, Muhr and Braunegg, 2014).

Figure 7 shows a schematic drawing of the photosynthetically important or commercially applied pigments of the most common microalgal groups.

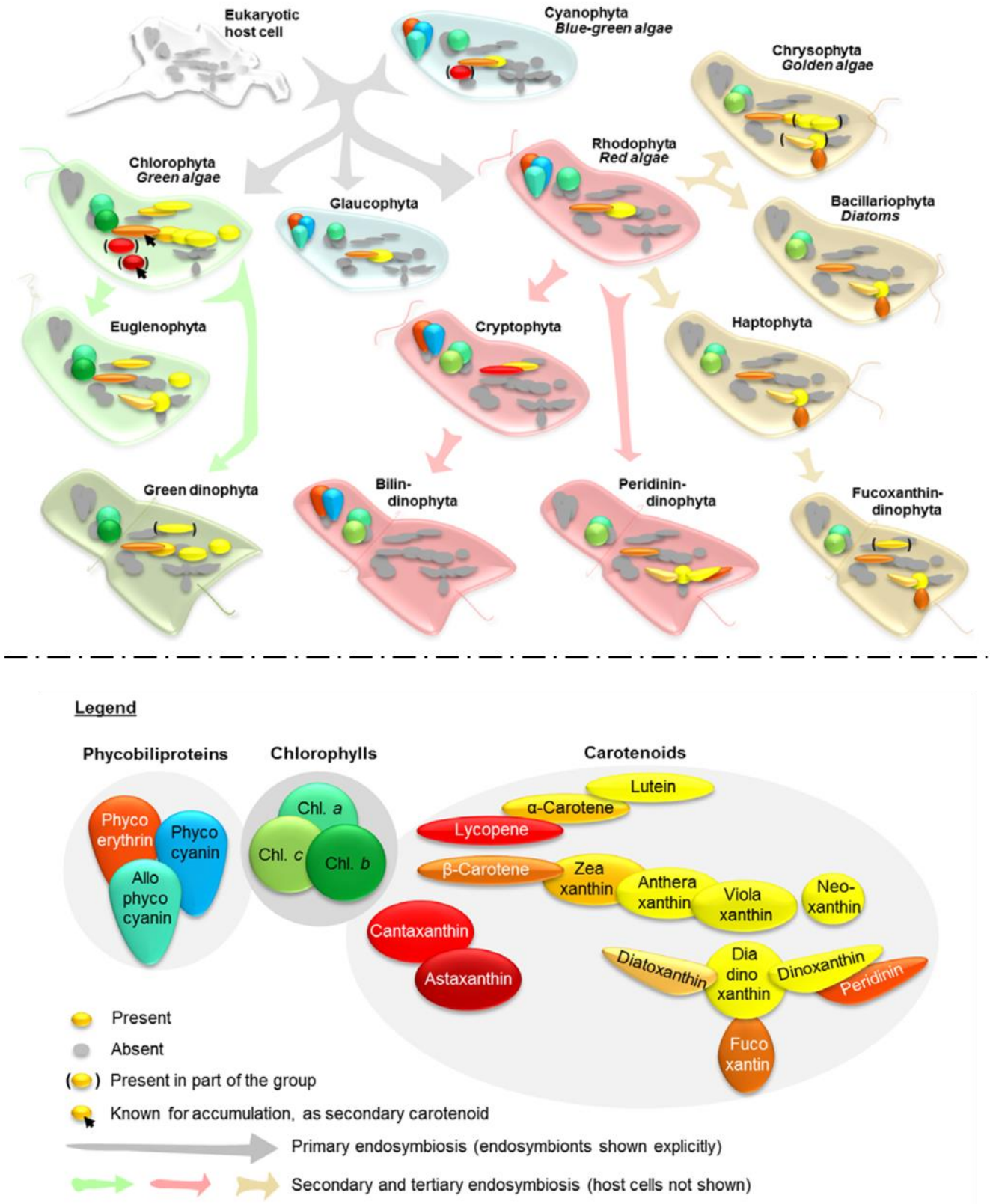

Figure 7 : Schematic representation showing the most common microalgal groups with their photosynthetically important and commercialized pigments (modified from Mulders et al., 2014)

Major microalgal lipids

Algal lipids are often investigated to produce biodiesel (Koller, Muhr and Braunegg, 2014). However, they can also be produced and commercialized for other applications such as therapeutic and pharmaceutical, health and food. The lipids found in microalgal cells (up to 70% DCW) can be separated into two types: polar lipids (or structural lipids) and non-polar lipids (neutral lipids).

Non-polar lipids are known as storage lipids and can be divided into three types: monoacylglycerol, diacylglycerol and triacylglycerol (TAG). Besides, they can also be found in the form of free fatty acids. TAGs can be converted into energy by transesterification; they are therefore vastly targeted for biodiesel production. Their structural formula is shown in Figure 8. Lipid productivity will mostly depend on the microalgae species. Several species were reported to potentially produce extremely high amounts of lipids: *Botryococcus* (*B. braunii*, 25% - 75 %, (Nautiyal, Subramanian and Dastidar, 2014)), *Chlorella*, *Nannochloropsis*, *Neochloris*, *Nitzschia*, *Scenedesmus*, *Dunaliella* and *Schizochytrium* (lipid content ranging from 50 to 77 % (Nautiyal, Subramanian and Dastidar, 2014)). Furthermore, the microalgae's lipid profile, highly investigated to produce quality biodiesel, is also dependent on the culture conditions. They are accumulated in the algal cells by submitting them to specific environmental stress conditions such as phosphate or nitrogen limitation/starvation and high light intensity.

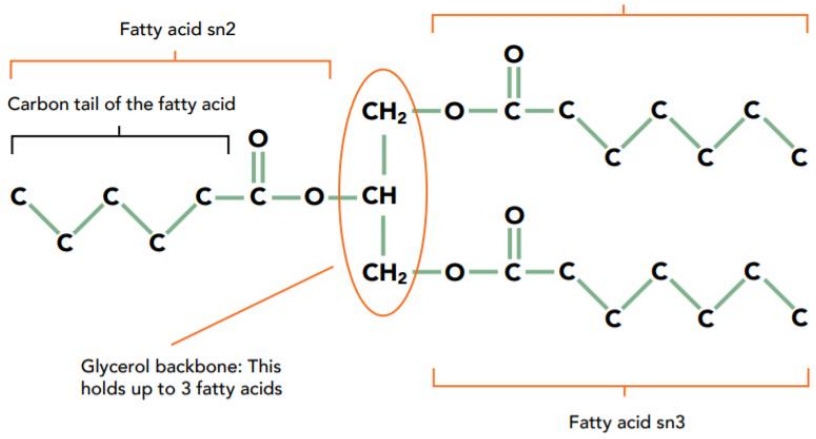

Figure 8: Structural formula of a triacylglycerol (TAG). The molecule can be composed of three fatty acids that are linked to the glycerol backbone by esterification (Berger, 2014).

Polar or structural lipids including phospholipids and sterols, play a major role in the structure of the cell membranes which represent a selective permeable barrier for both cells and organelles. They are responsible for the maintain of specific membrane functions (enabling various metabolic processes) and play a role in membrane fusion events and in responding to environmental changes. Moreover, some polar lipids, in addition to a structure function, act as important intermediates in cell signaling pathways (Sharma, Schuhmann and Schenk, 2012).

Structural lipids generally have a high content of **polyunsaturated fatty acids (PUFAs)** (Behera and Varma, 2016). These bioactive lipid compounds are crucial for the nutrition of humans and aquatic animals; they can maintain and improve cellular health, and they are necessary for the body to perform different vital functions. They can play a role in the

prevention of several diseases such as cardiovascular disorders, cancer, asthma, arthritis, kidney and skin disorders, depression and schizophrenia (Sharma and Sharma, 2017). Therefore, they can be produced and commercialized for therapeutic and pharmaceutical applications. Many algae species are composed of fats that contain PUFAs with high market values (omega-3 long chain fatty acids) such as eicosapentaenoic acid (EPA), docosahexaenoic acid (DHA), γ-linolenic acid (GLA) and arachidonic acid (AA). The following figure shows the composition of long chain PUFAs depending on the microalgal group.

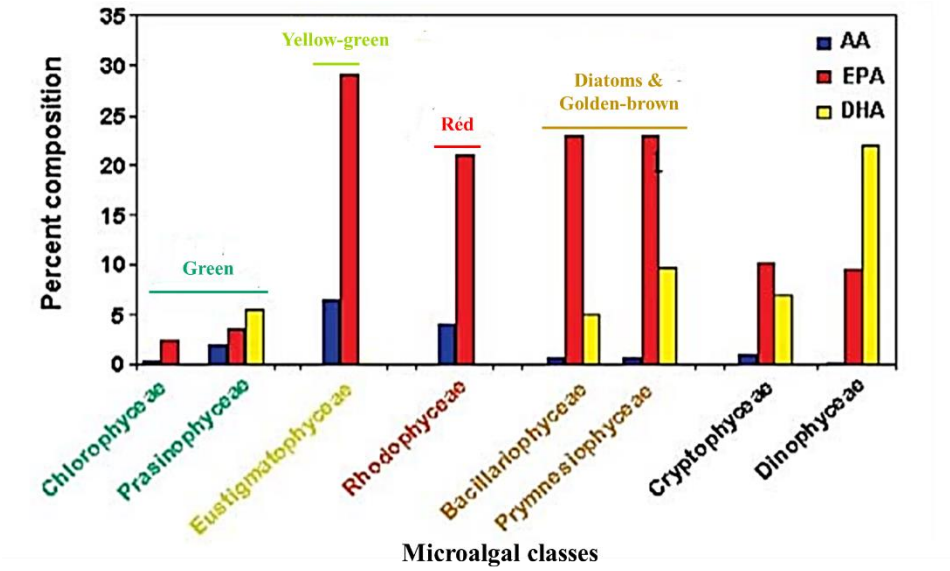

Figure 9: Composition in long-chain polyunsaturated fatty acids (LC-PUFA) depending on the microalgal class. Abbreviations: AA, arachidonic acid; EPA, eicosapentaenoic acid; DHA, docosahexaenoic acid (figure modified from Nichols et al., 2016).

Carbohydrates

Algal cells contain a wide variety of carbohydrates serving both structural (cell wall) and metabolic functions (they act as storage compounds that serve as energy providers for the metabolic processes when required and helps the cell survive in dark conditions). They are produced inside the chloroplast as well as the cytosol (Markou, Angelidaki and Georgakakis, 2012). Carbohydrates include sugars (monosaccharides) and their polymers (di-, oligo-, and polysaccharides like starch).

The amount carbohydrates vary depending on the microalgal species and the culture conditions. Among the major compounds of microalgae, carbohydrates are classified at the third position in the most energy-rich compounds (37.6 $kJ \cdot g^{-1}$ for lipids, 16.7 $kJ \cdot g^{-1}$ for proteins and 15.7 $kJ \cdot g^{-1}$ for carbohydrates (Wilhelm and Jakob, 2011)). They are however potential preferred for certain biofuel productions such as bioethanol (Markou, Angelidaki and Georgakakis, 2012). Moreover, some species present high carbohydrate content such as *Spirogyra sp.*, *Porphyridium cruentum*, *Chlorella emersonii* or *Chlorogloeopsis fritschii*. Carbohydrates are present in different proportions depending on the algal cell, however the most abundant ones are glucose (21%-87%), mannose (2%–46%), galactose (1%-20%) and arabinose, fucose, rhamnose, ribose and xylose (0%–17%).

Proteins

Like carbohydrates, proteins produced by algal cells have both structural and metabolic functions (CO2 fixation pathways, cell growth…). Due to the microalgae's capability to synthesize all essential amino acids within their cells (Guil-Guerrero *et al.*, 2004), they generate high levels of protein contents. Some species are known for their high protein content such as *Spirulina maxima*, *Synechoccus sp.*, *Anabaena cylindrical*, and *Chlorella vulgaris*. Their proteins can serve as an ideal source for nutrients, nutraceuticals and food additives.

In conclusion, microalgae are therefore often described as "chemical platforms" that are valuable for the production of biofuels (biodiesel, biohydrogen, bioethanol and biogas), and high-valuable compounds for cosmetics, food industry and pharmaceutical and therapeutic applications. Figure 10 displays an overview of the microalgal products and their potential applications.

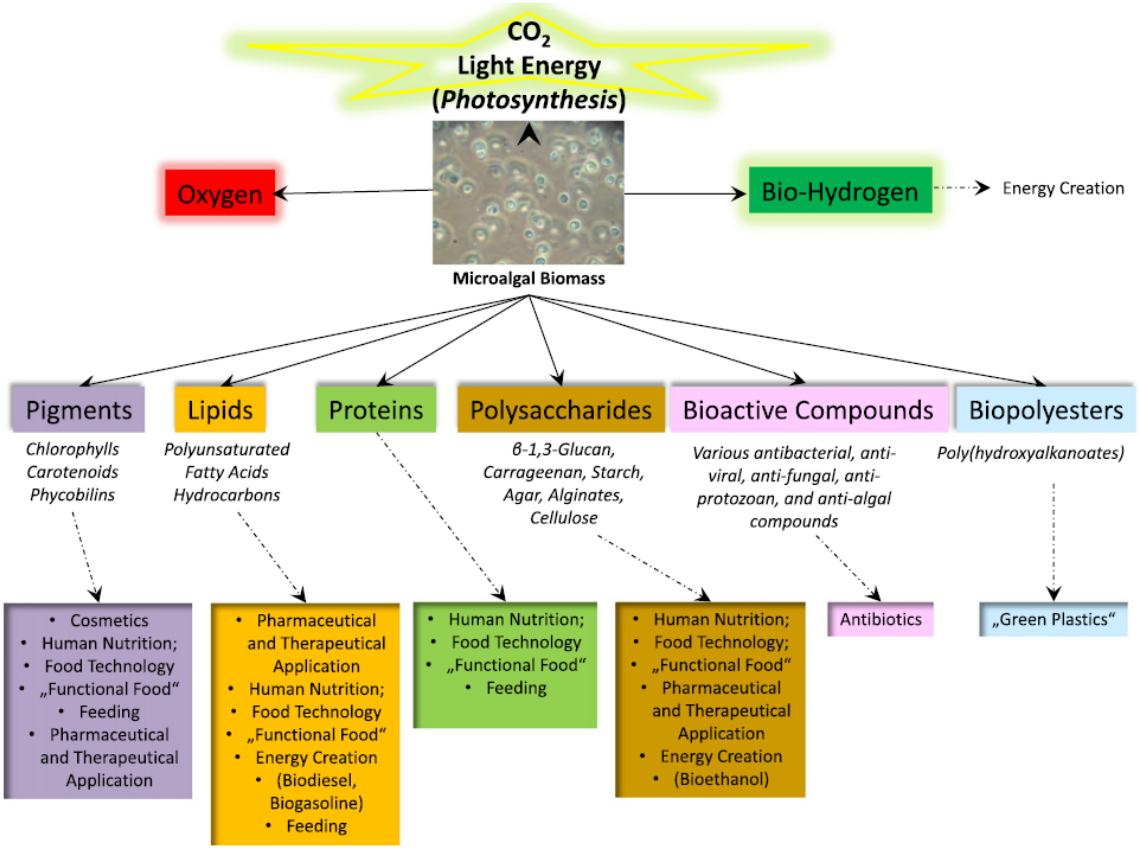

Figure 10: General description of the compounds produced by microalgae and their potential applications (Koller et al., 2014).

In food industry, microalgae are highly praised for health and functional food. For example, in Japan, by 1997, 2400t of microalgal biomass was commercialized per year for health food in the form of powder (the cultivated microalgae were *Chlorella* (2000t) and *Spirulina* (400t)) (Yuan-Kun, 1997). Currently, the use of microalgae for functional food dominates all other applications (Koller, Muhr and Braunegg, 2014)).

In the context of therapeutic and pharmaceutical applications, microalgae are also highly appreciated for the brand range of biological activities that they offer such as anti-oxidant, anti-inflammatory, anti-viral, anti-cancer and anti-bacterial activities. Indeed, they represent a potential source for a very wide range of bioactive molecules including pigments, PUFAs and polyphenols. Therefore, they are increasingly considered for their use for health benefits.

Furthermore, characteristics such as biomass productivity and compounds of interest will considerably depend on the cultivation conditions. From the original farming and harvesting to the advanced technological processes and controlled cultivations, various operational and environmental factors must be considered such as salinity, temperature, pH and light intensity. This will further be discussed in section 4.

Table 2 summarizes the most popular microalgae species and their growth type (photoautotrophic, heterotrophic or mixotrophic), cultivation conditions (open raceway ponds, photobioreactors…) and applications. The various growth type (s) and cultivation conditions will be discussed in further detail later in this work.

Table 2: Overview of the most popular microalgae species with their growth type(s), cultivation conditions and applications (Table modified from Saha and Murray, 2018).

Microalgae Species	Cultivation History	Growth Type	Cultivation Conditions	Applications
Chlorella vulgaris	1951	Photoautotrophic	Open raceway pond, tubular PBR, flat-plate photobioreactor	Whole biomass for human nutrition as tablets, powders, nectar noodles; cosmetics; aquafeed
Crypthecodinium cohnii	1999	Heterotrophic	Large stainless steel Fermentor	DHASCO™ oil for the infant formula as DHA source
Dunaliella salina	1980	Photoautotrophic (two phase cultivation)	Unstirred open pond, lagoons, paddle wheel stirred raceway ponds, tubular photobioreactors	Carotenoid β-carotene for food and in cosmetics, human nutrition as powder, animal feed, source for proteins and glycerol
Haematococcus pluvialis	2000	Photoautotrophic (two phase cultivation), Mixotrophic	Open raceway pond, tubular enclosed outdoor PBR, bubble column and airlift photobioreactors, large plastic bags	Carotenoid astaxanthin, aquafeed, poultry feed, animal feed, human nutrition, cosmetics, pharmaceuticals, food-colourant, food-supplement
Nannochloropsis sp.	1997	Photoautotrophic, Mixotrophic	Raceway pond, Helical-tubular photobioreactor	EPA oil for human nutrition, aquaculture
Odontella aurita	1996	Photoautotrophic, heterotrophic or mixotrophic	Outdoor open ponds, Pilot Tanks, cylindrical glass columns and flat-plate photobioreactors	Human nutrition, baby food as EPA and DHA source, cosmetics
Phaeodactylum tricornutum	1996	Photoautotrophic	Open pond, circular tanks, outdoor pilot-scale bubble column photobioreactor, large 400 L polyethylene bags supported by frames, air-lift photobioreactor	Aquaculture feed, EPA oil as health supplement
Porphyridium cruentum	1970	Photoautotrophic	Tubular PBR	Pink phycoerythrin pigment, sulfated polysaccharide, cosmetics
Schizochytrium sp.	1999	Heterotrophic	Large stainless steel Fermentor	Life's Omega™ oil as source for DHA and EPA
Arthrospira (Spirulina) platensis	1970	Photoautotrophic	Open raceway pond, tanks, earthen pots, basins, natural lakes	Whole biomass for human nutrition as tablets, capsules, powders; blue phycocyanin as colourant in food and in cosmetics; source for g-linolenic acid (GLA), vitamins and minerals

1.3.2 Biofuels

Several types of biofuels including **biodiesel**, **biohydrogen**, **bioethanol** and **biogas can be produced using microalgae**.

A microalgal biofuel production starts with the cultivation of microalgae in the chosen cultivation system (open ponds, PBRs…), then it is followed by a harvesting step, where the algal cells are separated from the culture medium, using a specific process (centrifugation, flocculation, filtration…). The harvested biomass is then processed through biochemical, thermochemical or chemical conversions to produce the wanted biofuel. The produced biofuel can be in solid (bio-char or bio-charcoal…), liquid (bioethanol, biodiesel…) or gas form (biohydrogen, biogas). The main types of biofuels produced by microalgae are described in the following section.

Biodiesel – produced from microalgal oil

Microalgal oils, just like vegetable oils, have a high viscosity, which means that they cannot be used directly as a biodiesel for engines. The most efficient way to produce biodiesel from microalgal oil is through a trans-esterification reaction which reduces the oil's viscosity and increases its fluidity (Figure 11). The reaction involves an oil (triglyceride, composed of three long hydrocarbon chains and a glycerol molecule) and an alcohol (methanol) as reactants, a catalyst and glycerol and esters (biodiesel) as products.

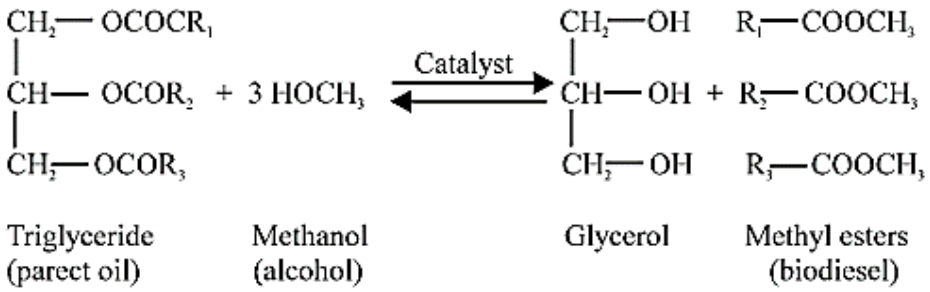

Figure 11: Transesterifaction reaction for biodiesel production (Hossain *et al.*, 2008).

Biohydrogen – produced from biophotolysis and fermentation

Hydrogen is the lightest element on earth (0.00005 % of the air). It is colorless, odorless and highly combustible, which makes it usable as a fuel. Biohydrogen is hydrogen made from a biological source. There are different methods available to produce biohydrogen (Gürtekin, 2014): dark fermentation, photo fermentation, combined fermentation, direct biophotolysis (algae), and indirect biophotolysis (cyanobacteria).

Bioethanol – produced via fermentation

Bioethanol is an alcohol that can be produced by fermentation mainly from carbohydrates. There are two types of methods to produce bioethanol: hydrolysis and fermentation of biomass.

Biogas – produced by anaerobic digestion

Biomethane can be produced by converting the cellular energy of algae into the chemical energy of methane through the anaerobic fermentation of algae by consortium of bacteria and Archae.

Major algae companies are listed hereafter in Table 3.

Company name	Location	Brief description
Algenol	Florida based company with head office in Fort Myers, founded in 2006	Industrial biotechnology company, commercializing its patented technology for ethanol production from algae and other fuels. Their technology includes production of four major fuels such as ethanol, gasoline, jet and diesel using a recovery process with involvement of algae, sunlight, carbon dioxide and salty water to produce ethanol and to produce other biofuels from spent algal biomass.
Solix Algredients	Colorado based company with headquarter in Fort Collins	Well known player in algae cultivation. Solix brings products like Solasta ® Astaxanthin, Solmega® DHA omega-3 and other natural algal ingredients to market.
Sapphire Energy	Desert scrub outside of Columbus, New Mexico	The company has world's first commercial demonstrated algae farm, with integration of total value chain starting from cultivation to production, to extraction. Sapphire Energy produces "Green Crude" from algae (100% renewable crude oil with reduced carbon emissions), providing a crude oil with many properties of fossil fuel oil.
TerraVia Holdings, Inc. (formerly Solazyme)	Biotechnology based public company in United States	Converts low cost plant sugars into high value oils and whole algae ingredients.
Aurora biofuels	California based energy company	Leading producer providing highly accomplished and excellent algae derived products with application in pharmaceutical, nutrition and fuel market.
Earthwise Spirulina	Sonoran Desert of southeastern California	High-quality *Spirulina* producer. Earthwise has the world's largest *Spirulina* farm. Their *Spirulina* is cultivated in protected environment without the use of pesticides, with an effort to be environmentally friendly.
Nutrex-Hawaii Hawaiian	Hawaii	Among one of the most popular brands of *Spirulina*.
Bulk Supplements	Harvested in China but tested and packaged in the US	*Spirulina* production.
Healthfoce Spirulina Azteca	Chile	Hard-core, vegan, therapeutic superfoods company.
Taiwan Chlorella Manufacturing Company (TCMC)	Taiwan	World's oldest and largest *Chlorella* producer.

Company name	Location	Brief description
Far East Bio-Tec Co., Ltd. (ALGAPHARMA BIOTECH CORP.)	Taiwan	Supplier and manufacturer of organic *spirulina*, organic *chlorella* and biotech microalgae research market (since 1976).
Nutress	Headquarters in Ochten, The Netherlands.	Biggest algae food company of Europe, founded in 2012. The company provides several value added products to feed, pharmacy and food sector.
Source Naturals®	California, USA	Created in 1982 by C.E.O. Ira Goldberg to support each individual's potential to enjoy optimal health. Source Naturals pioneered the concept of combining many nutrients, herbs and nutraceuticals in one formulation. Now the industry's #1 immune support product.
AstaReal®	India	Produces *Haemotococcus pluvialis* microalgae extract.
Herbal Hills	India	Cultivates, manufactures and exports various ayurvedic herbal products and various algae products such as *Spirulina* tablets.
Shibin Chlorella	India	Became the first company in India to start commercial production of *Chlorella* as a nutritional supplement (from July 2015).
Parry	India, headquarters in Chennai for Parry Nutraceuticals	One of the best providing microalgal health supplements,
Pondicherry Spirulina Farms (PyFarms)	India	South -India based food company with specialization in harvesting, production and marketing of Spirulina (established in May 2008).
The Algae Company	India	First company in India to have a dedicated focus on algae as nutraceuticals. The main products are brought by Chlorella and Spirulina.
Zenith Nutrition	India	Provides a wide range of products like vitamins, probiotics, herbal formulations and amino acids. It is involved in high quality research for providing formulations to benefit health.

Table 3: Summary of some of the main companies using microalgae as a source (modified from Sharma and Sharma, 2017).

1.4 **Economic position of microalgae – market potential**

Market prices for algal biomass and compounds of interest depend on various factors such as: the global geographic area of the production site, the current market situation and the type and purity of the product (Koller, Muhr and Braunegg, 2014). The product purity is an important factor that can significantly impact the final manufacturing prices because the isolation and purification of the high value products (that represent a minor proportion of the total algal biomass) requires considerable efforts.

To analyze the market potential of algal production, market price and volume relations can be used as indicators. The market volume indicates the market strength; a high volume can indicate strong interest from investors. Therefore, the market price/volume relations (2014) regarding different industrial applications using algae as feedstock are listed below (Koller, Muhr and Braunegg, 2014):

- For **biodiesel**, the general market price per kg corresponds to less than 0.5 US-$, and the global market volume to an extremely high value of 10^9 US-$. The estimated cost for a barrel of algae oil ranges from $300–2,600. In contrast, a barrel of fossil oil costs around 40 to 80 $ (McBride *et al.*, 2014).
- Regarding nutraceuticals for **animal feeding and aquaculture**, the final product's market price is around 10 US-$/kg, with a global market volume of 4 billion US-$.
- In contrast, regarding microalgal nutraceuticals for **human nutrition**, where the high market price of about 120 US-$/kg corresponds to a market volume estimated at only 70 million US-$. *Spirulina sp.* or *Chlorella sp.* biomass, are used as feedstock to human nutrition applications and cost about 40 to 50 US-$/kg with a market volume of 1.25 billion US-$.

When focusing on the **lipids and pigments**, the market price/volume relations are as follows:

- **ß-carotene**'s market value price is estimated in the range of 300 to 3000 US-$/kg, depending on the purity of the final product. Its global market volume is around 2 billion US-$ per year.
- In the case of **astaxanthin**, dependent on the origin, the market price ranges between 2500 and 7000 US-$/kg, depending on its origin. Its global market potential is estimated at 2 billion US-$ per year.
- **Phycobiliproteins**, extracted from *Spirulina* (phycoerythrin and phycocyanin), can approach 3000 and even reach 25 000 US-$/kg. The market volume was estimated in 1997 at 50 million US-$ per year).
- Finally, the market price of **polyunsaturated fatty acids** is estimate at around 50 US-$/kg for docosahexaenoic acid (DHA); this, if it originates from species such as *Crypthecodinium cohnii* or *Schizochytrium sp*. In the case of a production of eicosapentaenoic acid (EPA) from *Phaeodactylum Tricornutum*, 4600 US-$/kg was reported as the production price of a monoseptic cultivation in closed photobioreactors

and a downstream processing for the recovery of products with a very high purity. In contrast, the production price of a fish oil reaches 650 US-$/kg.

The following table summarizes the market price and volume of the above-mentioned microalgal products.

Product	Estimated market price (US-$/kg)	Global market volume (US-$)
Industrial applications		
Biomass for nutrition	40–50	$1.25 \cdot 10^9$
Biomass for feeding	10	$4 \cdot 10^9$
Microalgal nutraceuticals for human nutrition	120	$7 \cdot 10^7$
Biodiesel	0.5 (general market price for biodiesel) 3–4 (estimated production price from algal origin)	$1 \cdot 10^9$
Compounds of interest		
ß-Carotene	300–3000	$2 \cdot 10^8$
Astaxanthin	>2000	$2 \cdot 10^8$
Phycobiliproteins	3000–25 000	$5 \cdot 10^7$ $1 \cdot 10^8$ (estimate for USA)
ß-1,3-Glucan	5–20	$1 \cdot 10^8$ (estimate for USA)
Docosahexaenoic acid (DHA)	50	$1 \cdot 10^8$ (estimate for PR China); $4 \cdot 10^8$ (estimate for USA)
Eicosapentaenoic acid (EPA)	4600 (*Phaeodactylum Tricornutum*) 650 (from fish oil)	$1.25 \cdot 10^3$ (estimate for Japan)

Table 4: Estimated market prices and volumes for microalgal production (modified from Koller et al., 2014).

According to the "Algae Products Market- Global Opportunity Analysis and Industry Forecast (2017-2022)" report, the global algae products market is projected to reach 3.318 billion US-$ by 2022, at a CAGR (Compound Annual Growth Rate, it represents an investment's annual growth rate over time) of 6.7% from 2017 to 2022.

2. Microalgae

2.1 Origins: a little bit of history

Algae are part of the oldest life forms on earth. These photosynthetic organisms can be described as a type of plant with no roots, stems or leaves that can be found in the sea, in freshwater and other marine environments. Some species are capable to survive under extreme environmental conditions such as high temperature, high and low pH and high concentration of CO_2.

Microalgae, are unicellular eukaryotic microorganisms discovered in the 19th century that vary widely in size (from a few micrometers to hundreds of micrometers), shape, color and habit (i.e. green algae, red algae, golden-brown algae or diatoms). It has been estimated that there exist 200 000 to 800 000 species, but only 50 000 of them were discovered and only 100 of them are produced at laboratory scale.

The farming of plants has started thousands of years ago. Microalgae culturing in the laboratory is however only about 140 years old and commercial farming less than 60 years old.

The oldest culturing of microalgae includes Cohn's culture of *Haematococcus pluvialis* in situ (1850) and Famintzin's culture of *Chlorococcum infusionum* and *Protococcus viridis* (1871). Other advanced culture experiments then followed with Beijerinck's cultivation of *Chlorella vulgaris* (1890) and Miquel's axenic culture (growth and maintenance of only one type of microorganism in a culture free of other organisms) of diatoms (1892). The optimization of laboratory culture conditions continued and is reported through the work of other pioneers of phycology such as Pringsheim (1947) who worked on the culture of axenic strains, Ketchum, Red Field and other (1938-1949) who developed continuous cultures.

In 1952, one of the most important symposium in the history of algae research was held in California, USA, at the Stanford University (Algae Mass Culture Symposium). This meeting of scientists working on algae generated the publication of "Algae Culture. From Laboratory to Pilot Plant", edited by J.S. Burlew in 1953. This book included almost all the work done in the previous years, such as the first larger scale culturing attempts in the USA, Germany, Japan and Israel.

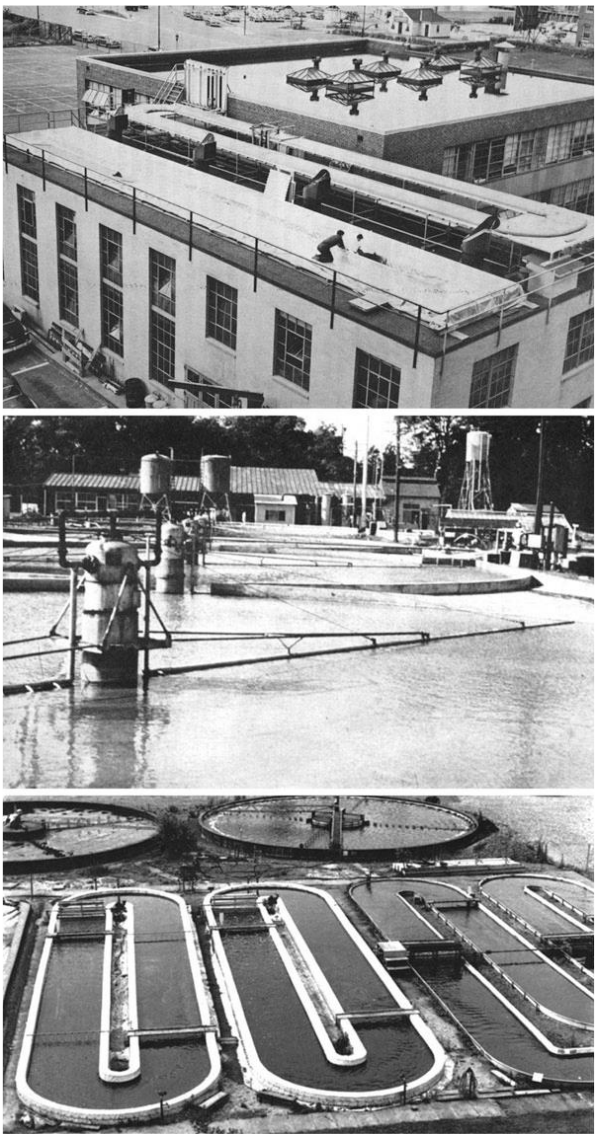

Figure 12 : Early large-scale algae culture systems (Borowitzka and Moheimani, 2013).

***Top photo*: Tube-type reactors on the roof of the building at Cambridge, Massachusetts, USA in 1951; *Middle photo*: Circular algae ponds at the Japanese Microalgae Research Institute at Kunitachi-machi, Tokyo (1960s); *Bottom photo*: The outdoor algae ponds at the Gesellschaft für Strahlen- und Umweltforschung, Dortmund, Germany (1970s).**

Research and interest in the commercial use of microalgae since then continued to grow and led to the publication of other important manuscripts such as Amos Richmond's book on microalgal biotechnology (1986 and 2004), Michael and Lesley Borowitzka's book, also on microalgal biotechnology (1988), Becker's compilation of the different methods employed worldwide for the artificial cultivation of different microalgae (1994) and other books focusing on particular species (Avron and Ben-Amotz, 1992; Vonshak, 1997).

2.2 Species and Strain Selection

Among the thousands of species of algae that have been discovered, each of them presents a potential for a specific production. For example, in the case of a biofuel production, some important criteria must be met: growth rate and photon conversion efficiency, easy harvest, lipid productivity and extractability.

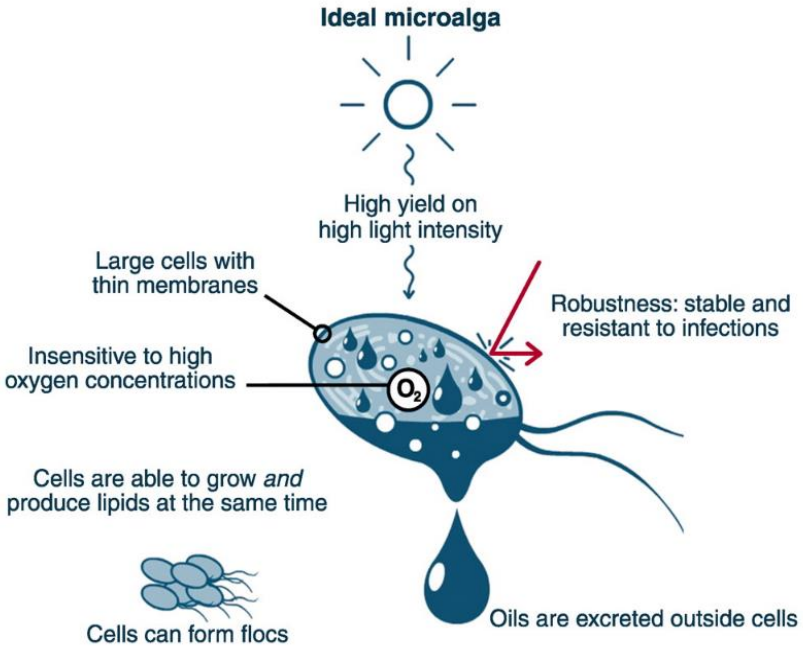

Figure 13: Characteristics of an ideal microalga (Wijffels and Barbosa, 2010)

For instance, some algal species are capable to double their biomass in less than one day, others can accumulate high lipid contents when submitted to nutritional stress conditions. Moreover, each species produces its own ratio of lipids, carbohydrates and proteins. Therefore, depending on the application, the chosen microalga as a source will vary. Some of the most currently investigated microalgae, other than the popular *Chlorella* and *Spirulina*, are briefly described below.

Microcystis aeruginosa

Like microalgae, cyanobacteria, also known as blue-green algae, are photosynthetic microorganisms highly studied because of their ecological and industrial interest. They are known to proliferate and produce various cyanotoxins in freshwater ecosystems worldwide. The most common toxins observed are microcystins and neurotoxins, which are extremely harmful for animals and humans. *Microcystis* are the most widespread bloom forming species, and *Microcystis aeruginosa* is known to proliferate massively and cause serious damages to fish (Padmavathi and Veeraiah, 2009; Briand *et al.*, 2012).

Although there is a significant amount of information on the ecology of freshwater blue-green algae, little is known on the impact of this microalga on the ecology and fish production in fish ponds. Moreover, the concentrations of microcystins produced are considerably different from

one bloom to another which makes it difficult to predict the potential risks on animal and human health.

It has also been reported that this species has appealing properties for biofuel production and could also be a potential source for natural butylated hydroxytoluene production, which is an antioxidant agent used for food additives.

Scenedesmus obliquus

Scenedesmus obliquus is a green microalga that, under unicellular growth conditions, has a long elliptical form of around 10 µm. Its lipid content is estimated at 40-55% of dry weight, with palmitate and oleate as main constituents. It is also known to be easily conditioned to grow efficiently and produce high lipid content. It is therefore highly investigated as a feedstock for biofuel production. Indeed, many studies using this microalgae in genetic and metabolic engineering were reported for the past few years, showing that it is possible to enhance its biomass production. In terms of lipid yield, Breuer et al. (2015) was able to produce a *Scenedesmus obliquus* mutant, carrying high contents of triacylglycerol, up to 57 ± 0.2 % of dry weight (Breuer *et al.*, 2015).

Furthermore, several studies demonstrate the interest of using *S. obliquus* to produce biofuels such as biodiesel, hydrogen and bioethanol or in the context of a biofuel production coupled with CO_2 mitigation and wastewater treatment (Miranda, Passarinho and Gouveia, 2012).

Haematococcus pluvialis

Astaxanthin is a high-value carotenoid that is a very important antioxidant, highly used in nutraceuticals, cosmetics, food and aquaculture industries. It showed a capacity to considerably reduce free radicals and oxidative stress, which is extremely useful for the human body. *Haematococcus pluvialis* is one of the most popular source for natural astaxanthin, which is believed to offer greater antioxidant capacities than the synthetic astaxanthin (Lorenz and Cysewski, 2000; Shah *et al.*, 2016). Therefore, the demand for natural astaxanthin has significantly increased, making *Haematococcus pluvialis* one of the most praised source for high-value products.

2.3 Microalgae metabolism, physiology and structure

2.3.1 Life cycle

The life cycle is defined as the series of changes that an organism undergoes, through asexual or sexual reproduction, that ends by its return to the starting state. In addition to displaying a wide diversity in their structural organization (unicellular organisms, microalgae, or multicellular ones, macroalgae) algae are unique in the way that they show a wide variety in terms of their life cycle patterns. They display different types of cell division during a single cell cycle; from binary fission (where the cell divides into two cells with the same DNA as the original cell), like bacteria, to multiple fission forming four to thousands of daughter cells, like green algae. The number of daughter cells is controlled by growth rate and can be influenced by factors such as light and temperature (Bišová and Zachleder, 2014).

Besides, the multiple fission observed in the algal species, is perceived as one of the most significant contribution of algal studies to the field of cell cycle studies (Zachleder, Bisova and Vitova, 2016). It has been reported that the evolution of this multiple fission capacity results from the fact that it enables algae to grow autotrophically during the day (where it is exposed to light), and then undergo cell and nuclear division as well as DNA replication, during the night (Bišová and Zachleder, 2014).

For example, when the algae are under a diurnal cycle involving 12 hours of light and 12 hours of dark, the cell cycle will synchronize in order to go through the growth phase during the presence of light, and cell division (including the mitotic and S phase) in the dark. For motile green algae, this adaptation has been previously explained by the fact that they use flagella-dependent phototaxis to optimize growth during the light phase and the cell division is only activated until dark. They remove their flagella before undergoing cell division (Koufopanou, 1994; Cross and Umen, 2015).

Also, algal species have shown a life cycle including both binary and multiple fission (Badour, Tan and Waygood, 1977; Zachleder, Bisova and Vitova, 2016).

Furthermore, some algae have the capacity to alternate between sexual and asexual reproduction during the same life cycle. Asexual reproduction can continuously be repeated, while sexual reproduction is generated by the change of environmental conditions (Grell, 1973).

In the case of *Chlamydomonas*, when the conditions of growth are favorable, it reproduces asexually. Sexual reproduction takes place only when it grows under unfavorable conditions (nitrogen limitation).

During asexual reproduction, the cells grow in volume by more than ten-fold (G1 phase) then undergo a certain number of cycles, altering between mitoses (M phase; cell division including nuclear and cytoplasm division) and S phases, also known as the interphase, where the DNA is replicated (Figure 14).

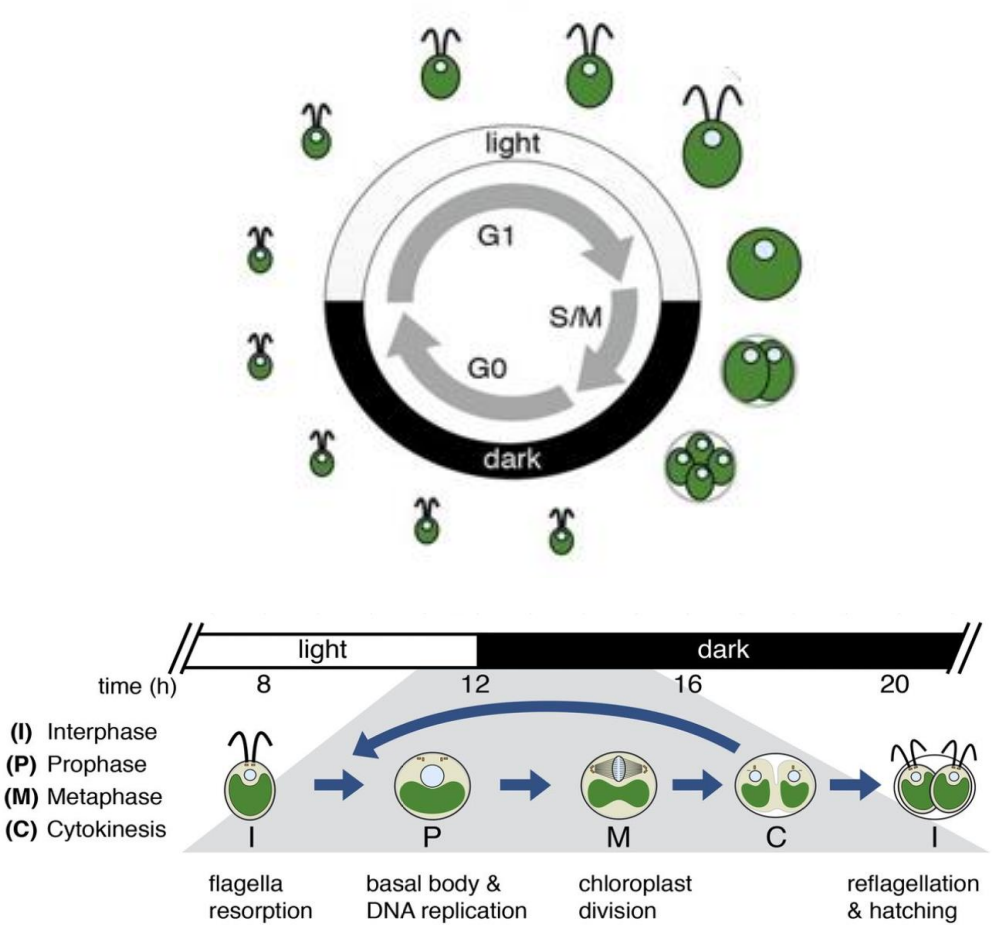

Figure 14: Chlamydomonas cell cycle showing the growth (G1), division (S/M), and resting (G0) stages. The bottom part of the figure displays the key stages and the relative timing of a single division cycle. The backward arrow shows the possible repetitions of S/M (modified from Zones et al., 2015).

Depending on the growth conditions, a mother cell can undergo two to five cycles of S/M, therefore producing 2 to 32 cell daughters (Lien and Knutsen, 1979; Cross and Umen, 2015). Furthermore, the larger the mother cell, the more it divides, which ensures the production of uniform size distribution daughter cells. Thus, the number of S/M cycles undergone by each mother cell will depend on the cell size (Craigie and Cavalier-Smith, 1982; Cross and Umen, 2015). The resulting cell daughters then hatch out of their mother cell, leaving the old cell wall behind. In the case of a sexual reproduction, the asexual cells (the plus mating type (mt+) and the minus mating type (mt-)) develop into gametes. Gametes of opposite mating types then fuse in pairs, their flagella agglutinate, to finally form a zygote. When the zygote matures and undergoes meiosis, four haploid cells are formed. They grow and become four asexual cells (two of each mating type). Figure 15 below, describes the asexual and sexual reproduction of *C. reinhardtii*.

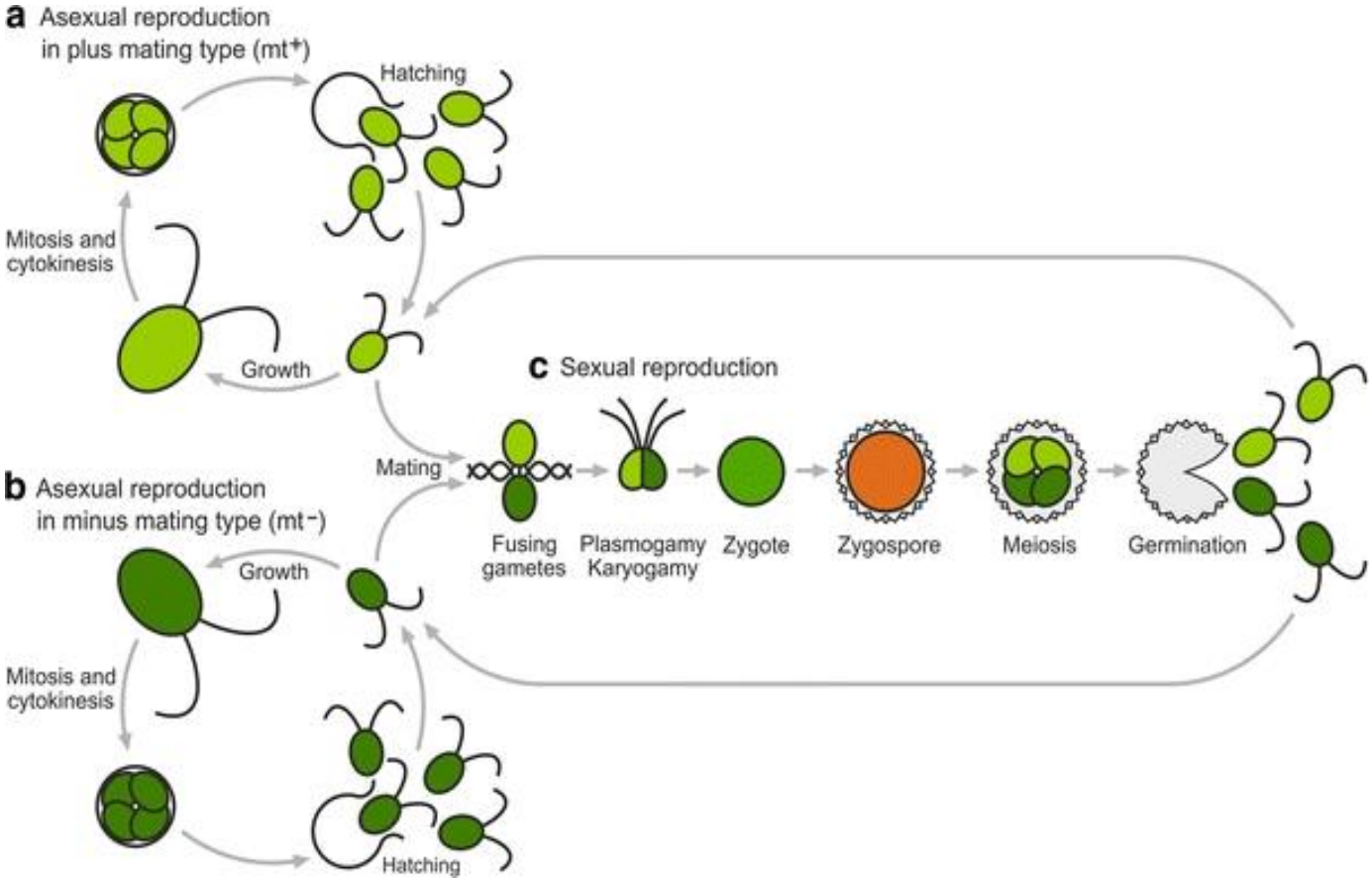

Figure 15: Life cycle of *Chlamydomonas reinhardtii*: asexual and sexual reproduction (Hallmann, 2011)

2.3.2 Metabolism: photosynthesis and respiration

Like plants, algae are oxygenic phototrophs, meaning that they capture energy from sunlight as photons to use it in their various metabolic functions (phototrophs), and take in oxygen to produce energy (oxygenic). These two biochemical and energy-transforming processes are what we call photosynthesis and respiration. During photosynthesis, the light energy captured is converted into carbohydrates (for example sugar) that can be used for cellular respiration and other metabolic processes. Cellular respiration is used to derive the energy from the sugar, producing ATP and various metabolites. Photosynthesis and respiration are therefore interdependent as the products of photosynthesis (carbohydrates and oxygen) are the reactants for cellular respiration (Figure 16).

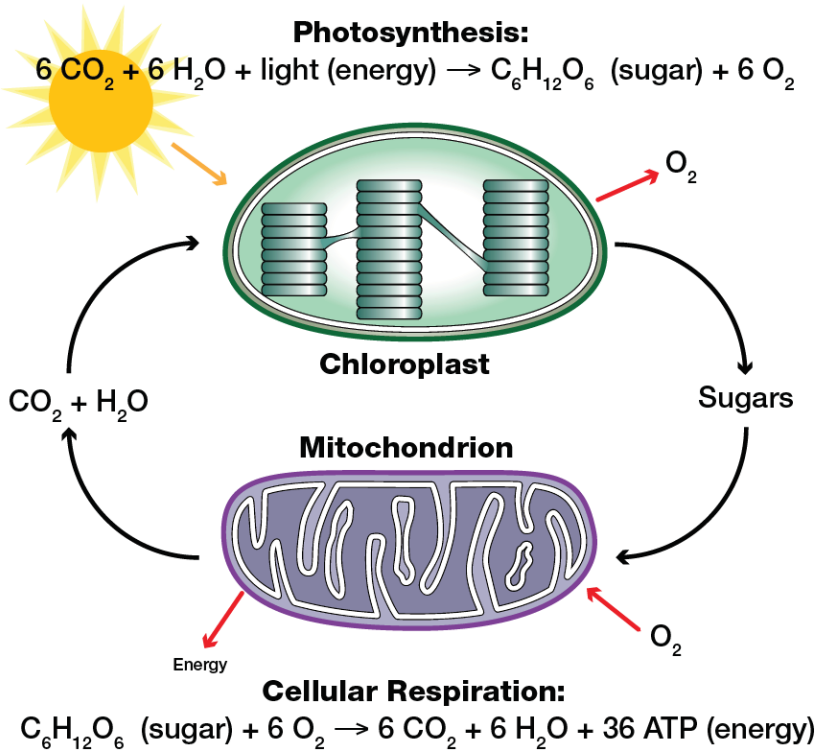

Figure 16: Relationship between photosynthesis and cellular respiration (Source: BioRad-Catalog #17001238EDU).

Autotrophs such as microalgae, carry out photosynthesis and cellular respiration within the same cell. More specifically, photosynthesis occurs within their chloroplasts and cellular respiration within their mitochondria.

Photosynthesis in the chloroplast

Photosynthesis occurs through two coordinated reactions: The Hill reaction (light-dependent reaction, first discovered by Robert Hill in 1937) in which the light energy is captured and converted into chemical energy and water (H_2O) fragmented to liberate oxygen (O_2) and the Calvin cycle (light-independent reaction) in which CO_2 is converted into sugar through the use of ATP and NADPH, produced in the Hill reaction.

The algae's chloroplast is composed of stacked and folded inner membranes, also known as thylakoids (the overall stacks are named grana). They contain the pigments (chlorophylls and carotenoids) and enzymes that are necessary to the Hill reaction. The spaces between grana are known as stroma and are where the carbon fixation reactions occur. The chloroplast is composed of three membranes (inner and outer membranes of the envelope and thylakoid membrane; different from the mitochondrion that only has two membranes), therefore forming three compartments (Figure 17).

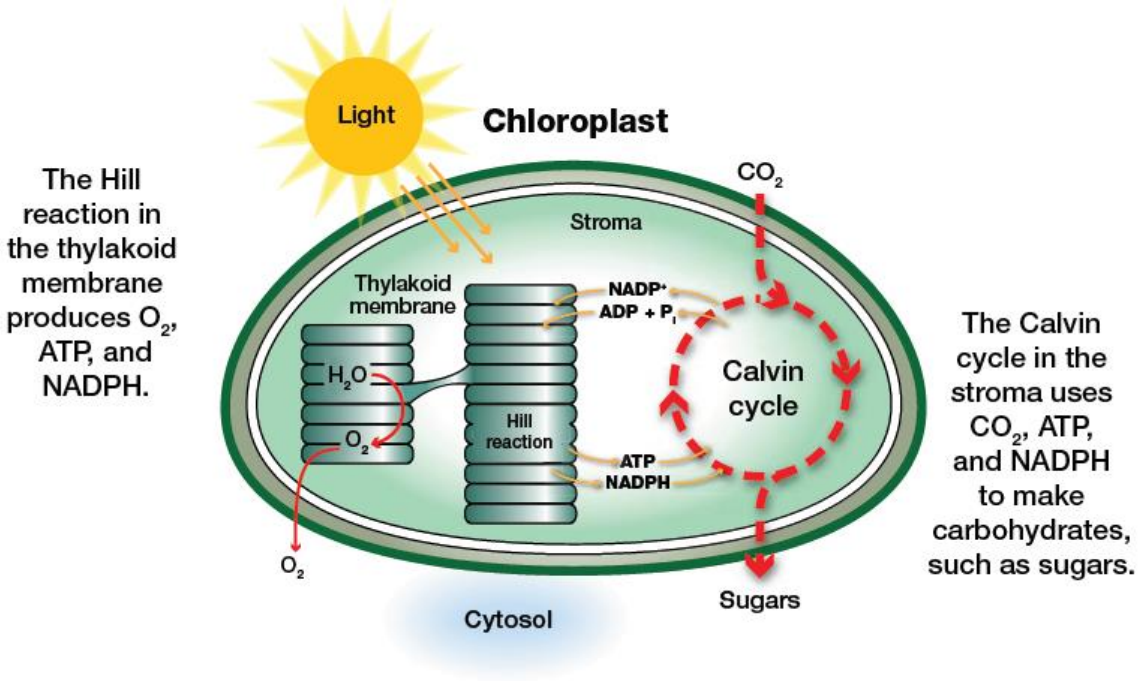

Figure 17: Schematic representation of a chloroplast showing the two key reactions involved during photosynthesis (Source: BioRad-Catalog #17001238EDU)

The Hill reaction when discovered, proved that the oxygen produced during photosynthesis originates from water (H_2O) and not carbon dioxide (CO_2), as it was previously believed. It is a light-dependent process where the energy from sunlight is captured by the chlorophyll and other pigments and converted into an energy with a higher, excited energy state (photoexcitation) (Figure 18). This ionizes the chlorophyll molecule, which means that the electron leaves the molecule that consequently becomes a positively charged ion (photoionization). The net reaction is as follows:

$$2\ H_2O + 3\ ADP + 3\ P_i + 2\ NADP^+ + \text{energy (light)} \rightarrow 3\ ATP + 2\ NADPH + O_2$$

The overall system involves an electron transfer chain where electrons are transported through a series of electron transporters that undergo reduction/oxidation reactions. It ultimately releases enough energy to convert ADP and phosphate into ATP. In fact, the discovery of the Hill reaction has also demonstrated that the reduction/oxidation reaction corresponds to the first step of photosynthesis and that an electron acceptor is mandatory for the reaction to occur.

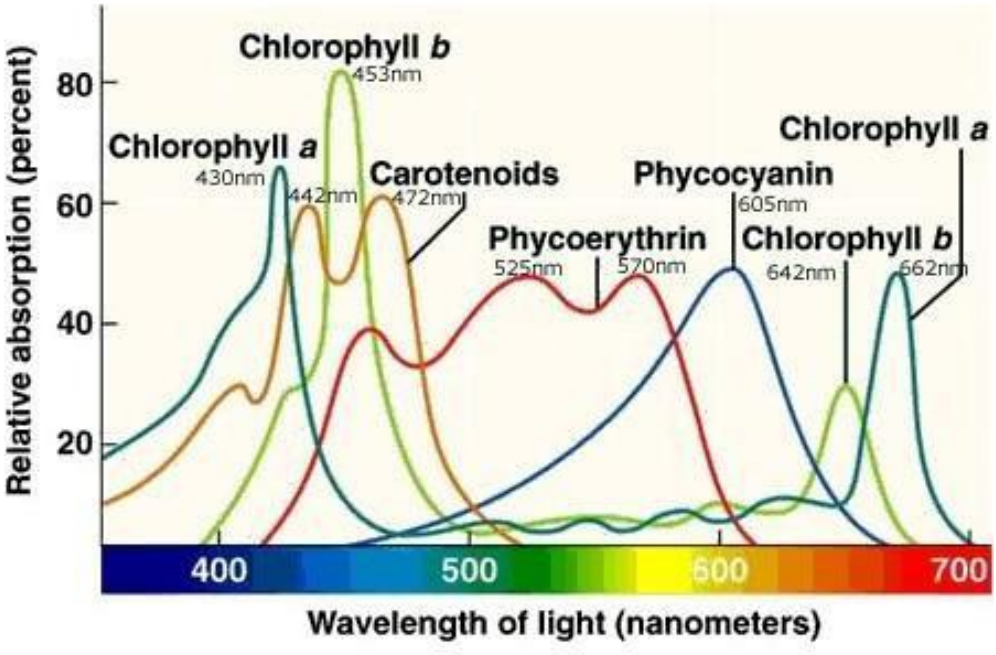

Figure 18: Light absorbance spectra of photosynthetic pigments (Source: Quora.com)

There are two large complexes (light-absorbing molecules), called photosystems, that are composed of proteins and pigments and that play a major role during the light-dependent reaction. The first one, discovered in the 1950s, is known as the Photosystem I (PSI), and the second one, discovered a few years later (1960), is named the Photosystem II (PSII).

These photosystems contain (in the reaction center) a unique pair of chlorophyll molecules that is also known as the **special pair**. PSI is also named P700 because its special pair absorbs best at 700nm and in the same way, PSII is named because it absorbs better at 680nm.

The following figure (Figure 19) shows the overall process. The different steps are as follows:

- It all starts with the **photosystem II**. Light is absorbed by the pigments (i.e. chlorophyll) that are inside the PSII. This energy is then passed from one pigment to another until it arrives to the reaction center, where it reaches the special pair (P680) and takes an electron to a higher level of energy. This electron is then captured by an electron acceptor. A water molecule also undergoes a cleavage, thus releasing the O_2 molecule and H^+ ions that are pumped towards the thylakoid lumen. The electron resulting from the water cleavage replaces the empty space left by the high-energy electron when it joined the electron acceptor.

- The electron with a high level of energy then passes through the electron transport chain, where it progressively loses its energy. Part of this released energy powers the pumping of **H^+ ions** from the chloroplast stroma to the thylakoid lumen, forming a gradient. This

leads to a flow of H^+ ions through the **ATP synthase** which produces ATP (this is also known as **chemiosmosis**).

- The electron then reaches the **photosystem I** and arrives towards the special pair of the P700. In the same way as with the PSII, light is absorbed by pigments and transferred to the reaction center. The electron reaches a high level of energy and joins the electron acceptor. This leaves a place for a new electron that comes from the PSII via the electron transport chain.

- The high-energy electron then passes through the electron transport chain where it ultimately reaches NADP+ and, with the help of a second electron (coming from the same process), converts it into **NADPH**.

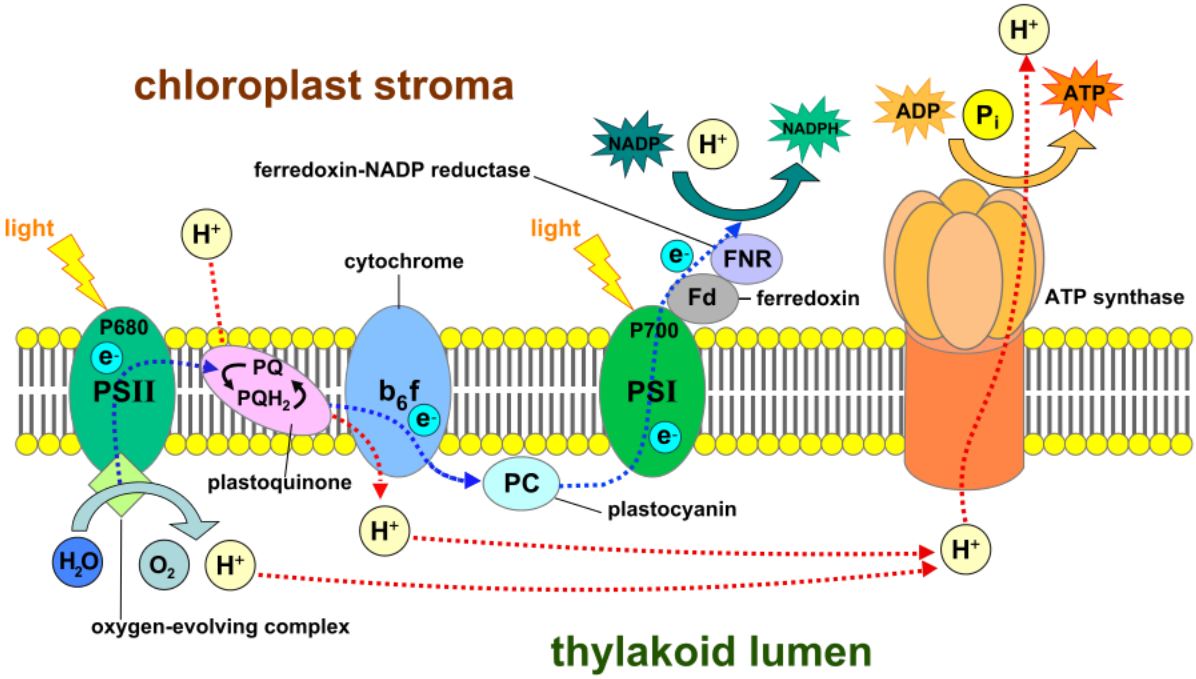

Figure 19: Light-dependent reactions of photosynthesis (Source: Wikipedia/Photosystem I)

The NADPH and ATP produced during this process are then used by the Calvin cycle to make carbohydrates such as sugar. Oxygen is also generated, which is then used for the cellular respiration.

The Calvin cycle

The Calvin cycle is a light-independent process, also known as dark reaction. The carbon-fixing reactions involved in the Calvin cycle convert CO_2 into carbohydrates by using the ATP and NADPH from the Hill reaction. The net reaction is as follows:

$$6\ CO_2 + 18\ ATP + 12\ NADPH \rightarrow C_6H_{12}O_6\ (glucose) + 12\ NADP^+ + 18\ ADP + 18\ P_i$$

The enzyme Rubisco (**R**ib**u**lose **Bis**phosphate **C**arboxylase **O**xygenase) catalyzes the CO_2 fixation step. It is the most abundant protein on Earth. It enables the fixation of a 5-carbon ribulose biphosphate (RuBP) with a CO_2. This gives an unstable molecule composed of 6 carbons. This molecule is then rapidly broken into a stable, 3-carbon chemical called phosphoglycerate (PGA) that is subsequently converted into glyceraldehyde phosphate (G3P). Finally, as a final step of the cycle, RuBP molecules are regenerated by using ATP energy. The cycle can then start again (Figure 20).

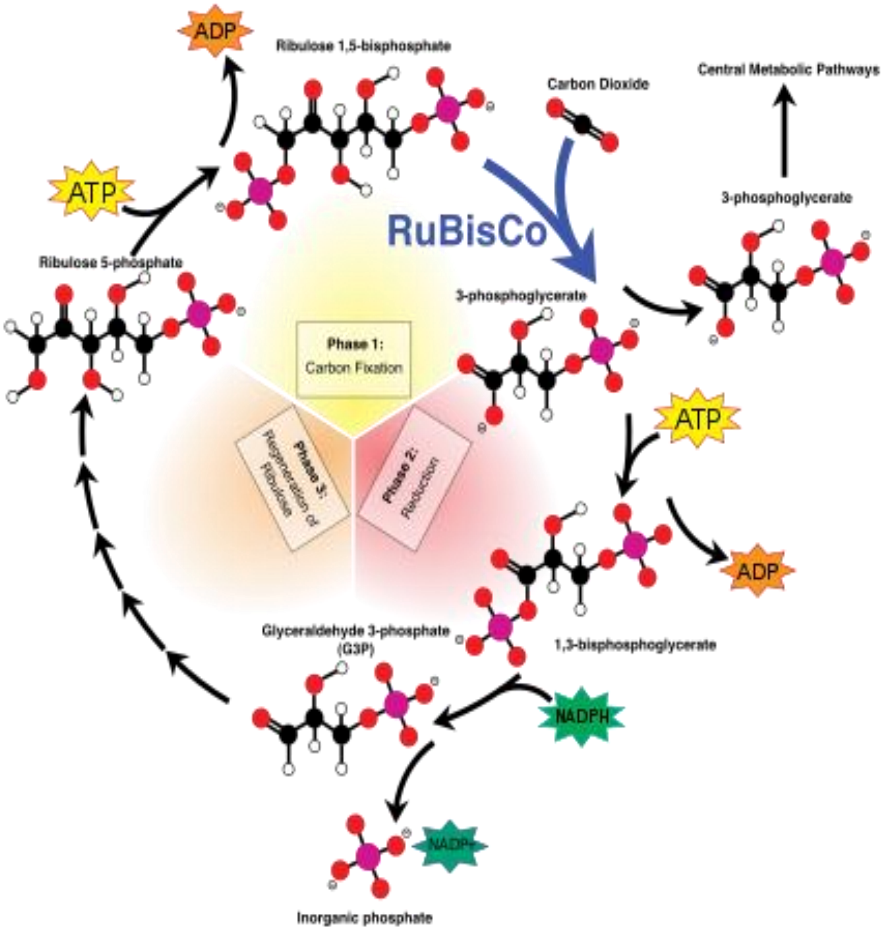

Figure 20: The Calvin cycle: light-independent reaction (Source: Wikipedia/Light-independent reactions).

Respiration in mitochondria

Glycolysis and cellular respiration could be described as the reverse processes of photosynthesis. In the same way as photosynthesis, the reactions are compartmentalized (eukaryote particularity). Cell respiration occurs within mitochondria, and involves, much like during the photosynthesis, an electron transport chain and an ATP synthase.

Glycolysis is the first step of the breakdown of glucose that generates energy as well as the molecule pyruvate which itself produces ATP after entering the citric acid cycle. It occurs within the cytosol.

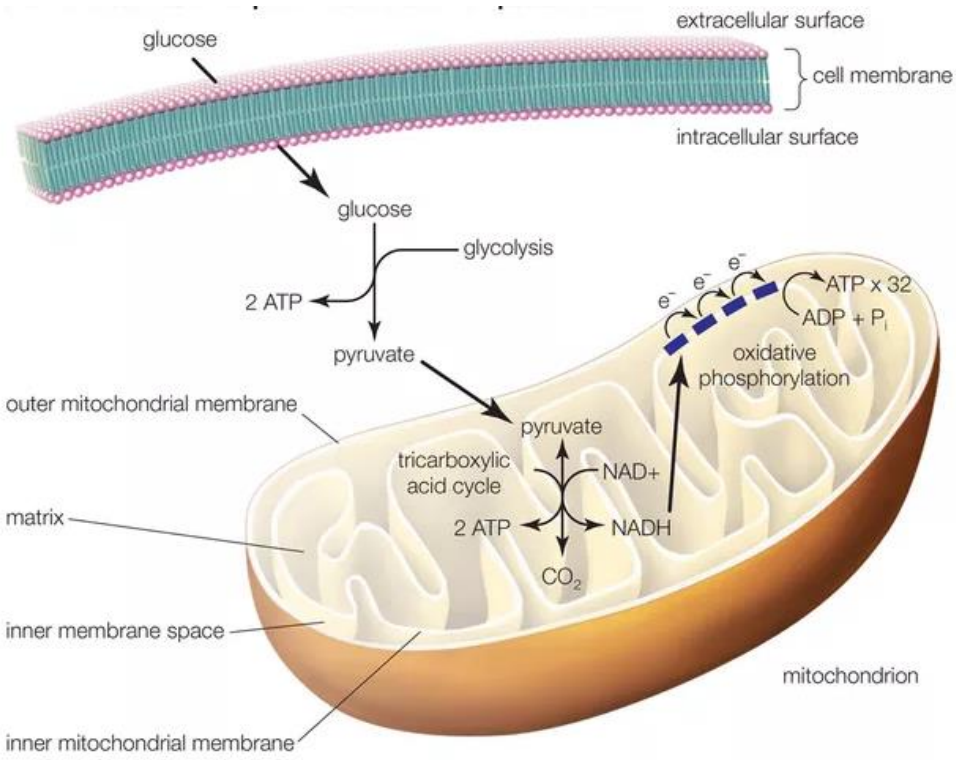

Figure 21: Overview of the cellular respiration and glycolysis (Source: Encyclopædia Britannica/UIG/Getty Images).

2.3.3 Lipid production

Microalgae potentially offer promising advantages when it comes to energy production. It is now clearly stated that their oil productivity surpasses all other crops. From a biological perspective, this promising potential is demonstrated through the high lipid yield that they are capable to offer (which is also dependent on the microalgae species). Under stress conditions, often applied by removing nitrogen from the culture medium, microalgae are capable to accumulate a significant amount of lipids, up to 70 % dry cell weight (Chisti, 2007; Hu *et al.*, 2008; Saha and Murray, 2018).

However, when under stress conditions, biomass productivity, which is as important in the context of a large-scale production, significantly decreases. Therefore, in the development and optimization of a biofuel production, a compromise must be reached between finding solutions to increase the lipid yield from the microalga and maintaining a convenient biomass productivity. This implies a thorough comprehension of the microalgae's lipid composition and biosynthesis, particularly when it is submitted to stress conditions.

C. reinhardtii is a very well-known green microalga as it has been studied for many years and was chosen as a model of study to further understand biological metabolisms (photosynthesis, starch synthesis, hydrogen production…) and develop genetic engineering models. It is therefore one of the most characterized microalgae species. Naturally, it is also a coherent

model for the study of lipid biosynthesis in microalgae cells, which is what it became recently (Figure 22).

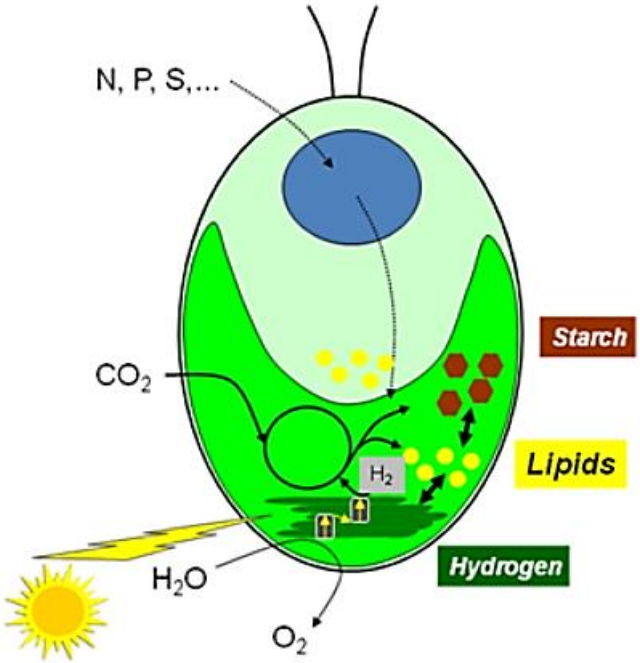

Figure 22: *Chlamydomonas reinhardtii*, a model for the study of photosynthesis, lipid and starch synthesis and H2 production (Nguyen *et al.*, 2012)

The following section describes *C. reinhardtii*'s lipids (composition and profile) and their biosynthesis. This organism was chosen as model in our study (see section 3).

Lipid composition

Compared to prokaryotes, *C. reinhardtii*'s green algae group (chlorophyceae) produces a very wide range of biological compounds (also due to their adaptability to different types of environmental conditions including the location, light, pH and temperature). Figure 23 displays the fatty acid and lipid composition of *C. reinhardtii* as well as a schematic drawing showing the location of its major lipid classes.

A

Fatty acids	Mol %
C16:0	22
C16:1 (7)	5
C16:1 (9)	Tr
C16:1 (3t)	2
C16:2 (7,10)	2
C16:3 (4,7,10)	1
C16:3 (7,10,13)	2
C16:4 (4,7,10,13)	13
C18:0	2
C18:1 (9)	13
C18:1 (11)	3
C18:2 (9,12)	8
C18:3 (5,9,12)	9
C18:3 (9,12,15)	16
C18:4 (5,9,12,15)	2

B

Lipid classes	Mol %
MGDG	40.6
DGDG	12.8
PG	7.2
SQDG	10.5
DGTS	14.9
PE	8.6
PI	5.3

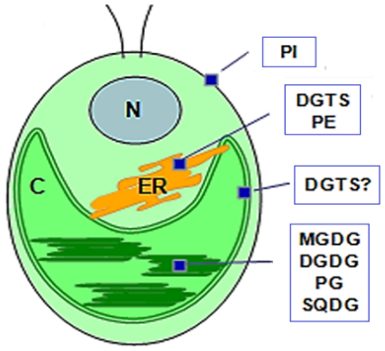

Figure 23: *Chlamydomonas reinhardtii*'s fatty acid (A) and lipid (B) composition. The fatty acids are presented through the number of carbon atoms, the number and position of the double bond (Figure modified from Nguyen et al., 2012, data was based on that of Giroud, Gerber, & Eichenberger, 1988).

Abbreviations: Tr, trace; MGDG, monogalactosyldiacylglycerol; DGDG, digalactosyldiacylglycerol; SQDG, sulfoquinovosyldiacylglycerol; PG, phosphatidylglycerol; PE, phosphatidylethanolamine; PI, phosphatidylinositol; DGTS, diacylglyceroltrimethylhomoserine

Under stress conditions, *C. reinhardtii* produces and stores triacylglycerols and free fatty acids (FFA) in the form of cytoplasmic lipid bodies (storage is often associated to a response to stress). The stress can be triggered using different methods such as high light intensity, high salinity or nutrient removal from the medium. It has been reported that the most efficient way for *C. reinhardtii* to accumulate lipids is by nitrogen deprivation. Under these conditions, it accumulates abundant cytoplasmic lipid bodies and starch granules. Some studies have also investigated on the relation between this accumulation of lipid bodies and starch, whether they are codependent and if lipid biosynthesis is enhanced when starch accumulation is absent (Wang *et al.*, 2009). They demonstrated that the starchless mutant strain cw15 sta6, was able to accumulate and double the amount of lipid bodies, compared to the mother strain cw15. However, the lipid bodies of both strains had the same composition: 90 % of TAGs, 10 % of FFAs and traces of charged glycerolipids.

C. reinhardtii's TAG biosynthesis pathway

C. reinhardtii has a unique TAG biosynthesis pathway (Wang *et al.*, 2009) that involves however three distinct steps that are common to plant and algae: *de novo* fatty acid biosynthesis, triacylglycerol biosynthesis (or Kennedy pathway) and the mobilization of triacylglycerol.

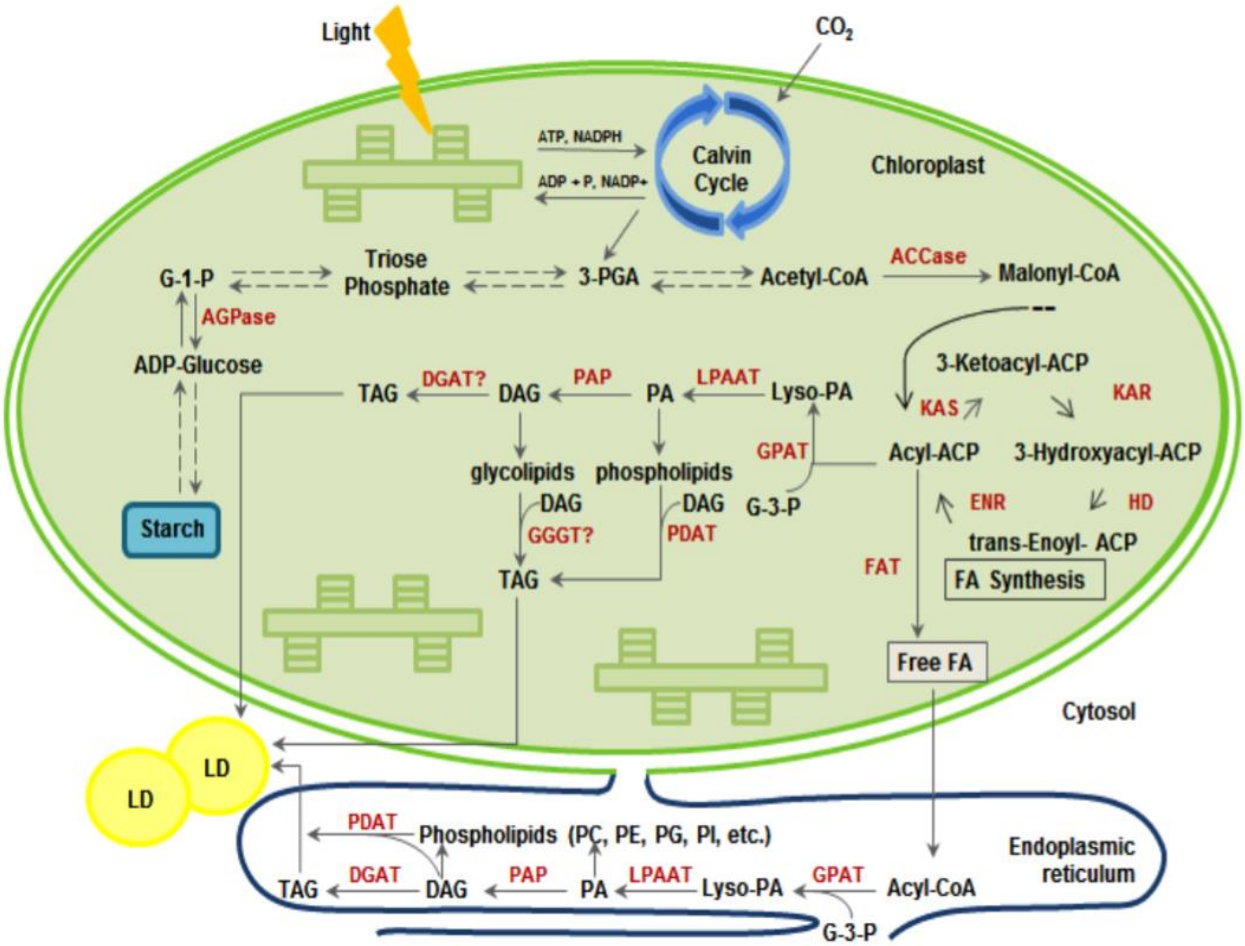

Figure 24: Overview of the microalgae's *de novo* fatty acid and TAG biosynthesis.

Abbreviations: PC, phosphatidylchloline; PE: phosphatidylethanolamine; PG: phosphatidylglycerol; PI: phosphatidylinositol; LD: lipid droplets, ENR, enoyl-ACP reductase; FAT, fatty acyl-ACP thioesterase; HD, 3-hydroxyacylACP dehydratase; KAR, 3-ketoacyl-ACP reductase. Question marks indicate enzymes or reactions that are not established to exist in the chloroplast of microalgae (Lenka *et al.*, 2016).

The *de novo* fatty acid synthesis occurs in the chloroplasts. The sugar produced by microalgae during photosynthesis can be processed to produce acetyl-CoA (acetyl coenzyme A). This molecule can be involved in various pathways (Calvin cycle, starch, steroid and acetylcholine biosynthesis…). It plays a role of precursor for the fatty acid biosynthesis. These fatty acids are important structural components for many types of cellular lipids including TAGs.

The ***de novo* fatty acid synthesis** starts with the production of malonyl-CoA from acetyl-CoA and bicarbonate (that serves as the source of CO_2). The enzyme acetyl CoA carboxylase (ACCase) catalyzes this carboxylation of acetyl-CoA, which is irreversible. The malonyl-CoA:acyl carrier protein malonyltransferase then transfers the malonyl group to the acyl carrier

protein, named 3-ketoacyl ACP (or KAS enzyme). The fatty acid chains undergo a chain elongation (catalyzed by the fatty acid synthase) before they enter the TAG biosynthesis in the chloroplast (in the form of acyl-ACP chains). For each cycle of elongation, a consecutive addition of two carbon units is held to form 16:0 fatty acids, which are then elongated again to form 18:0 fatty acids (Most 18:0 fatty acids are then desaturated by the stearoyl-ACP desaturase to form 18:1 fatty acids). For most algae species, the resulting fatty acyl chains are 16 or 18 carbon long.

Photosynthesis, other than providing a carbon source, plays a major role in the fatty acid synthesis. Indeed, stoichiometric amount of ATP, acetyl-CoA and NADPH are essential for the addition of each two carbons to the growing acyl chain. The required energy ATP and reducing power (NADH and NADPH) are provided by photosynthesis (Fan, Andre and Xu, 2011; Nguyen *et al.*, 2012; Farine *et al.*, 2015; Lenka *et al.*, 2016).

The **biosynthesis of triacylglycerols** in the endoplasmic reticulum (ER) is generally described as follows: a group of enzymes, known as acyltransferases, catalyze the sequential acylation of G3P (sn-glycerol-3-phosphate) backbone with three acyl-CoAs. This pathway, named the Kennedy pathway (described in the 1950s by Professor Eugene Kennedy and his colleagues) has however since been reviewed through various studies (Bates *et al.*, 2009; Li-beisson *et al.*, 2010; Tjellstrom *et al.*, 2012). Indeed, there exists several alternative metabolic pathways for TAG synthesis that vary for example with tissue or species (Bates *et al.*, 2009).

In the case of *C. reinhardtii*, the biosynthesis of TAGs in the ER (and ultimately the lipid droplets) can be described through the following steps:

- The acylation of the *sn*-1 position of G3P by an *sn*-glycerol-3-phosphate acyltransferase (GPAT). This produces lysophosphatidic acid (Lyso-PA).

- Lyso-PA is then acylated by the lysophosphatidic acid acyltransferase (LPAAT) which forms phosphatidic acid (PA).

- The enzyme phosphatidic acid phosphatase (PAP) then further catalyzes the removal of the phosphate group from phosphatidic acid to produce *sn*-1,2-diacylglycerol (DAG). DAG is the central intermediate in the synthesis and turn-over of all major glycerolipids.

- Finally, the last step is catalyzed by diacylglycerol acyltransferase (DGAT).

These reactions are acyl-CoA dependent since all three acyltransferases use acyl-CoA as the acyl donor.

There is also an alternative pathway to the lipid droplet synthesis (commonly found in plants and yeast) where phospholipid:diacylglycerol acyltransferase (PDAT) catalyzes the reaction between phosphatidylcholine (as an acyl donor) and sn-1,2-diacylglycerol (as an acyl acceptor) to synthesize triacylglycerol.

C. reinhardtii shows several particularities in its lipid composition compared to land plants. For example, land plants and *Chlamydomonas* have some common membrane lipids such as phosphatidylglycerol (PG) or phosphatidylethanolamine (PE). However, *Chlamydomonas* doesn't have phosphatidylcholine (PC), the major cytoplasmic lipid of land plants. Instead, it shows a large amount of a betaine lipid named diacylglyceroltrimethylhomoserine (DGTS) that structurally resembles PC (Li-beisson *et al.*, 2010; Nguyen *et al.*, 2012).

Furthermore, a recent study of *C. reinhardtii* (Fan, Andre and Xu, 2011), has demonstrated the particularity of its TAG biosynthesis. In the conventional pathway, TAG is finalized in the ER using DAG and the different ER-specific acyltransferases before being deposited exclusively in lipid droplets, dispersed in the cytosol. In the study, the authors demonstrated that *C. reinhardtii* uses a different unique pathway. It produces TAG by using DAG derived almost exclusively from the chloroplast. This unique pathway is highly dependent on the *de novo* fatty acid synthesis. Moreover, the synthesized TAG in this pathway is then stored in lipid droplets in both the chloroplast and the cytosol (Figure 25).

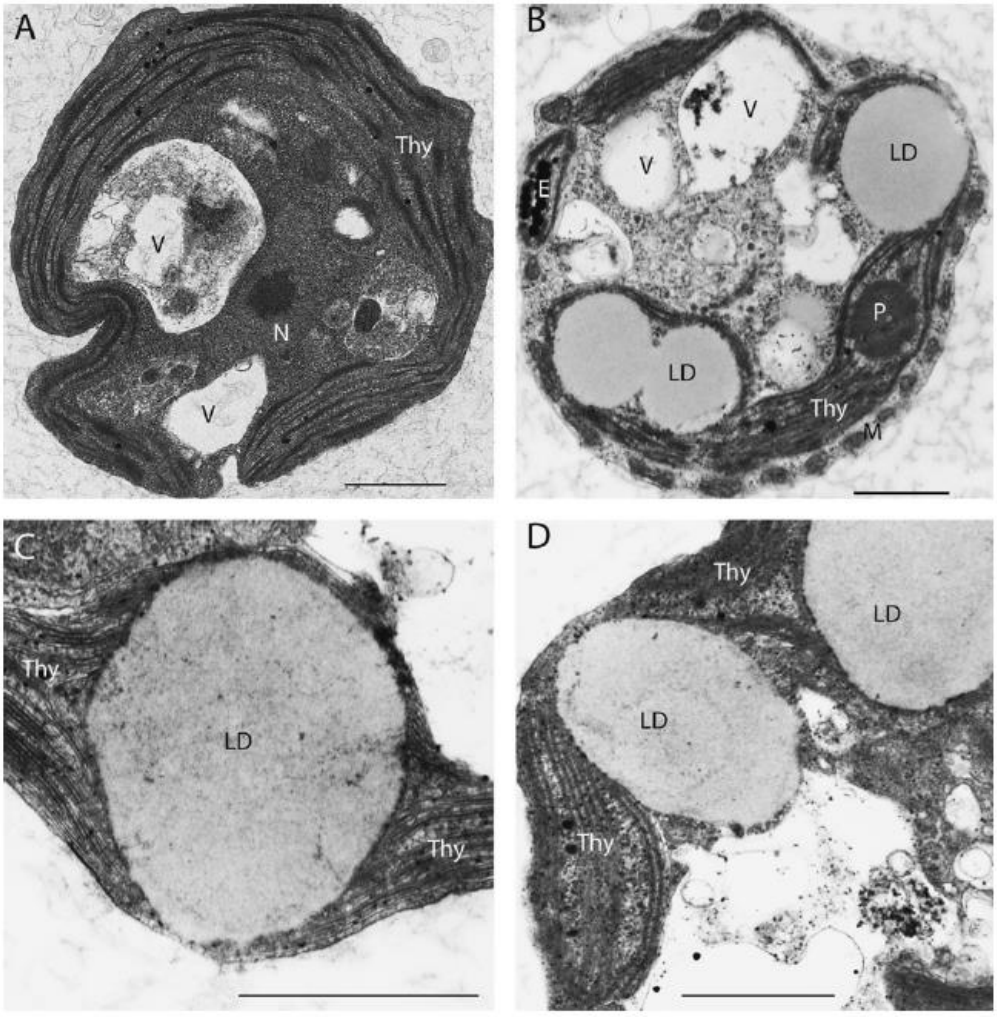

Figure 25: Representative electron micrographs showing lipid droplets present in the chloroplast and the cytosol of the starchless mutant BAJF5. (A), cells grown in complete medium; (B-D), stressed cells (medium lacking N for 2 days). Scale bars: 2 µm.

Abbreviations: E, eyespot; LD, lipid droplets; M, mitochondria; N, nucleus; P, pyrenoid; Thy, thylakoid membranes; V, vacuoles (Fan, Andre and Xu, 2011).

When the TAGs are formed in the ER, the following step is their **mobilization** towards the cytoplasm. After a certain amount of TAGs produced, they are mobilized in lipids droplets (or oleisin, or oil bodies) that bud off from the ER. These lipids droplets are then distinct cellular organelles (Figure 26). Being highly hydrophobic, their dispersion in the cytoplasm is possible by the fact that they are surrounded by a single-layer membrane that is composed of phospholipids (their hydrophilic heads assemble on the surface).

These lipid droplets are also composed of proteins. Major lipid droplet protein (MLDP), a structural protein, was found in the lipid droplets of *Chlamydomonas reinhardtii* as well as *Haematococcus pluvialis* and *Dunaliella*. Other than structural proteins, there also exists lipid metabolic enzymes and numerous lipid-trafficking proteins in the oil bodies of *Chlamydomonas* (Moellering and Benning, 2010; Siaut *et al.*, 2011; Nguyen *et al.*, 2012).

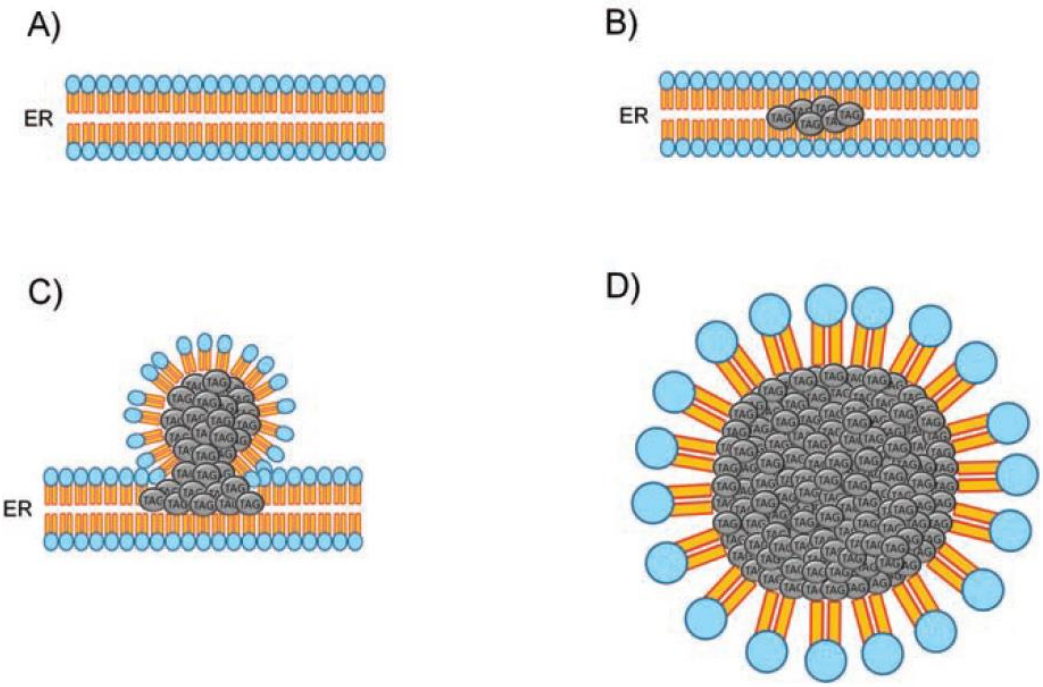

Figure 26: Representation of the progressive formation (A to D) of a lipid droplet in plants and algae (Cagliari *et al.*, 2011).

Algal oils are mostly composed of various TAGs with fatty acid chains, 16 or 18 carbons long, chemically like the hydrocarbons found in typical diesel fuel (10 to 15 carbons long). However, algal and plant oil is usually more viscous than conventional diesel, which is why it requires an additional step before being used as a biodiesel: the transesterification process. The transesterification of triacylglycerols produces, in the presence of methanol, fatty acid methyl esters (FAME), which are the primary molecules composing biodiesel.

Other than the fatty acid chain length, the number of double bonds must also be considered to produce a good quality biodiesel. Indeed, the presence of a high proportion of saturated fatty

acids gives a biodiesel in the form of a gel, while a dominant presence of unsaturated fatty acids gives a biodiesel that is prone to oxidation (Nguyen *et al.*, 2012).

Figure 27 displays a diagram, used to evaluate the quality of the biodiesel according to the European Standard UNE-EN 14214 (Ramos *et al.*, 2009). The biodiesels are represented through their composition in monounsaturated, polyunsaturated and saturated methyl esters. In these standards, the following parameters are taken into consideration: cetane number (indicates the combustion speed and compression needed for ignition), iodine value (gives the measure of the relative degree of unsaturation, number of double bonds in the sample) and cold filter plugging point (CCFP, used to estimate the lowest temperature at which a fuel will freely flow through filters in the fuel system).

The yellow area on the graph corresponds to biodiesels with a good cetane number and iodine value. The blue area corresponds to biodiesels with a good CFPP. Finally, the green area corresponds to biodiesels that satisfy the European Standard UNE-EN 14214; in this area we find as good candidates olive, almond, corn, HOS (high oleic sunflower) and rape.

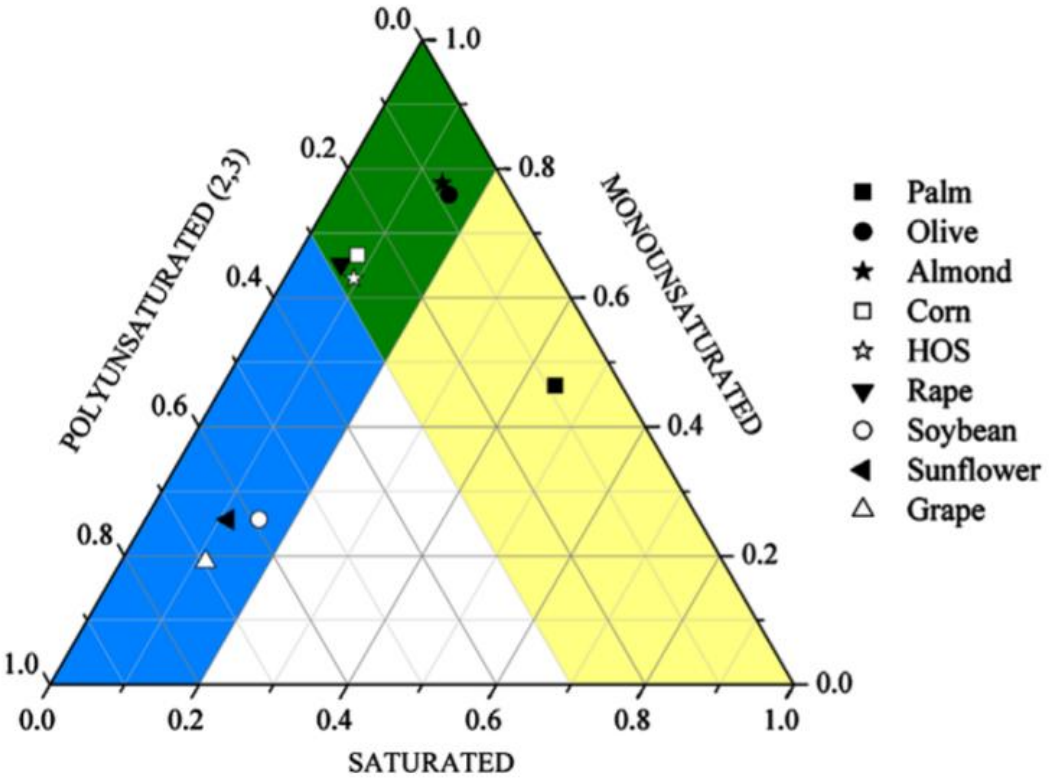

Figure 27 : Triangular graph showing biodiesels by their composition in monounsaturated, polyunsaturated and saturated methyl esters (Ramos et al., 2009; UNE-EN 14 214).

Recently, several studies have focused on the production of oils containing shorter fatty acid chains with fewer double bonds, for example, through genetic engineering. A recent study has demonstrated that it was possible to produce medium-chain fatty acids from the eukaryotic microalga *Phaeodactylum tricornutum* by overexpressing thioesterases (Radakovits, Eduafo and Posewitz, 2011).

Furthermore, using genetic engineering, other studies have focused on the improvement of the lipid yield (Miller *et al.*, 2010). A recent study on *C. reinhardtii* has succeeded in increasing its lipid yield by approximately 50 %. This was obtained by overexpressing novel proteins that triggers the lipid production in *C. reinhardtii* (Yohn et al., 2011; Fang, 2013). Another study has demonstrated an increase in the lipid content of the starchless mutant of *C. reinhardtii* (CC-4325) under salt stress conditions (Hounslow *et al.*, 2016).

3. The microalga *Chlamydomonas reinhardtii* as our study model

3.1 The species Chlamydomonas reinhardtii

In our study, *Chlamydomonas reinhardtii* was chosen as the model microalga. This unicellular green microalga has her own history that started about a century ago. The genus *Chlamydomonas* (Origins: Greek *chlamys*, a cloak; *monas*, solitary) was first described by its morphology before being investigated as a model for genetic studies. Since the early 20th century, many studies were published, demonstrating the possibility to isolate mutant strains from this alga that could be characterized and studied in laboratories. In the mid-20th century, *Chlamydomonas* species, especially *C. reinhardtii* and *C. eugametos*, started to be highly developed for laboratory research. This microorganism has since become part of the premier models for a diverse range of research areas such as cell and molecular biology.

The main and common components of *Chlamydomonas* species are: two anterior flagella of equal length, a basal chloroplast containing one or more pyrenoids and a cell wall (Figure 28).

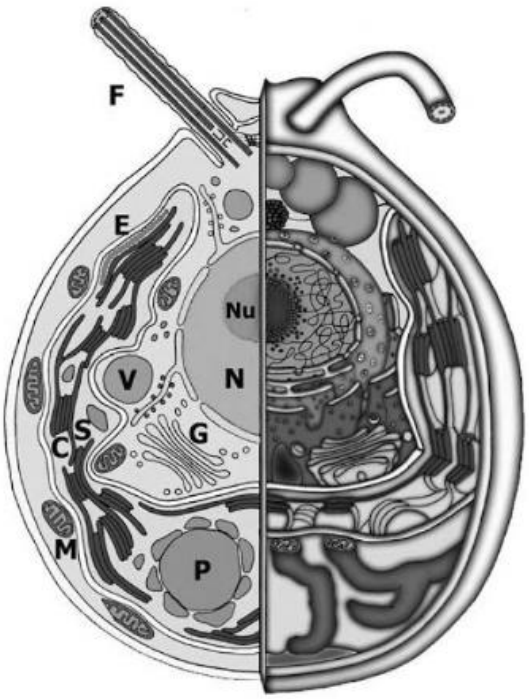

Figure 28: *Chlamydomonas reinhardtii*'s cell structure.

Abbreviations: N, central nucleus; Nu, the nucleolus; F, the two isoform flagella; C, the cup-shaped chloroplast; E, the eyespot; P, the starch-containing pyrenoid; M, the mitochondria; G, the Golgi; S, starch grains; V, vacuoles (Harris, Stern and Witman, 1960).

Chlamydomonas species (about 500 recognized species) have been differeniated by their body shape and size, number and position of the contractile vacuoles, shape and position of the chloroplast and pyrenoids, as well as the length of the flagella.

3.2 Cell architecture

3.2.1 General components

The major components of *Chlamydomonas reinhardtii* are its cell wall, nucleus, mitochondria, chloroplasts, vacuoles, pyrenoids, flagella, basal bodies and eyespot (Figure 29).

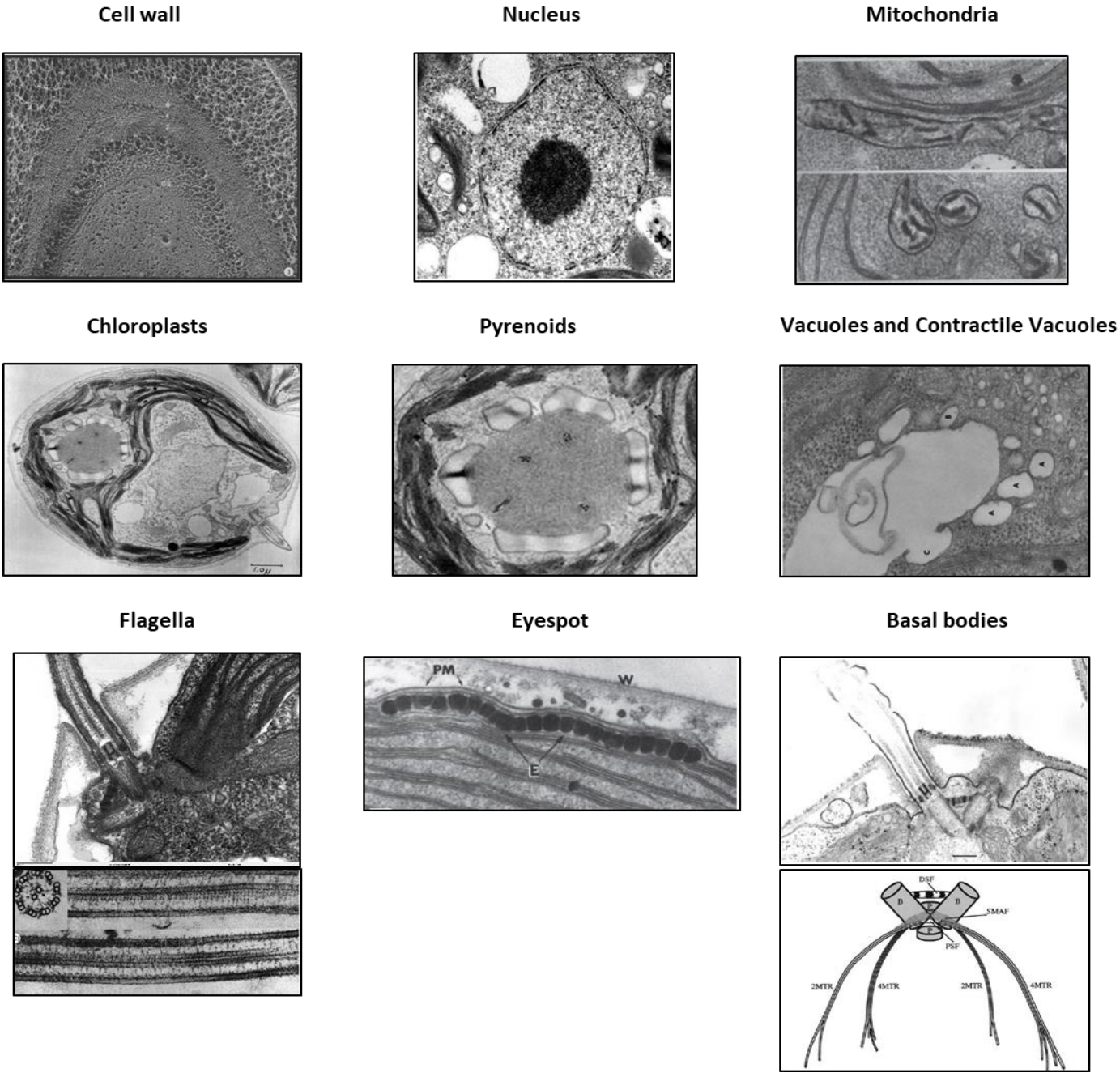

Figure 29: General components of *Chlamydomonas reinhardtii* (modified from Harris, Stern and Witman, 2009).

C. reinhardtii's average diameter is around 5 µm and it is surrounded and protected by a non-cellulosic, **7-layered cell wall** that is primarily composed of hydroxyproline-rich glycoproteins. Like all green algae, *C. reinhardtii*'s cell is composed of eukaryotic cell components such as the **nucleus** and several **mitochondria** for the energy production (photosynthesis). The nucleus is generally located in an anterior position. The double nuclear membrane is continuous with the endoplasmic reticulum, and one to four Golgi bodies are usually visible near the nucleus.

The nucleus membrane pores are generally concentrated primarily on the posterior side of the nucleus (Colon-Ramos *et al.*, 2003).

Also, *C. reinhardtii* contains a **single large cup-shaped chloroplast** that settles in all parts of the cell, between other cell components. The chloroplast contains a single round or oval **pyrenoid** (for most *Chlamydomonas* species, it is situated in the posterior half part of the cell) that is easily visible under light microscopy. The pyrenoid among algae in general, is associated to the carbon-concentrating mechanism (CCM) (Harris, Stern and Witman, 2009). The pyrenoid's granular region appears to contain mostly ribulose-1,5-bisphosphate carboxylase/oxygenase (RuBisCo) and Rubisco activase (He *et al.*, 2003; Harris, Stern and Witman, 2009). It appears to play a major role in maintaining a CO_2-rich environment around the rubisco.

In addition, *C. reinhardtii* has an **eyespot** (photoreceptive organelle) that is associated with the chloroplast and allows light detection. When it senses light direction and intensity, the cell responds by swimming towards it or away from it (this is known as positive or negative phototaxis); it has been reported that *C. reinhardtii* shows both positive and negative phototaxis (Bennett and Golestanian, 2014). The cell also contains contractile vacuoles that help prevent plasma membrane lysis and maintain the osmotic balance. *C. reinhardtii* also contains **two flagella** for motility (swims in a forward direction). This particularity isn't common to all green algae; some aren't motile such as *Chlorella*, *Desmids* and *Acetabularia*. Furthermore, base of each flagellum is formed by a **basal body** containing a cylinder of nine triplet microtubules (Dutcher and O'Toole, 2016; Wingfield and Lechtreck, 2018).

Figure 30 shows the cell and component volumes of *C. reinhardtii*'s according to two cells analyzed through electron microscopy in serial sections.

	Cell#1		Cell#2	
Cell component	**Volume (μm^3)**	**% of cell volume**	**Volume (μm^3)**	**% of cell volume**
Whole cell, including cell wall	56.08		80.38	
Cell inside the plasma membrane	44.08	100.00	59.07	100.00
Nucleus	4.42	10.04	4.33	7.31
Chloroplast	17.41	39.46	5.17	42.66
Total mitochondria (individual mitochondria 0.1–0.5 μm^3)	1.36	3.09	2.01	3.39
Total Golgi (two dictyosomes in each cell)	0.40	0.90	0.31	0.51
Total vacuoles (individual vacuoles 0.01–1.5 μm^3)	2.85	6.46	5.38	9.14
Total lipid bodies (individual bodies 0.01–0.08 μm^3)	0.09	0.22	0.28	0.47
Total cytoplasm (including small vesicles as well as endoplasmic reticulum)	17.55	39.83	21.59	36.52

Figure 30: Volumes of *Chlamydomonas reinhardtii*'s cell and components analyzed by electron microscopy on two cells (Harris, Stern and Witman, 2009).

Results show that the chloroplast alone occupies a major part of the total cell volume and lipid bodies represent less than 1 % (cells in growth conditions).

3.2.2 Cell membrane

All organisms such as plants and algae have cells with a cell membrane which separates the intracellular medium from the extracellular medium (Figure 31).

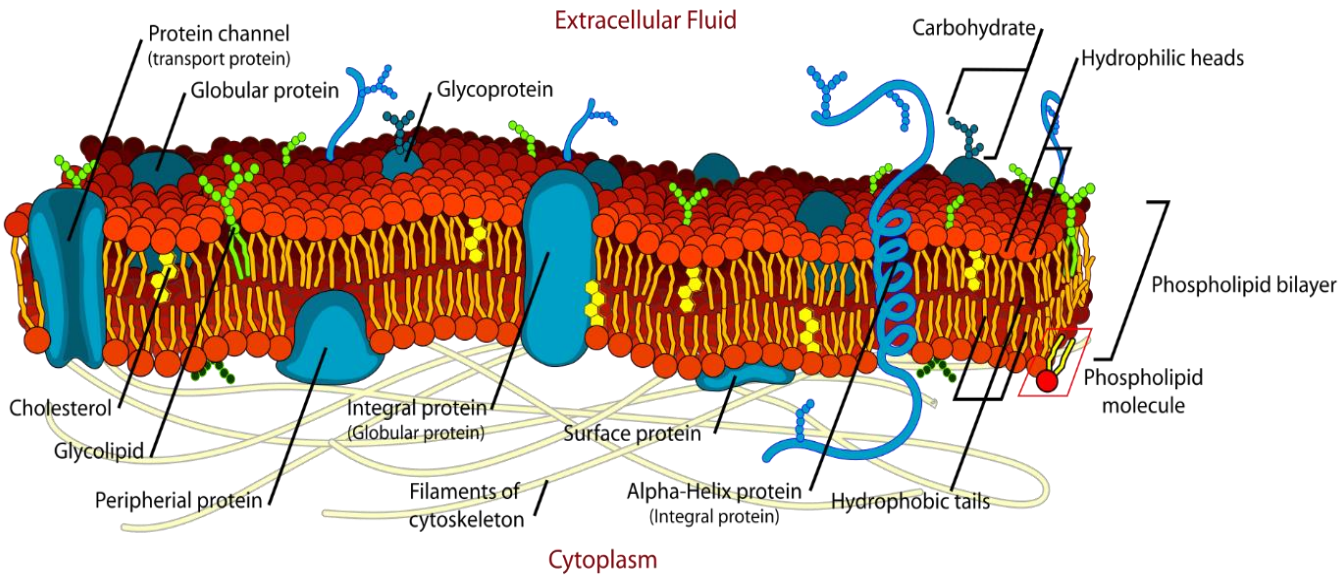

Figure 31: Diagram of the cell membrane (Mariana Ruiz, Wikimedia Commons).

The cell membrane is composed of a phospholipid bilayer with proteins embedded in it. These proteins have various functions such as enzymatic activity (for the catalyzation of the reactions) or transport activity (transmembrane proteins act as channels that permit the transport of various molecules in and out of the cell).

The phospholipids have a non-polar hydrophobic (repulsed by water) end and a polar hydrophilic (attracted to water) end. The hydrophobic ends of the phospholipids face each other, and the hydrophilic heads face the outside or inside of the cell. They are therefore in contact with the fluids of the extracellular and intracellular media.

Finally, a complex network of filaments known as the cytoskeleton is linked to the cell membrane. It serves as support for the plasma membrane, gives the cell an overall shape, assists in the correct positioning of organelles and provides tracks for the transport of vesicles. Like all eukaryotes, it is composed of three types of protein fibers: microfilaments, intermediate filaments, and microtubules.

3.2.3 Cell wall

C. reinhardtii is surrounded and protected by an extracellular coat composed of hydroxyproline-rich glycoproteins; a cell wall of 7 layers named W1 to W7 (Goodenough and Heuser, 1985) (Figure 32):

- **W1**: this layer varies from one cell to another. It extends from the cell membrane and it is composed of fibers (with various calibers) that are associated to various, relatively large granules (most of them with a diameter of 15-20 nm). The fibers make side-to-side anastomoses with one another, which creates a three-dimensional trabeculum.
- **W2**: also composed of a network of anastomosing fibers. It appears however much "tighter" than the W1 layer below it.
- **W3 and W5**: they consist of granules that are thin strands. They are electron-transparent layers (Roberts, Phillips and Hills, 1974) therefore hardly visible under electron microscopy.
- **W4**: this layer is primarily composed of large granules (with a diameter around 14 nm); they line up, which forms the layer.
- **W6**: this layer seems to be composed of two discrete sublayers which differ by their linkage. One is very densely woven (formed from stout parallel fibers, interconnected by cross-fibrils. In contrast, the other one is an open weave, creating a polygonal lattice.

- **W7**: this outer layer has fibers similar to W1 that make side-to-side anastomoses, forming a trabeculum.

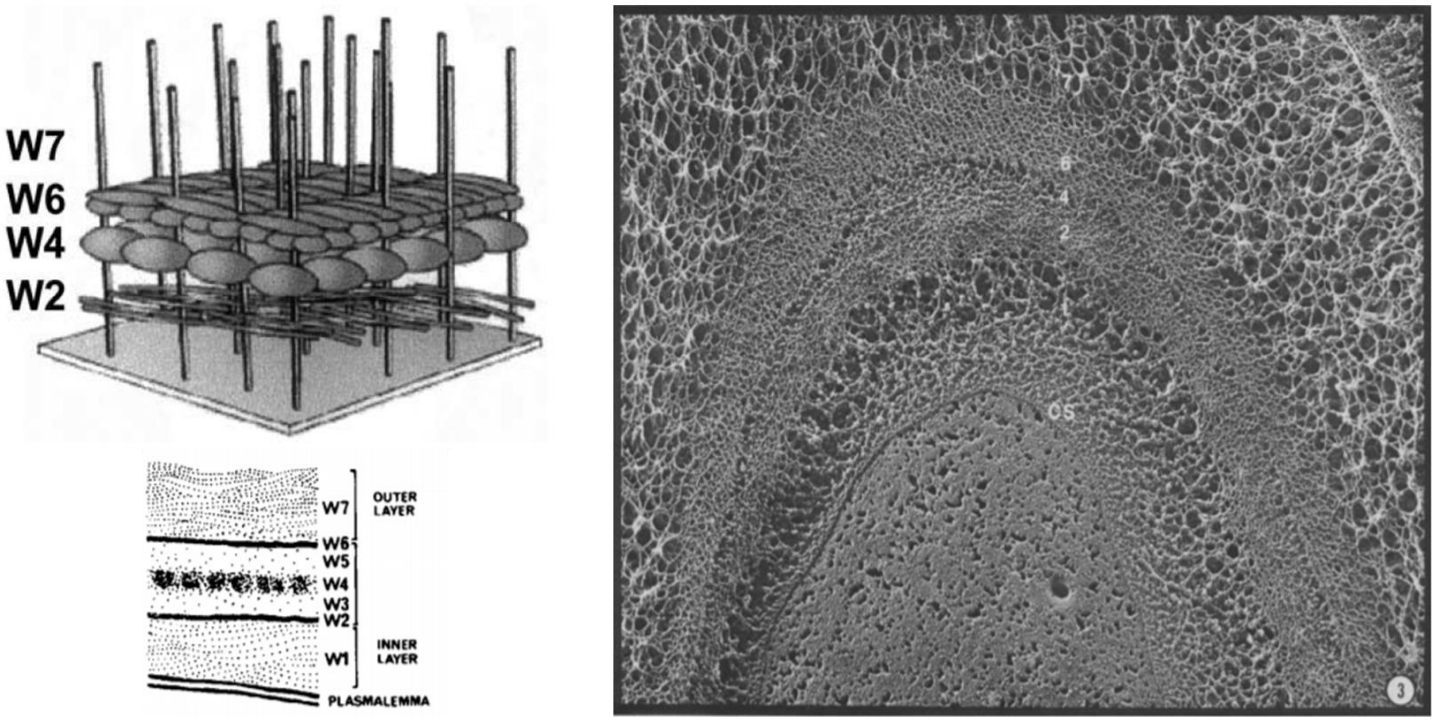

Figure 32: Cell wall of *Chlamydomonas reinhardtii*. The left side of the figure shows a diagram of the cell wall and the right side the cell wall of wild-type *C. reinhardtii* gamete after being treated with detergent and after tangential fracture of quick-freeze, deep etch (Harris et al., 2009-The Chlamydomonas sourcebook, second edition, Chapter 2; Goodenough and Heuser, 1985).

3.3 General culture conditions

Cell composition during growth conditions

When *C. reinhardtii* is under growth conditions, it has been reported that the distribution of its major compounds (in % of its dry cell weight) is typically as follows: 52 % of carbohydrates, 27 % of proteins, 19 % of lipids and 2 % of chlorophyll.

The 19 % of total lipid content include polar and neutral lipids. As we can see on Figure 33, the proportion of TAGs in these conditions represents only 1 %. The lipid content is primarily composed of monogalactosyldiacylglycerols (MGDG) representing 40 % of the total amount.

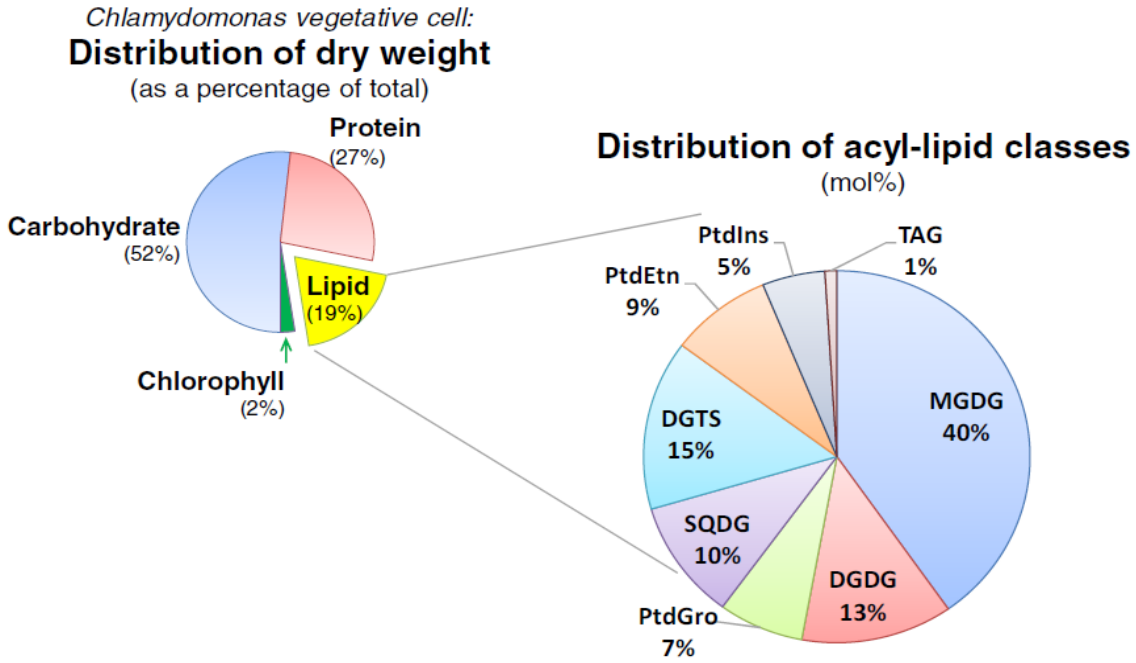

Figure 33: Distribution of acyl-lipid classes in *Chlamydomonas reinhardtii* under growth conditions (Li-Beisson, Beisson and Riekhof, 2015).

Abbreviations: MGDG: monogalactosyldiacylglycerol; DGDG: digalactosyldiacylglycerol; DGTS: diacylglycerol-N,N,N-trimethylhomoserine; SQDG: sulfoquinovosyldiacylglycerol; PtdGro: phosphatidylglycerol; PtdEtn: phosphatidylethanolamine; PtdIns: phosphatidylinositol; TAG: triacylglycerol.

Of course, depending on the culture medium and the cultivation technique used for their growth phase, the biochemical composition will vary.

Biochemical composition under stress conditions

In the same way as for growth conditions, the biochemical composition of *Chlamydomonas reinhardtii* will vary depending on the strategy employed to induce stress conditions (such as salinity, nitrogen or phosphorous depletion). Figure 34 shows the biochemical composition of

Chlamydomonas sp. JSC4 cells cultivated on modified Bold 3 N medium and stressed by depriving the culture medium of nitrogen for three days (Ho *et al.*, 2014).

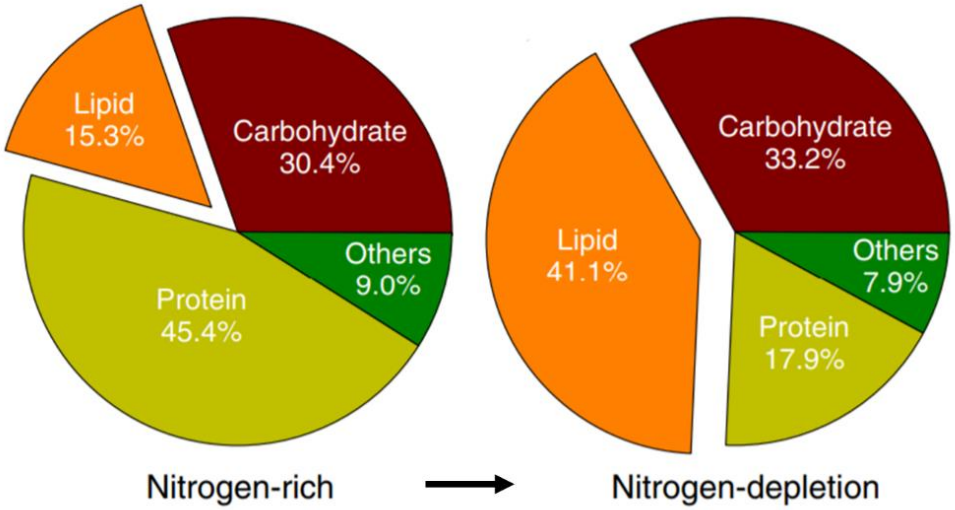

Figure 34: Biochemical composition of *Chlamydomonas* sp. under growth and nitrogen stress conditions (figure modified from Ho *et al.*, 2014).

4. Microalgae production systems (upstream and downstream processes)

4.1 Microalgae culturing

Microalgae culturing systems have been investigated for many years now. In the context of microalgae production at large scale, optimal culture conditions must be identified and maintained. Parameters such as temperature, light (intensity, quality and frequency), nutrient and salt concentrations, pH and mixing are among the factors that affect greatly microalgae growth, biomass and metabolites productivities.

4.1.1 Environmental factors

Temperature

Temperature influences microalgae growth rates and metabolism. CO_2 fixation by photosynthesis is strongly affected by temperature. Indeed, the activity of the enzyme ribulose-1,5-bisphosphate (Rubisco) increases with temperature up to a certain limit where it starts to decline. Low temperatures also impact the cell's carbon assimilation activity by reducing it while high temperatures can lead to the inactivation of photosynthetic proteins, alter the energy balance in the cell, reduce cell size and respiration (Ras, Steyer and Bernard, 2013).

For most species, the optimal temperature ranges from 20 °C to 30 °C (they are categorized as mesophiles, micro-organisms capable to grow at a temperature range of 15 °C – 50 °C). Some species, categorized as thermophilic strains are however capable to grow under high temperatures, above 45 °C (i.e. *Anacystis nidulans* and *Chaetoceros*) (Zeldes *et al.*, 2015). Some species, also named hyperthermophiles can grow with temperatures above 80 °C. Others, known as psychrophiles can grow optimally under temperatures lower than 15 °C (snow or ice algae like *Chlamydomonas nivalis* can grow at 1 °C).

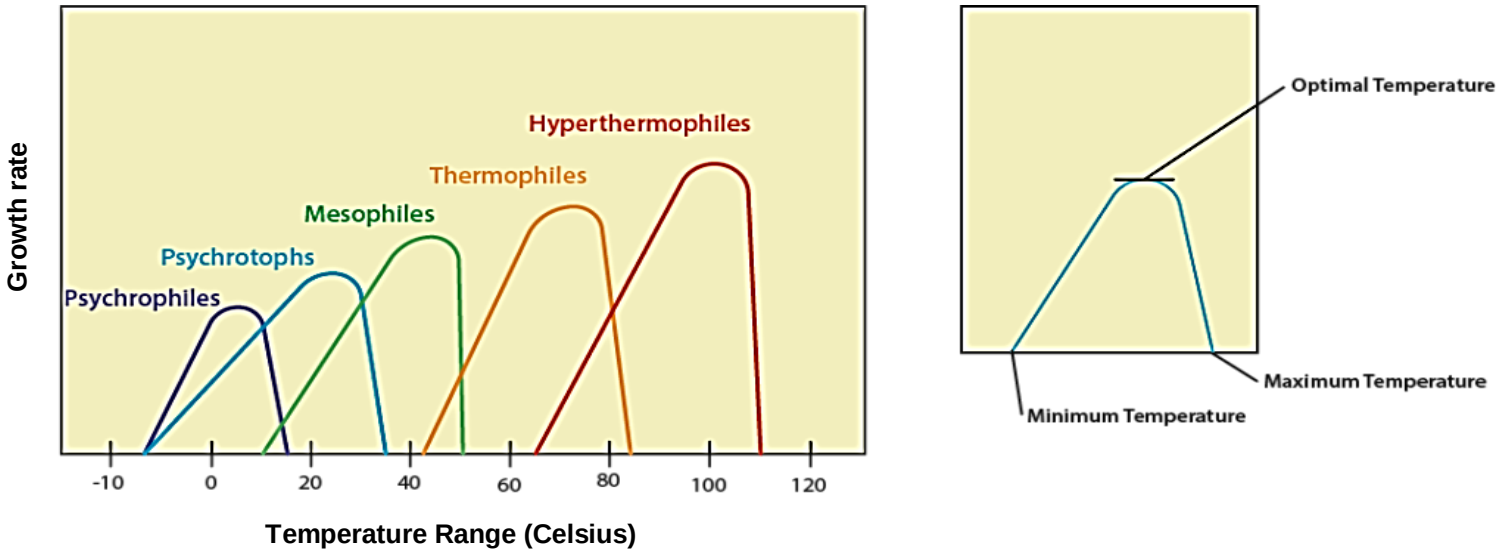

Figure 35: Growth rate and temperature (modified from Bruslind, Environmental Factors-Microbiology).

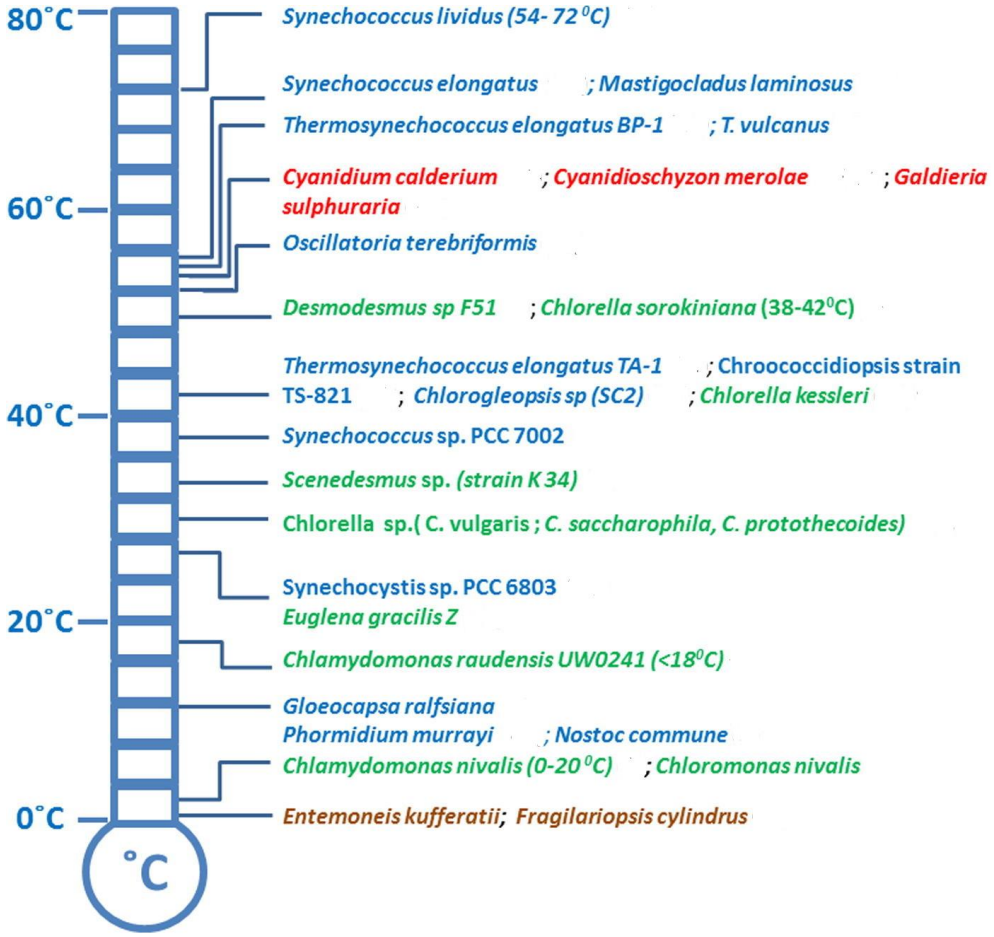

Figure 36: Microalgae species and temperature limit (modified from Varshney et al., 2015)

Light

Light duration and intensity impact algae's metabolism, biochemical composition, growth rate and biomass productivity. It is one of the major factors affecting the microalgae production. For each species, the optimal light intensity must be determined to maximize growth and biomass accumulation. Concerning kinetics, at low levels of light intensity, microalgae growth will be limited. However, if the light intensity is too high, growth will be inhibited. Following published studies, the optimum light intensity is in the range of 200-400 µmol photons·m^{-2}·s^{-1} and the optimum light duration is 16h light/8h dark (light/dark periods, significant for algal photosynthesis) for most microalgae. Both light duration and intensity are important to control to avoid photooxidation and growth inhibition

It has also been reported that light intensity can have an impact on structural and storage lipids and high light intensities can damage lipid composition. It can for example, generate oxidative damage to polyunsaturated fatty acids (PUFAs), cause a reduction in EPA production or increase the level of TAG storage.

Furthermore, the way the microalgae are exposed to light in a cultivation system is also important to avoid photoinhibition or self-shading effect from the algae themselves (Figure 37, 38).

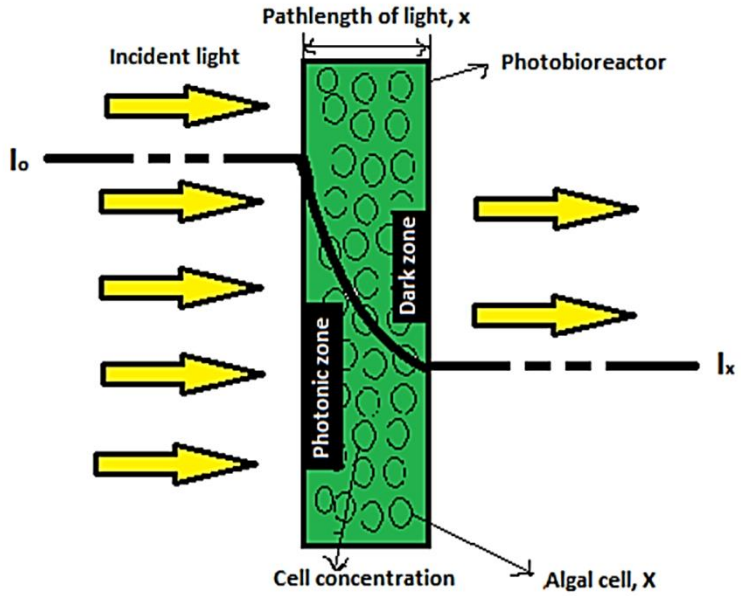

Figure 37: Distribution of light in a photobioreactor (Rajendran and Anderson, 2013).

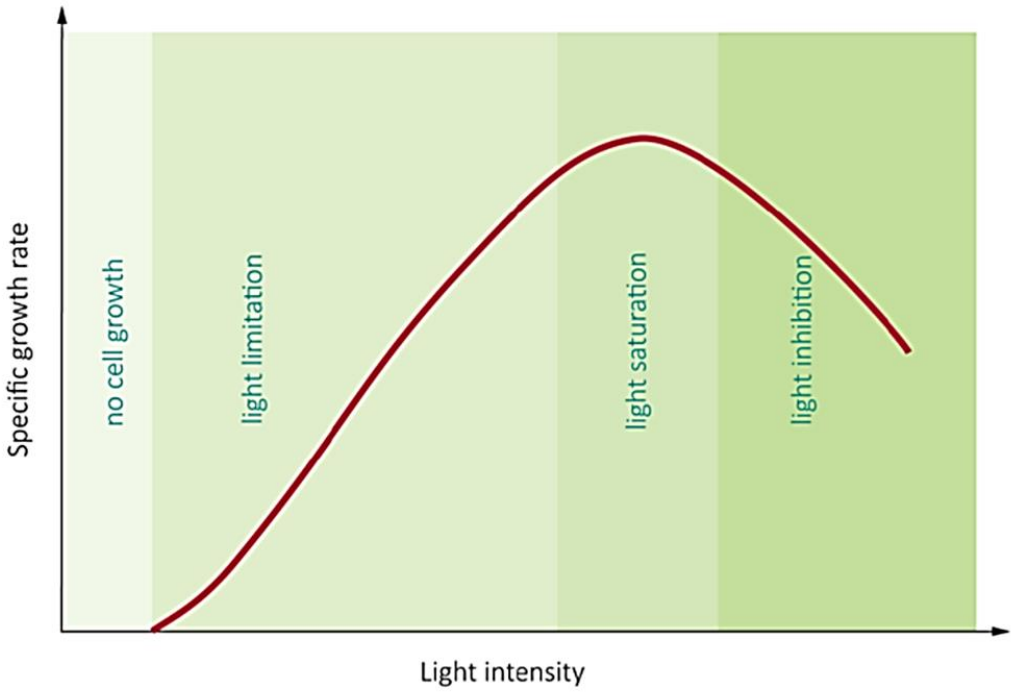

Figure 38: Effect of light intensity on microalgae growth rate (Ogbonna and Tanaka, 2000; Zhang, 2015).

pH

The pH of the culture medium is also an important factor because it has a significant impact on the microalgae's growth and on its metabolites. Each species requires a specific pH for an optimal growth; most of them grow efficiently at a pH range of 6-8.76. Only few species, discovered up to now, can tolerate a broad range of pH (i.e. *Chlorella vulgaris*).

In the case of a pH increase, some consequent effects have been reported such as the altering of lipid and fatty acid composition. In 1990, Guckert and Cooksey have published results showing that high pH led to an increase in the proportion of accumulated TAG and a decrease of the membrane lipid content in *Chlorella* sp..

Another study showed that low pH could increase the proportion of fatty acids in membrane lipids of *Chlamydomonas* sp. (Tatsuzawa and Takizawa, 1996); it was suggested that this was an adaptive response of the algal cells when surrounded by a low pH medium to protect themselves by decreasing the fluidity of their membranes.

Tatsuzawa et al. has also stated that, when grown at pH 1, *Chlamydomonas* sp. increases its proportion of TAG relative to the total lipid content.

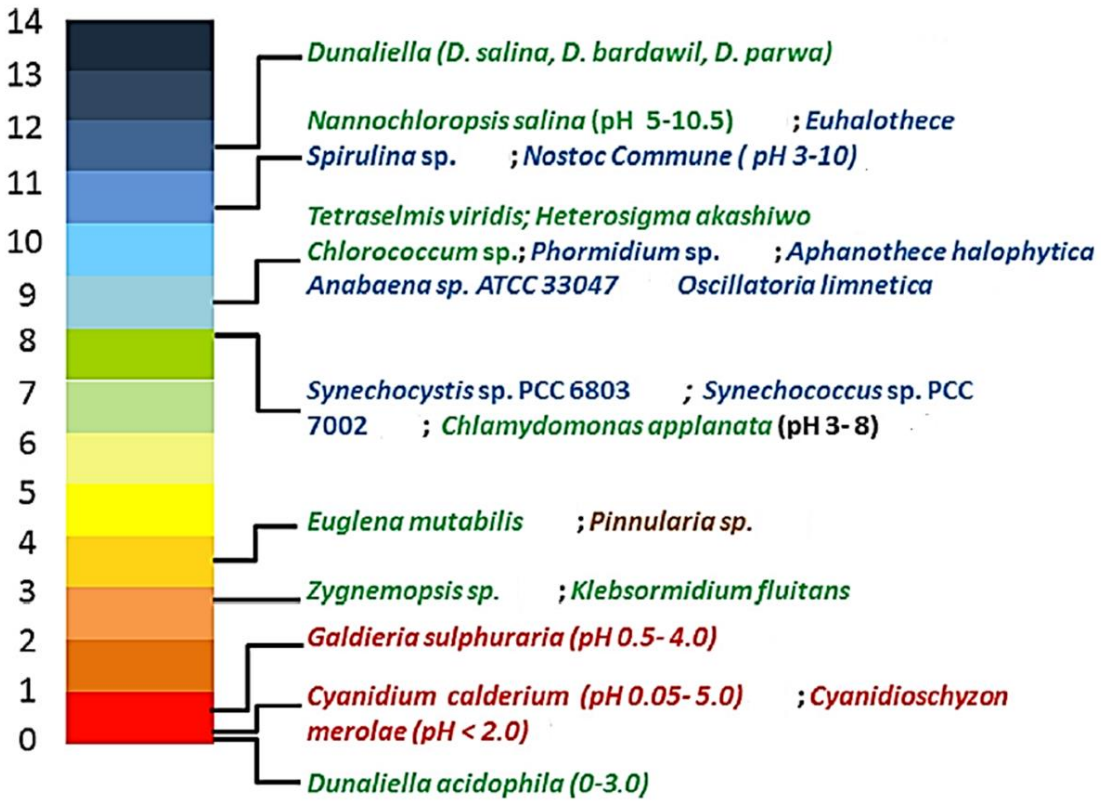

Figure 39: Microalgae species and pH limit (modified from Varshney et al., 2015).

Salt Concentrations

Several articles were published in the recent years to report salinity as a stress factor for microalgae, leading to an increase in lipid content. Very few studies however are available on freshwater microalgae. Some algae like *Dunaliella*, are capable to tolerate very high concentrations of salt, which makes it a perfect model to study the mechanisms behind the salinity stress. As an example, *Dunaliella tertiolecta* showed an increase in lipid content, up to 70 %, when submitted to a high salinity concentration (Takagi, Karseno and Yoshida, 2006). In the case of *Dunaliella salina*, salinity stress also increased the relative proportion of PUFAs (Hanaa H. Abd El-Baky, 2004). Understanding and controlling the mechanisms behind a salinity stress on algal cells is therefore of prime importance. Moreover, each microalga will react differently to these conditions, therefore each study will have to be species specific.

Furthermore, a study using *D. salina* as a model, showed that the combination of NaCl stress (high NaCl concentration), nitrogen limitation and ultraviolet B radiation (UV-B radiation 290-320 nm) can increase the lipophilic (carotenoids and α-tocopherol) and hydrophilic (glutathione and ascorbic acid) antioxidant contents (Hanaa H. Abd El-Baky, 2004).

This approach, using cheap and available elements such as NaCl could therefore have a great potential in reducing biofuel production costs (higher lipid productivity, algal biomass and better biofuel quality).

Nutrients

The nutritional needs are also specific for each microalgae species. There are however common and major nutrients found in every algae culture medium, that are necessary for the development and growth of algae: nitrogen, phosphorous, an organic or inorganic carbon source and iron. Then macronutrients such as Na, Mg, Ca and K, micronutrients such as Mo, Mn, B, Co, Fe, and Zn and other trace elements are needed to complete the necessary requirements for microalgae growth.

Nutrient concentration can significantly impact the growth and lipid composition of the algae. Many scientific publications showed how nutrient concentration could affect growth, biomass and lipid productivities (Pancha *et al.*, 2014; Li *et al.*, 2016). It is generally explained that nutrient starvation decelerates the algal growth and stimulates the synthesis of storage lipids because the algae transfer their fatty acids into their storage lipids instead of synthesizing membrane components that are no longer needed. For the past few years many studies exposed the microalgae's ability to more than double their lipid and TAG content (Guschina and Harwood, 2013) when submitted to a nutrient depletion. One of the most promising oil-rich microalga, *Neochloris oleoabundans*, showed an increase in its fatty acid content (about 50 %) with no significant impact on the fatty acid profile when submitted to a cultivation under nitrogen starvation and after 5 days of nitrogen depletion (Gouveia and Oliveira, 2009). Different nutrient sources were also investigated over these past few years. *Chlorella sp.* showed the highest total lipid content when cultured with a very low concentration of urea (0.025 $g \cdot L^{-1}$) and a maximal lipid productivity with a urea concentration of 0.100 $g \cdot L^{-1}$ (Hsieh and Wu, 2009).

Although the highest accumulation of lipids was obtained under nitrogen deficiency/starvation, other limitations for example in phosphorus, silicon, sulfur, phosphate led to an increase in the cellular total lipid content (Lynn *et al.*, 2000; Sato *et al.*, 2000; Khozin-Goldberg and Cohen, 2006).

These investigations are of prime importance in the context of a commercial lipid production using microalgal biomass. A rapid growth rate is essential; therefore, it is important to know which nutrients should be given to the specific alga used and in what proportions. Furthermore, in some cases, bacteria are used as an enhancer for microalgae growth as they are capable to degrade nutrients into assimilable nutrients for microalgae (Zhu, Li and Ketola, 2011).

Mixing

Mixing is done by using paddle wheels in raceways and through aeration in some photobioreactors. The latter may be implemented by CO_2 enriched air also providing carbon to the system. Mixing and aeration are also significant factors in microalgae culturing for many reasons. Both improve mass transfer (CO_2, nutrients) and light access to the cells in the culture medium. They also prevent the algal cells from sedimentation and cell aggregation. Therefore, continuous mixing is mandatory in a photo-bioreactor and raceway (these culture systems will be further detailed in the following section) for an optimal biomass productivity, growth and compound productivity.

Autotrophy, heterotrophy and mixotrophy

Microalgae cultivation can be classified into three different conditions: autotrophy, heterotrophy and mixotrophy. In autotrophic conditions, carbon dioxide is the carbon source which is captured using light energy; in the case of heterotrophic conditions, organic carbon compounds are the carbon and energy source (i.e. glucose, glycerol and acetate). Mixotrophic cultivation involves both autotrophic and heterotrophic conditions. In this case, growth rates are higher, and the synthesized compounds can derive both from autotrophic and heterotrophic pathways.

4.1.2 Microalgae culture systems

As mentioned previously, the cultivation of microalgae for commercial use has only started a few decades ago and have given great information leading to different suggestions and ideas for the development of a cheap and efficient large-scale production systems. Currently, there are various microalgal cultivation systems in use that can be described by their placement (**outdoor or indoor**), the container used (**open or closed**), the sterility of their medium (axenic, meaning only one species or strain is present in the medium, or xenic), and the mode of production (**batch, continuous or semi-continuous**).

Generally, the conventional microalgal cultivation systems can be categorized into open or closed systems.

Open culture systems, open ponds or raceways have the advantage of being cheap. The most popular system is the paddle-wheel raceway pond, including as their name mentions, a paddle wheel that circulates the culture medium. The microalgae can thus use CO_2 from the atmosphere. The advantage of these systems, other than the fact that they are cheap, is that they are usually easier to construct and operate than closed systems. However, few drawbacks have been pointed out: it requires a lot of land, it is highly vulnerable to contamination, it presents a low light efficiency and important water loss because of evaporation.

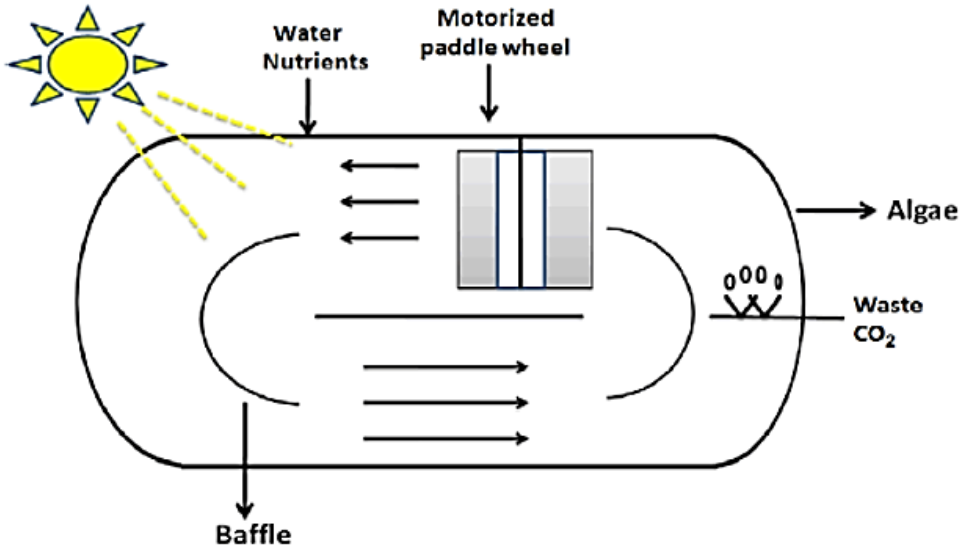

Figure 41: Schematic representation of an open raceway pond system (Sharma et al., 2015)

Figure 40: Open raceway ponds for commercial microalgae production (Source: Global CCS Institute). Left image: *Spirulina* production, Ponds ~ 1 acre (Earthrise Nutritionals, LLC, California); Right image: *Haematococcus pluvialis* (red ponds) and *Spirulina* (Cyanotech Co., Hawaii).

On the other hand, **closed bioreactor systems or photobioreactors (PBRs)**, offer the benefit of a high level of control (of culture conditions and growth parameters), which increases

productivity, but they are more expensive in construction and running. There is a wide range of PBR designs with different kinds of sizes and shape. The most popular ones however are the tubular PBRs, flat panel PBRs and airlift column PBRs (Figure 42). Tubular PBRs are widely used and can have a vertical, horizontal, inclined or helix position. They are made of plastic or glass tubes connected to a mechanical or airlift pump to ensure a culture mixture and prevent the formation of aggregates or the settling of the algal cells.

Photobioreactors offer numerous advantages and have overcome most of the problems observed with open systems. Other than permitting a fully controlled and automatic system, the contamination risk is lower, evaporation is prevented, and it permits increased biomass and products productivity.

There are also other alternative systems of cultivation for microalgae production that have been reported and that present original features. Some of them are briefly discussed below:

- **Hybrid photobioreactors**: they are a combination of closed PBRs and open systems. This configuration permits two cultivation stages, one in the PBR, which minimizes the contamination risk, permits the control of the culture conditions, therefore achieving high biomass productivity, then a second one in an open pond system to cultivate the microalgae under nutrient stresses for an enhanced lipid production.

- **Algal Turf Scrubber (ATG)**: this system concerns immobilized biomass (biofilm) production; it has been used for wastewater treatment (Woertz *et al.*, 2009). The algal culture medium is pumped onto runways, enabling the algae to attach on screens. Water is pumped continuously through the runways and the attached algal community remove the nutrients from the water for their growth, therefore removing pollutants out of the water.

- There exist other types of biofilm systems such as **Rotating Algal Biofilm Reactor (RABR)** involving a partially submerged rotating cylinder where microalgae growth occurs on a substratum attached to the cylinder and with an original harvesting mechanism. In this system, microalgae are cultivated in consortium with bacteria (Christenson and Sims, 2012; Fica and Sims, 2016). In this co-culture system where a synergistic relationship is established, bacteria use the oxygen and extracellular substances produced by microalgae, and microalgae use the carbon dioxide and vitamins from bacteria.
  In general, algal **biofilm-based cultivation** was first developed in the 1980s, presenting a design with a rotating polystyrene disk and used for the removal of nitrogen and phosphorus from municipal wastewater (Przytocka-Jusiak *et al.*, 1984). Algal biofilm systems offer the benefit of easy harvesting of algae by simply scraping them from the material surface on which they are attached.

- **Deep sea water cultures (DSW)**: DSW refers to seawater pumped from a depth of over 200 m. DSW contains high concentrations of nutrients which is an attractive property to produce from microalgae. Tan et al. (2015) reported that the oil-rich microalga *Chlorella sorokiniana* CY1 gave a higher biomass and lipid yield when cultured in 50 % DSW

enriched BG-11 medium. DSW is also characterized by high purity and low temperature (Mohd Nani *et al.*, 2016).

Production system	Advantages	Limitations
Raceway pond 	✓ Relatively cheap ✓ Easy to clean ✓ Utilizes non-agricultural land ✓ Low energy inputs ✓ Easy maintenance	x Poor biomass productivity x Large area of land required x Limited to a few strains of algae x Poor mixing, light and CO2 utilization x Cultures are easily contaminated
Tubular photobioreactor 	✓ Large illumination surface area ✓ Suitable for outdoor cultures ✓ Relatively cheap ✓ Good biomass productivities	x Some degree of wall growth x Fouling x Requires large land space x Gradients of pH, dissolved oxygen and CO2 along the tubes
Flat plate photobioreactor 	✓ High biomass productivities ✓ Easy to sterilise ✓ Low oxygen build-up ✓ Readily tempered ✓ Good light path ✓ Large illumination surface area ✓ Suitable for outdoor cultures	x Difficult scale-up x Difficult temperature control x Small degree of hydrodynamic stress x Some degree of wall growth
Column photobioreactor 	✓ Compact ✓ High mass transfer ✓ Low energy consumption ✓ Good mixing with low shear stress ✓ Easy to sterilize ✓ Reduced photoinhibition and photo-oxidation	x Small illumination area x Expensive compared to open ponds x Shear stress x Sophisticated construction

Figure 42: Advantages and disadvantages of various algal productions systems: raceway pond, tubular photobioreactor, flat plate photobioreactor and column photobioreactor (modified from Paper, City and Scientific, 2015).

4.2 Microalgae harvesting and concentrating

Algal cells have a high-water content (about 70%), that is either removed for a dry extraction or maintained for a wet extraction. A typical harvesting process for a dry biomass usually includes two steps: separating the biomass from the bulk suspension then concentrating the slurry to obtain a thick algal paste. In any case, harvesting strongly depends on the microalgae strain, its size and properties (Valdivia-lefort, 2011). Due to their small size and low concentrations, microalgae harvesting is costly. Thus, different techniques have been developed for the past years. The most common harvesting techniques are briefly described below with their main application, advantages and disadvantages, and some suggested investigations.

Sedimentation and flotation are based on the particularity of microalgae to either sediment or float in the absence of mixing.
Main application: open pond cultivation systems
Advantage: low power consumption, easy to operate and useful as a pre-concentration step.
Disadvantage: algae species specific, slow process, low cell recovery.

> **Suggested investigations**: it can be used as a co-method with another harvesting technique such as flocculation.

Flocculation refers to a state in which algal cells aggregate and form large clumps that are easily filtered or sediment faster. Microalgae can either auto-flocculate or flocculation can be assisted by chemical flocculants (inorganic flocculants such as Zn^{2+} and Fe^{3+} or organic flocculants such as chitosan and starch), for example when the algae strain has poor sedimentation properties. Other types of flocculation enhancers have been explored such as the use of positively charged electrodes or cationic polymers.
Main application: PBR
Advantage: easy to operate, a wide range of flocculants is available.
Disadvantage: highly sensitive to the pH level, possible chemical contamination, and flocculants can be costly and algae species specific.

> **Suggested investigations**: developing cheaper and nontoxic flocculants, inducing autoflocculation by changing the culture conditions (90 % flocculation efficiencies were obtained when increasing the medium pH (Wu *et al.*, 2012) but also decreasing it (Liu *et al.*, 2013) and bio-flocculation method in which two microalgae are co-cultured, one flocculating microalga that helps the other non-flocculating microalga to sediment faster.

Centrifugation relies on a separation based on the size and density of the algal cells. The centrifugal force is used to accelerate the rate of sedimentation. It highly depends on the algae strain. It is mainly used as a biomass concentration step.
Main application: PBR

Advantage: easy to operate, rapid process, high efficiency, suitable for a wide range of algae species and the harvested biomass does not contain flocculants or any other chemical contamination.
Disadvantage: high capital and operational costs, algal cells can be damaged, and bulk harvesting can be difficult.

> **Suggested investigations**: it can be used together with another harvesting method such as flocculation or sedimentation.

Filtration is a method that could be highly efficient for microalgae with a large size. However, most microalgae are small and can rapidly clog filters. There are different types of filtration in terms of the techniques used such as pressure filtration, vacuum filtration or tangential flow filtration and in terms of filter pores sizes used such as macrofiltration (pore size above 10 µm), microfiltration (pore size between 0.1 and 10 µm) or ultrafiltration (pore size between 0.02 and 2 µm).
Main application: PBR
Advantage: water and nutrients can be reused, and a wide range of filters and membranes is available.
Disadvantage: slow process, algae species specific (only large microalgae) and fouling problems.

> **Suggested investigations**: it can possibly be combined with other methods.

Some novel techniques have also been introduced in the past recent years such as **ultrasound for microbial harvesting** (Bosma *et al.*, 2003), **electrochemical harvesting** (ECH) that showed promising results for the harvesting of different types of algae species (Mishra *et al.*, 2014), and **cell palletization** (Xia *et al.*, 2011).

4.3 Extraction techniques for a biodiesel production

The lipid extraction step is also a bottleneck in algal large-scale productions. Indeed, this part of the process have seen many obstacles for the past few years, leading to the following conclusion: the extraction step in a microalgal oil production is excessively costly compared to a palm oil extraction step. An optimal extraction method should be fast, cheap, eco-friendly and should not affect the extracted lipids.

The extraction of algal oil can be carried out by various methods, categorized into three types: chemical method, physical method or the combination of both methods.

4.3.1 Chemical approach: Organic solvents for the extraction of lipids

The extraction of lipids using solvents is based on the solvents' property (hydrophobicity, affinity with lipids…). The solvents used for the extraction of lipids can be either non-polar (i.e. hexane, chloroform, benzene and toluene), polar (i.e. methanol, ethanol and ethyl acetate)

or a combination of both types. Lipids that are largely hydrophobic (e.g., neutral lipids) will favorably interact with the relatively non-polar solvent molecules (Cooney, Young and Nagle, 2009).

Solvent extraction is very popular for the extraction of lipids. Some of most common solvents used include chloroform, hexane, acetone and benzene. Previous studies have reported that solvent extraction of intracellular compounds on dry biomass is more efficient than on wet biomass. Indeed, such solvents are insoluble in water, making their access to intracellular lipids more difficult when the biomass is wet. The major downsides of using solvents for the extraction of microalgal oil is the fact that they can be dangerous for the human health and the environment. However, in order to minimize the use of such solvents while maintaining an efficient lipid extraction, the coupling of a solvent extraction with biomass pretreatments and the use of ecofriendly solvents known as green solvents is currently highly investigated (Sahad, Md. Som and Sulaiman, 2014; Jeevan Kumar *et al.*, 2017; Kumar *et al.*, 2017).

Current methods

In the microalgae field, there are two major solvent extraction methods: the Folch method and the Bligh and Dyer method.

Folch method

The Folch method involves the use of a mixture of two solvents, chloroform: methanol with a ratio of 1:2 (v/v). This method was introduced by Folch et al. (1957) many years ago and has been since used for the analysis of algal lipids by gravimetry but has also been the initial basis for the development of other methods of algal lipid extraction. Today, other methods are more sensitive; it has however the benefit of being fast and easy for the analysis of multiple samples.

Bligh and Dyer method

The Bligh and Dyer method differs from the Folch method by the solvents and solvent/cell ratios used. This method uses methanol and chloroform as solvents, with water as co-solvent. Many suggestions of modification of the protocol have since been published such as replacing water by a 1 M NaCl salt solution to prevent acidic lipids from binding to denatured lipids or adding a phosphate buffer to the chloroform, methanol and water mixture (Ranjith Kumar, Hanumantha Rao and Arumugam, 2015).

Other than the choice of the solvent, several systems are in use for an efficient lipid such as Soxhlet extractions, magnetic stirring, ultrasonic baths, or pressurized fluid extractions (Pieber, Schober and Mittelbach, 2012). For example, in the case of a **Soxhlet extraction**, (reported as relatively safe and easy to operate), a specific apparatus (invented by Franz von Soxhlet in 1879) was developed, composed of a flask that is constantly heated, the Soxhlet extractor that contains the algal biomass, and a condenser for cooling.

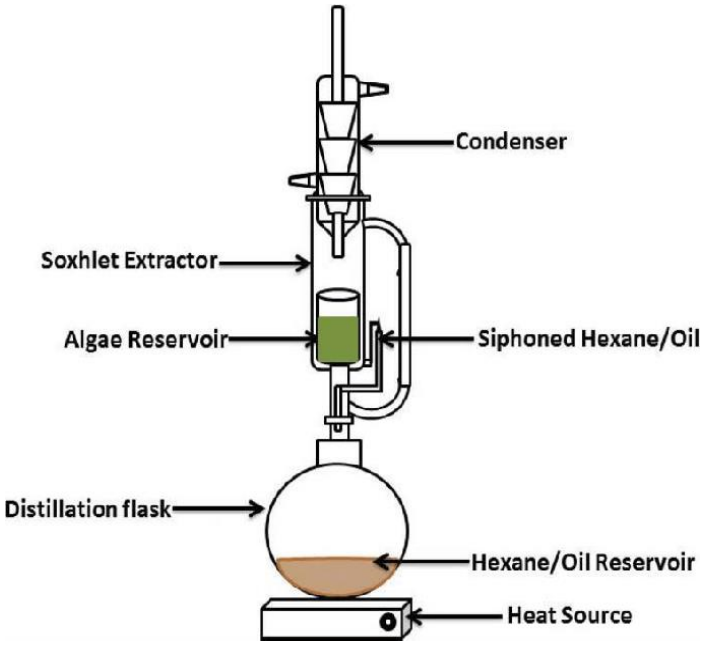

Figure 43: Schematic representation of the Soxhlet extraction setup (Tulashie and Salifu, 2017).

Chemical approach: supercritical fluids

Supercritical fluids are used as extraction solvents due to their capability to evolve in terms of extraction efficiency by varying the extraction pressure and temperature. The supercritical fluid

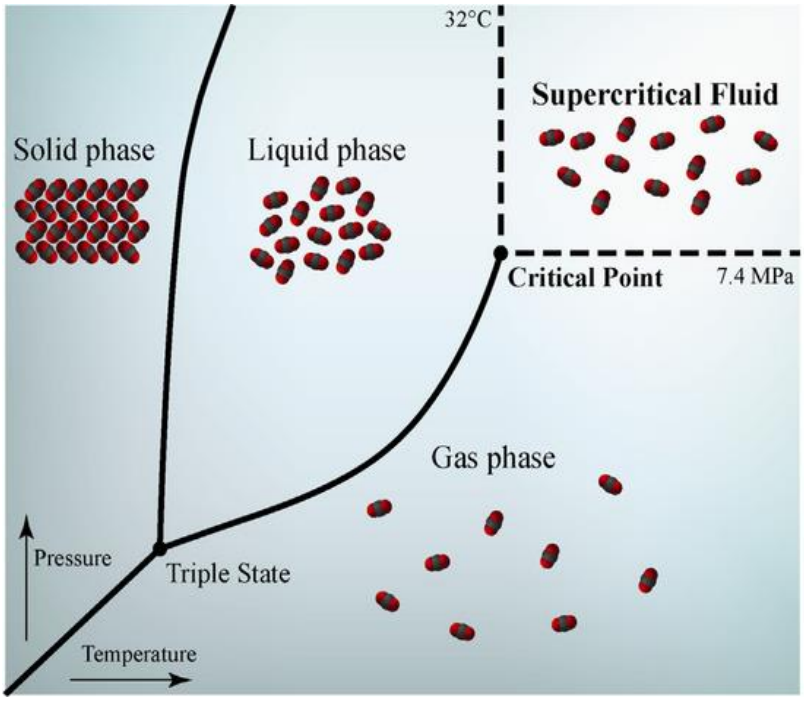

Figure 44: Phase diagram. CO_2 Critical point: 32°C, 7.4 MPa (Capuzzo et al., 2013).

state is achieved when the fluid is above its critical temperature (Tc) and pressure (Pc) (Figure 44).

In this context, carbon dioxide is commonly used as an extracting solvent, sometimes accompanied by solvents such as ethanol or methanol (Cooney et al. 2009, Mendes et al. 2006). For example, Halim et al. (2011) investigated on the potential of supercritical CO_2 as an extraction method and demonstrated that increasing the temperature and pressure led to a decrease in lipid yield, however, the use of co-solvents such as ethanol helped increase the lipid yield.

The advantage of this method is its ability to generate highly purified extracts without using toxic solvents. Moreover, this process is fast and harmless for thermosensitive materials. It does however require high costs in terms of investment and maintenance.

4.3.2 Cell disruption: a key step for the extraction of lipids

In the context of biodiesel production, biomass pretreatments are usually applied to attack the cell barriers (cell wall and membrane) and therefore increase the lipid yield. Indeed, some microalgae can be protected by a very tough cell wall, composed of multiple layers of polysaccharides (i.e. cellulose, mannose, uronic acid…), glycoproteins, algaenan or minerals (i.e. calcium, silicates…). Therefore, a cell disruption step which facilitates the access to the intracellular lipids by breaking the cellular wall and membrane is usually integrated in most of the extraction procedures. The optimization of this process step is therefore of utmost importance for lipid production from microalgae.

Cell disruption techniques can involve **physical, chemical or enzymatic mechanisms** and be categorized into two groups: **mechanical or non-mechanical disruption**. Each technique offers its own benefits and drawbacks. In addition, it is important to judge the proposed process by its energy demand, impact on the further downstream process (separation and purification), effect on product quality, cost and scalability from the laboratory to industrial scale.

Mechanical approach

Mechanical cell disruption can either use a single force (i.e. pressing, bead milling, blending…) or multiple forces (i.e. grinding, homogenization…) to destruct the cell integrity. One of its main advantages, for example for protein extraction, is that most of the intracellular proteins and therefore their functionality is preserved compared to a chemical approach. This method also permits a processing of larger sample sizes which is an attractive advantage for large scale productions.

Oil expeller or press extraction

This method refers to the use of a mechanical press to crush the cells, disrupt them and squeeze the oil out of them (Topare *et al.*, 2011). It's an efficient method, since it can extract about 75 % of the algal oil, however it requires large amounts of biomass and it's a slow process.

High pressure homogenization (HPH)

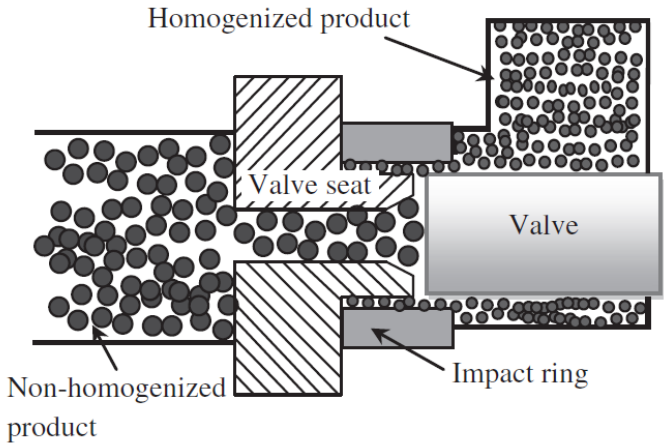

Figure 45: Schematic representation of a standard homogenizer (Yusaf and. Al-Juboori, 2014)

High pressure homogenizers (HPH) are widely used for large-scale applications; they have shown a great potential for the disruption of microalgae (Chisti and Moo-Young, 1986). In this system, the liquid flow, containing algal cells, is pumped under high pressure (5 - 400 MPa) through an orifice. The cells ultimately collide against a valve seat to rupture their cell wall and release the intracellular content. There exists a wide range of designs including a screw, an expeller or a piston.

Several mechanisms behind the cell disruption due to HPH are highlighted; some state that the disruption is only due to the collapsing of cavitation bubbles, formed by the sudden pressure drop in the medium, on the cells. Others believe that the cell disruption is also due to the impingements of cells on the hard surfaces of the valve seat and impact ring, the high shear stress and the turbulence of the flow. In this process, the controllable parameters are the pressure applied and consequently the pressure drop that occurs in the orifice, valve seats and impact ring. Finally, other important parameters can influence the disruption efficiency such as the number of cycles or passes, temperature, impingement and valve design.

Rotor-stator homogenizers

This homogenization system is also widely used for the disruption of cells. It usually includes a static tube (stator) that contains a high-speed rotating blade (rotor). The shear inside the vessel can be maximized by the design of the stator, particularly the design of its slots or gaps located on the tip. The disruption efficiency is also influenced by the sizes of the rotor and stator, the medium viscosity, the flow rate and the cell concentration. In the case of rotor-stator homogenizers, heating during the operation is highly minimized or even inexistent, foaming and aeration problems are minimized, and small biomass volumes are very well processed.

Overall, high shear homogenization systems require a lot of energy, they are therefore preferably proposed for the extraction of high-value products rather than for biodiesel production.

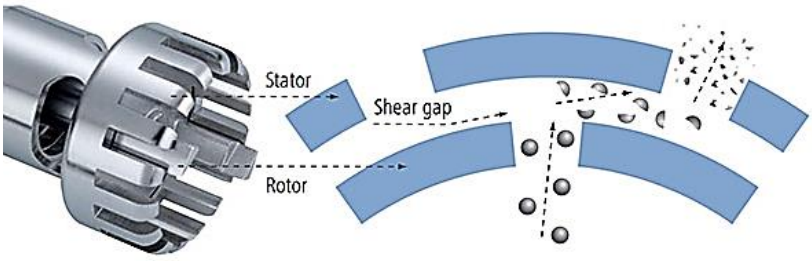

Figure 46: Rotor-stator and schematic representation of its principle (Terra Universal).

Bead milling

Bead mills can either include shaking vessels or agitated beats. The first one disrupts the cells by shaking the entire vessel and is suitable for multiple samples. In the case of the second one,

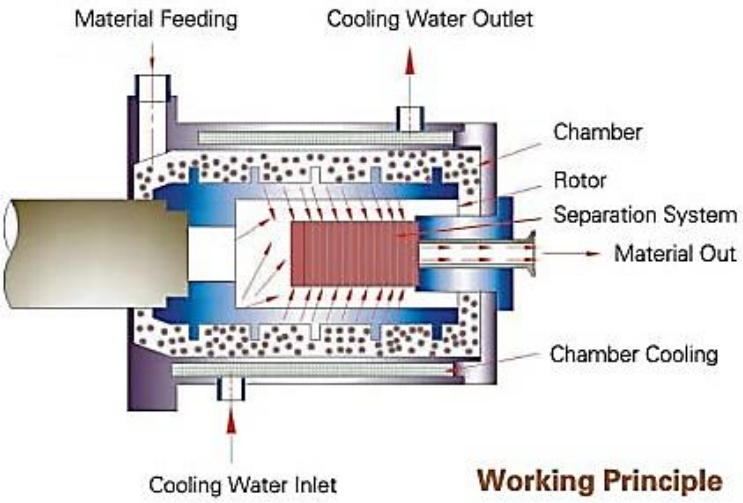

Figure 47: Schematic representation of a bead mill (Source: Beadmill88.com).

cell disruption is ensured by inserting the desired material in a vertical or horizontal cylindrical compartment with beads (steel, ceramic, glass, zirconia-silica, zirconium oxide…) that are then submitted to a high-speed spinning. The grinding of beads against the cells is the cause of their breakage.

The disruption efficiency will depend on various factors such as: the size and composition of the beads, and the temperature, viscosity and cell concentration of the feed. The optimal bead diameter depends on type of cells; 0.1 mm for bacteria and spores, 0.5 mm for yeast, microalgae and unicellular animal cells were reported (Chisti and Moo-Young, 1986; Middelberg, 1995; Lee, Lewis and Ashman, 2012). The bead mills with an agitated system are more suitable for large scale productions than the shaking vessels.

Microwave assisted extraction (MAE)

The potential of MAE to assist and enhance a solvent extraction has been mentioned in different publications, some demonstrating that it successfully increases algal lipid extractions with solvents (Dai, Chen and Chen, 2014). Microwaves lead to rapid oscillating electric fields (with frequencies ranging from 300 MHz to 300 GHz), in which water and dielectric or polar compounds vibrate (Gude *et al.*, 2013). In the case of a molecule with a dipole moment, the dipole is constantly trying to realign with the oscillating movement of the electric field. This results in friction forces and generates heat which leads to the evaporation of water and the disruption of cells due to the pressure on the cell wall and membrane. For extraction purposes, the operating frequency is around 2.5 GHz.

Moreover, this method offers an advantage compared to ultrasonication as it can enhance the efficiency of the solvent to extract by increasing its molecular energy and therefore enabling it to penetrate and extract more efficiently the algal oil ((Nomanbhay and Ong, 2017).

Besides, it has been mentioned that this technique doesn't degrade the algal lipids and that it could be considered as the most effective and simple cell disruption method for the extraction of microalgal lipids (Lee *et al.*, 2010). Currently, microwaves are used in the food and pharmaceutical industry for drying and compound extraction purposes.

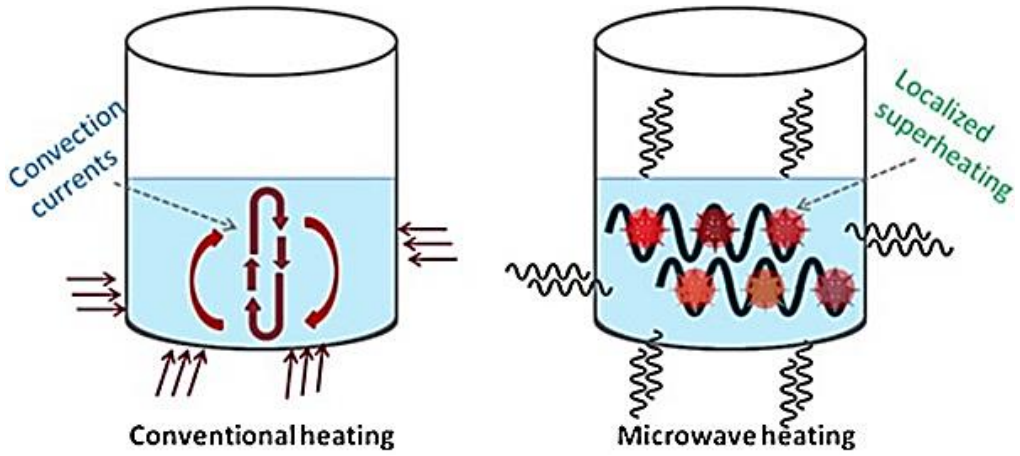

Figure 48: Conventional vs microwave heating (Gude et al., 2013).

Ultrasound assisted extraction (UAE)

Ultrasonication generates cavitation, accompanied by high pressure and high liquid jets that create shearing forces around the algal cells. They mechanically disrupt the cells. This method can be used as an assistant to solvents extractions. Some results have shown an increase in solvent extraction efficiency (Saifuddin and Fazlili, 2009).

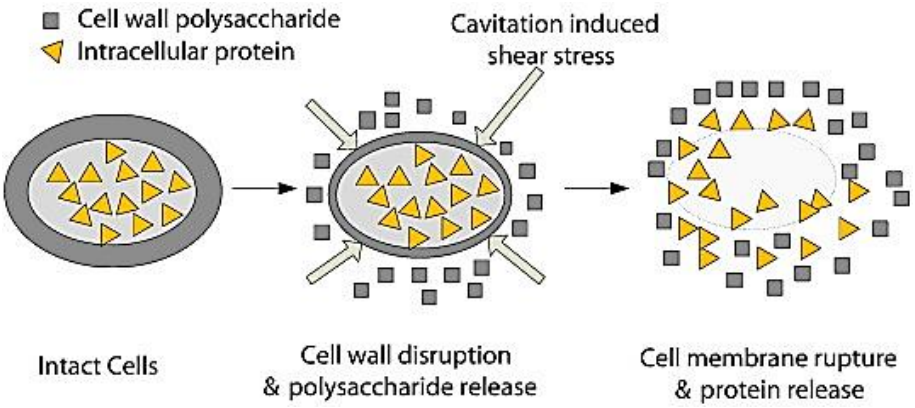

Figure 49: Schematic representation of the ultrasonic cell disruption mechanism (Wu *et al.*, 2015).

Ultrasound extraction is based on the formation of microbubbles in the liquid medium that grow up to a point where they collapse brutally, generating an energy-rich shock wave that efficiently disrupts the cells and enable the release of intracellular compounds. This mechanism is also referred as a cavitation phenomenon. The temperature inside the cavitation bubbles can reach 5000 K and a few hundred atmospheres. Overall, this disruption technique generates considerable heat during processing.

Non-mechanical approach

Non-mechanical disruptions refer to techniques that have a potential to extract algal lipids without using a mechanical force to rupture the cell's membrane and cell wall. There are three non-mechanical methods: chemical, physical or enzymatic. These methods are usually preferred for the following cases: small samples, cells that do not have very tough cell walls, or when specific molecules or cells are targeted and when contaminants and lysate residues are undesired.

Freeze drying (lyophilization)

Freeze drying is based on the dehydration of the cells through two steps, 1) freezing the sample, 2) lowering the pressure (to about 1kPa) and the temperature (to about – 40 °C) to which the sample is submitted. The latter conditions correspond to the required settings for the formation of ice crystals. These ice crystals are primordial because they enhance the porosity of the cell wall which also increases the extraction efficiency of intracellular compounds. Moreover, if the sample is submitted to an even slower freezing, the ice crystals will be larger which increases the cell's disruption. Although optimization is possible, this process has however been reported to be very expensive. Indeed, it requires a high energy consumption and high costs in terms of maintenance and operation.

Pulsed Electric Fields (PEFs)

PEFs, first introduced in the 1960s, are also investigated as a strategy to enhance algal lipid extractions using solvents. They have shown great potential as a mild, fast and non-chemical technique. It is highly appreciated for food processing, commercialized PEF systems are today available for food processing, and has also been developed for large scale wastewater treatments (Mesa and Arizona, 2006).

PEFs are short pulses (micro to milliseconds) of high electric field modifying the transmembrane potential, which in turn causes the rearrangement of the bilayer's phospholipids and induces the formation of pores in the cell membrane (it is therefore sometimes referred as an electroporation). The past few years have seen an emergence in the publication of studies including PEFs as a pretreatment to solvent extractions.

This technique has been investigated in this present work and will therefore be further discussed in Chapter 2.

Osmotic method

Osmotic shock is caused by the sudden change of the solute concentration surrounding the algal cells. This causes a sudden change in the movement of water across the algal cell membrane, which in turn, leads to the rupture of cells and the release of their intracellular content. It has

been mentioned that this method requires high costs and a time-consuming treatment, making it difficult to apply at an industrial scale (Kapoore *et al.*, 2018).

Enzymatic method

Enzymes are used in this case facilitate the hydrolysis of algal cell walls. This enables the intracellular release of the algal compounds such as lipids. Extraction using enzymes is however very costly. It is therefore highly studied as a co-extractor with another pretreatment. Some promising results have been published, demonstrating that the combination of this method with other pretreatments such as ultrasound could lead to higher yields (Mercer and Armenta, 2011).

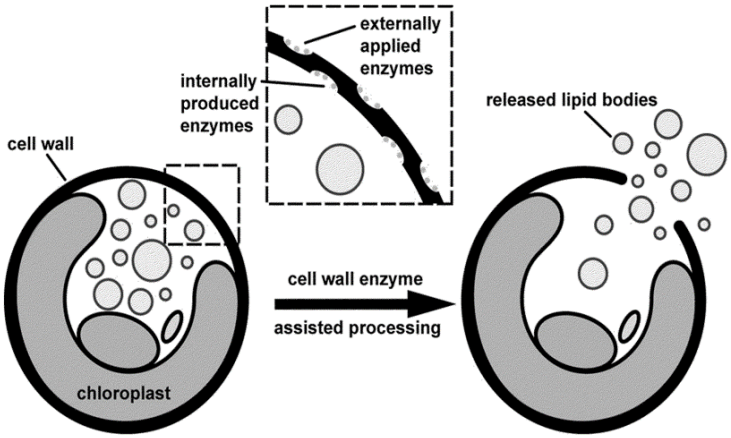

Figure 50 Enzyme-assisted extraction principle (Gerken, Donohoe and Knoshaug, 2013).

The advantages and disadvantages of several current cell disruption techniques are presented in the table below (Table5).

Method	Operates at Industrial Scale	Suitability for Commercial Application	Advantages	Disadvantages
High pressure homogeniser	✓	-	Destruction of cell walls at room temperature, effective for neutral lipid extraction	High energy input, not effective for extraction of high molecular weight proteins
Mechanical cell press	✓	-	Industry standard for oil recovery from oilseeds	Inefficient cell disruption, high energy input
Hydrodynamic cavitation	✓	-	Relatively low energy input	Cavitation area limited
Bath sonication	x	+++	Effective cell wall disruption, minimal maintenance cost, relatively rapid, no hazardous substances required	High operational costs and energy input
Microwaves	x	++++	Effective cell wall disruption and excellent recovery of bioactives, relatively low energy input, fast heating and short reaction time, reduced solvent usage	Generates heat, high maintenance cost
Bead milling/beat beating	✓	++	Effective cell wall disruption, rapid extraction	Varied efficiency across species, additional step required to remove beads, high maintenance costs and energy input
Osmotic shock	x	-	Low energy input, easier to scale-up	Inefficient cell disruption, generation of waste saltwater, time consuming
Enzymatic hydrolysis	✓	++	Effective cell wall hydrolysis, high selectivity, mild treatment, carotenoid bioactivity not affected	High cost of enzymes, longer treatment time, enzymes must be disposed of after use
Supercritical fluid extraction	✓	+	Polarity of solvent is tunable, fast process, uses non-toxic solvents such CO_2, effective for carotenoid extraction	Expensive, not suitable for scale-up
Pulse electric field	✓	+	High selectivity, mild treatment, carotenoid bioactivity not affected, relatively low energy input	Still in its infancy
Soxhlet extraction	✓	+	Cost-effective, easy to scale-up	Long extraction time, uses large amounts of solvents (often toxic)

Table 5: Current cell disruption techniques for microalgal biotechnology with their advantages and disadvantages (modified from Kapoore et al., 2018).

✓ : Yes; x: No; -: Not suitable; +: Weak; ++: Moderate; +++: High; ++++: Higher; +++++: Very high.

5. Challenges and aim of project

5.1 Challenges at the different stages of the production

It is now clearly accepted that fossil fuels are not a sustainable energy resource, and that the current environmental situation shows an alarming accumulation of greenhouse gas emissions. In addition, the depletion of fossil fuels is accompanied by a strong population growth, thus an increasing energy demand. Therefore, renewable and ecofriendly energy productions such as biodiesel production, are of prime importance for a sustainable economy and the environment. Microalgae has a huge potential as a renewable energy source. Research on this "green gold" is therefore primordial for our future. For the past 60 years, large scale production of microalgae has been highly investigated. Since then, several bottlenecks have been pointed out such as high production costs (harvesting costs over 30% of the total production cost in the case of an open pond cultivation (Chini Zittelli *et al.*, 2006) and energy intensive processes. Overall, there are three key steps in the algal industry that need to be optimized: the cultivation, harvesting and extraction step.

5.2 Aim and objectives of this study

Many would agree on the fact that microalgal productions have a tremendous potential for the future (microalgae investments reached over $900 million worldwide (Deng, Li and Fei, 2009). Many scientists have therefore devoted their time for research on microalgae, whether it is on cell physiology or on their potential as a source of a wide range of compounds of interest for different commercial applications or for environmental purposes.

It is also widely accepted that there are remaining bottlenecks for achieving environmentally friendly and/or economically competitive large-scale production such as for biofuel production.

Few suggestions and proposed solutions have emerged recently. As an example, in 2009, the OriginOil algae company presented a breakthrough algal technology that involves only one single-step extraction (harvesting, concentrating and oil extracting and separation, all in one step and in less than one hour), instead of the conventional three-step processing (solids separation, dewatering and extraction).

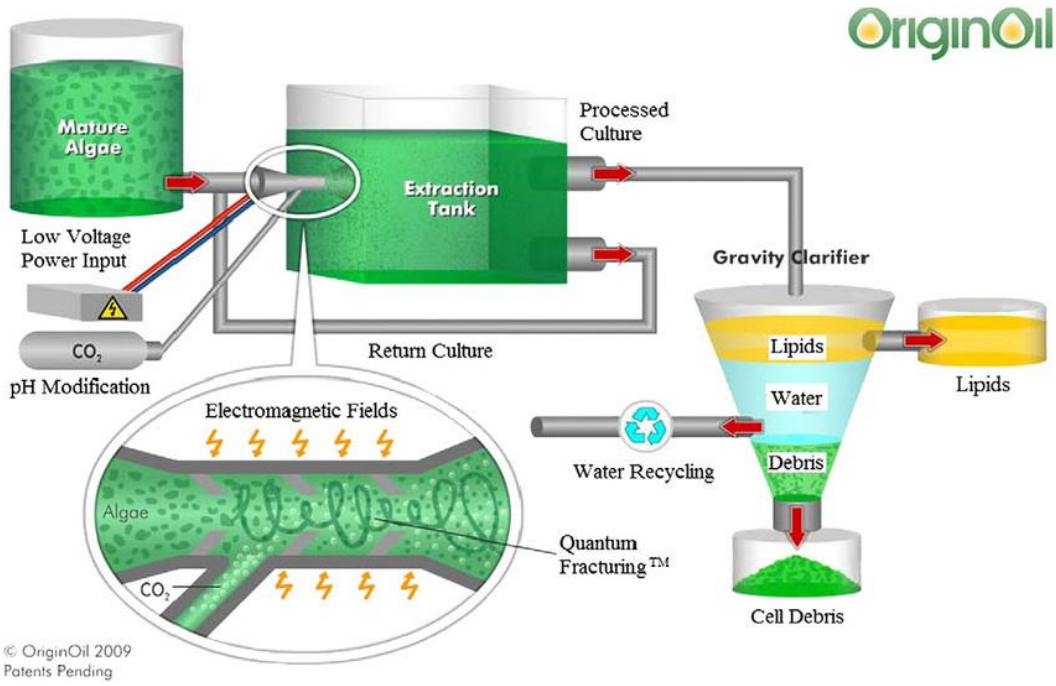

Figure 51: Single-step extraction (OriginOil, 2009)

The study presented in this work concerned the extraction step. As mentioned previously, this step of the process is currently significantly expensive and energy intensive. Moreover, in the case of lipid extraction, it is commonly performed using toxic organic solvents. Further investigations are therefore needed to propose solutions for this step of the process and ultimately improve and enhance lipid recovery from microalgae cells.

Several solutions have been proposed in the literature (discussed in Chapter 1) that include the use of pretreatments (mechanical or non-mechanical), prior to the solvent extraction, in order to enhance lipid recovery. These pretreatments, as well as the microalga *Chlamydomonas reinhardtii*, are widely studied and many information is available in the literature. However, very few information is available on the **effect of these pretreatments on the microalgae cells** (their morphology, structure, components…) and their mechanisms of action on the **enhancement of lipid extraction** remain unclear. This is significantly important and required for the final objective of developing a sustainable and economically feasible algae-based biofuel production at a large scale.

This work therefore proposes a study of two types of pretreatments, **Pulsed Electric Fields (PEFs) and mechanical compressions**, in the context of lipid extraction from the microalga *C. reinhardtii*. Their potential to enhance lipid recovery was first evaluated before investigating their mechanism of action at a cellular scale. Overall, several techniques were used to investigate, at a cellular scale, the effect of electrical (PEF), mechanical (compressions induced on the cells) and chemical (solvent extraction) treatments on the microalgae cells. These include flow cytometry analysis and microscopic tools such as Confocal Scanning Laser Microscopy (CLSM) and Transmission Electron Microscopy (TEM) coupled with a microfluidic device that was specifically designed and fabricated for this study. This permitted us for example to observe

and investigate the possible effects of mechanical compressions on the microalgae cells. **Cell permeability, viability, and lysis** were evaluated, as well as the cell's **morphology and structure** (plasma membrane, cell wall and inner components). Moreover, to further understand and optimize the lipid production process, the effect of nitrogen stress conditions (used induce lipid accumulation in *C. reinhardtii* cells) was also investigated.

The following chapter presents the materials and methods used during this work and results are presented and discussed in Chapter 3 and Chapter 4. In these chapters, the articles resulting from this work are presented, including the obtained results and further details on the methods and materials used.

References

Badour, S. S., Tan, C. K. and Waygood, E. R. (1977) 'Observations on cell development in Chlamydomonas Segnis (Chlorophyceae) at low and high carbon dioxide tension'.

Bates, P. D. *et al.* (2009) 'Analysis of Acyl Fluxes through Multiple Pathways of Triacylglycerol Synthesis in Developing Soybean Embryos', *Plant Physiology*, 150(1), pp. 55–72. doi: 10.1104/pp.109.137737.

Becker, E. W. (2007) 'Micro-algae as a source of protein', *Biotechnology Advances*, 25(2), pp. 207–210. doi: 10.1016/j.biotechadv.2006.11.002.

Behera, B. K. and Varma, A. (2016) *Microbial resources for sustainable energy*, *Microbial Resources for Sustainable Energy*. doi: 10.1007/978-3-319-33778-4.

Benedetti, S. *et al.* (2004) 'Antioxidant properties of a novel phycocyanin extract from the blue-green alga Aphanizomenon flos-aquae', *Life Sciences*, 75(19), pp. 2353–2362. doi: 10.1016/j.lfs.2004.06.004.

Bennett, R. R. and Golestanian, R. (2014) 'A steering mechanism for phototaxis in Chlamydomonas'. doi: 10.1098/rsif.2014.1164.

Berger, B. A. and Structure, A. E. O.- (2014) 'Polar Lipids — Phospholipids and Glycolipids - An Enhanced Omega-3 Structure Polar Lipids — Phospholipids and Glycolipids', (October).

Bišová, K. and Zachleder, V. (2014) 'Cell-cycle regulation in green algae dividing by multiple fission', *Journal of Experimental Botany*, 65(10), pp. 2585–2602. doi: 10.1093/jxb/ert466.

Bondioli, P. *et al.* (2012) 'Oil production by the marine microalgae Nannochloropsis sp. F&M-M24 and Tetraselmis suecica F&M-M33', *Bioresource Technology*. Elsevier Ltd, 114, pp. 567–572. doi: 10.1016/j.biortech.2012.02.123.

Borowitzka, M. A. (2013) 'High-value products from microalgae-their development and commercialisation', Journal of Applied Phycology, 25(3), pp. 743–756. doi: 10.1007/s10811-013-9983-9.

Bosma *et al.* (2003) 'Ultrasound, a new separation technique to harvest microalgae', *Evidence Based Midwifery*, 15, pp. 143–153. doi: 10.1023/A.

Breuer, G. *et al.* (2015) 'Opportunities to improve the areal oil productivity of microalgae', *Bioresource Technology*. Elsevier Ltd, 186, pp. 294–302. doi: 10.1016/j.biortech.2015.03.085.

Briand, E. *et al.* (2012) 'Evidence of the cost of the production of microcystins by Microcystis aeruginosa under differing light and nitrate environmental conditions', *PLoS ONE*, 7(1). doi: 10.1371/journal.pone.0029981.

Cagliari, A. *et al.* (2011) 'Biosynthesis of triacylglycerols (TAGs) in plants and algae', *International Journal of Plant Biology*, 2(1), pp. 40–52. doi: 10.4081/pb.2011.e10.

Capuzzo, A., Maffei, M. E. and Occhipinti, A. (2013) 'Supercritical fluid extraction of plant flavors and fragrances', Molecules, 18(6), pp. 7194–7238. doi: 10.3390/molecules18067194.

Del Campo, J. A., García-González, M. and Guerrero, M. G. (2007) 'Outdoor cultivation of microalgae for carotenoid production: Current state and perspectives', *Applied Microbiology and Biotechnology*, 74(6), pp. 1163–1174. doi: 10.1007/s00253-007-0844-9.

Chen, C. Y. *et al.* (2013) 'Microalgae-based carbohydrates for biofuel production', *Biochemical*

Engineering Journal. Elsevier B.V., 78, pp. 1–10. doi: 10.1016/j.bej.2013.03.006.

Chini Zittelli, G. *et al.* (2006) 'Productivity and photosynthetic efficiency of outdoor cultures of Tetraselmis suecica in annular columns', *Aquaculture*, 261(3), pp. 932–943. doi: 10.1016/j.aquaculture.2006.08.011.

Chisti, Y. (2007) 'Biodiesel from microalgae.', *Biotechnology advances*, 25(3), pp. 294–306. doi: 10.1016/j.biotechadv.2007.02.001.

Chisti, Y. and Moo-Young, M. (1986) 'Disruption of microbial cells for intracellular products', *Enzyme and Microbial Technology*, 8(4), pp. 194–204. doi: 10.1016/0141-0229(86)90087-6.

Choi, S. P., Nguyen, M. T. and Sim, S. J. (2010) 'Enzymatic pretreatment of Chlamydomonas reinhardtii biomass for ethanol production', *Bioresource Technology*. Elsevier Ltd, 101(14), pp. 5330–5336. doi: 10.1016/j.biortech.2010.02.026.

Christenson, L. B. and Sims, R. C. (2012) 'Rotating algal biofilm reactor and spool harvester for wastewater treatment with biofuels by-products', *Biotechnology and Bioengineering*, 109(7), pp. 1674–1684. doi: 10.2478/mspe-2018-0005.

Cross, F. R. and Umen, J. G. (2015) 'The Chlamydomonas cell cycle', Plant Journal, 82(3), pp. 370–392. doi: 10.1111/tpj.12795.

Cohen, Z. *et al.* (1993) 'Production and partial purification of γ-linolenic acid and some pigments from Spirulina platensis', *Journal of Applied Phycology*, 5(1), pp. 109–115. doi: 10.1007/BF02182428.

Colon-Ramos, D. A. *et al.* (2003) 'Asymmetric Distribution of Nuclear Pore Complexes and the Cytoplasmic Localization of', 4, pp. 1–12. Available at: papers3://publication/uuid/70C7BA14-A5AB-4250-8798-4848F62A1730.

Cooney, M., Young, G. and Nagle, N. (2009) 'Extraction of bio-oils from microalgae', *Separation and Purification Reviews*, 38(4), pp. 291–325. doi: 10.1080/15422110903327919.

Craigie, R. A. and Cavalier-Smith, T. (1982) 'Cell Volume and the Control of the Chlamydomonas Cell Cycle', *Journal of Cell Science*, 54(1), pp. 173–191. Available at: http://jcs.biologists.org/cgi/content/abstract/54/1/173.

Cross, F. R. and Umen, J. G. (2015) 'The Chlamydomonas cell cycle', *Plant Journal*, 82(3), pp. 370–392. doi: 10.1111/tpj.12795.

Dai, Y. M., Chen, K. T. and Chen, C. C. (2014) 'Study of the microwave lipid extraction from microalgae for biodiesel production', *Chemical Engineering Journal*. Elsevier B.V., 250, pp. 267–273. doi: 10.1016/j.cej.2014.04.031.

Deng, X., Li, Y. and Fei, X. (2009) 'Microalgae: A promising feedstock for biodiesel', *African Journal of Microbiology Research\n* , 3(13), pp. 1008–1014.

Díaz, G. D., Li, Q. and Dashwood, R. H. (2003) 'Caspase-8 and apoptosis-inducing factor mediate a cytochrome c-independent pathway of apoptosis in human colon cancer cells induced by the dietary phytochemical chlorophyllin', *Cancer Research*, 63(6), pp. 1254–1261. doi: 10.1109/EMBC.2013.6610334.

Dutcher, S. K. and O'Toole, E. T. (2016) 'The basal bodies of Chlamydomonas reinhardtii', *Cilia*. BioMed Central, 5(1), pp. 1–7. doi: 10.1186/s13630-016-0039-z.

Eriksen (2016) 'Research Trends in the Dominating Microalgal Pigments, β-carotene,

Astaxanthin, and Phycocyanin Used in Feed, in Foods, and in Health Applications', *Journal of Nutrition & Food Sciences*, 06(03). doi: 10.4172/2155-9600.1000507.

Fan, J., Andre, C. and Xu, C. (2011) 'A chloroplast pathway for the de novo biosynthesis of triacylglycerol in Chlamydomonas reinhardtii', *FEBS Letters*. Federation of European Biochemical Societies, 585(12), pp. 1985–1991. doi: 10.1016/j.febslet.2011.05.018.

Fang, S. C. (2013) *Metabolic Engineering and Molecular Biotechnology of Microalgae for Fuel Production, Biofuels from Algae*. Elsevier B.V. doi: 10.1016/B978-0-444-59558-4.00003-6.

Farine, L. *et al.* (2015) 'Phosphatidylethanolamine and phosphatidylcholine biosynthesis by the Kennedy pathway occurs at different sites in Trypanosoma brucei', *Scientific Reports*. Nature Publishing Group, 5(September), pp. 1–11. doi: 10.1038/srep16787.

Fica, Z. T. and Sims, R. C. (2016) 'Algae-based biofilm productivity utilizing dairy wastewater: Effects of temperature and organic carbon concentration', *Journal of Biological Engineering*. Journal of Biological Engineering, 10(1), pp. 1–7. doi: 10.1186/s13036-016-0039-y.

Gerken, H. G., Donohoe, B. and Knoshaug, E. P. (2013) 'Enzymatic cell wall degradation of Chlorella vulgaris and other microalgae for biofuels production', Planta, 237(1), pp. 239–253. doi: 10.1007/s00425-012-1765-0.

Giroud, C., Gerber, A. and Eichenberger, W. (1988) 'Lipids of Chlamydomonas reinhardtii . Analysis of Molecular Species and Intracellular Site (s) of Biosynthesis', 29(4), pp. 587–595.

Goodenough, U. W. and Heuser, J. E. (1985) 'The Chlamydomonas Cell Wall Glycoproteins Analyzed by the Technique and Its Constituent Quick-Freeze, Deep-Etch', 101(October).

Gouveia, L. and Oliveira, A. C. (2009) 'Microalgae as a raw material for biofuels production', *Journal of Industrial Microbiology and Biotechnology*, 36(2), pp. 269–274. doi: 10.1007/s10295-008-0495-6.

Gude, V. *et al.* (2013) 'Microwave energy potential for biodiesel production', *Sustainable Chemical Processes*, 1(1), p. 5. doi: 10.1186/2043-7129-1-5.

Guil-Guerrero, J. L. *et al.* (2004) 'Functional properties of the biomass of three microalgal species', *Journal of Food Engineering*, 65(4), pp. 511–517. doi: 10.1016/j.jfoodeng.2004.02.014.

Gürtekin, E. (2014) 'Biological Hydrogen Production Methods'. Available at: http://i-sem.info/PastConferences/ISEM2014/ISEM2014/papers/A10-ISEM2014ID80.pdf.

Guschina, I. A. and Harwood, J. L. (2013) *Algae for biofuels and energy*, *Algae for Biofuels and Energy*. doi: 10.1007/978-94-007-5479-9.

Halim, R. *et al.* (2010) 'Chlorophyll extraction from microalgae: A review on the process engineering aspects', *International Journal of Chemical Engineering*, (June 2016). doi: 10.5268/IW-6.4.874.

Hallmann, A. (2011) 'Evolution of reproductive development in the volvocine algae', *Sexual Plant Reproduction*, 24(2), pp. 97–112. doi: 10.1007/s00497-010-0158-4.

Hanaa H. Abd El-Baky, F. K. E. B. and G. S. E.-B. (2004) 'Production of Antioxidant by the Green Alga Dunaliella salina', *International Journal of Agriculture and Biology*, (July), pp. 49–57. Available at: file:///C:/Users/jordina.casademunt/Downloads/50463515a36fa0784a.pdf.

Harris, E. H., Stern, D. B. and Witman, G. B. (1960) 'Chapter-1---The-Genus-Chlamydomonas_2009_The-Chlamydomonas-Sourcebook', 1786. doi: 10.1556/ABot.53.2011.1.

Harris, E. H., Stern, D. B. and Witman, G. B. (2009) 'Chapter 2 - Cell Architecture', *The Chlamydomonas Sourcebook*, pp. 25–64. doi: 10.1016/B978-0-12-370873-1.00002-2.

He, P. *et al.* (2003) 'Gold immunolocalization of Rubisco and Rubisco Activase in pyrenoid of Chlamydomonas reinhardtii', 18(2), pp. 121–127. doi: 10.4490/ALGAE.2003.18.2.121.

Ho, S.-H. *et al.* (2014) 'Perspectives on engineering strategies for improving biofuel production from microalgae — A critical review', *Biotechnology Advances*. Elsevier Inc., 32(8), pp. 1448–1459. doi: 10.1016/j.biotechadv.2014.09.002.

Ho, S. H. et al. (2014) 'Optimizing biodiesel production in marine Chlamydomonas sp. JSC4 through metabolic profiling and an innovative salinity-gradient strategy', Biotechnology for Biofuels, 7(1), pp. 1–16. doi: 10.1186/1754-6834-7-97.

Hossain, A. B. M. S. *et al.* (2008) 'Biodiesel fuel production from algae as renewable energy', *American Journal of Biochemistry and Biotechnology*, 4(3), pp. 250–254. doi: 10.3844/ajbbsp.2008.250.254.

Hounslow *et al.* (2016) '7Kh 6Hdufk Iru D /Lslg 7Uljjhu 7Kh (Iihfw Ri 6Dow 6Wuhvv Rq Wkh /Lslg 3Uriloh Ri Wkh 0Rgho 0Lfurdojdo 6Shflhv', *Current Biotechnology*, 5, pp. 305–313. doi: 10.2174/2211550105666160322344.

Hsieh, C. H. and Wu, W. T. (2009) 'Cultivation of microalgae for oil production with a cultivation strategy of urea limitation', *Bioresource Technology*. Elsevier Ltd, 100(17), pp. 3921–3926. doi: 10.1016/j.biortech.2009.03.019.

Hu, Q. *et al.* (2008) 'Microalgal triacylglycerols as feedstocks for biofuel production: Perspectives and advances', *Plant Journal*, 54(4), pp. 621–639. doi: 10.1111/j.1365-313X.2008.03492.x.

IEA (2017) 'WEO 2017 Chapter 1: Introduction and scope.', *IEA: World Energy Outlook*, pp. 33–61. doi: 10.1787/weo-2017-en.

Igielska-Kalwat, J., Wawrzyńczak, A. and Nowak, I. (2012) 'β-Carotene as an exemplary carotenoid and its application in cosmetic industry', *Chemik*, 66(2), pp. 140–144.

IRENA (2018) 'Renewable Energy and Jobs: Annual Review 2018, International Renewable Agency', p. 28. doi: 10.1158/1078-0432.CCR-16-2586.

Jeevan Kumar, S. P. *et al.* (2017) 'Sustainable green solvents and techniques for lipid extraction from microalgae: A review', *Algal Research*. Elsevier B.V., 21, pp. 138–147. doi: 10.1016/j.algal.2016.11.014.

Kang, C. D. *et al.* (2005) 'Comparison of heterotrophic and photoautotrophic induction on astaxanthin production by Haematococcus pluvialis', *Applied Microbiology and Biotechnology*, 68(2), pp. 237–241. doi: 10.1007/s00253-005-1889-2.

Kapoore, R. *et al.* (2018) 'Microwave-Assisted Extraction for Microalgae: From Biofuels to Biorefinery', *Biology*, 7(1), p. 18. doi: 10.3390/biology7010018.

Khozin-Goldberg, I. and Cohen, Z. (2006) 'The effect of phosphate starvation on the lipid and fatty acid composition of the fresh water eustigmatophyte Monodus subterraneus', *Phytochemistry*, 67(7), pp. 696–701. doi: 10.1016/j.phytochem.2006.01.010.

Koller, M., Muhr, A. and Braunegg, G. (2014) 'Microalgae as versatile cellular factories for valued products', *Algal Research*. Elsevier B.V., 6(PA), pp. 52–63. doi: 10.1016/j.algal.2014.09.002.

Koufopanou, V. (1994) 'The Evolution of Soma in the Volvocales', *Source: The American Naturalist*, 143(5), pp. 907–931. doi: 10.1086/285639.

Kumar, S. P. J. *et al.* (2017) 'Green solvents and technologies for oil extraction from oilseeds Green solvents and technologies for oil extraction from oilseeds', *Chemistry Central Journal*. Springer International Publishing, (January). doi: 10.1186/s13065-017-0238-8.

Lee, A. K., Lewis, D. M. and Ashman, P. J. (2012) 'Disruption of microalgal cells for the extraction of lipids for biofuels: Processes and specific energy requirements', *Biomass and Bioenergy*. Elsevier Ltd, 46, pp. 89–101. doi: 10.1016/j.biombioe.2012.06.034.

Lee, J. Y. *et al.* (2010) 'Comparison of several methods for effective lipid extraction from microalgae', *Bioresource Technology*. Elsevier Ltd, 101(1 SUPPL.), pp. S75–S77. doi: 10.1016/j.biortech.2009.03.058.

Lenka, S. K. *et al.* (2016) 'Current advances in molecular, biochemical, and computational modeling analysis of microalgal triacylglycerol biosynthesis', *Biotechnology Advances*. Elsevier B.V., 34(5), pp. 1046–1063. doi: 10.1016/j.biotechadv.2016.06.004.

Li-beisson, Y. *et al.* (2010) 'Acyl-Lipid Metabolism'. doi: 10.1199/tab.0161.

Li-Beisson, Y., Beisson, F. and Riekhof, W. (2015) Metabolism of acyl-lipids in Chlamydomonas reinhardtii, Plant Journal. doi: 10.1111/tpj.12787.

Li, C. *et al.* (2016) 'Combined effects of carbon, phosphorus and nitrogen on lipid accumulation of Chlorella vulgaris in mixotrophic culture', *Journal of Chemical Technology and Biotechnology*, 91(3), pp. 680–684. doi: 10.1002/jctb.4623.

Lien, T. and Knutsen, G. (1979) 'Synchronous Growth of Chlamydomonas Reinhardtii (Chlorophyceae): a Review of Optimal Conditions', *Journal of Phycology*, pp. 191–200. doi: 10.1111/j.0022-3646.1979.00191.x.

Liu *et al.* (2013) 'Freshwater microalgae harvested via flocculation induced by pH decrease', *Biotechnology for Biofuels*. Biotechnology for Biofuels, 6, p. 98. doi: 10.1186/1754-6834-6-98.

Lorenz, R. T. and Cysewski, G. R. (2000) '2000_Commercial potential for Haematococcus(commmerical pproduction', 18(April), pp. 160–167. doi: 10.1016/S0167-7799(00)01433-5.

Lynn *et al.* (2000) 'Effect of nutrient availability on the biochemical and elemental stoichiometry in the freshwater diatom', *J. Phycol.*, 522(February), pp. 510–522.

Mansor, M. R. *et al.* (2015) *Life cycle assessment of natural fiber polymer composites, Agricultural Biomass Based Potential Materials*. doi: 10.1007/978-3-319-13847-3_6.

Markou, G., Angelidaki, I. and Georgakakis, D. (2012) 'Microalgal carbohydrates: An overview of the factors influencing carbohydrates production, and of main bioconversion technologies for production of biofuels', *Applied Microbiology and Biotechnology*, 96(3), pp. 631–645. doi: 10.1007/s00253-012-4398-0.

McBride, R. C. *et al.* (2014) 'Contamination Management in Low Cost Open Algae Ponds for Biofuels Production', *Industrial Biotechnology*, 10(3), pp. 221–227. doi: 10.1089/ind.2013.0036.

Mercer, P. and Armenta, R. E. (2011) 'Developments in oil extraction from microalgae', *European Journal of Lipid Science and Technology*, 113(5), pp. 539–547. doi: 10.1002/ejlt.201000455.

Medipally, S. R. et al. (2015) 'Microalgae as Sustainable Renewable Energy Feedstock for Biofuel Production, Microalgae as Sustainable Renewable Energy Feedstock for Biofuel Production', BioMed Research International, BioMed Research International, 2015, 2015, p. e519513. doi: 10.1155/2015/519513, 10.1155/2015/519513.

Middelberg, A. P. J. (1995) 'Process-scale disruption of microorganisms', *Biotechnology Advances*, 13(3), pp. 491–551. doi: 10.1016/0734-9750(95)02007-P.

Miller, R. *et al.* (2010) 'Changes in Transcript Abundance in Chlamydomonas reinhardtii following Nitrogen Deprivation Predict Diversion of Metabolism', *Plant Physiology*, 154(4), pp. 1737–1752. doi: 10.1104/pp.110.165159.

Miranda, J. R., Passarinho, P. C. and Gouveia, L. (2012) 'Bioethanol production from Scenedesmus obliquus sugars: The influence of photobioreactors and culture conditions on biomass production', *Applied Microbiology and Biotechnology*, 96(2), pp. 555–564. doi: 10.1007/s00253-012-4338-z.

Mishra, S. K. *et al.* (2014) 'Rapid quantification of microalgal lipids in aqueous medium by a simple colorimetric method', *Bioresource Technology*. Elsevier Ltd, 155, pp. 330–333. doi: 10.1016/j.biortech.2013.12.077.

Moellering, E. R. and Benning, C. (2010) 'RNA interference silencing of a major lipid droplet protein affects lipid droplet size in Chlamydomonas reinhardtii', *Eukaryotic Cell*, 9(1), pp. 97–106. doi: 10.1128/EC.00203-09.

Mohd Nani, S. Z. *et al.* (2016) 'Potential health benefits of deep sea water: A review', *Evidence-based Complementary and Alternative Medicine*, 2016. doi: 10.1155/2016/6520475.

Mulders, K. J. M. et al. (2014) 'Phototrophic pigment production with microalgae: Biological constraints and opportunities', Journal of Phycology, 50(2), pp. 229–242. doi: 10.1111/jpy.12173.

Nautiyal, P., Subramanian, K. A. and Dastidar, M. G. (2014) *Recent Advancements in the Production of Biodiesel from Algae: A Review, Reference Module in Earth Systems and Environmental Sciences*. Elsevier Inc. doi: 10.1016/B978-0-12-409548-9.09380-5.

Nguyen, H. M. *et al.* (2012) 'Proteomic profiling of oil bodies isolated from the unicellular green microalga Chlamydomonas reinhardtii: With focus on proteins involved in lipid metabolism', *Proteomics*, 11(21), pp. 4266–4273. doi: 10.1002/pmic.201100114.

Nomanbhay, S. and Ong, M. Y. (2017) 'A Review of Microwave-Assisted Reactions for Biodiesel Production', *Bioengineering*, 4(4), p. 57. doi: 10.3390/bioengineering4020057.

Nichols, P. D. et al. (2016) 'NEW AUSTRALIAN SINGLE CELL AND CROP PLANT SOURCES OF HEALTH-ENHANCING LONG-CHAIN OMEGA-3 OILS', (October 2003).

Ogbonna, J. C. and Tanaka, H. (2000) 'Light requirement and photosynthetic cell cultivation – Development of processes for efficient light utilization in photobioreactors', Journal of Applied Phycology, 12(X), pp. 207–218. doi: 10.1023/A:1008194627239.

Olaizola, M. (2000) '2000 Commercial production of astaxanthin from Haematococcus.pdf', pp. 499–506.

Padmavathi, P. and Veeraiah, K. (2009) 'Studies on the influence of Microcystis aeruginosa on the ecology and fish production of carp culture ponds', *Journal of Biotechnology*, 8(9), pp. 1911–1918.

Pancha, I. *et al.* (2014) 'Nitrogen stress triggered biochemical and morphological changes in the microalgae Scenedesmus sp. CCNM 1077', *Bioresource Technology*. Elsevier Ltd, 156, pp. 146–154. doi: 10.1016/j.biortech.2014.01.025.

Paniagua-Michel, J. (2015) *Microalgal Nutraceuticals, Handbook of Marine Microalgae: Biotechnology Advances*. Elsevier Inc. doi: 10.1016/B978-0-12-800776-1.00016-9.

Paper, C., City, R. A. and Scientific, O. (2015) 'Green Renewable Energy for Sustainable Socio-Economic Development', (SEPTEMBER).

Parmar, A. *et al.* (2011) 'Purification, characterization and comparison of phycoerythrins from three different marine cyanobacterial cultures', *Bioresource Technology*. Elsevier Ltd, 102(2), pp. 1795–1802. doi: 10.1016/j.biortech.2010.09.025.

Patel, A. *et al.* (2005) 'Purification and characterization of C-Phycocyanin from cyanobacterial species of marine and freshwater habitat', *Protein Expression and Purification*, 40(2), pp. 248–255. doi: 10.1016/j.pep.2004.10.028.

Pieber, S., Schober, S. and Mittelbach, M. (2012) 'Pressurized fluid extraction of polyunsaturated fatty acids from the microalga Nannochloropsis oculata', *Biomass and Bioenergy*. Elsevier Ltd, 47(December 2012), pp. 474–482. doi: 10.1016/j.biombioe.2012.10.019.

Pruvost, J. *et al.* (2011) 'Systematic investigation of biomass and lipid productivity by microalgae in photobioreactors for biodiesel application', *Bioresource Technology*. Elsevier Ltd, 102(1), pp. 150–158. doi: 10.1016/j.biortech.2010.06.153.

Przytocka-Jusiak, M. *et al.* (1984) 'Removal of nitrogen from industrial wastewaters with the use of algal rotating disks and denitrification packed bed reactor', *Water Research*, 18(9), pp. 1077–1082. doi: 10.1016/0043-1354(84)90221-5.

Radakovits, R., Eduafo, P. M. and Posewitz, M. C. (2011) 'Genetic engineering of fatty acid chain length in Phaeodactylum tricornutum', *Metabolic Engineering*. Elsevier, 13(1), pp. 89–95. doi: 10.1016/j.ymben.2010.10.003.

Rajendran, A. and Anderson, G. A. (2013) 'Light in a Photobioreactor', 2013 Kansas City, Missouri, July 21 - July 24, 2013, (January). doi: 10.13031/aim.20131620672.

Ramos, M. J. *et al.* (2009) 'Influence of fatty acid composition of raw materials on biodiesel properties', *Bioresource Technology*, 100(1), pp. 261–268. doi: 10.1016/j.biortech.2008.06.039.

Ranjith Kumar, R., Hanumantha Rao, P. and Arumugam, M. (2015) 'Lipid Extraction Methods from Microalgae: A Comprehensive Review', *Frontiers in Energy Research*, 2(January), pp. 1–9. doi: 10.3389/fenrg.2014.00061.

Ras, M., Steyer, J. P. and Bernard, O. (2013) 'Temperature effect on microalgae: A crucial factor for outdoor production', *Reviews in Environmental Science and Biotechnology*, 12(2), pp. 153–164. doi: 10.1007/s11157-013-9310-6.

Ravindran, B. et al. (2016) 'Microalgae potential and multiple roles-current progress and future prospects-an overview', Sustainability (Switzerland), 8(12), pp. 1–16. doi: 10.3390/su8121215.

Rittmann, B. E. (2008) 'Opportunities for renewable bioenergy using microorganisms', *Biotechnology and Bioengineering*, 100(2), pp. 203–212. doi: 10.1002/bit.21875.

Roberts, K., Phillips, J. M. and Hills, G. J. (1974) 'Structure, composition and morphogenesis of the cell wall of Chlamydomonas reinhardi. VI. The flagellar collar', *Micron (1969)*, 5(4), pp. 341–357. doi: 10.1016/0047-7206(74)90021-1.

Saha, S. and Murray, P. (2018) 'Exploitation of Microalgae Species for Nutraceutical Purposes: Cultivation Aspects', *Fermentation*, 4(2), p. 46. doi: 10.3390/fermentation4020046.

Sahad, N., Md. Som, A. and Sulaiman, A. (2014) 'Review of green solvents for oil extraction from natural products using different extraction methods', *Applied Mechanics and Materials*, 661(June), pp. 58–62. doi: 10.4028/www.scientific.net/AMM.661.58.

Saifuddin and Fazlili (2009) 'Effect of Microwave and Ultrasonic Pretreatments on Biogas Production from Anaerobic Digestion of Palm Oil Mill Effleunt', *American Journal of Engineering and Applied Sciences*, 2(1), pp. 139–146. doi: 10.3844/ajeas.2009.139.146.

Sato, N. *et al.* (2000) 'Environmental effects on acidic lipids of thylakoid membranes.', *Biochemical Society transactions*, 28(6), pp. 912–914. doi: 10.1042/BST0280912.

Shah, M. M. R. *et al.* (2016) 'Astaxanthin-Producing Green Microalga Haematococcus pluvialis: From Single Cell to High Value Commercial Products', *Frontiers in Plant Science*, 7(April). doi: 10.3389/fpls.2016.00531.

Shahidi, F. and Brown, J. (1998) 'Carotenoid Pigments in Seafoods and Aquaculture', *Food Science and Nutrition*, pp. 37–41.

Sharma, K. K., Schuhmann, H. and Schenk, P. M. (2012) 'High lipid induction in microalgae for biodiesel production', *Energies*, 5(5), pp. 1532–1553. doi: 10.3390/en5051532.

Sharma, P. and Sharma, N. (2017) 'Industrial and Biotechnological Applications of Algae: A Review', *Journal of Advances in Plant Biology*, 1(1), pp. 1–25. doi: 10.14302/issn.2638-4469.japb-17-1534.

Siaut, M. *et al.* (2011) 'Oil accumulation in the model green alga Chlamydomonas reinhardtii: characterization, variability between common laboratory strains and relationship with starch reserves.', *BMC biotechnology*, 11(1), p. 7. doi: 10.1186/1472-6750-11-7.

Takagi, M., Karseno and Yoshida, T. (2006) 'Effect of salt concentration on intracellular accumulation of lipids and triacylglyceride in marine microalgae Dunaliella cells', *Journal of Bioscience and Bioengineering*, 101(3), pp. 223–226. doi: 10.1263/jbb.101.223.

Tatsuzawa, H. and Takizawa, E. (1996) 'Fatty Acid and Lipid Composition of T H E Acidophilic', *Symposium A Quarterly Journal In Modern Foreign Literatures*, 601, pp. 598–601.

Tjellstrom, H. *et al.* (2012) 'Rapid Kinetic Labeling of Arabidopsis Cell Suspension Cultures: Implications for Models of Lipid Export from Plastids', *Plant Physiology*, 158(2), pp. 601–611. doi: 10.1104/pp.111.186122.

Topare, N. S. *et al.* (2011) 'Extraction of oil from algae by solvent extraction and oil expeller method', *International Journal of Chemical Sciences*, 9(4), pp. 1746–1750. doi: 10.1016/j.psychres.2013.12.056.

Tulashie, S. K. and Salifu, S. (2017) 'Potential production of biodiesel from green microalgae', Biofuels. Taylor & Francis, 0(0), pp. 1–8. doi: 10.1080/17597269.2017.1348188.

Valdivia-lefort, P. (2011) 'An Optimal Harvesting and Dewatering System Mechanism for Microalgae', *Jornal of Agricultural Machinery Science*, 7(2), pp. 211–215.

Varshney, P. et al. (2015) 'Extremophilic micro-algae and their potential contribution in biotechnology', Bioresource Technology. Elsevier Ltd, 184, pp. 363–372. doi: 10.1016/j.biortech.2014.11.040.

Vonshak, A. (1997) *Spirulina platensis (Arthrospira) Physiology, cell-biology and biotechnology*.

Wang, Z. T. *et al.* (2009) 'Algal lipid bodies: Stress induction, purification, and biochemical characterization in wild-type and starchless chlamydomonas reinhardtit', *Eukaryotic Cell*, 8(12), pp. 1856–1868. doi: 10.1128/EC.00272-09.

Wijffels, R. H. and Barbosa, J. M. (2010) 'Perspective. An Outlook on Microalgal Biofuels', Science \r, Vol. 329(November), pp. 796–799.

Wilhelm, C. and Jakob, T. (2011) 'From photons to biomass and biofuels: Evaluation of different strategies for the improvement of algal biotechnology based on comparative energy balances', *Applied Microbiology and Biotechnology*, 92(5), pp. 909–919. doi: 10.1007/s00253-011-3627-2.

Wingfield, J. and Lechtreck, K.-F. (2018) 'Chlamydomonas Basal Bodies as Flagella Organizing Centers', *Cells*, 7(7), p. 79. doi: 10.3390/cells7070079.

Woertz, I. *et al.* (2009) 'Algae Grown on Dairy and Municipal Wastewater for Simultaneous Nutrient Removal and Lipid Production for Biofuel Feedstock', *Journal of Environmental Engineering*, 135(11), pp. 1115–1122. doi: 10.1061/(ASCE)EE.1943-7870.0000129.

Wu *et al.* (2012) 'Evaluation of flocculation induced by pH increase for harvesting microalgae and reuse of flocculated medium', *Bioresource Technology*. Elsevier Ltd, pp. 496–502. doi: 10.1016/j.biortech.2012.01.101.

Wu, T. et al. (2015) 'Ultrasonic disruption of yeast cells: Underlying mechanism and effects of processing parameters', Innovative Food Science and Emerging Technologies. Elsevier Ltd, 28, pp. 59–65. doi: 10.1016/j.ifset.2015.01.005.

Xia, C. *et al.* (2011) 'A new cultivation method for microbial oil production: Cell pelletization and lipid accumulation by Mucor circinelloides', *Biotechnology for Biofuels*, 4(September). doi: 10.1186/1754-6834-4-15.

Yuan-Kun, L. (1997) 'Commercial production of microalgae in the Asia-Pacific rim', *Journal of Applied Phycology*, 9, pp. 403–411.

Yusaf, T. and Al-Juboori, R. A. (2014) 'Alternative methods of microorganism disruption for agricultural applications', Applied Energy. Elsevier Ltd, 114, pp. 909–923. doi: 10.1016/j.apenergy.2013.08.085.

Zachleder, V., Bisova, K. and Vitova, M. (2016) *The Physiology of Microalgae*. doi: 10.1007/978-3-319-24945-2.

Zeldes, B. M. *et al.* (2015) 'Extremely thermophilic microorganisms as metabolic engineering platforms for production of fuels and industrial chemicals', *Frontiers in Microbiology*, 6(NOV). doi: 10.3389/fmicb.2015.01209.

Zhang, X. (2015) 'Microalgae removal of CO2 from flue gas', (April 2015), p. 95. doi: 10.1016/j.biortech.2012.01.008.

Zhu, L. D., Li, Z. H. and Hiltunen, E. (2016) 'Strategies for Lipid Production Improvement in Microalgae as a Biodiesel Feedstock', *BioMed Research International*, 2016, pp. 7–9. doi: 10.1155/2016/8792548.

Zhu, L., Li, Z. and Ketola, T. (2011) 'Biomass accumulations and nutrient uptake of plants cultivated on artificial floating beds in chinas rural area', *Ecological Engineering*. Elsevier B.V., 37(10), pp. 1460–1466. doi: 10.1016/j.ecoleng.2011.03.010.

Zones, M. J. et al. (2015) 'High-Resolution Profiling of a Synchronized Diurnal Transcriptome from Chlamydomonas reinhardtii Reveals Continuous Cell and Metabolic Differentiation', The Plant Cell, 27(October), pp. 2743–2769. doi: 10.1105/tpc.15.00498.

CHAPTER II - Materials and methods

Table of contents

References

1. Culture conditions

The microalgae strains studied during this work were: *Chlamydomonas reinhardtii* SAG-34.98 (**Wild type**) and *C.reinhardtii* SAG-83.81(**Cell wall deficient mutant strain**). The cells were cultured in TAP growth media with the following components: NH_4Cl, $MgSO_4.7H_2O$ and $CaCl_2$. $2H_2O$ for the salt solution, K_2HPO_4 and KH_2PO_4 for the phosphate solution, tris and Hutner's trace elements (the detailed protocol is in the Annex section).

1.1. Growth conditions

Both microalgae strains (wild type and mutant) were cultured under photo-autotrophic conditions in a total culture volume of 50 mL. They were incubated shake incubator (Minitron, Infors HT, Bottmingen, Switzerland) and agitated at 100 rpm under a light intensity of 20 $\mu mol \cdot m^{-2} \cdot s^{-1}$. The temperature and air injection were held constant at 25 °C and 1.5 % CO_2 respectively.

Figure 1: Shake incubator used for the growth cultivation step.

1.2. Characterization of the algae culture

Flow cytometry analysis was sued to determine the **cell viability, permeability and lysis**. Cell permeability was evaluated using the following dyes: Propidium Iodide (PI, binds to double stranded DNA) or Sytox Green (SG, nucleic acid binding). Fluorescein diacetate (FDA) was used for the cell viability analysis as it indicates the enzymatic activity of the cell. Viable cells have active esterases that enable the hydrolysis of the non-fluorescent FDA which leads to the emission of fluorescence (detected through the green channel of the cytometer).

The cell concentration (analyzed to evaluate cell lysis) and fluorescence intensities were measured using a Guava easyCyte microcapillary flow cytometer (EMD Millipore Corporation, 25801 Industrial Blvd., Hayward, CA 94545, USA). This cytometry system includes a single blue excitation laser (488 nm) and 3 fluorescence detector channels plus forward scatter (FSc)

and side scatter (SSc). Once the sample is labeled with a specific fluorescent dye, it is placed for analysis, and aspirated into the flow cell.

The algal cells within the sample are then detected once they pass through the laser, and individually analyzed (Figure 2). The system then uses the scattered light to sort out the cells. The forward scatter is proportional to the size of the cell and the side scatter is proportional to the shape and the internal complexity of the cell.

After determining our population of cells (excluding cell debris) and its concentration from the light scatter signal, it is then possible to analyze the fluorescent signals from each detector channel with the software InCyte 2.7. For each sample, the number of cells analyzed was typically in the range of 2500 to 5000.

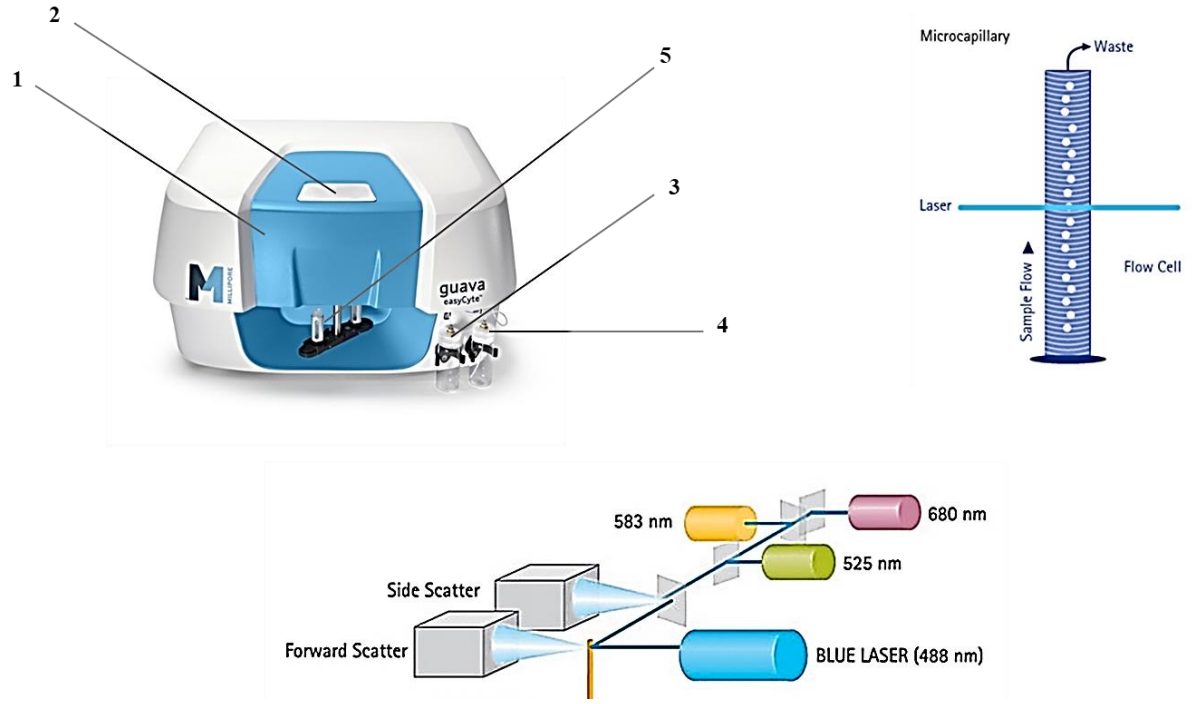

Figure 2: Flow cytometer used during our experiments for the analysis of cell concentration, viability and permeability. 1: detection zone (up to 12 parameters); 2: Microcapillary flow cell (shown also on the upper right); 3: waste vial; 4: cleaning solution vial; 5: sample loader. On the bottom of the figure: the blue laser trajectory through the forward and side scatter and the 3 fluorescence detector channels (Source: Guava InCyte manual).

All staining procedures were first developed and optimized to determine the following conditions for an optimal labelling: incubation time and final dye concentration in the cell sample. During staining the sample was incubated in the dark, and rotatively agitated at an ambient temperature.

To analyze cell lysis in our microalgae sample, cell concentration was first validated by comparing the cell concentration given by the flow cytometer with the cell concentration given by the Hemocytometer. This enabled us to determine the adequate cell concentration range for

the analysis using the flow cytometer. The obtained range was from 8 x 10^4 cells·mL^{-1} to 2 x 10^6 cells·mL^{-1}.

1.3. Stress conditions for a lipid accumulation

To induce lipid accumulation, cultures from the growth conditions were transferred to the experimental setup permitting stress conditions for the accumulation of lipids (figure x). It involves an agitator (100 rpm continuous agitation), higher light intensity (150 µmol·m^{-2}·s^{-1}), atmospheric CO_2 (0.004 %) and a constant temperature of 25 ° C ± 0.5. In addition, the culture medium was also modified to induce nitrogen starvation stress: NH_4Cl was removed.

Figure 3: Experimental setup for the stress conditions.

1.4. Characterization of the lipid accumulation

Lipid quantification is another important step in the production of microalgal biofuels. Indeed, to select the most appropriate algae strain (for example, in terms of its lipid yield, or its adaptability to environmental changes) and culture conditions, it is necessary to be able to quantify in a simple and fast way the lipid content. It is also required in the optimization step of the lipid extraction, for example to test the potential of a pretreatment on the extraction efficiency. Thus, lipid screening techniques are also highly investigated for algal lipids, mainly by studying the techniques previously established since the early 30's for the screening of non-algal lipids. Moreover, screening techniques are usually suitable for specific needs including the sample volume, the lipid content and the algae strain. The development of techniques that could adapt to different conditions are even more praised. Some of the most recent techniques are based on gravimetric analysis, staining techniques or colorimetric methods.

Gravimetric quantification methods are very popular for an accurate and precise macro-quantitative analysis. It is based on the measurement of the analyte's mass. After determining the targeted ion's mass, it is then possible to determine its proportion in a mixture. There are various ways to apply this method, each baring their own advantages and disadvantages: precipitation, volatilization or electro-analytical methods.

Before a gravimetric analysis, the algae are first harvested then submitted to a lipid extraction (on a dry or wet biomass); the extract is then dried for analysis. This method requires a relatively large amount of sample and is time consuming. It is however known as one of the most accurate method for lipid analysis.

Staining methods refer to the use of lipophilic dyes such as Nile Red and Bodipy because they have a high selective affinity to the intracellular neutral lipids. In the case of algal lipids, Bodipy or Nile Red staining is useful for the optimization of pretreatments for an optimal lipid extraction; however, the staining method should be optimized for each algal species. **Bodipy 505/515** staining was used in this work as a first step to characterize and optimize the lipid accumulation of *C. reinhardtii*. The staining protocol was initially optimized in terms of dye concentration, incubation time, and washing or no washing before cytometric analysis. Subsequently, for the lipid quantification, for example in the solvent extraction experiment, the colorimetric **Sulfo-Phospho-Vanillin (SPV) method** was used.

The colorimetric **SPV method** was first introduced by Chabrol and Charonnat in 1937 (Chabrol and Charonnat, 1937), then further modified by other investigators. This method is based on the reaction between lipids and other molecules that ultimately generates a colored compound (Figure 4) that is photometrically measured (absorbance at 530 nm was read using a Thermo Scientific spectrophotometer). It is usually used to validate a high throughput method for total lipids analysis. It presents various advantages such as rapid and simple, suitable for small volumes of samples and permits the analysis of multiple samples at once, without being excessively time-consuming.

The detailed protocol is described in the Annex section.

Figure 4: Samples after SPV protocol.

After solvent extraction, the total lipid content in the remaining aqueous phase after was calculated using the following equations:

$$Total\ remaining\ lipid\ content\ (\%) = (1 - \frac{Abs_1}{Abs_0}) \times 100$$

The total remaining lipid content in µg was calculated as an equivalent of Triolein, as follows:

$$Total\ remaining\ lipid\ content(\mu g) = \frac{Abs_{sample}}{0.003}$$

where Abs1 corresponds to the absorbance of the tested sample (after extraction) and Abs0 the absorbance of cells before extraction.

2. Pretreatments

2.1. Mechanical treatment

Microfluidic devices for microalgal applications

Many microfluidic lab-on-chip systems have emerged for the past few years for an application in microalgal biotechnology. They have the potential to offer several advantages such as: **cost and time efficient** technique to further advance in microalgal biofuel and bioproduction research, analysis at a cellular scale with **high precision** and **high-throughput assays**.

The first fabricated microsystems were semiconductor devices in 1968 (i.e. diodes, transistors and integrated circuits) and the primary semiconductor material used was and still is silicon (Dietzel, 2016). From the semiconductor fabrication technology, numerous techniques have emerged such as photolithography, soft lithography, replica molding, and etching (Fiorini and Chiu, 2005). They enable micromachining of various materials such as polymers, silicon, glass and metals. Therefore today, there is a wide range of microsystems such as microelectromechanical systems (**MEMS**), microoptoelectromechanical systems (**MOEMS**), biomedical (or biological) microelectromechanical systems (**BioMEMS**) and **lab-on-chip** and **organ-on-chip** systems.

A typical fabrication of a microfluidic chip (involving the use of a clean room) includes: a **photolithography** process (also known as UV-lithography) for the fabrication of a SU-8 patterned master composed of an epoxy-based photoresist (SU-8) layer (or multiple layers) and a substrate (wafer) and a **soft lithography** process for fabrication of the microfluidic chip, and where a wide range of elastomeric materials can be used such as polymers and gels (Figure 5). The most widely used elastomer however is **PDMS** (PolyDiMethylSiloxane) as it offers several advantages such as low cost, biocompatibility, low toxicity and mechanical flexibility and durability.

In the context of biofuel and bioproduction research, microfluidic systems are highly investigated. Numerous microfluidic devices were developed in the last years for microalgal applications including strain selection and development (i.e. identification of species, cell characterization, cell sorting and cell transformation), cell cultivation and harvesting, lipid extraction and biomass processing (Kim, Devarenne and Han, 2018).

Experimental setup

The microfluidic device, designed and fabricated (using photolithography and soft lithography) for our study consisted of a series of microfluidic channels with restrictions of 5 µm (width and height). 7-days stressed *C. reinhardtii* cells (mean diameter: 10 µm) would enter these channels and flow through the restrictions (with a flow rate of 1.11 $\mu L \cdot s^{-1}$). This generated successive compressive stress on the microalgae cells.

The experimental setup consisted of a microfluidic pressure pump (AF1 Pressure Generator, Elveflow), the algal solution in a container connected to the pressure pump, a magnetic stirrer (to avoid cell sedimentation and therefore maintain a constant cell concentration during the experiment) and the microfluidic chip (Figure 6).

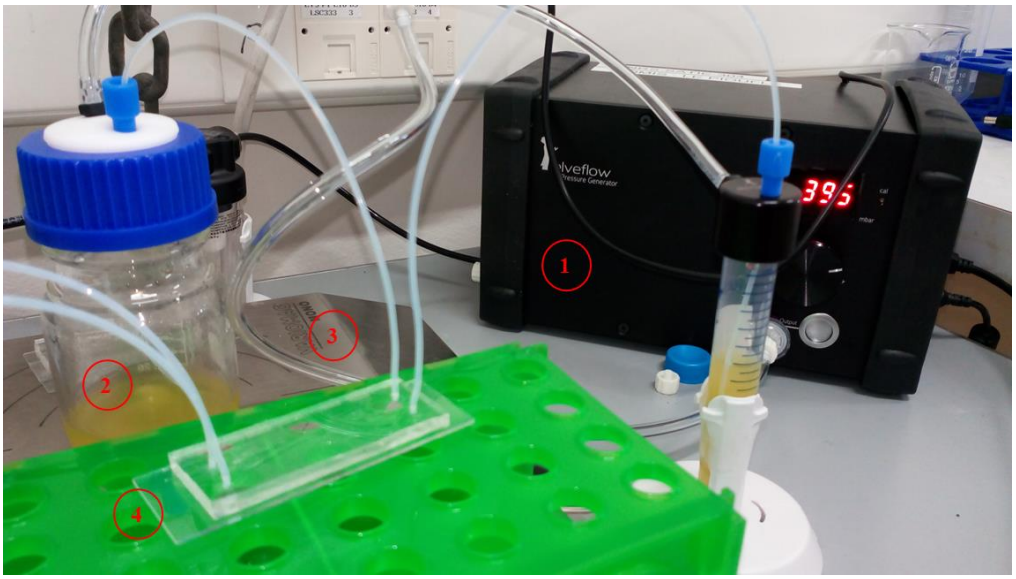

Figure 5: Experimental setup for the mechanical compression treatment (1: pressure pump; 2: algal solution container; 3: magnetic agitator; 4: microfluidic chip).

The microfluidic chip included 8 analysis frames, each composed of 24 parallel thin microchannels with the successive restrictions.

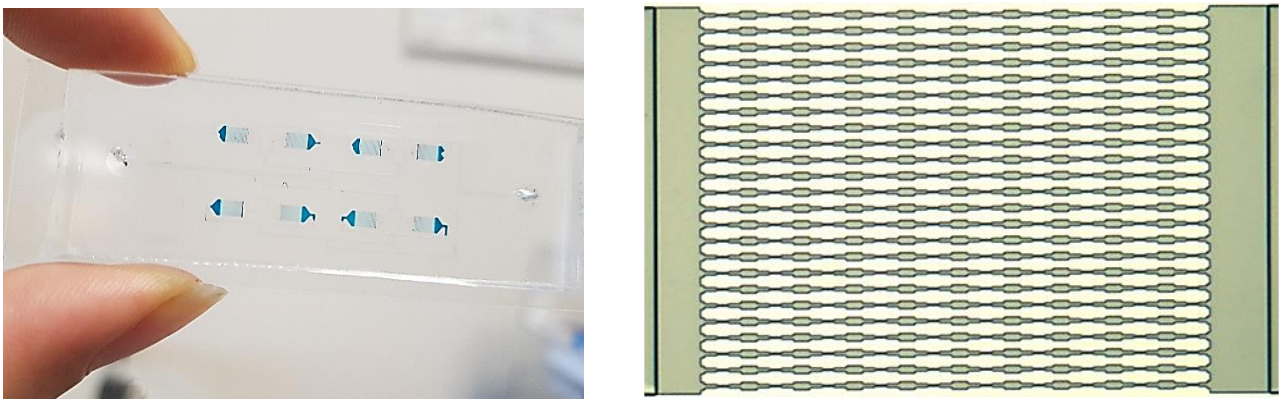

Figure 6: Microfluidic chip showing the 8 analysis frames (blue colorant) on the left and one analysis frame including the restrictions on the right.

2.2. **PEF treatment**

Principle

Pulsed Electric Field (PEF) technology involves the application of **repeated short pulses** of an electric field E with duration of microsecond to milliseconds (ms) and intensity ($V \cdot m^{-1}$) that is **created between two electrodes** (the distance between the electrodes is also known as the PEF chamber's treatment gap). This application of repeated pulses, typically employed on cells or tissues, generates pores on the membrane (Figure 8).

Pore creation is first initiated by a water defect into the phospholipid bilayer interior (**pore initiation**) and the phospholipid polar head groups then reorganize around the defect (**pore construction**). This proceeds with the migration of additional water and polar head groups into the pore, until it stabilizes into a mature pore structure (**pore maturation**). When the electric field application is terminated, it leads to the annihilation of the pore. At this point, the pore size starts decreasing with the polar head groups that migrate out of the membrane interior and back to their initial position, separated into two groups (**pore degradation deconstruction**). The remaining polar molecules, including water, also follow this trend and move out of the interior membrane (**pore dissolution**). Finally, the initial structure of the bilayer is restored.

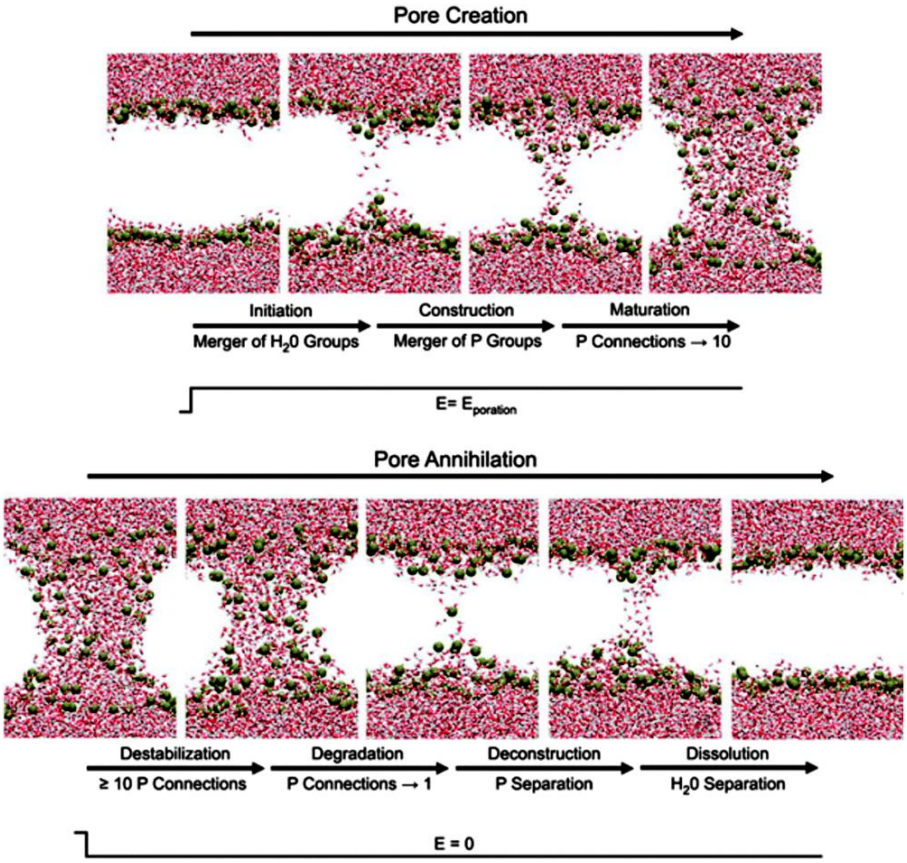

Figure 7: Pore creation and destruction dynamics (Levine and Vernier, 2010). Polar molecules (water) are shown in red and polar head groups in green.

Overall, the applied electric field E generates a **charge displacement** in the intracellular medium (cytoplasm) and in the extracellular medium which leads to an induced voltage called the membrane potential. This membrane voltage or transmembrane potential ($\Delta\Phi_m$), induced by the electric field, reaches a critical value ($\Delta\Phi_c$) which destabilizes the phospholipid bilayer and creates a pore. The pore creation leads to a new charge displacement that modifies the intracellular charge gradient leading to the formation of additional pores (Zimmermann, 1986; Kotnik *et al.*, 2012).

Electroporation (defined as the electrical breakdown of cell membranes) can be characterized as **reversible or irreversible** (Figure 9). Reversible electroporation means that the cell is capable to reseal back its membrane while irreversible electroporation involves a cell membrane that is unable to reseal back and regain its initial structure (Joannes *et al.*, 2015).

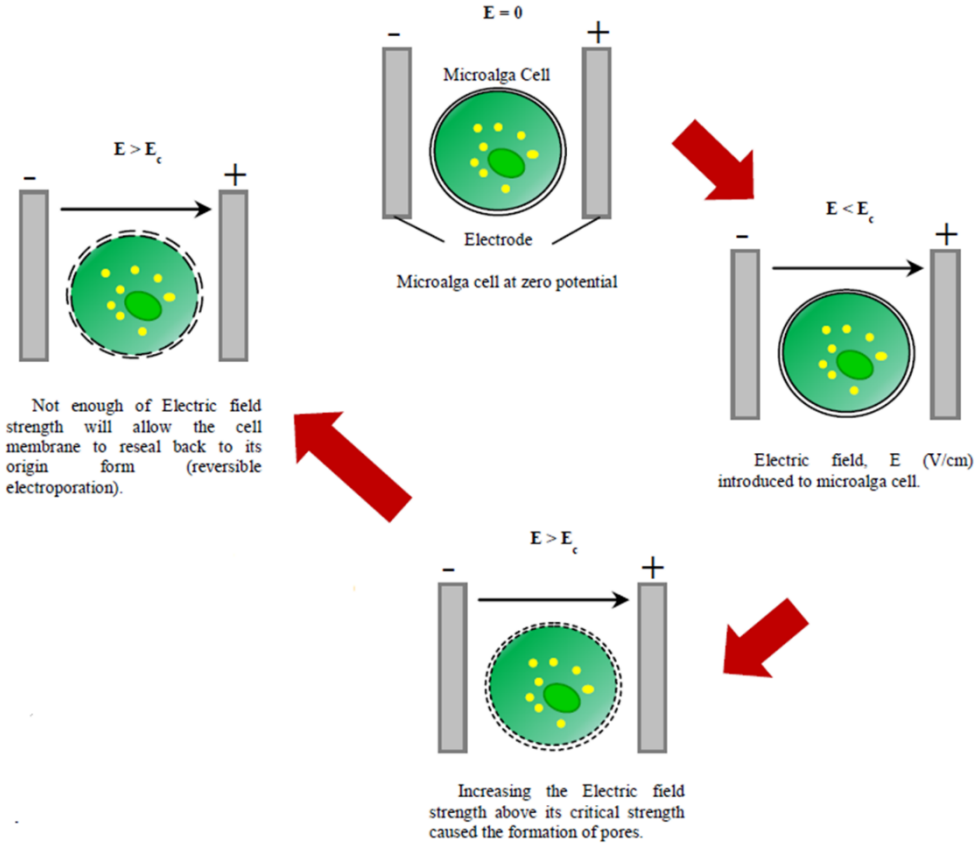

Figure 8: Schematic representation of the permeabilization mechanism when the microalga's membrane is exposed to an electric field E (modified from Joannes et al., 2015). Ec: critical electric field strength.

Typically, a PEF system will include the following components: a **control system**, that monitors the parameters for the applied treatment, a **high voltage pulse generator** for the voltage supply and a **treatment chamber** which includes the treated sample (Figure 10). There are various designs for the treatment chamber such as parallel plate (Foltz, 2012; Goettel *et al.*, 2013; Zbinden *et al.*, 2013) and co-field (Flisar *et al.*, 2014; Kempkes, Roth and Gaudreau, 2015) treatments chambers. The parallel plate design is considered as the simplest chamber treatment in batch systems and for laboratory scale; the plate electrodes are disposed in parallel,

which ensures a uniform field strength. The co-field treatment chamber is mainly used in continuous systems and for large scale applications (Joannes *et al.*, 2015).

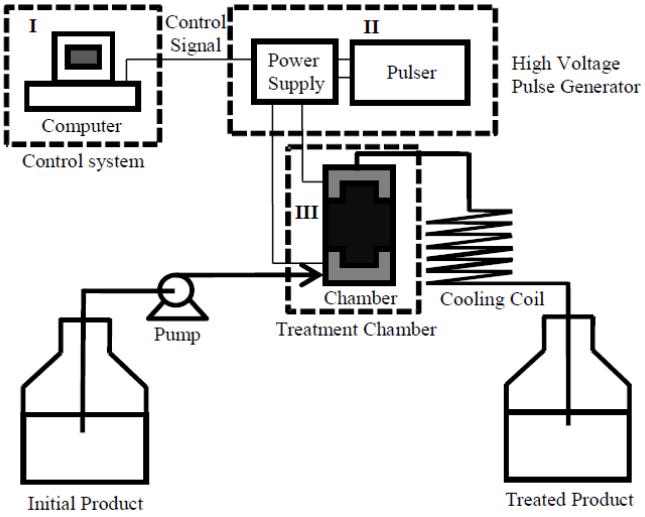

Figure 9: Typical PEF system showing the basic components (Joannes et al., 2015).

In the context of PEF treatment, several important points must be taken into consideration:

- Although it isn't always represented in simulations such as the one presented in Figure 1, the **plasma membrane is a complex system**, composed of a wide diversity of molecules such as lipids (phospholipids and cholesterol), proteins (transport channels…), carbohydrates groups attached to some of the lipids and proteins (glycolipids and glycoproteins) and cytoskeleton filaments.

- Even in the case where pores reseal, there may be possible long-term effects (lasting from seconds to hours) after a PEF treatment; this is called **memory effect** (Teissie, Golzio and Rols, 2005; Pavlin *et al.*, 2008).

- The **characterization of the microalgae**, such as the size and structure (for example the presence or not of a cell wall), can influence the efficiency of the PEF treatment (Foltz, 2012).

- The type of **electrode material** used is also a crucial factor in the good efficiency of the treatment. Electrode materials such as nickel, silver or gold are considered to permit a homogeneous electric field distribution (Reberšek *et al.*, 2014).

- As a result of the application of high currents, **side effects** such as joule heating and undesirable electrochemical reactions (most likely to occur at the interface between the electrode and the electrolyte) are possible (Pataro *et al.*, 2015; Ho, 2017).

Theoretical considerations

The resting and induced transmembrane potential are calculated using the following equations:

The **resting membrane potential** (or resting voltage) can be calculated with the Goldman–Hodgkin–Katz voltage equation, known as the **Goldman equation**, that takes into account the all ions that are permeant through the membrane:

$$Vm = \frac{RT}{F}\ln\left(\frac{p_K[K^+]_0 + p_{Na}[Na^+]_0 + p_{Cl}[Cl^+]_i}{p_K[K^+]_i + p_{Na}[Na^+]_i + p_{Cl}[Cl^+]_0}\right)$$

V_m is the resting membrane potential (Volt) and generally has a negative value. It varies depending on the cell type and typically ranges from - 20mV to - 100mV. For example, its value is around - 70 mV in a typical neuron cell. It has been reported to be around - 50 mV (- 0.05 V) for mammalian cells.

Constants, variables and parameters:

R corresponds to the universal gas constant (8.314 $J \cdot K^{-1} \cdot mol^{-1}$) and **F**, the Faraday's constant (96 485 $C \cdot mol^{-1}$).

T is the temperature in Kelvin (K = °C + 273.15).

p_K, **p_{Na}** and **p_{Cl}** are the relative membrane permeabilities for K^+, Na^+ and Cl^+ respectively.

$[K^+]_o$, **$[Na^+]_o$**, and **$[Cl^-]_o$** correspond to the concentration in the extracellular fluid of K^+, Na^+ and Cl^+ respectively.

$[K^+]_i$, **$[Na^+]_i$** and **$[Cl^-]_i$** are the concentration in the intracellular medium of K^+, Na^+ and Cl^+ respectively.

The **critical potential difference** ($\Delta\Phi_c$) which induces membrane permeabilization has in most cases, a positive value (mammalian cells) or is equal to zero (liposomes). It is known to be around 200 mV for various types of cell systems (Teissié and Rols, 1993).

The induced transmembrane potential difference ($\Delta\Phi_m$) is obtained using the **Schwan equation**, considering a spherical cell at a time t:

$$\Delta\Phi_m = -\frac{3}{2} \cdot r \cdot E \cdot \cos(\theta_M) \cdot [\,1 - e^{-\frac{t}{\tau_m}}\,]$$

Variables and parameters:

E ($V \cdot m^{-1}$) corresponds to the applied electric field (the potential V applied is divided by the distance between the electrodes).

r (m) is the cell radius. The cell size is therefore important to consider for the treatment. The larger the cell, the stronger the induced potential.

θ_M corresponds to the angle between the direction of the field and the normal to the cell surface at M with the direction out of the cell (Figure 11).

t (s) corresponds to the time after the field is turned on and τ_m (s) the **membrane charging time constant**. This parameter, generally in the range of 0.4 to 1 µs for mammalian cells (Frank S. Barnes, 2006), can be obtained using the following equations, depending on the model used; **single shell model** (commonly used for mammalian cells) and **double shell model** (preferred for plant cells since it takes into account the presence of a cell wall):

Single shell model: $$r \cdot C_m \left(\frac{1}{\sigma_{cyt}} + \frac{1}{2\sigma_{med}}\right)$$

Double shell model: $$r \cdot C_m \left(\frac{1}{\sigma_{cyt}} + \frac{\sigma_{med}+\sigma_{cw}}{2\sigma_{med}\sigma_{cw}}\right)$$

C_m ($F \cdot m^{-2}$) is the membrane capacitance, generally around 0.01 (Arnold and Zimmermann, 1982).

σ_{cyt}, σ_{med}, and σ_{cw} ($S \cdot m^{-1}$) correspond to the conductivities of the cytoplasm, medium and cell wall conductivities respectively. The membrane charging time is in the range 0.4 to 1 µs (Frank S. Barnes, 2006) and is generally considered much shorter than the pulse duration (Teissié and Rols, 1993).

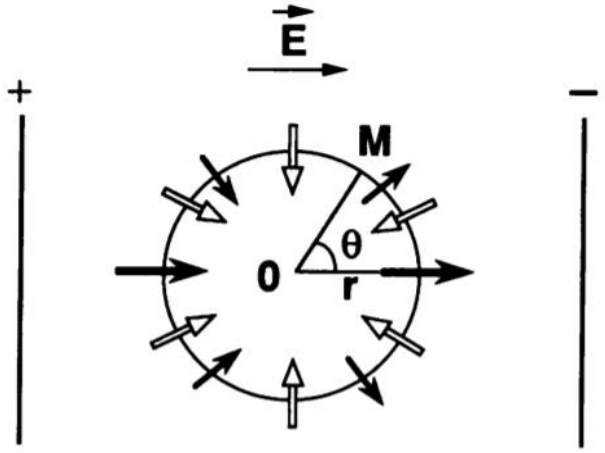

Figure 10: Schematic representation of a cell submitted to an external field E. The arrows correspond to the vectorial representation of the electrical potential gradient direction; open arrows = resting potential; closed arrows = electric field induced potential. Their length indicates the magnitude of the potential difference (Teissie and Rols, 1993).

Other important parameters

The total **temperature increase**, ΔT_{treat} (°K or °C), related to the treatment (in the absence of cooling) is proportional to the temperature increase of a single pulse (due to the Joule effect), ΔT_{pu} and the number of pulses applied during the treatment, N_{pu}. It is obtained using the following equation:

$$\Delta T_{treat} = \Delta T_{pu} \cdot N_{pu}$$

It is directly proportional to the spent energy **W** ($J \cdot m^{-3}$):

$$\Delta T = \frac{W}{C_p \cdot \rho} \quad \text{and} \quad W = |E|^2 \cdot \Delta t \cdot \sigma_{med}$$

Furthermore, the temperature increase of a single pulse depends on the medium conductivity, $\boldsymbol{\sigma_{med}}$ ($S \cdot m^{-1}$), medium heat capacity, $\mathbf{C_p}$ ($J \cdot K^{-1}$), medium volumetric mass density $\boldsymbol{\rho}$ ($kg \cdot m^{-3}$), the electric field strength, E ($V \cdot m^{-1}$) and the pulse duration $\boldsymbol{\Delta t_{pu}}$ (s):

$$\Delta T_{pu} = \frac{\sigma_{med}}{C_p \cdot \rho} \cdot |E|^2 \cdot \Delta t_{pu}$$

Pulse duration and electric field strength strongly influence the treatment's effect (Figure 12); the reversibility and irreversibility of the electroporation is correlated to the applied electric field strength and pulse duration. For example, if one desires to induce a same effect by using shorter pulses, the electric field strength will need to be increased.

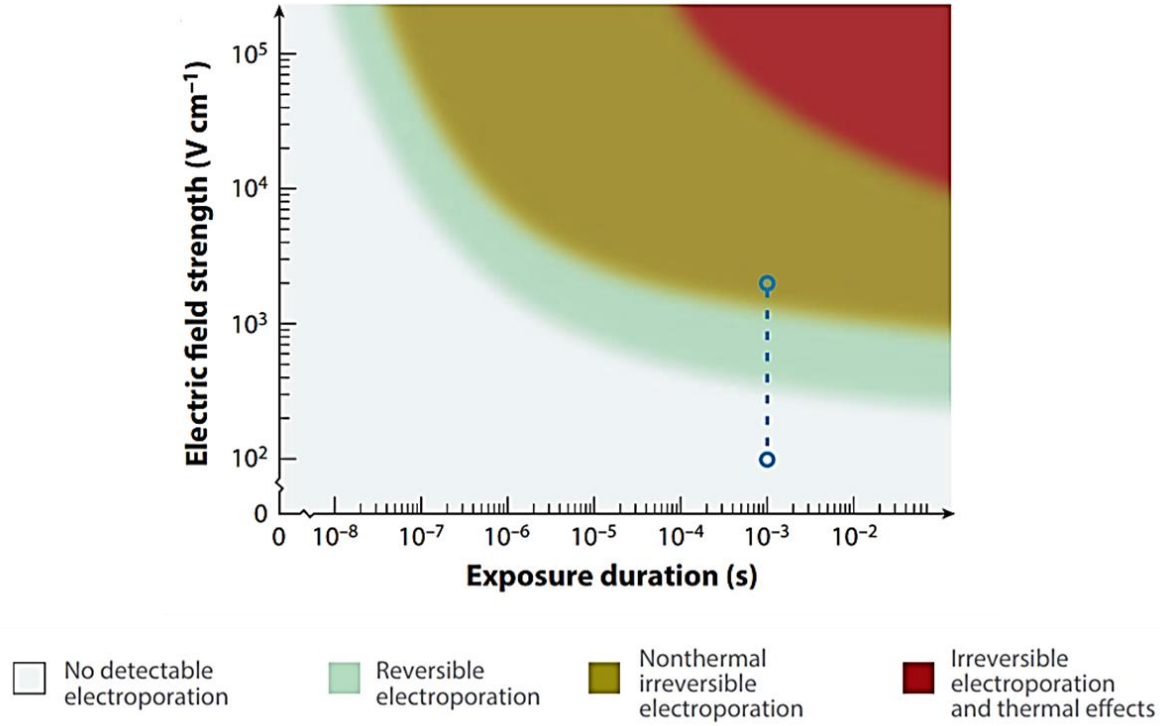

Figure 11: Relation between reversible/irreversible electroporation and thermal effects with the electric field strength (Yarmush et al., 2014).

Medium conductivity is an important factor that can influence the temperature increase during the treatment. Therefore, microalgae PEF treatments usually involve a low conductivity medium (Coustets *et al.*, 2013; Luengo *et al.*, 2014) or a cooling system (Zbinden *et al.*, 2013) in order to minimize heating.

A pulse can be characterized by its shape (square, exponential, trapezoidal, sinusoidal…) and frequency (Hz). Squared shaped pulses can either be monopolar or bipolar. Several studies have investigated the difference of effect between **monopolar and bipolar pulses** (Kotnik, Miklavčič and Mir, 2001; Ostapenko *et al.*, 2004; Brito *et al.*, 2012).

PEF applications

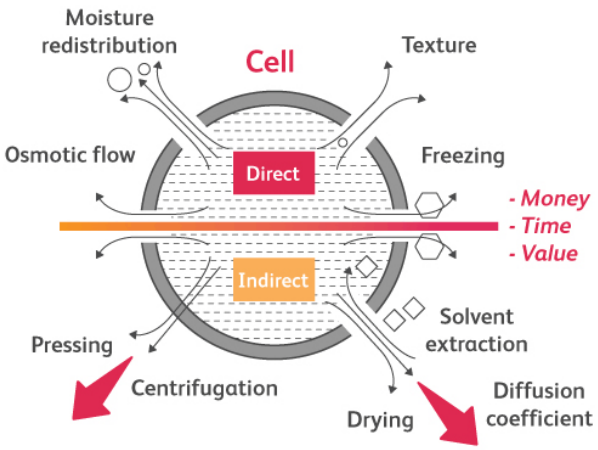

Figure 12: PEF processes and applications (Source: Pulsemaster)

Electroporation is widely used in various medical and biotechnological applications (Figure 13). Today, reversible electroporation is an established method in **electrochemotherapy**. It is used to introduce chemotherapeutic drugs into tumor cells (Haberl *et al.*, 2013). It is also an important technique in the field of **gene therapy** for DNA electrotransfer in various types of cells (André and Mir, 2004) On the other side, irreversible electroporation is widely used in biotechnology (for the extraction of biomolecules such as proteins, pigments and carbohydrates), bioengineering (lipid extraction, see Table 1), clinical medicine (tissue ablation) (Lee, Thai and Kee, 2010; Ho, 2017), food preservation (microbial deactivation) (Puc *et al.*, 2003) and water treatment (sterilization by killing pathogens and bacteria) (Schlager, 2005).

PEF treatment is highly investigated for a direct application or as a pretreatment prior to solvent extraction. The following Table summarizes numerous studies on the use of PEF treatment as a method for microalgae lipid extraction.

References	Flisar et al., 2014	Goettel et al., 2013	Foltz et al., 2012	Kempkes et al., 2015	Lai et al., 2014	Eing et al., 2013	Zbinden et al., 2013	Sheng et al., 2011
Purpose of Study	Lipid extraction	Intracellular and lipid extraction	Cell lyse observation	Lipid extraction	Lipid extraction	Lipid extraction	Lipid extraction	Lipid extraction
Batch or Continuous Treatment System	Continuous	Continuous	Batch	Continuous	Batch	Continuous	Batch	Batch
PEF Chamber Design	Co-field flow chamber	Paired in parallel with polycarbonate housing	Cubic millimeter chamber	Co-field flow chamber	Co-field flow chamber	Paired in parallel with polycarbonate housing	Modified UV cuvette	Co-field flow chamber
Electric Field Strength, E	2.7 kV/cm	23 k - 43 kV/cm	a: 0.15 kV/cm; b: 1.6 kV/cm; c: 4.0 kV/cm	20 k - 30 kV/cm	1st pass treatment: 30.6 kWh/m^3; 2nd pass treatment: 33.7 kWh/m^3	35 kV/cm	45 kV/cm	>35 kWh/m3
Pulse shape	Square wave	Square wave	a: Square wave; b & c: Exponential Decay	Square wave	Square wave	Square wave	Exponential decay	Square wave
Pulse duration, t	100 µs	1 µs	a: 33.3 s; b: 50 s; c: 20 s	1 – 10 µs	> 500 µs	1 µs	100 ms	> 500 µs
Type of electrode material	Stainless steel	Stainless steel	a & b: Silver/Silver chloride; c: Stainless steel	NA	NA	Stainless steel	Stainless steel	NA
Microalga Strain (s)	Chlorella vulgaris	Auxenochlorella protothecodies	a: Chlamydomonas reinhardtii; b: Dunaliella salina; c: Chlorella vulgaris	Isocrysis sp.	Scenedesmus spp.	Auxenochlorella protothecoides	Ankistrodesmus falcatus	Synechocystis PCC 6803 (cyanobacteria)
Lipid content by % of dry weight	14 - 40	20 - 25	a: NA; b: 14 – 20; c: 14 - 40	NA	19.6 – 21.1	20 - 25	40	NA
Extraction method								
Pre-treatment	PEF	PEF	PEF	PEF	FP	PEF	PEF	FP
Solvent extraction	-	-	-	-	Bligh & Dyer, Hexane, Isopropanol	Ethanol	Modified Bligh & Dyer	Isopropanol
Extracted Lipid	22 % wt	NA	NA	NA	Bligh & Dyer ≈ 23 % wt; Hexane≈ 10 %wt; Isopropanol ≈ 6 % wt	22 % wt	6.1 mg/L	25 – 75 % wt (FAME)

Table 1: Summary of studies on microalgae lipid extraction using PEF as a singular or co-method to a solvent extraction (modified from Joannes et al., 2015). FP corresponds to Focused-Pulsed (FP) technology which is an adaptation of PEF technology. In a study published by Lee et al. (2010), it was characterized as the application of a series of shorts high-voltage pulses. FP technology can lead to the expansion of existing pores (electroporation) and create new pores in the

Experimental setup

The experimental setup for PEF treatment was composed of: a bipolar pulse generator (Betatech Electrocell B10 HVLV) for the application of unipolar pulses. An electroporation cuvette (Bio-Rad, plastic material) including stainless steel electrodes with a gap (d=1 mm) and a sample volume of 130 µL was used (Figure 15).

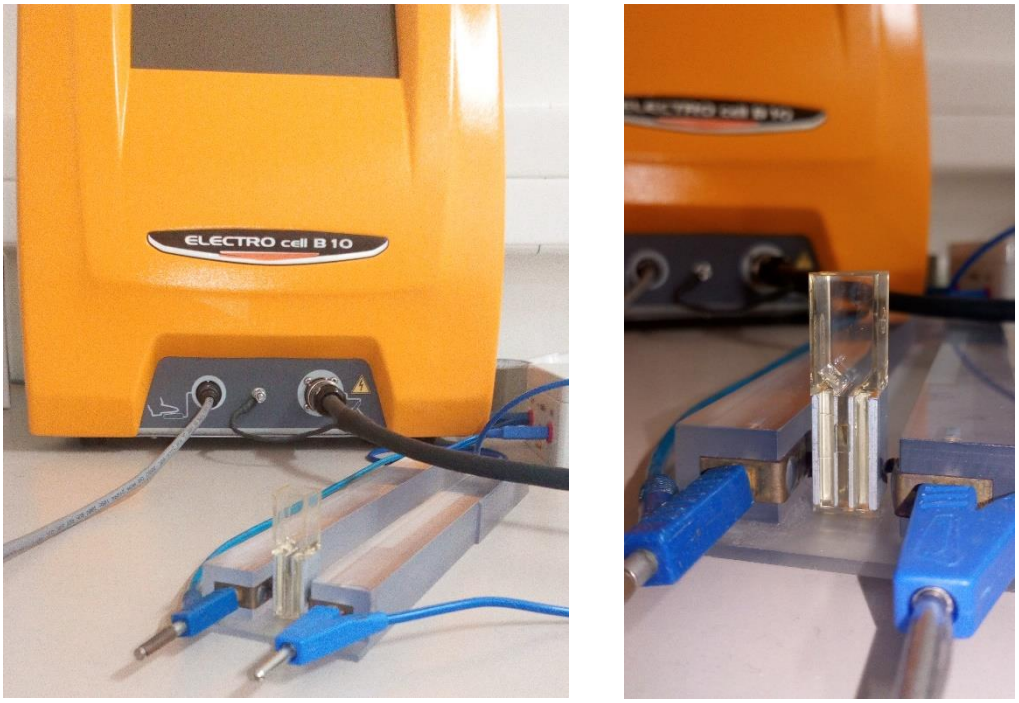

Figure 13: Experimental setup for the PEF treatment. The left image shows the pulse generator and the cuvette holder containing the cuvette and the right image focuses on the electroporation cuvette (1mm electrode gap).

3. Solvent extraction

3.1. Selected solvents

For the extraction of *C. reinhardtii*'s lipids, we used the solvent hexane for its well-known efficiency for the extraction of algal lipids. Hexane is part of the organic solvents commonly used for microalgae applications such as methanol, ethanol, chloroform and ethyl acetate. They all differ by properties such as: boiling point, polarity, solubility in water and density.

Another study was held to evaluate the effect of different solvents on the microalgae cells with the aim of understanding the mechanisms behind solvent extraction and determining a possible solvent duo including a polar solvent (low logP, toxic) and a biocompatible solvent (high logP, non-toxic) that would reduce the negative effects of the polar solvent while staying efficient for the extraction of lipids. The following solvents were tested as biocompatible ones: decane (logP ≈ 6), dodecane (logP ≈ 7); as toxic solvents, we used: dichloromethane (logP ≈ 1.25), hexane (logP ≈ 3.9), methyl ethyl ketone (MEK, logP ≈ 0.29) and ethanol (logP ≈ 0.23).

3.2. Experimental setup

The organic solvent hexane (Fisher Scientific, laboratory reagent grade) was added to obtain a final ratio of 2:1 (2 volumes of solvent for 1 volume of algae solution) to the concentrated samples collected after each pretreatment and mixed thoroughly during 15 min (Intelli-Mixer RM-2, Elmi Ltd.). The sample was then centrifuged in order to separate the different phases. The resulting aqueous phase (cells with the medium) was collected to be analyzed with the sulfo phospho vanillin method (see hereafter).

The above-mentioned extraction conditions (hexane, ratio 2:1, 15 min) were also used to evaluate the impact of cell wall evolution over time on lipid extraction. A mixture of decane and dichloromethane was also tested (with a ratio 1:1) on mutant and wild type cells. The mixture was added to the cell sample to obtain a final ratio of 2:1 (2 volumes of solvent for 1 volume of algae solution). The cells were exposed to the mixture for 30 min.

Figure 14: Agitating system used for the lipid extraction using solvents.

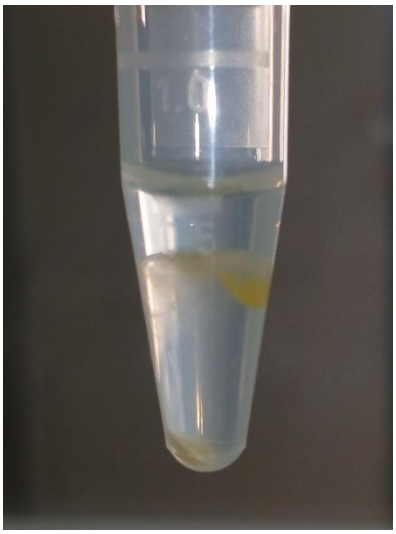

Figure 15: Algal sample after a solvent extraction. The cell pellet and the yellow interface are visible on the image.

4. Evaluating the impact of pretreatments and nitrogen starvation on *C. reinhardtii*

4.1. Analyzing the impact on the microalga's morphology and cell structure

The impact of pretreatments on the microalgae cells was evaluated using three microscopic techniques: **epifluorescence, confocal laser scanning and transmission electron microscopy**.

For the confocal laser scanning microscope (CLSM) and epifluorescence microscope, the following dyes were used: **Concanavalin A conjugated with tetramethylrhodamine** (ConA, yellow-orange fluorescence) and **Bodipy 505/515** (green fluorescence) were used for wall and lipid imaging, respectively. Chlorophyll was detected by red autofluorescence. ConA is a lectine that selectively binds to the α-glucopyranosyl residues of the cell wall.

A Nikon eclipse Ti-U inverted microscope was also used to observe cells flowing through the microfluidic constrictions using a 20X objective (Nikon Plan fluor 20× DICN2NA= 0.6).

The Transmission Electron Microscopy (TEM) experiment was held at the laboratory of I2BC (Institut de Biologie Intégrative de la cellule) in Gif-sur-Yvette.

The protocol for the preparation of the microalgae cells before observation is described below:

Cell preparation for ultra-structural study by transmission electron microscopy

Cells were fixed over night at 4°C with 4% glutaraldehyde in 0.1 M cacodylate buffer pH 6.8. Cells were washed with cacodylate 0.1 M, pH 6.8. Cells were incubated for 1h in 1% osmium tetroxide reduced with 1.5% potassium ferrocyanide in distilled water. Pellets were then centrifuged in 2% low melting point agarose to obtain concentrated pellets in 1 mm3 cubes. Dehydration in graded ethanol series (10-20-30-50-70-90-100%) and finally in propylene oxide and embedding in increasing proportions (25-33-50-75-100-100%) of epoxy resin (Low Viscosity Premix Kit Medium, Agar Scientific, Oxford instruments) mixed with propylene oxide were processed manually on 3 days. Blocs were polymerised for 24 h at 60°C.

Sectioning and contrast

Semithin (250 nm) or ultrathin sections (80 nm) were cut with an ultramicrotome EM UC6 (Leica Microsystems) and respectively collected on glass slide or formvar carbon-coated copper grids (Agar). Semithin sections were stained with methyleneblue-azur II and observed with a Leica DM750 microscope for screening the blocks. Ultrathin were stained 2% uranyl acetate (Merck) and lead citrate (Agar) before observation.

Observation

Observations were made with a JEOL JEM-1400 transmission electron microscope operating at 120 kV. Images were acquired using a postcolumn high-resolution (11 megapixels) high-speed camera (SC1000 Orius; Gatan) and processed with Digital Micrograph (Gatan) and ImageJ.

Figure 16 Transmission electron microscope (I2BC).

4.2. Impact on the plasma membrane: pore characterization

The characterization of the pore size (this method is detailed in Chapter 4 (Part 2)) induced by different pretreatments was held using a Confocal Laser Scanning Microscope (CLSM, Confocal Leica SP8), FITC-Dextrans and the dye Con A for the observation of the cell wall. The chlorophyll was observed by autofluorescence.

FITC-Dextrans

For this experiment, various fluorescein-labeled (Excitation/Emission (nm): 488/495 - 540) and anionic dextrans were tested; all differ by their molecular weight: 3 kDa, 10 kDa, 40 kDa and 70 kDa. The incubation time of all dextrans before confocal analysis was equal to 20 min.

The different dextrans were added to the cell sample (volume: 100 µL; cell concentration in the range of $6x10^6$ – $1x10^7$ cells·mL^{-1}) at a constant final concentration of 50 µM for 3 kDa dextran, 37.5 µM for 10 kDa dextran, 10 µM for 40 kDa dextran and 2.5 µM for 70 kDa dextran.

The radius of each dextran molecule was calculated using Flory's equation for the determination of a radius of gyration:

$$R_g = \frac{R_0}{\sqrt{6}}$$

where $R_0 = aN^{\nu}$, with a, the monomer size, N, the degree of polymerization (number of bond segments), and ν, the Flory exponent. For a good solvent, ν is equal to 3/5 (we used DMSO, considered as a good solvent).

The calculated radius for each dextran molecule were: 0.77 nm for 3 kDa dextran, 1.59 nm for 10 kDa dextran, 3.66 nm for 40 kDa dextran and 5.11 nm for 70 kDa dextran.

4.3. **Impact on the protein content**

The proteomic analysis of *C. reinhardtii*, under various conditions (cells in exponential growth and cells after 4, 7, 15 and 20 days of stress conditions), was held using a SDS-PAGE method at the laboratory of the Faculty of Pharmacy in Châtenay-Malabry.

The algal cell samples were first prepared using an extraction buffer. The obtained proteins were then separated by SDS-Polyacrylamide Gel Electrophoresis (SDS-PAGE) and compared to a prestained protein ladder (PageRuler Plus Prestained Protein Ladder, Thermo Scientific) of known protein size standards (in the range of 10 kDa to 250 kDa).

References

André, F. and Mir, L. M. (2004) 'DNA electrotransfer: its principles and an updated review of its therapeutic applications', *Gene Therapy*, 11, pp. S33–S42. doi: 10.1038/sj.gt.3302367.

Arnold, W. M. and Zimmermann, U. (1982) 'Rotating-field-induced rotation and measurement of the membrane capacitance of single mesophyll cells of avena sativa', *Zeitschrift fur Naturforschung - Section C Journal of Biosciences*, 37(10), pp. 908–915. doi: 10.1515/znc-1982-1010.

Brito, P. S. *et al.* (2012) 'Comparison between monopolar and bipolar microsecond range pulsed electric fields in enhancement of apple juice extraction', *IEEE Transactions on Plasma Science*, 40(10 PART 1), pp. 2348–2354. doi: 10.1109/TPS.2012.2209444.

Coustets, M. *et al.* (2013) 'Flow process for electroextraction of total proteins from microalgae', *Journal of Membrane Biology*, 246(10), pp. 751–760. doi: 10.1007/s00232-013-9542-y.

Chabrol EC, Charonnat R (1937). 'Une nouvelle reaction pour l'études des lipides: l'oleidemie. La Presse Medicale', 45, 1713–1714.

Dietzel, A. (2016) *Microsystems for pharmatechnology: Manipulation of fluids, particles, droplets, and cells*, *Microsystems for Pharmatechnology: Manipulation of Fluids, Particles, Droplets, and Cells*. doi: 10.1007/978-3-319-26920-7.

Fiorini, G. S. and Chiu, D. T. (2005) 'Disposable microfluidic devices: Fabrication, function, and application', *BioTechniques*, 38(3), pp. 429–446. doi: 10.2144/05383RV02.

Flisar, K. *et al.* (2014) 'Testing a prototype pulse generator for a continuous flow system and its use for E. coli inactivation and microalgae lipid extraction', *Bioelectrochemistry*. Elsevier B.V., 100, pp. 44–51. doi: 10.1016/j.bioelechem.2014.03.008.

Foltz, G. (2012) 'Algae Lysis with Pulsed Electric Fields', *Master's Theses and Project Reports*.

Frank S. Barnes, B. G. (2006) *Biological and Medical Aspects of Electromagnetic Fields (Handbook of Biological Effects of Electromagnetic Fields) 3Ed*.

Goettel, M. *et al.* (2013) 'Pulsed electric fi eld assisted extraction of intracellular valuables from microalgae', *ALGAL*. Elsevier B.V., 2(4), pp. 401–408. doi: 10.1016/j.algal.2013.07.004.

Haberl, S. *et al.* (2013) 'Cell membrane electroporation-Part 2: The applications', *IEEE Electrical Insulation Magazine*, 29(1), pp. 29–37. doi: 10.1109/MEI.2013.6410537.

Ho, M. P. (2017) 'Combining electrolysis and electroporation for tissue ablation', *Handbook of Electroporation*, 3(December), pp. 1733–1753. doi: 10.1007/978-3-319-32886-7_63.

Joannes, C. *et al.* (2015) 'The Potential of Using Pulsed Electric Field (PEF) Technology as the Cell Disruption Method to Extract Lipid from Microalgae for Biodiesel Production', *International Journal of Renewable Energy Research (IJRER)*, 5(2), pp. 598–621. Available at: http://www.ijrer.org/ijrer/index.php/ijrer/article/view/2240.

Kempkes, M. A., Roth, I. and Gaudreau, M. P. J. (2015) 'Pulsed Electric Field (PEF) method for continuous enhanced extraction of oil and lipids from small aquatic plants, Diversified Technologies Inc., US 9,029,108', 2(12).

Kim, H. S., Devarenne, T. P. and Han, A. (2018) 'Microfluidic systems for microalgal biotechnology: A review', *Algal Research*, 30(November), pp. 149–161. doi: 10.1016/j.algal.2017.11.020.

Kotnik, T. *et al.* (2012) 'Cell membrane electroporation - Part 1: The phenomenon', *IEEE*

Electrical Insulation Magazine, 28(5), pp. 14–23. doi: 10.1109/MEI.2012.6268438.

Kotnik, T., Miklavčič, D. and Mir, L. M. (2001) 'Cell membrane electropermeabilization by symmetrical bipolar rectangular pulses: Part II. Reduced electrolytic contamination', *Bioelectrochemistry*, 54(1), pp. 91–95. doi: 10.1016/j.dhjo.2014.02.002.

Lee, E. W., Thai, S. and Kee, S. T. (2010) 'Irreversible electroporation: A novel image-guided cancer therapy', *Gut and Liver*, 4(SUPPL. 1), pp. 99–104. doi: 10.5009/gnl.2010.4.S1.S99.

Levine, Z. A. and Vernier, P. T. (2010) 'Life cycle of an electropore: Field-dependent and field-independent steps in pore creation and annihilation', *Journal of Membrane Biology*, 236(1), pp. 27–36. doi: 10.1007/s00232-010-9277-y.

Luengo, E. *et al.* (2014) 'Effect of pulsed electric field treatments on permeabilization and extraction of pigments from Chlorella vulgaris.', *The Journal of membrane biology*, 247(12), pp. 1269–77. doi: 10.1007/s00232-014-9688-2.

Mishra, S. K. *et al.* (2014) 'Rapid quantification of microalgal lipids in aqueous medium by a simple colorimetric method', *Bioresource Technology*. Elsevier Ltd, 155, pp. 330–333. doi: 10.1016/j.biortech.2013.12.077.

Ostapenko, O. V. *et al.* (2004) 'Influence of electroporation conditions on transfection of muscle fibers in vivo', *Russian Journal of Genetics*, 40(1), pp. 33–39.

Pataro, G. *et al.* (2015) 'On the modeling of electrochemical phenomena at the electrode-solution interface in a PEF treatment chamber: Methodological approach to describe the phenomenon of metal release', *Journal of Food Engineering*. Elsevier Ltd, 165, pp. 34–44. doi: 10.1016/j.jfoodeng.2015.05.009.

Pavlin, M. *et al.* (2008) 'Chapter Seven Electroporation of Planar Lipid Bilayers and Membranes', *Advances in Planar Lipid Bilayers and Liposomes*, 6(07), pp. 165–226. doi: 10.1016/S1554-4516(07)06007-3.

Puc, M. *et al.* (2003) 'Quantitative model of small molecules uptake after in vitro cell electropermeabilization', *Bioelectrochemistry*, 60(1–2), pp. 1–10. doi: 10.1016/S1567-5394(03)00021-5.

Reberšek, M. *et al.* (2014) 'Cell membrane electroporation-Part 3: The equipment', *IEEE Electrical Insulation Magazine*, 30(3), pp. 8–18. doi: 10.1109/MEI.2014.6804737.

Schlager (2005) 'Electroporation System for Sterilizing Water Amounts of chemicals needed for sterilization are reduced .', (October), pp. 25–26.

Teissie, J., Golzio, M. and Rols, M. P. (2005) 'Mechanisms of cell membrane electropermeabilization: A minireview of our present (lack of?) knowledge', *Biochimica et Biophysica Acta - General Subjects*, 1724(3), pp. 270–280. doi: 10.1016/j.bbagen.2005.05.006.

Teissié, J. and Rols, M. (1993) 'An Experimental Evaluation of the Critical Potential Difference', *Biophysical Journal*, 65(July), pp. 409–413.

Zbinden, M. D. A. *et al.* (2013) 'Pulsed electric field (PEF) as an intensification pretreatment for greener solvent lipid extraction from microalgae', *Biotechnology and Bioengineering*, 110(6), pp. 1605–1615. doi: 10.1002/bit.24829.

Zimmermann, U. (1986) 'Electrical breakdown, electropermeabilization and electrofusion', *Reviews of Physiology, Biochemistry and Pharmacology, Volume 105*, 105, pp. 175–256. doi: 10.1007/BFb0034499.

Annex

TAP medium composition and protocol

From Gorman, D.S., and R.P. Levine (1965) *Proc. Natl. Acad. Sci. USA***54**, 1665-1669.

This isprobably the most widely-used medium at present for experimental work.

Make the following stock solutions:

1. TAP salts

NH_4Cl	15.0 g
$MgSO_4 . 7H_2O$	4.0 g
$CaCl_2 . 2H_2O$	2.0 g
water to 1 liter	

2. phosphate solution

K_2HPO_4	28.8 g
KH_2PO_4	14.4 g
water to 100 ml	

3. **Hutner's trace elements**

Hutner et al. (1950) *Proc. Am. Philos. Soc.***94**, 152-170

This mixture is used both in TAP and in the Sueoka high salt medium.

For a detailed analysis of how well this trace elements solution meets the nutritional requirements of *C. reinhardtii*, see Merchant et al. (2006) *Biochim. Biophys. Acta***1763**, 578-594.

For 1 liter final mix, dissolve each compound in the volume of water indicated.

The EDTA should be dissolved in boiling water, and the $FeSO_4$shouldbeprepared last to avoid oxidation.

compound	**amount**	**water**
EDTA disodiumsalt	50 g	250 ml
$ZnSO_4 . 7 H_2O$	22 g	100 ml
H_3BO_3	11.4 g	200 ml
$MnCl_2 . 4 H_2O$	5.06 g	50 ml
$CoCl_2. 6 H_2O$	1.61 g	50 ml
$CuSO_4 . 5 H_2O$	1.57 g	50 ml
$(NH_4)_6Mo_7O_{24}. 4 H_2O$	1.10 g	50 ml

$FeSO_4$. 7 H_2O	4.99 g	50 ml

Mix all solutions except EDTA. Bring to boil, then add EDTA solution. The mixture should turn green. When everything is dissolved, cool to 70 degrees C. Keeping temperature at 70, add 85 ml hot 20% KOH solution (20 grams / 100 ml final volume). Do NOT use NaOH to adjust the pH.

Bring the final solution to 1 liter total volume. It should be clear green initially. Stopper the flaskwith a cotton plug and let it stand for 1-2 weeks, shaking it once a day. The solution shouldeventuallyturnpurple and leave a rust-brown precipitate, whichcanberemoved by filteringthroughtwolayers of Whatman#1 filter paper, repeating the filtration if necessary until the solution is clear. Store refrigerated or frozen convenient aliquots. Some people shorten the time for formation of the precipiate by bubbling the solution with filtered air.

If no precipitate forms, the solution isstill usable. However, you might want to check the pH in this case and adjust it to around 7.0 using either KOH or HCl as needed.

To make the final medium, mix the following:

2.42 g Tris
25 ml solution #1 (salts)
0.375 ml solution #2 (phosphate)
1.0 ml solution #3 (trace elements)
1.0 ml glacial aceticacid
water to 1 liter

For solid medium, add 15 g agar per liter

Autoclave.

For Tris-minimal medium omit the acetic acid and titrate the final solution to pH 7.0 with HCl

Quantification of total lipids using the colorimetric Sulphophosphovanillin (SPV) method

Principle

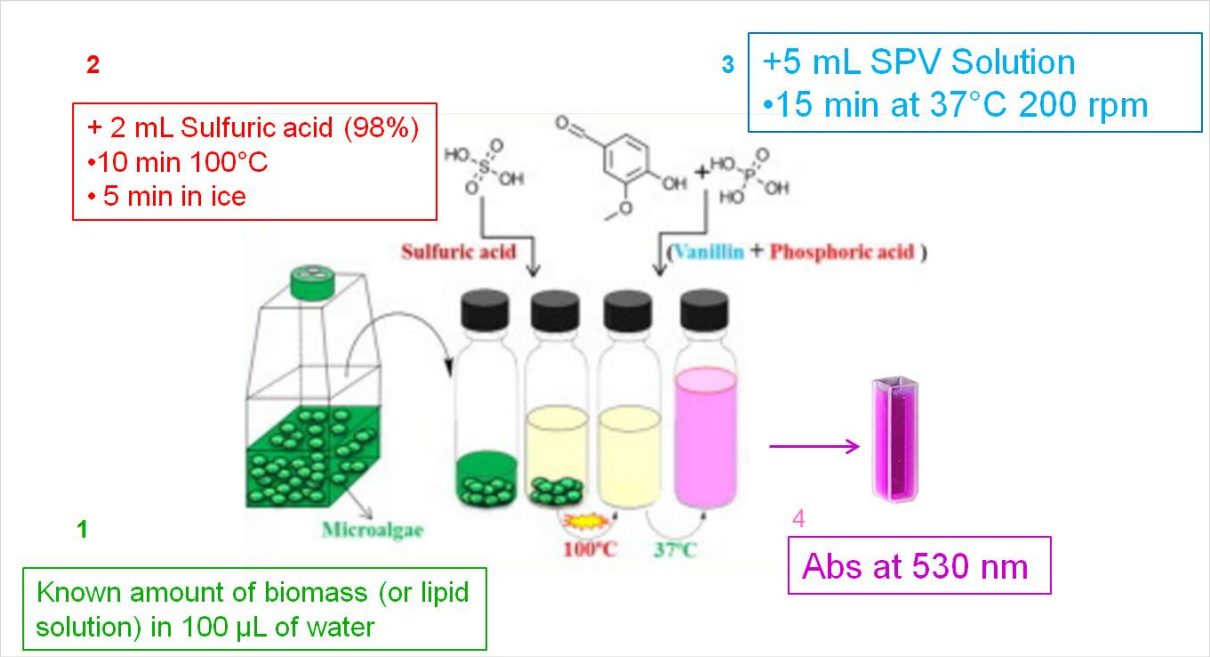

Figure 17: Principle of the method (Mishra *et al.*, 2014)

Material

Vanilin 99% (ref: 10387020)	0.6 g
Absolute ethanol	10 ml
Deionized water	(-) ml
Distilled water	(-) ml
Orthophosphoric acid 85% (ref: 10102060)	400 mL
Glycerine trioleate 99% (ref: 10190612)	20 mg
Chlorophorm	10 ml
Sulfuric Acid (98%)	2 ml (per sample)
100 °C Heater	x1
37°C, 200 Rpm incubator	x1
Glass cuvettes for spectro	x1
glass tubes + caps (15 mL min)	x9
Ice	(-)
Vanilin solution	5 ml (per sample)
-20 °C freezer	X1
37°C, 200 rpm incubator	X1

Preparation of SPV Solution

- Dissolve 0.6 g of vanilin in 10 ml absolute ethanol
- add 90 ml of deionized water
- add 400 ml of concentrated phosphoric acid
- store the 500 mL bottle in the dark before use
- Fresh SPV solution needs to be prepare before use

Preparation a calibration curve (Triolein in chloroform)

- Dissolve 20 mg of triolein in 10 mL of chloroform (2 mg/ml)
- store at -20°C before use
- Add different quantities of triolein in glass tubes:

Lip qty (µg)	0	10	20	30	40	50	60	70
Triolein sol (µl)	0	5	10	15	20	25	30	35

- Evaporate the chloroform at 60°C during 10 minutes
- In each tube, add 100 µl of distilled water
- In each tube, add 2 mL of concentrated sulfuric acid (98%)
- Heat at 100°C during 10 min
- Cool the tubes in ice during 5 min
- add 5 mL of SPV solution (caution, solution becomes very hot after mixing)
- incubate the tubes at 37°C, 200 rpm during 15 min
- transfer the content in glass absorbance cuvettes
- read the absorbance at 530 nm. Dilute if needed with the blank solution (0 µg lipid).

Figure 18: Tube heater (WTW CR3200) and ice cooling

Figure 19: Mixing device (ELMI Inteli-Mixer, Mode F2, 99 Rpm) in a oven at 37°.

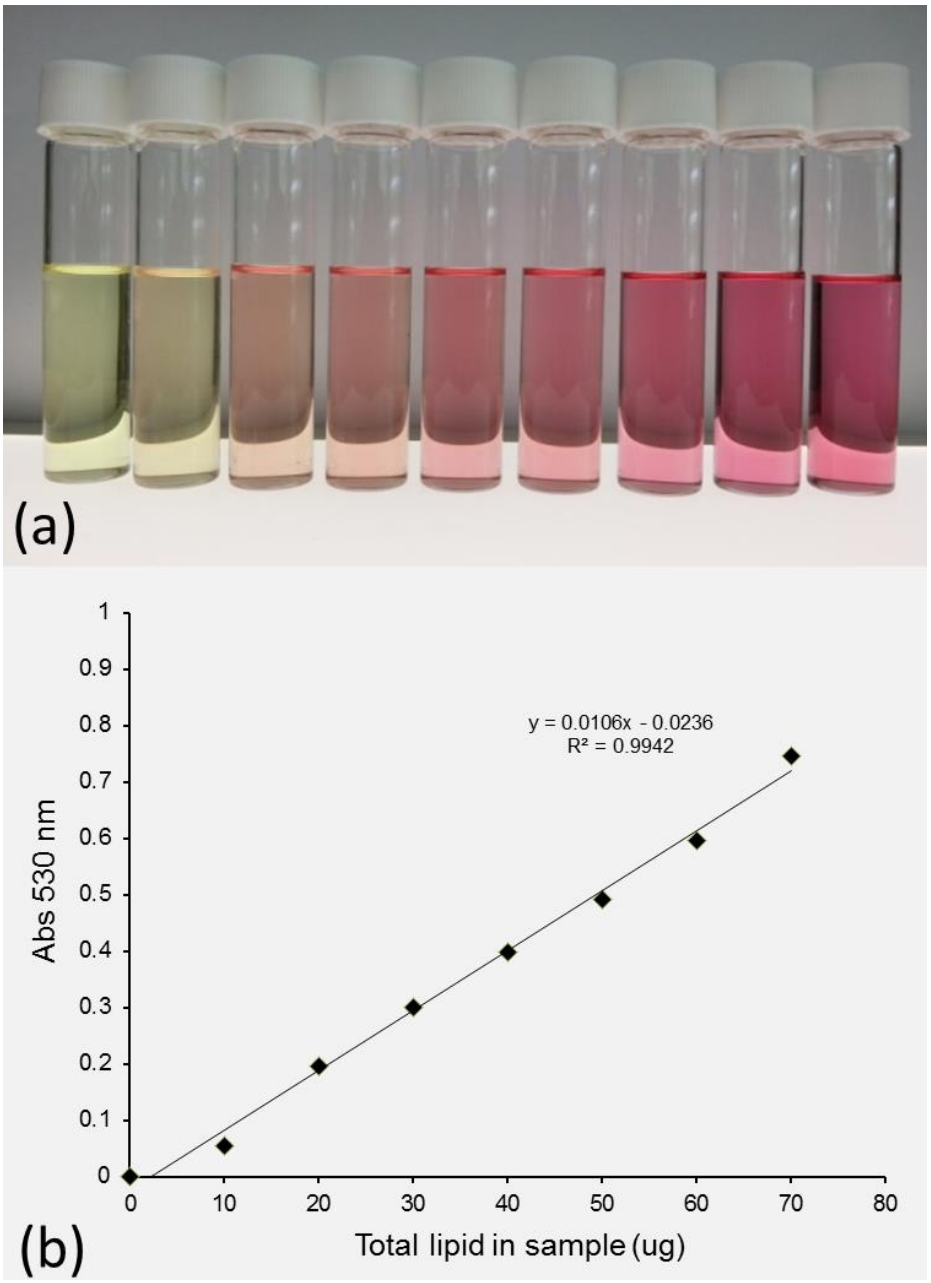

Figure 20: (a) From the left to right, the color change with the increasing concentration of lipid (Canola Oil) and (b) the corresponding linear relationship of absorption enhancement at 530 nm against lipid quantity in the sample (canola oil in the picture from (Mishra *et al.*, 2014)**).**

Results

Lip qty (µg)	0	10	20	30	40	50	60	70	80	90	100
Abs 530 (i)	0	2	4,07	6,66	7,66	10,6	15,24	17,36	14,98	17,32	20,2
Abs 530 (ii)	0	1,81	3,1	3,51	5,28	8,12	10,48	8,84	13,7	13	17
Abs 530 (iii)	0	1,66	2,97	4,02	6,43	9,84	12,46	12,28	17,1	19,04	22,2
Mean Abs 530	0	1,82	3,38	4,73	6,46	9,52	12,73	12,83	15,26	16,45	19,80
SD	0	0,17	0,60	1,69	1,19	1,27	2,39	4,29	1,72	3,11	2,62

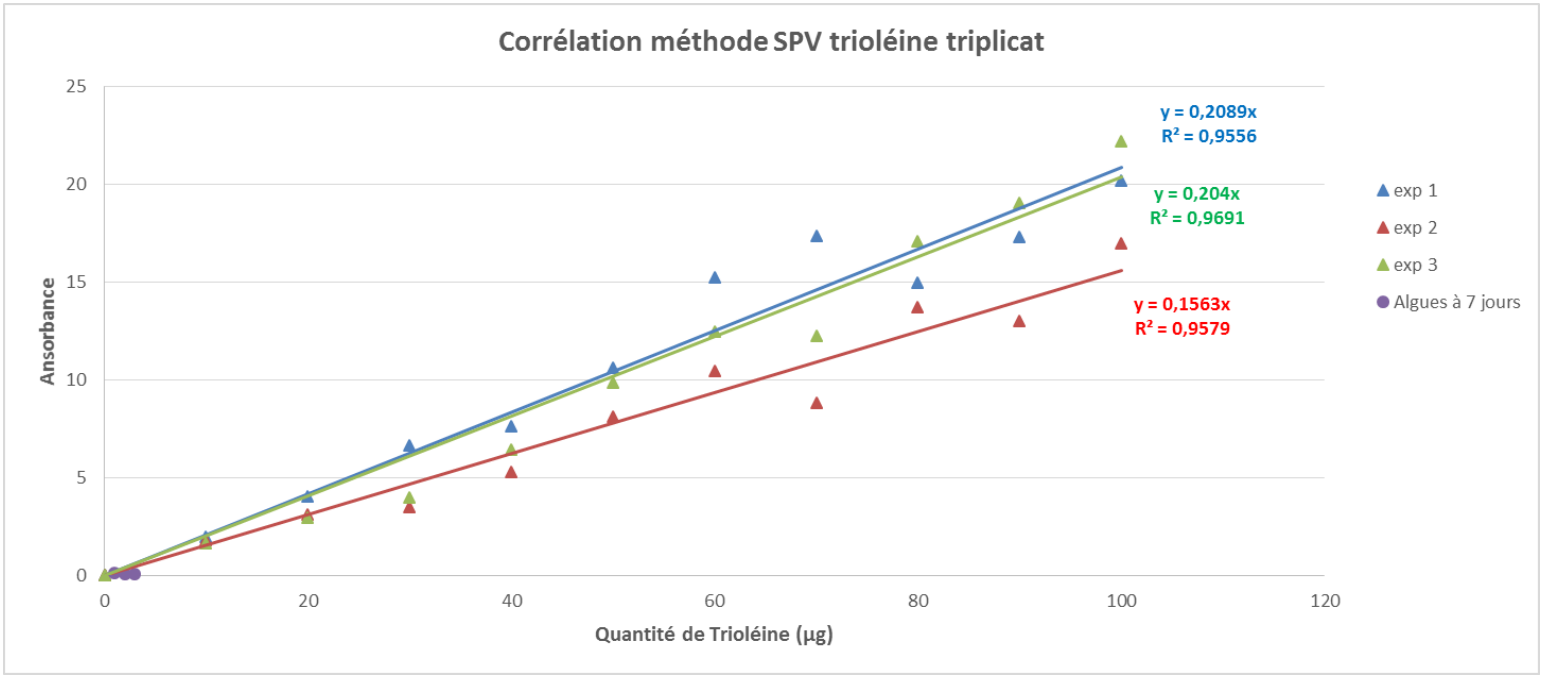

Figure 21: Absorbance at 530 nm obtained with the increased concentration of triolein from three experiments. (Dilution by a factor from 10 to 40 was needed).

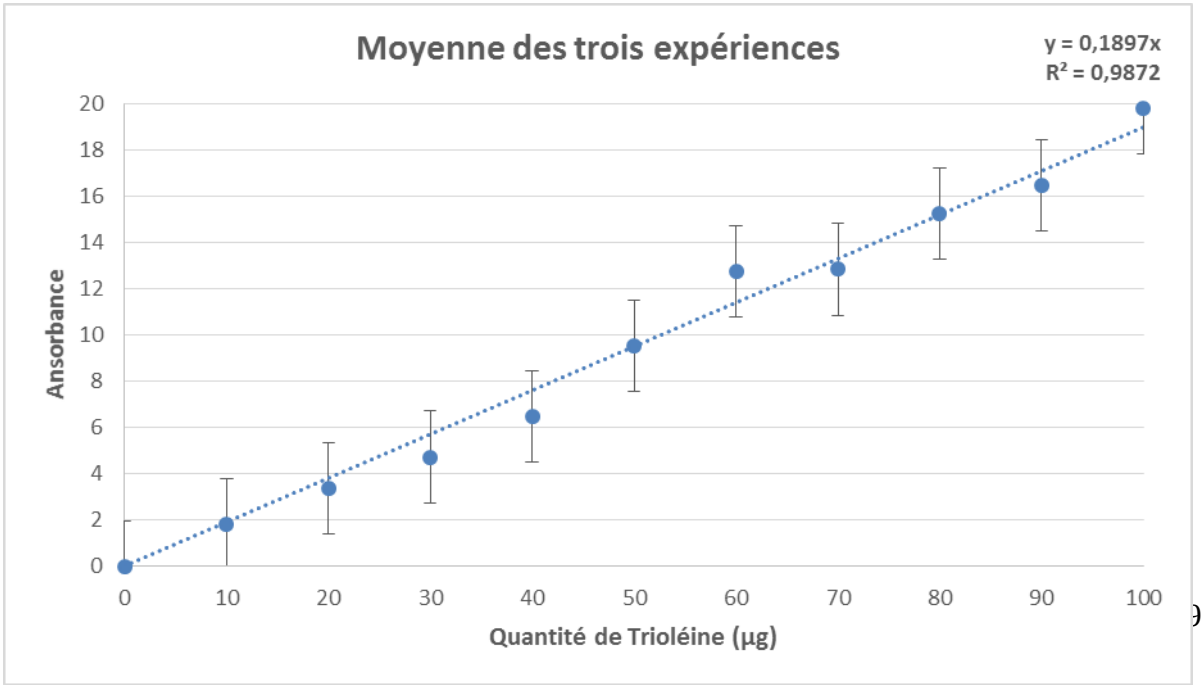

Protocole SPV sur la gamme de 0 à 10µg

Lip qty (µg)	0	2	4	6	8	10
Abs 530 (i)	0,000	0,402	0,894	0,620	0,919	0,491
Abs 530 (ii)	0,000	0,366	0,826	0,612	0,827	0,559
Abs 530 (iii)	0,000	0,380	0,665	0,557	0,834	0,575
Mean Abs 530	0,000	0,383	0,795	0,596	0,860	0,542
SD	0,000	0,018	0,118	0,034	0,051	0,045
Abs réelle	0,000	0,383	0,795	1,193	1,720	2,167

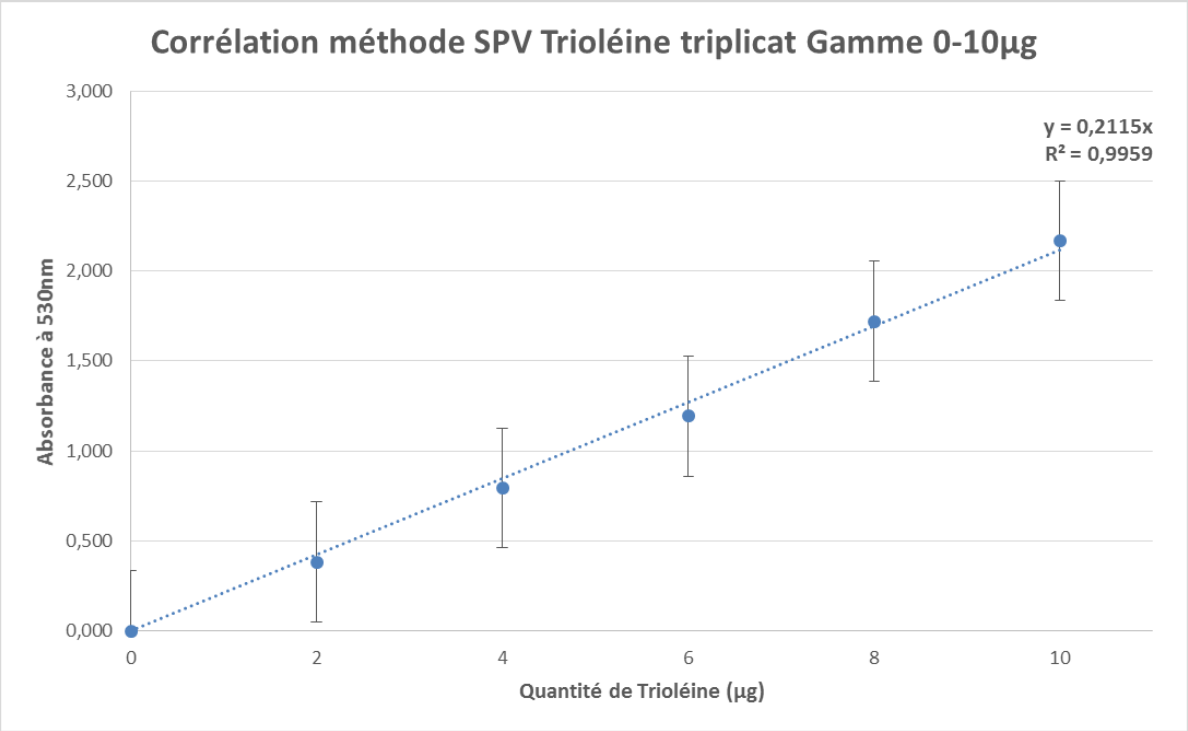

Algae, 7 days of stress 22/07/2016

- Measure algae concentration by flow cytometry. Mean concentration = 9,94E+06 cells/ml
- In order to concentrate or dilute the algae samples apply centrifugation-resuspension on the initial algae solution.
- A sample of algae in exponential growth is analysed (**WT26exp**)

Table 2: Dilution for the algae solution (7 days of stress)

Concentration factor	0	0.5	1	2	4	8
Initial volume (µL)	0	800	800	800	800	800
Final volume (µL)	0	1600	800	400	200	100

Results

Facteur de Dilution/Concentration	**0**	**0,5**	**1**	**2**	**4**	**8**	**WT26exp**
Number of cells in the sample (100µl)	0	497000	994000	1988000	3976000	7952000	4560000
Mean Abs	0,000	0,055	0,130	0,250	0,455	0,724	0,323
Masse de Trioléine équivalente (µg)	0,000	0,291	0,682	1,316	2,396	3,812	1,698
Rapport Trioléine équivalente/cellule	0	5,8597E-07	6,8658E-07	6,6187E-07	6,0274E-07	4,7941E-07	3,7242E-07

Figure 6: Absorbance

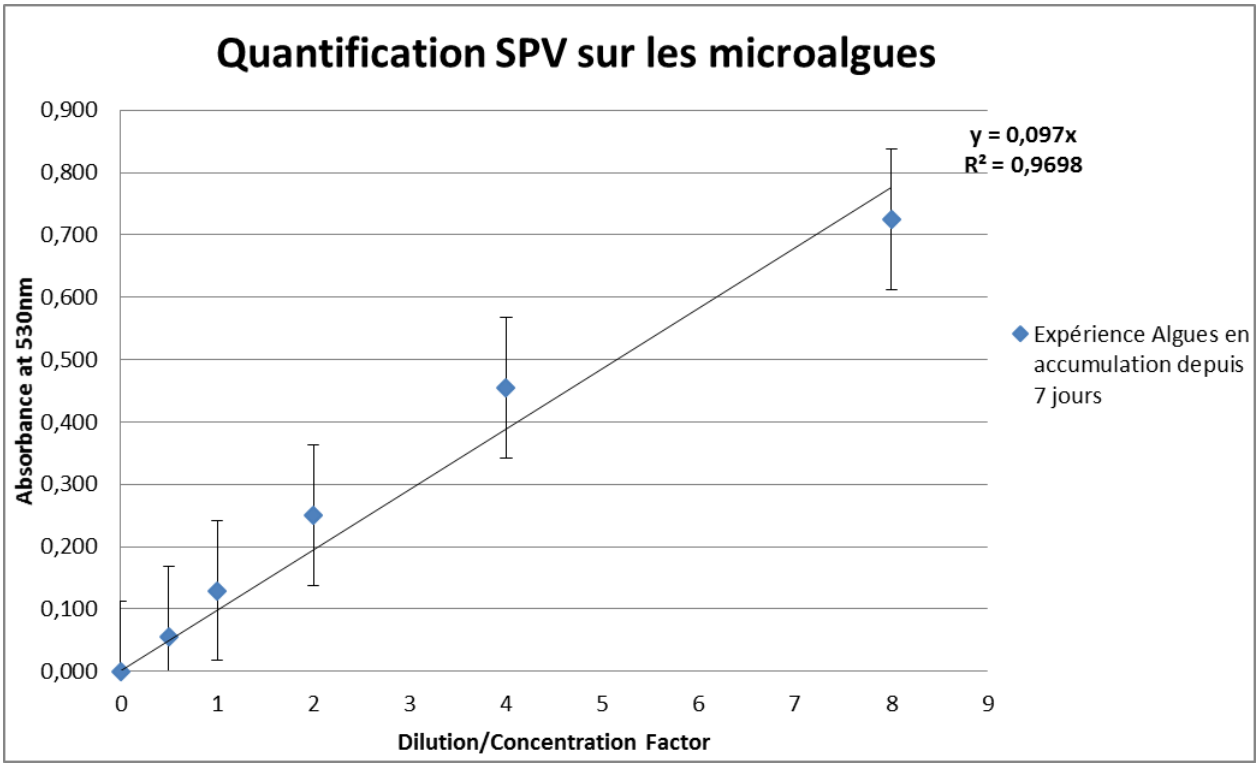

Chapter III - Lipid extraction

Table of contents

Preamble - *Motivation and Objectives*

As mentioned previously (Chapter 1), various strategies are being explored by industrial and research teams to overcome the environmental and economic challenges encountered in the algal-based large scale productions. In the case of the extraction of algal lipids, improvements must be made in terms of lipid yield and process sustainability. Techniques for lipids recovery are therefore strongly studied.

Usually pretreatments are used to improve lipid extraction. In this context, cell disruption is usually used. Indeed, cell disruption is a key step for an efficient lipid extraction from microalgae. An effective solvent extraction system must be able to overcome two different barriers: 1) water: it is highly present (up to 80 %) in the microalgae suspensions and is considered as a challenging polar barrier to the solvent; this barrier must be overcome in order to remove the drying step from the production process and becoming economically competitive, 2) the microalgae's cell wall: in the case of a monophasic solvent extraction on unruptured cells, lipids are extracted by the solvent through a slow and costly process, mainly due to the presence of the microalgae's cell wall that is very rigid and thick (i.e. Folch or Bligh and Dyer extractions) (Yap et al., 2014; Cooney et al., 2009; Halim et al., 2012).

There are many different disruption techniques that are mechanical, physical, chemical or enzymatic. Some however are not adequate as they can lead to damages of the target product (degradation of the lipids which leads to a biodiesel with a lower quality, decrease in protein solubility which involves a decrease in their extractability…) and generation of small cellular debris that makes the following downstream process difficult. The chosen pretreatment to lipid extraction should be therefore be "biocompatible" in the sense that it maximizes the preservation of the cell and the target compound.

In this context, it is necessary to understand the mechanisms behind each technique to determine the right cell disruption method for an efficient lipid extraction. There is currently few information at the cell level of the effect of disruption techniques prior to the solvent extraction. Therefore further investigations of cell disruption techniques at the cellular scale would provide significant information for the development and optimization of an extraction process from microalgae.

In this project, we have chosen to study two pretreatments: **pulsed electric fields (PEFs)**, for the many advantages that have been previously reported such as being considered a simple and a reproducible technique able to preserve the cell integrity and a **controlled mechanical process** where cell compression is obtained within a **dedicated microfluidic device.** The latter device coupled to microscopic observations is used to evaluate the effects of mechanical stress at cell level. The combination of pretreatments is also studied.

To do so, we rely on different analytical techniques (described in Chapter 2 and Part 1 of this chapter) enabling us to study the impact and efficiency of each of those pretreatments (alone and coupled) and their combination with extracting solvents on the **cell's permeability and viability,** cell **lysis**, **cell's structure and morphology** and the extracted lipids yield.

As a first step, **different configurations of pretreatments** were studied: PEFs alone (10 unipolar pulses, 5.5 kV·cm-1, pulse duration 5 µs and repetitio frequency of 10 Hz; these tested conditions lead to a reversible electroporation (see Part 1 of Chapter 4) therefore a temporary permeabilization where the created pores reseal after a specific time), mechanical compressions alone, PEFs followed by mechanical compressions and mechanical compressions followed by PEFs. Each configuration was evaluated as an enhancer to the extraction of lipids using several solvents. We first focused on extraction with hexane.

After determining the best configuration, leading to the highest lipid yield, we focused on the **study of solvents**, to evaluate the possibility of replacing toxic solvents such as hexane with more biocompatible ones such as decane. The objective was to evaluate the extraction efficiency and the mechanisms behind the extraction of solvents such as dichloromethane (high LogP, high hydrophobicity and high affinity for lipids), the so called biocompatible solvents (low LogP, hydrophilic, low affinity for lipids) and the combination of both types of solvents. In addition, the idea was to combine the previously determined configuration of pretreatments that gave the best extraction efficiency with a solvent mixture that could lead to a minimized damage on the cells.

From data, we understood the major importance of cell lysis in the efficiency of lipid extraction from *C. reinhardtii* with solvents. This was further confirmed with the mutant strain of *C. reinhardtii* (cell wall deficient, see Complementary data, Part 1 of this chapter). Indeed, microalgae are known to have rigid and thick cell walls that can be held responsible for the difficulty to extract the inner compounds from the cells.

In addition, culture conditions may change cell structure with further impact of compounds recovery. The effect of nitrogen stress applied to enhance lipid accumulation on *C. reinhardtii* cell structure, and in particular cell wall, and lipid extraction efficiency was evaluated.

The first part of this Chapter relates to the quantitative analysis of the effect of both electrical and mechanical pretreatments on *C. reinhardtii* and their respective efficiency for lipid extraction. The work is presented through our published journal article in Bioresource Technology in 2018, "**Understanding the mechanisms of lipid extraction from microalga *Chlamydomonas reinhardtii* after electrical field solicitations and mechanical stress within a microfluidic device**". Complementary results are also presented involving: the cell wall deficient *Chlamydomonas reinhardtii* (mutant strain), the different investigated solvents (biocompatible and toxic solvents with a high LogP) and their coupling for an efficient extraction, and a different configuration of our combined pretreatments (mechanical compression followed by PEFs) and its effect on the cell permeability.

The second part of this Chapter relates to the structural changes induced on the microalgae by the stress conditions allowing its lipid production and the effect of different types of solvents (ethyl acetate, decane, dichloromethane) on the cell structure and in particular, on the intracellular lipid droplets. Here again, the work is presented through an article published in Data in Brief in 2018: "**Structural changes of *Chlamydomonas reinhardtii* cells during lipid enrichment and after solvent exposure**".

This second part also includes complementary results involving the statistical analysis on the cell wall of *C. reinhardtii* at different stages of stress conditions as well as additional confocal images showing the structural changes endured by the algae cells.

Acknowledgements

Section 1 of this chapter, in full, is a reprint of the material as it appears in Bioresource Technology 2018 (DOI: 10.1016/j.biortech.2018.01.139). The dissertation author is the primary investigator and first author of this paper. The other authors on this paper are: Pierre Bodénès, Dominique Pareau, Filipa Lopes, Olivier Français and Bruno Le Pioufle

Section 2 of this chapter, in full, is a reprint of the material as it appears in Data in Brief 2018 (DOI: 10.1016/j.dib.2018.02.042). The dissertation author is the primary investigator and first author of this paper. The other authors on this paper are: Filipa Lopes, Pierre Bodénès, Dominique Pareau, Olivier Français and Bruno Le Pioufle.

Part 1 Comprehensive study of lipid extraction from the microalga Chlamydomonas reinhardtii

1. Understanding the mechanisms of lipid extraction from microalga Chlamydomonas reinhardtii after electrical field solicitations and mechanical stress within a microfluidic device

1.1 Abstract

One way envisioned to overcome part of the issues biodiesel production encounters today is to develop a simple, economically viable and eco-friendly process for the extraction of lipids from microalgae. This study investigates the lipid extraction efficiency from the microalga *Chlamydomonas reinhardtii* as well as the underlying mechanisms. We propose a new methodology combining a pulsed electric field (PEF) application and mechanical stresses as a pretreatment to improve lipid extraction with solvents. Cells enriched in lipids are therefore submitted to electric field pulses creating pores on the cell membrane and then subjected to a mechanical stress by applying cyclic pressures on the cell wall (using a microfluidic device). Results showed an increase in lipid extraction when cells were pretreated by the combination of both methods. Microscopic observations showed that both pretreatments affect the cell structure. Finally, the dependency of solvent lipid extraction efficiency with the cell wall structure is discussed.

Highlights

- Lipid extraction is increased when using combined pretreatments.
- PEF and mechanical compression affect differently cell structure and viability.
- In situ visualization of the mechanical cyclic compression in a microfluidic device.

Keywords: Microalgae - Pulsed electric field (PEF) - Solvent extraction - Cell permeability – Microfluidics

1.2 Introduction

Over the past few years, the worldwide energy demand has significantly increased.

In the fuel industry, two major issues have been highlighted: the fast consumption of fossil fuels and global warming, since the increasing demand in fuel for transportation goes along with an increase in atmospheric greenhouse gases.

1st and 2nd generation biofuels can be associated to concerns such as economic, environmental or social negative consequences. In this context, microalgae, which are carbon

dioxide consuming organisms, are considered one of the most promising sources for biodiesel production (Behera et al., 2015; Takeshita, 2011). Indeed, some species, described as oleaginous, can store large fractions of neutral lipids (triacylglycerol, TAG) in the form of droplets which can be further turned into biodiesel or other high value products such as omega-3 fatty acids (Adarme-Vega et al., 2012).

Microalgae bear several advantages compared to other biodiesel producing crops such as high growth rate, high biomass production, and high biodiesel productivity with low need in landscape. The competition for arable lands with other crops also used for human consumption is therefore largely reduced (Atabani et al., 2012).

However, despite the high potential of microalgae, several scientific, technological and economical bottlenecks must be overcome before large-scale production of biodiesel from microalgae takes place (Bravo-Fritz et al., 2016) and ultimately compete with the petroleum based fuels.

It is now clearly recognized that harvesting/dewatering and lipids extraction steps are highly energy intensive. In the particular case of extraction, significant breakthroughs are needed to improve the oil recovery, the sustainability and ultimately the cost efficiency of the overall bioprocess (Kim et al., 2013; Slegers et al., 2014; Vanthoor-Koopmans et al., 2013). Among those, improvements must be made to reduce and ultimately replace the use of toxic organic solvents.

Lipid extraction from microalgae is usually performed with solvents, some highly toxic (Miazek et al., 2017). But mechanisms of extraction with solvents are hardly described or based on experimental data (Cooney et al., 2009; Halim et al., 2012). For instance, according to Halim and coworkers (Halim et al., 2012), extraction occurs at several steps including the diffusion of the solvent through the cell wall and cell membrane before reaching the cytoplasmic lipid droplets. On the contrary, the study of Yap et al. (2014) clearly demonstrates that cell rupture must occur to extract intracellular lipids from Chlorella species with solvents (Yap et al., 2014).

Amongst the commonly used solvents, hexane is known for its high selectivity to neutral lipids (Olmstead et al., 2013).

In addition, research on greener solvents to extract lipids is increasing strongly lately (Kumar et al., 2017; Nezammahalleh et al., 2016). The main characteristics taken into consideration while choosing an adequate solvent for extraction are its ability to extract or polarity (Mojaat et al., 2008), its solubility with lipids, its miscibility with water (a water-immiscible solvent won’t require additional energy to be recovered) and its toxicity.

Several suggestions are proposed in the literature to determine the appropriate solvent (with a low solvent toxicity). One of these suggestions includes the use of a mixture of a solvent that is biocompatible but with a low ability of extraction (high polarity) with a solvent showing a high ability of extraction (low polarity) (Mojaat et al., 2008; Ryckebosch et al., 2012). This approach was investigated in this work.

In order to improve lipid extraction from microalgae, mechanical and non-mechanical methods are proposed such as bead milling (Postma et al., 2015), ultrasound (Araujo et al., 2013), supercritical fluid extraction (Santana et al., 2012), enzymatic extractions (Kim et al., 2013), and microwave (Ranjith Kumar et al., 2015). Most of these techniques rely on the weakening of the cell wall as a pretreatment before extraction with solvents inducing partial or total disruption of the cells to collect lipids from the cytoplasm. Most of them are highly energy demanding and all are characterized by a lack of specificity that cause cell debris along with the compound of interest. Therefore, successive separation steps, which are costly, are required to recover the compound of interest. However, in the case of high pressure homogenization, under certain conditions (algae specie, TAG content and biomass concentration), the energy required becomes reasonable (Yap et al., 2015).

In this context, mechanical compression is commonly used to disrupt microalgae cells in units such as those of homogenizers (Halim et al., 2013; Lee et al., 2012; Min et al., 2014; Rakesh et al., 2015) and is highly investigated as a pretreatment for the improvement of lipid extraction solvent extraction (Günerken et al., 2015).

Recently, electroporation has also proven to be simple, fast and highly efficient as a pretreatment to extract compounds from microalgae as intracellular lipids (Goettel et al., 2013; Lai et al., 2014). The principle behind is the following: high intensity of electric field pulses leads to a transmembrane voltage, that at a certain critical threshold value (~0.2 – 1.5V for mammalian cells) (Geng et al., 2010), triggers creation of pores in the cell membrane. In addition, PEF has been coupled to solvents to extract lipids from microalgae (Eing et al., 2013). Though the high potential of this technology has been stated (Pataro et al., 2017), only few studies describe the mechanisms underlying lipid extraction when PEF is coupled to solvent (Lai et al., 2014; Zbinden et al., 2013).

In order to improve microalgae production systems, making them sustainable and cost effective, it is therefore of utmost importance to study new pretreatments to improve lipid recovery and to understand the underlying mechanisms of extraction of lipids with those treatments coupled with solvents.

In this work, two pretreatments were investigated: Pulsed Electric Fields (PEF) and mechanical compression. We examined the lipid extraction from *Chlamydomonas reinhardtii* with those pretreatments, combined or not, followed by further solvent extraction. Hexane, ethyl acetate, dichloromethane and dodecane were used as solvents in our study.

In order to get a better insight on the underlying physical mechanisms related to the tested pretreatments, the effect of electric and mechanical stresses on cell structure (cell membrane/wall, lipid droplets structure) and viability is thus assessed. Finally, in order to evaluate the impact of cell wall on lipid extraction, a cell wall deficient mutant of *Chlamydomonas reinhardtii* was used.

In our study, mechanical cyclic compression is assured by flowing cells through constrictions in a microfluidic device that we specifically designed. The latter is an ideal tool for studying the effect of mechanical stress on cell structure in precise and fully controlled environmental

conditions. Indeed, microdevices coupled to microscopic tools were used to evaluate the effects of electric and mechanical stress on the cell in this study.

The green unicellular alga *Chlamydomonas reinhardtii* was chosen as a model of study. Stress factors such as nutrient deficiency, light intensity and temperature can cause various cellular response mechanisms in microalgal cells (Minhas et al., 2016). In the case of *Chlamydomonas reinhardtii*, a deprivation of nitrogen and high light intensities cause an accumulation of lipid droplets for the storage of triacylglycerols (TAGs) and a chlorophyll breakdown, leading to a major slowdown in cell growth.

It is a well-studied microalga for which a cell wall deficient mutant has been developed. Assays aiming at understanding the effect of the cell wall are therefore feasible. This microalga has also been studied on its response to pulse electric field as well as to mechanical membrane distortion solicitations lately (Bodénès et al., 2016; Min et al., 2014). Although mechanical disruption on *Chlamydomonas reinhardtii* and other strains have been demonstrated previously (Gerde et al., 2012; Min et al., 2014), it is still unclear how it affects cell viability and permeability. Moreover, no information on the precise physical effect of mechanical compression on the cell wall and cell lipid droplets is described. This study addresses therefore this gap.

1.3 Materials and methods

1.3.1 Microalgae strain

The microalgae strains were obtained from the University of Goettingen (EPSAG, Nikolausberger Goettingen, Germany). The strains studied in this work were: *Chlamydomonas reinhardtii* SAG-34.98 (Wild type) and *C. reinhardtii* SAG-83.81(Cell wall deficient mutant strain). The cells were cultured in TAP growth media (Gorman, D.S., 1965). The aforementioned was depleted from nitrogen when the cells were put into stress conditions.

1.3.2 Cultivation of *C. reinhardtii*

Growth conditions

Algal cells were cultured under photo-autotrophic conditions in a total volume of 50 mL. They were incubated under light intensity of 20 $\mu mol \cdot m^{-2} \cdot s^{-1}$ in a shake incubator (Minitron, Infors HT, Bottmingen, Switzerland) at 100 rpm. The temperature and air injection were held constant at 25 °C and 1.5 % CO_2 respectively.

Stress conditions

In order to induce lipid accumulation, cultures from the exponential phase, with a cell concentration in the range of 2 x 10^5 to 1 x 10^7 cells·mL^{-1}, were centrifuged at 6000 g for 5 min. The pellet was resuspended at a concentration of 3 x 10^6 cells·mL^{-1} in 60 mL of nitrogen depleted TAP media. The culture flasks were then placed under high light intensity at 150 µmol·m^{-2}·s^{-1} and agitated at 100 rpm. The temperature was held constant at 24 °C ± 1 °C and the air at 0.004 % CO_2. These stress conditions were conducted during 7 to 8 days before experimental analysis.

1.3.3 Pretreatments

Pulsed Electric Field (PEF) treatment

A bipolar pulse generator (Betatech Electrocell B10 HVLV) was used to apply unipolar pulses with a peak to peak amplitude that could vary from 0 V to 1000 V, depending on the electric field we want to apply.

The electroporation cuvette (Bio-Rad) was made of plastic involving stainless steel electrodes with a gap (d=1 mm), admitting a sample volume of 130 µL.

The applied electric field strength was calculated as follows:

$$E = \frac{U}{d} \quad (1)$$

where U denotes the applied voltage and d the distance between the electrodes.

The following conditions were tested: 10 unipolar pulses of 5.5 kV·cm^{-1}, a pulse duration of 5 µs, and a repetition frequency of 10 Hz.

Mechanical compression treatment

The microfluidic device was designed to generate cyclic compressive stress on the microalgae cells. Cells enter the microfluidic channels and pass through a series of constrictions that are dimensioned in a way that the size is smaller than the cell diameter (Constrictions height and width: 5 µm; Mean cell diameter: 10 µm), resulting in a cyclic compression on the cell passing through successive restrictions (Fig. 1, 2).

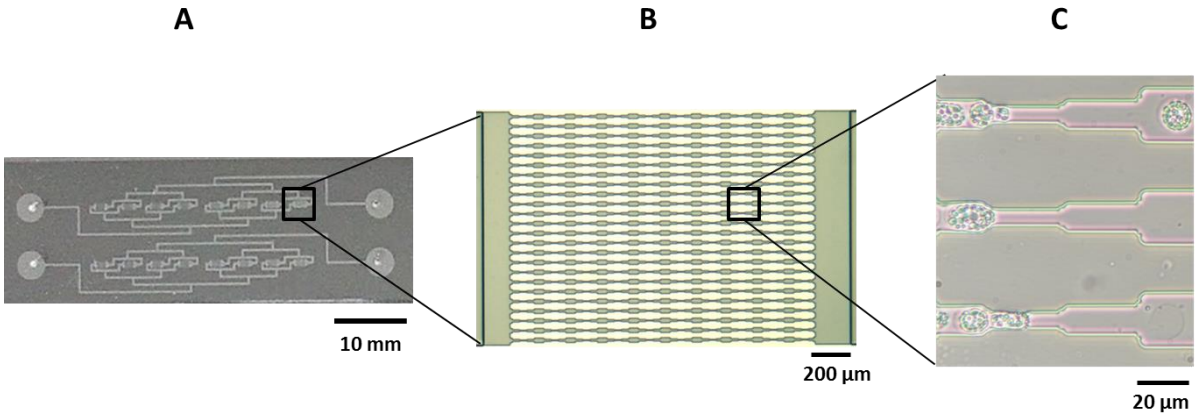

Fig. 1 (A) image of the microfluidic device : double layer PDMS on a microscopic glass slide, (B) microscopic observation of one analysis frame, (C) microscopic observation of *Chlamydomonas reinhardtii* cells flowing through constrictions (under bright field).

The device was fabricated by means of standard soft lithography protocol (Qin et al., 2010), consisting of molding a soft polymer (polydimethylsiloxane, PDMS) on a mold made of thick resist (SU8). The mold is made by superposing and patterning a 5 µm thick SU8-2005 layer (corresponding to the height of restrictions) and 25 µm thick SU8-2025 layer (corresponding to the fluid accesses on a silicone substrate). PDMS was then poured on the mold and treated with oxygen plasma in order to ensure bonding to a glass slide. The overall process is described by Picot et al. (2015).

The microfluidic chip involves 8 analysis frames connected in parallel to the fluidic inlet. On each analysis frame, the flow is separated and forced through 24 parallel thin microchannels, involving the restrictions (Fig. 1). A microfluidic pressure pump (AF1 Pressure Generator, Elveflow) was used to transfer the microalgal solution in the chip with a constant pressure of 1000 mbar which corresponded in our experiment to a flow rate of 1.11 µL·s^{-1}.

A theoretical maximum cell elongation length (21 µm) was calculated as follows:

$$l_{elongation} = \frac{4}{3}\pi \times \frac{r_{cell}^3}{S_f} \quad (2)$$

Experimental setup

In order to study the effect of mechanical and electric stresses *on Chlamydomonas reinhardtii* wild type and mutant strains enriched in lipids (7 to 8 days of nitrogen stress), three distinct pretreatment protocols were tested: (1) mechanical, (2) PEF and (3) PEF followed by mechanical.

After undergoing any of those pretreatments, the cells were submitted to solvent extraction with hexane. In the control assay, cells not being submitted to any of the pretreatments were also put in contact with the organic solvent.

Cell permeability, viability and cell lysis were measured for cells sampled just before and after each treatment (PEF, mechanical treatment, PEF followed by mechanical treatment and solvent contact). Those cells were also observed by optical and Confocal Laser Scanning Microscope (CLSM).

1.3.4 Lipid extraction using organic solvents

The organic solvent hexane (Fisher Scientific, laboratory reagent grade) was added to obtain a final ratio of 2:1 (2 volumes of solvent for 1 volume of algae solution) to the concentrated samples collected after each pretreatment and mixed thoroughly during 15 min (Intelli-Mixer RM-2, Elmi Ltd.).

The sample was then centrifuged in order to separate the different phases. The resulting aqueous phase (cells with the medium) was collected to be analyzed with the sulfo phospho vanillin method (see hereafter).

The above mentioned extraction conditions (hexane, ratio 2:1, 15 min) were also used to evaluate the impact of cell wall evolution over time on lipid extraction.

A mixture of decane and dichloromethane was also tested (with a ratio 1:1) on mutant and wild type cells. The mixture was added to the cell sample to obtain a final ratio of 2:1 (2 volumes of solvent for 1 volume of algae solution). The cells were exposed to the mixture for 30 min.

1.3.5 Cell regrowth

The capability of the cells to grow again after being treated by PEF, mechanical treatment and PEF followed by mechanical treatment was examined by submitting them to the same growth conditions described above (20 $\mu mol \cdot m^{-2} \cdot s^{-1}$; 100 rpm; 25 °C and 1.5 % CO_2) in a total volume of 20 mL and an initial concentration between 1 x 10^5 $cells \cdot mL^{-1}$ and 2 x 10^5 $cells \cdot mL^{-1}$.

1.3.6 Analytical methods

Total lipid quantification

The colorimetric method based on sulfo phospho vanillin reaction (Knight et al., 1972) was used for total lipid estimation after validation in our experimental conditions. The literature

highlighted the advantages of SPV, compared to other methods in particular gravimetric analysis (reliability, less time consuming and applicable to small scale analysis) (Byreddy et al., 2016; Mishra et al., 2014).

A known concentration of biomass in a volume of 100 µL was prepared. The absorbance at 530 nm of each sample was read using a Thermo Scientific spectrophotometer.

The phospho-vanillin reagent was freshly prepared before each experiment and triolein was used as standard.

The total lipid content remaining in the aqueous phase after extraction was calculated as following:

$$Total\ remaining\ lipid\ content\ (\%) = (1 - \frac{Abs_1}{Abs_0}) \times 100 \quad (3)$$

The total remaining lipid content in µg was calculated as an equivalent of Triolein, as follows:

$$Total\ remaining\ lipid\ content(\mu g) = \frac{Abs_{sample}}{0.003} \quad (4)$$

where Abs1 corresponds to the absorbance of the tested sample (after extraction) and Abs0 the absorbance of cells before extraction.

Measurements using flow cytometry

Cell concentration, permeability and viability were measured using flow cytometry (Guava easyCyte microcapillary flow cytometer; EMD Millipore Corporation, 25801 Industrial Blvd., Hayward, CA 94545, USA. For each sample, the number of cells analyzed was typically in the range of 2500 to 5000).

Cell lysis

Cell lysis was evaluated by measuring the cell concentration on samples before and after each pretreatment (PEF, mechanical treatment and PEF followed by mechanical treatment) and solvent contact.

Permeability

Sytox Green (Molecular probes, Lifetechnologies, S7020) was used to assess cell permeability. This dye stains DNA from cells with a permeabilized cell membrane. The dye solution (200 µM) was prepared from a stock solution (5 mM, previously prepared by dissolving Sytox Green in DMSO) by further diluting it in TAP medium. The cellular suspensions (cell concentration: 2 x 10^5 cells·mL^{-1}) were incubated and agitated with a final dye concentration of 0.5 µM for 4 min before analysis. Sytox Green uptake was expressed as the ratio of permeabilized cells (cells stained in green by the dye) over total cells.

Viability assessment: FDA staining

The fluorescent dye FDA was dissolved in acetone to a concentration of 1.1 mM and stored at 4 °C in the dark. FDA solution was added to 1 mL of 1-2 x 10^5 cells·mL^{-1} for a final concentration of 5.5 µM. The sample was then incubated and agitated in the dark for 6 min. The fluorescence intensity was subsequently analyzed through the green channel detector signal of the cytometer. Viable cells have active esterases that enable the hydrolysis of the non-fluorescent FDA into a fluorescent molecule that is fluorescein. Therefore cells are considered viable when they exhibit green fluorescence intensity (Excitation: 430 nm and emission: 525 nm). FDA viability is therefore given by the ratio of green fluorescent cells over total cells.

Microscopic observations

In order to visualize the cell wall and lipid droplets, observations with confocal laser scanning microscope (CLSM 700, Carl Zeiss Microscopy GmbH, Germany) were performed.

Concanavalin A conjugated with tetramethylrhodamine (ConA, yellow-orange fluorescence) and Bodipy 505/515 (green fluorescence) were used for wall and lipid imaging, respectively. Chlorophyll was detected by red autofluorescence. ConA is a lectine that selectively binds to the α-glucopyranosyl residues of the cell wall.

Bodipy 505/515 is a dye that stains exclusively neutral lipids (Benito et al., 2015; Bono Jr. et al., 2015; Govender et al., 2012). A stock solution of the green lipophilic fluorescent dye Bodipy 505/515 (Molecular probes, Lifetechnologies, D-3921) was prepared by dissolving it in DMSO to a concentration of 100 mg·L^{-1}. After an optimization step, bodipy was added to 1 mL cell suspensions (cell concentration of 10^6 cells·mL^{-1}) giving a final concentration of 1.5 µg·mL^{-1}. Fluorescence intensity was recorded after 10 min of incubation and agitation.

The stock solution of ConA (Molecular Probes, Lifetechnologies, C860) was prepared by dissolving it in 0.1 M sodium bicarbonate (pH ≈ 8.3) to a final concentration of 2 mg·mL^{-1}.

A Nikon eclipse Ti-U inverted microscope was also used to observe cells flowing through the microfluidic constrictions using a 20X objective (Nikon Plan fluor 20× DICN2NA= 0.6).

1.4 Results and discussion

1.4.1 Extraction efficiency

In this study, the effect of the electrical and/or the mechanical pretreatments on the extraction efficiency of lipids using hexane as the extraction solvent was evaluated (Fig. 2).

The results were compared to the extraction of lipids from cells that weren't submitted to any pretreatment.

Figure 2 highlights the fact that a higher extraction yield was obtained using the coupled pretreatments followed by solvent extraction ($p < 0.05$). The variability of data among replicates observed is probably due to differences in microalgae cultures though experiments were carefully performed under the same conditions. This observation will be further discussed (subsection 3.4). No statistically significant differences in lipid extraction were obtained when cells were submitted to PEF and mechanical stress compared to the control (this point will be further discussed in subsection 3.2).

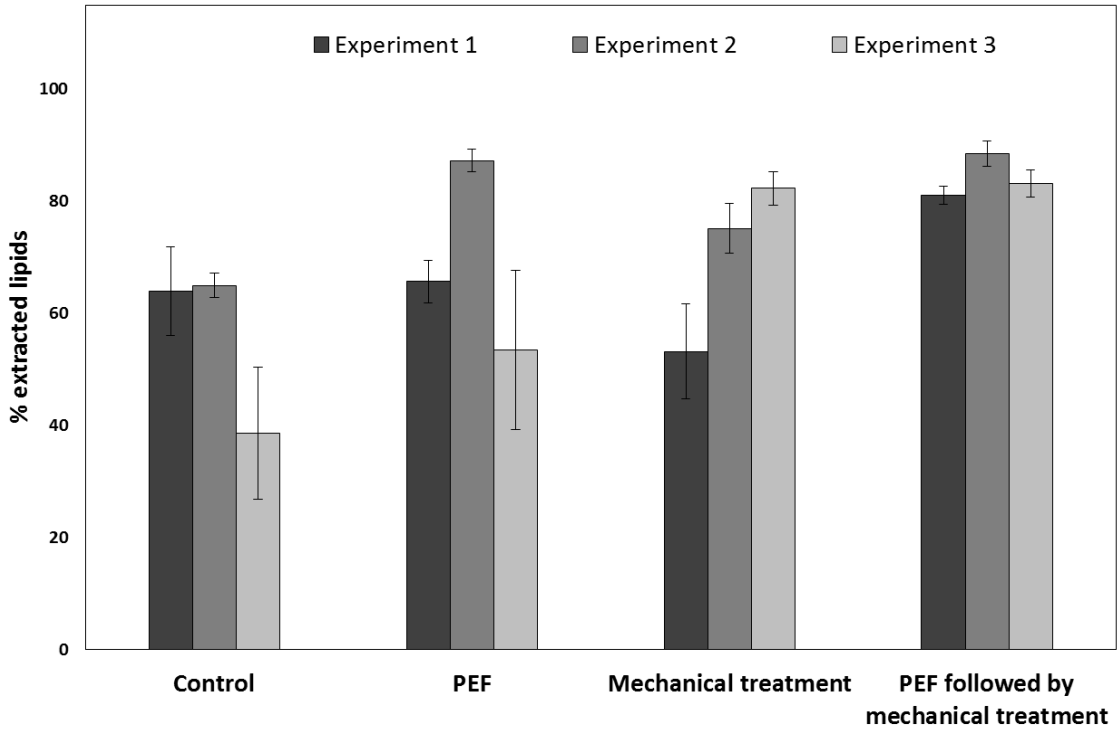

Fig. 2 Percentage of extracted lipids from pretreated *Chlamydomonas reinhardtii* using the solvent hexane (15 min of exposure time). *C.reinhardtii* was submitted to three distinct pretreatments before solvent extraction with hexane: Pulsed electric field treatment, mechanical compression, a combination of both pretreatments. The control corresponds to a solvent extraction using hexane on cells that haven't been pretreated. Results show three independent experiments performed on three different algae cultures. Error bars represent the standard deviation of triplicate samples.

In order to understand the mechanism behind the observed increase in lipid extraction efficiency, the impact of each treatment (PEF, mechanical compression and solvent) on cell structure (membrane and cell wall), cell lysis and physiology (viability and cell regrowth) were evaluated. It should be stressed that parameters such as cell viability and growth must be followed closely when considering cell reusal in bioprocesses.

1.4.2 Understanding mechanisms of extraction

Impact of pretreatments on cell structure and physiology

In order to evaluate the effect of the different pretreatments on cell membrane, permeability was assessed (Fig. 3).

Results show that 4.2 ± 2.5 % of the cells were, before any treatment (PEF, mechanical treatment and PEF followed by mechanical treatment), naturally permeabilized. This is due to the stress conditions (nitrogen starvation) in which the cells were exposed during 7 to 8 days before the experiment, as previously reported (Bodénès et al., 2016). Indeed, conditions inducing lipid storage clearly impact cell physiology (Velmurugan et al., 2013).

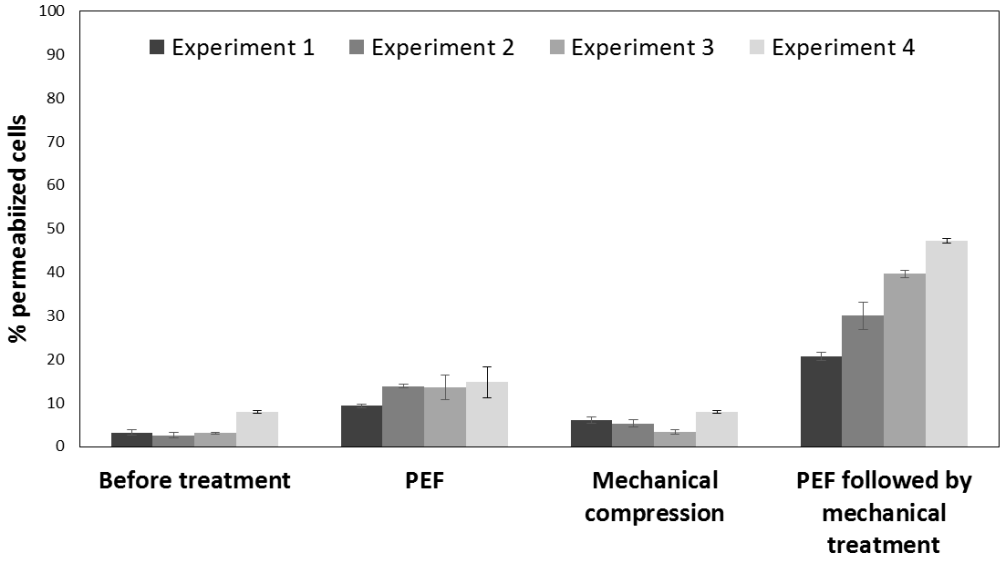

Fig. 3 Percentage of permeabilized cells (Sytox Green uptake) before and after being submitted to the following pretreatments: Pulsed electric field treatment, mechanical compression and a combination of both pretreatments. Results were analyzed by flow cytometry. Data show four independent experiments performed on four different algae cultures. Error bars represent the standard deviation of triplicate samples.

Overall, the three configurations (PEF treatment, mechanical treatment, or both conjugated treatments) have shown an impact on cell permeability with less extent for the mechanical compression pretreatment.

Most importantly, the results of figure 3 show that pretreating cells with PEF followed by mechanical treatment leads to the highest increase in the percentage of permeable cells. As mentioned previously, variability of data among assays was observed (see hereafter).

C.reinhardtii showed a high resistance to all pretreatments: no cell lysis was observed in these experiments. The cell viability, assessed using FDA staining, was however impacted differently depending on the pretreatment used. Mechanical compression led to a decrease in cell viability from 91.7 % to 78.3 %, while PEF treatment showed a final cell viability of 67.5 %. The decrease was more obvious in the case of a combination of both pretreatments; only 46.4 % of the cells remained viable.

Complementary assays were carried out to evaluate the cell ability to divide after each pretreatment, as shown in figure 4 where *C.reinhardtii* has proven to be able to grow after any of the three pretreatments.

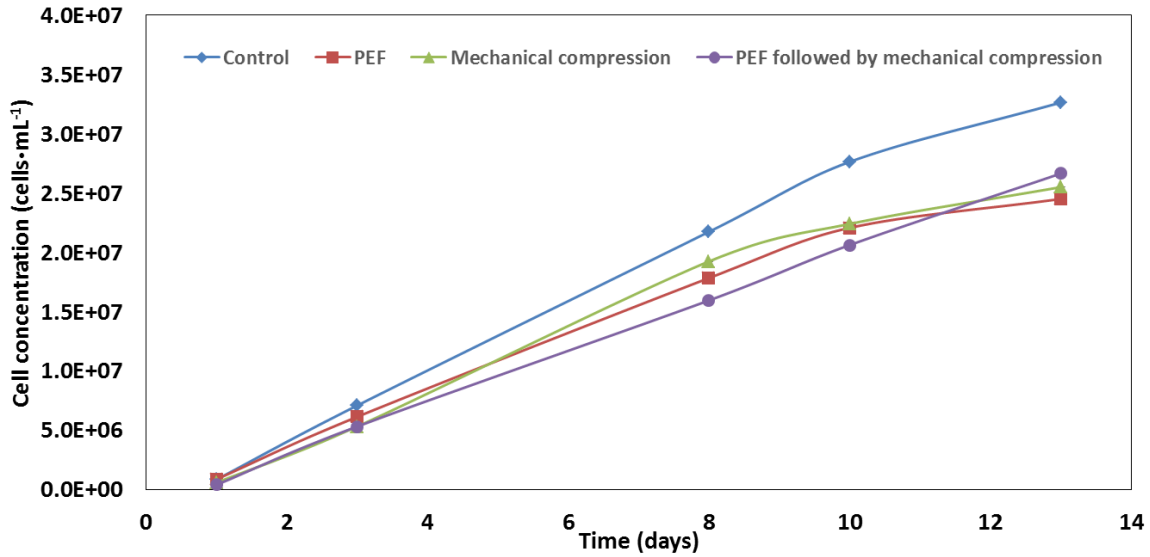

Fig. 4 *Chlamydomonas reinhardtii*'s growth after different pretreatments: Pulsed electric field, mechanical compression and a combination of both pretreatments. The control corresponds to cell that have only been submitted to 7 days of stress and weren't submitted to any pretreatment.

In order to further evaluate pretreatment impact on cell structure, cells were observed by CLSM microscopy.

Cells passing through the constrictions and thus submitted to mechanical effects are shown in Fig. 5. A deformation of the cells seems to be observed after their passage through the series of constrictions suggesting an impact of mechanical stress on cell morphology. Indeed, in some cases, after mechanical compression, the cells seemed to present a different morphology (keeping an oval shape instead of the original round shape). We hypothesize therefore an impact of the mechanical stress on the cell wall.

On the contrary, cell wall does not seem to be affected by PEF treatment. This is in agreement with data from Azencott et al. (Azencott et al., 2007), suggesting that electroporation primarily transports molecules across the plasma membrane. On the other hand, PEF clearly leads to lipid droplets fusion, as previously demonstrated (Bodénès et al., 2016) (Fig. 5). Interestingly, lipid droplets structure is also affected by PEF. Such morphological effects of lipid droplets are not observed when cells are submitted to mechanical stress.

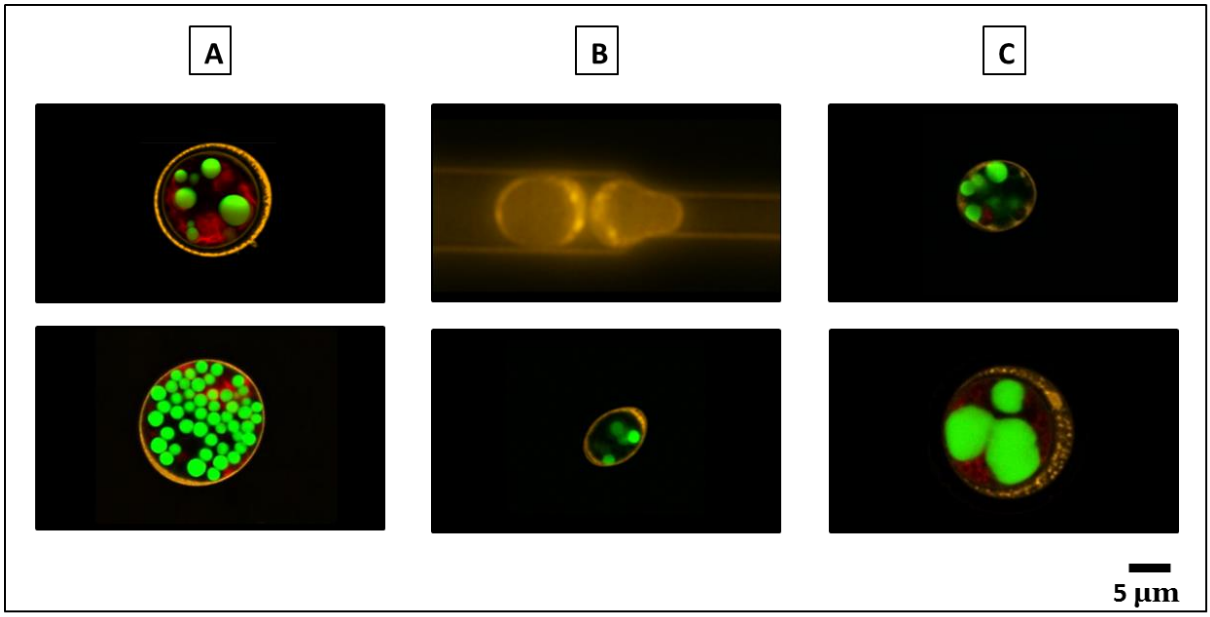

Fig. 5 Confocal microscopic observation of *Chlamydomonas reinhardtii* under different conditions: (A) Control; cells submitted to lipid accumulation conditions during 7 days, (B) cells after 7 days of lipid accumulation flowing through the constriction within the microfluidic device (upper image) and after the mechanical treatment, (C) cells after 7 days of lipid accumulation and PEF treatment. Lipid droplets were stained with Bodipy 505/515 (green), the cell wall with Concanavalin A (orange). Scale bar : 5 µm

Solvent extraction

Assays are then carried out to assess mechanisms of lipid extraction from the cell with hexane coupled or not with pretreatments.

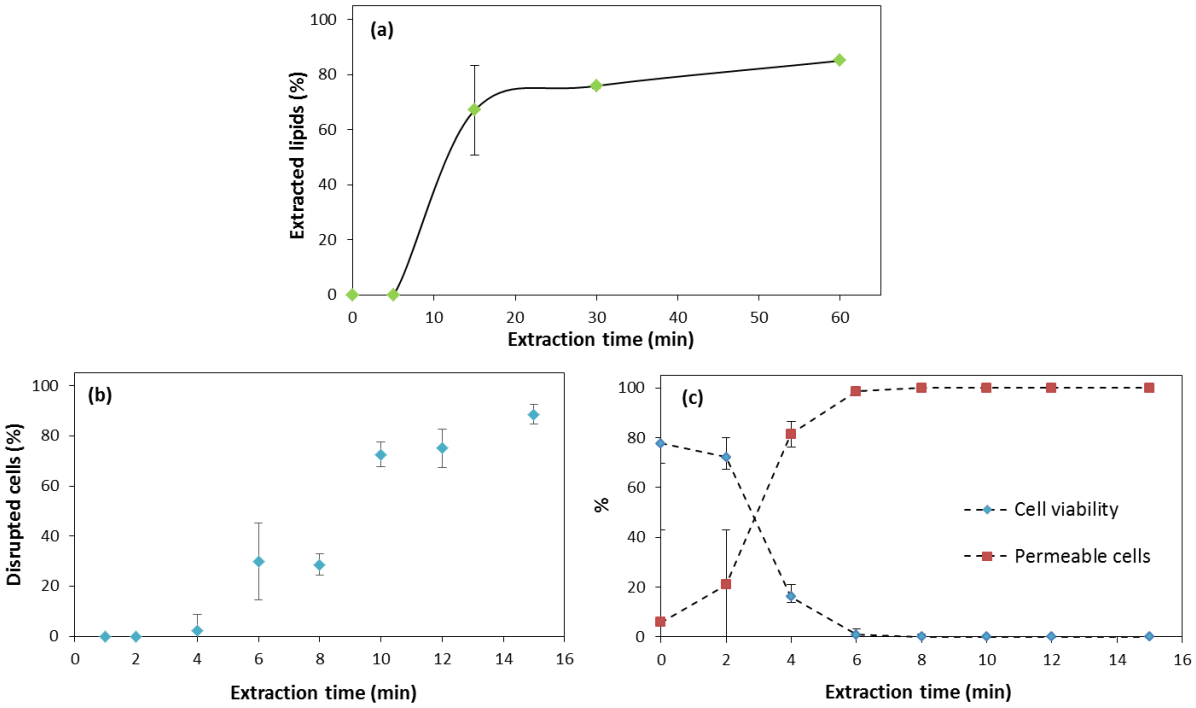

Fig. 6 Hexane lipid extraction on *Chlamydomonas reinhardtii*: correlation between the extraction efficiency and cell lysis. Solvent/cell ratio = 2:1 (a) Evolution of the lipid extraction with time, (b) Cell lysis as a function of time, (c) Percentage of viable and permeable cells with time during lipid extraction with hexane: the dye FDA was used to assess cell viability and Sytox green for the permeable cells (amongst the non-disrupted cells) and the cell concentration for the disrupted cells. Error bars represent the standard deviation of triplicate samples.

Results (Fig. 6) clearly show that the extraction efficiency of the solvent is closely related to cell lysis. Indeed, hexane started extracting lipids after a minimum contact of 5 min (Fig. 6a). It is also at this same moment that we could observe a rise in cell disruption (Fig. 6b). Therefore, the mechanism proposed by Halim et al. (Halim et al., 2012) by which hexane, a non-polar organic solvent, is believed to enter the cytoplasm of the algae cells by passing through the membrane, form a complex with the lipids followed by the diffusion of the complex through the cell membrane does not apply to our study. Our results are though in agreement with data presented by Yap et al. (Yap et al., 2014) showing that cell disruption must occur to extract lipids from the green algae, *C. vulgaris*.

When considering lipid extraction with hexane coupled with PEF treatment, the latter does not seem to impact significantly the cell lysis (Table 1, “PEF”) as previously stated (subsection 3.2). PEF treatment led to 91.5 ± 0.2 % of disrupted cells in one case and in

another 94.5 ± 0.03 %. In parallel, hexane alone led to 88.3 ± 0.3 % and 93.8 ± 0.1 % respectively. Indeed, cell lysis in this case is mainly due to the presence of the solvent. This is in agreement with data in figure 2 showing similar extraction efficiencies with PEF followed by hexane extraction and the control.

In future work, other PEF conditions (more aggressive) may be applied in order to evaluate whether PEF definitely affect lipid extraction.

		PEF		**PEF followed by mechanical treatment**	
		Control	After pretreatment	Control	After pretreatment
% extracted lipids		81.4 ± 2.3	88.2 ± 2.0	81.7 ± 4.9	87.9 ± 4.2
% disrupted cells	*Experiment 1*	93.8 ± 0.1	94.5 ± 0.03	79.3 ± 4.0	92.2 ± 0.9
	Experiment 2	88.3 ± 0.3	91.5 ± 0.2		

Table 1 Impact of different pretreatments on lipid extraction and cell lysis after hexane solvent extraction (Contact time: 15 min) . The control represents a hexane extraction on unpretreated cells; cells submitted to PEF and PEF followed by mechanical treatment were subject to solvent extraction afterwards.

In the case of the combination of both pretreatments (PEF and mechanical stress), a higher lipid extraction efficiency was determined compared to that of the solvent (Fig. 2). This is consistent with a higher lysis extent obtained when cells were submitted to electrical and mechanical stress prior to solvent (92.2 ± 0.9 % of disrupted cells compared to 79.3 ± 4 % for solvent alone). Therefore, it seems that cells submitted to both pretreatments are weakened and more prone to lysis which is also in agreement with data on cell permeability (Fig. 3).

In conclusion, in all tested conditions (solvent coupled or not to pretreatments), lipid extraction is clearly associated to cell lysis. Furthermore, assays were also performed with other solvents (ethyl acetate, methyl ethyl ketone, dichloromethane…) and mixtures of those with biocompatible solvents (decane and dodecane) conducting to similar trends where the extraction is correlated with cell disruption (data not shown). These results indicate that the disintegration of the cell wall is a key condition for lipid extraction from *Chlamydomonas reinhardtii*, which was previously reported in the literature for certain microalgae species (Kim et al., 2016; Lee et al., 2017).

Moreover, the results in figure 6.c show that the cell viability of the non-disrupted cells declined rapidly to 0 % after 4 min of contact with the solvent along with an increase in cell permeability which is due to hexane toxicity as stated by Miazek et al. (Miazek et al., 2017).

1.4.3 Impact of the cell wall on lipid extraction

In order to further evaluate the impact of cell wall in lipid extraction, experiments were performed with the cell wall deficient *C. reinhardtii* using a mixture of decane (so called biocompatible solvent) and dichloromethane.

Results clearly demonstrate (Table 2) that lipid extraction occurs only with lysed cells (as previously stated) which confirms the role of the cell wall as a barrier to the solvent action. The viability of the remaining cells of the mutant and the wild type *Chlamydomonas reinhardtii* is highly affected by such treatment. This is in agreement with data obtained for hexane solvent (see Fig. 6).

	Disrupted cells (%)	Cell viability (%)	Extracted lipids (%)
Wild type strain	0	0	0
Mutant strain	67.6	0	53.9

Table 2 Percentage of disrupted cells (cell lysis), cell viability and recovered lipids after lipid extraction. The following solvent mixture was used: Decane-Dichloromethane (1:1) with a solvent contact time of 30 min. Solvent/cell ratio = 2:1.

Similar results were obtained using the biocompatible decane solvent. In the presence of the cell wall, no lysis and no lipid extraction was observed even in case of coupling this solvent with PEF pretreatment (data not shown). The latter seems to confirm that PEF has no effect on the cell wall. In addition, the critical membrane concentration of this solvent is not expected to be attained (Mojaat et al., 2008) and therefore, no effect of this solvent on the cell is observed.

The overall data are in agreement with our CLSM observations (data not shown) where lipids are entrapped by the cell wall.

1.4.4 Variability of cell wall structuration

Variability on extraction efficiency and cell permeability data was observed previously for independent experiences (Fig. 2 and 3). This could be associated to variability on cell structure among the different cultures tested though similar conditions were applied. The same observation was stated by Goettel et al. (2013).

As it has been shown in previous articles, *Chlamydomonas reinhardtii* is composed of a 7 layers cell wall (Goodenough and Heuser, 1985; Roberts et al., 1974). However, throughout our experiments, a high variability of the structure of the cells was observed: cells in division, cells with one very thick layer of cell wall, cells with one thinner layer of cell wall, 2 to 3

layers of cell wall, and more than 3 layers. The occurrence of multiple layers is correlated to culture conditions and/or the time of the culture.

For instance, at 7 days of lipid accumulation, the percentage of cells in division (Mean %: 5.9), cells with one very thick layer of cell wall (Mean %: 7.8), cells with one thinner layer of cell wall (Mean %: 62.4), 2 to 3 layers of cell wall (Mean %: 17.4), and more than 3 layers (Mean %: 6.5) could be found and this is clearly different from one algal culture to another. This is in agreement with the variability in the extraction efficiency, observed throughout the experiments. On the other hand, experiments were carried out to evaluate the impact of cell wall evolution over time on lipid extraction.

Results showed that when *C. reinhardtii* is stressed during 2 to 3 days, the majority of the cells in the culture would have a thin layer cell wall or be in division (69 % and 15.4 % respectively). After 7 to 8 days of stress conditions, we could start observing more cells with 2 to 3 layers and more than 3 layers, but the majority would still have one thin layer (62%). When it is stressed for more than 20 days, the majority of the cells would have 2 to 3 layers (41.3 %) or more than 3 layers; up to 7 layers (39.1 %).

Concerning lipid extraction, unexpectedly, results showed that the extraction efficiency was higher when the culture was stressed during a longer time (lipid yield of 40 %, 79% and 90 % for cells at 3, 7 and 21 days of accumulation, respectively). In addition, the cell lysis after solvent extraction was higher when the culture was stressed for a longer time (cell disruption 63 %, 76 % and 82 % for cells at 3, 7 and 21 days of accumulation, respectively). A relation between the structure and/or composition of the cell wall and the efficiency of extraction of the solvent is hypothesized and should be studied in a further study.

1.5 Conclusions

In this study, the lipid extraction efficiency of several pretreatments (electrical, mechanical or both pretreatments) coupled to solvents was investigated. The studied pretreatments affect differently cell structure and viability. It was demonstrated that cell lysis must occur to extract lipids with the tested solvents. An increase in the extraction efficiency was observed for the coupled treatments suggesting that cells were more prone to the lysing inducing solvent action. The impact of the cell wall (in particular thickness) on lipid extraction was further confirmed. This should be further studied and compared with other treatment methods in a future work.

1.6 Acknowledgements

This work was funded by the financial support of the LabeX LaSIPS (ANR-10-LABX-0040-LaSIPS) managed by the French National Research Agency under the "Investissements d'avenir" program (n°ANR-11-IDEX-0003-02).

1.7 References

Adarme-Vega, T., Lim, D.K.Y., Timmins, M., Vernen, F., Li, Y., Schenk, P.M., 2012. Microalgal biofactories: a promising approach towards sustainable omega-3 fatty acid production. Microb. Cell Fact. 11, 96. https://doi.org/10.1186/1475-2859-11-96

Araujo, G.S., Matos, L.J.B.L., Fernandes, J.O., Cartaxo, S.J.M., Gonçalves, L.R.B., Fernandes, F. a N., Farias, W.R.L., 2013. Extraction of lipids from microalgae by ultrasound application: Prospection of the optimal extraction method. Ultrason. Sonochem. 20, 95–98. https://doi.org/10.1016/j.ultsonch.2012.07.027

Atabani, a. E., Silitonga, a. S., Badruddin, I.A., Mahlia, T.M.I., Masjuki, H.H., Mekhilef, S., 2012. A comprehensive review on biodiesel as an alternative energy resource and its characteristics. Renew. Sustain. Energy Rev. 16, 2070–2093. https://doi.org/10.1016/j.rser.2012.01.003

Azencott, H.R., Peter, G.F., Prausnitz, M.R., 2007. Influence of the cell wall on intracellular delivery to algal cells by electroporation and sonication. Ultrasound Med. Biol. 33, 1805–17. https://doi.org/10.1016/j.ultrasmedbio.2007.05.008

Behera, S., Singh, R., Arora, R., Sharma, N.K., Shukla, M., 2015. Scope of algae as third generation biofuels 2, 1–13. https://doi.org/10.3389/fbioe.2014.00090

Benito, V., Goñi-de-Cerio, F., Brettes, P., 2015. BODIPY vital staining as a tool for flow cytometric monitoring of intracellular lipid accumulation in Nannochloropsis gaditana. J. Appl. Phycol. 27, 233–241. https://doi.org/10.1007/s10811-014-0310-x

Bodénès, P., Lopes, F., Pareau, D., Français, O., Le Pioufle, B., 2016. Microdevice for studying the in situ permeabilization and characterization of Chlamydomonas reinhardtii in lipid accumulation phase. Algal Res. 16, 357–367. https://doi.org/10.1016/j.algal.2016.03.023

Bono Jr., M.S., Garcia, R.D., Sri-Jayantha, D. V., Ahner, B.A., Kirby, B.J., 2015. Measurement of Lipid Accumulation in Chlorella vulgaris via Flow Cytometry and Liquid-State ^{1}H NMR Spectroscopy for Development of an NMR-Traceable Flow Cytometry Protocol. PLoS One 10, e0134846. https://doi.org/10.1371/journal.pone.0134846

Bravo-Fritz, C.P., S??ez-Navarrete, C. a., Herrera-Zeppelin, L. a., Varas-Concha, F., 2016. Multi-scenario energy-economic evaluation for a biorefinery based on microalgae biomass with application of anaerobic digestion. Algal Res. 16, 292–307. https://doi.org/10.1016/j.algal.2016.03.028

Byreddy, A.R., Gupta, A., Barrow, C.J., Puri, M., 2016. A quick colorimetric method for total lipid quantification in microalgae. J. Microbiol. Methods 125, 28–32. https://doi.org/10.1016/j.mimet.2016.04.002

Cooney, M., Young, G., Nagle, N., 2009. Extraction of bio-oils from microalgae. Sep. Purif. Rev. 38, 291–325. https://doi.org/10.1080/15422110903327919

Eing, C.J., Goettel, M., Straessner, R., Gusbeth, C., Frey, W., 2013. Pulsed Electric Field Treatment of Microalgae—Benefits for Microalgae Biomass Processing. IEEE Trans. Plasma Sci. 41, 2901–2907. https://doi.org/10.1109/TPS.2013.2274805

Geng, T., Zhan, Y., Wang, H.Y., Witting, S.R., Cornetta, K.G., Lu, C., 2010. Flow-through electroporation based on constant voltage for large-volume transfection of cells. J. Control. Release 144, 91–100. https://doi.org/10.1016/j.jconrel.2010.01.030

Gerde, J. a., Montalbo-Lomboy, M., Yao, L., Grewell, D., Wang, T., 2012. Evaluation of microalgae cell disruption by ultrasonic treatment. Bioresour. Technol. 125, 175–181. https://doi.org/10.1016/j.biortech.2012.08.110

Goettel, M., Eing, C., Gusbeth, C., Straessner, R., Frey, W., 2013. Pulsed electric fi eld assisted extraction of intracellular valuables from microalgae. ALGAL 2, 401–408. https://doi.org/10.1016/j.algal.2013.07.004

Goodenough, U.W., Heuser, J.E., 1985. The Chlamydomonas Cell Wall Glycoproteins Analyzed by the Technique and Its Constituent Quick-Freeze, Deep-Etch 101.

Gorman, D.S., R.P.L., 1965. TAP and Tris-minimal* medium. Proc. Natl. Acad. Sci. USA 1665–1669.

Govender, T., Ramanna, L., Rawat, I., Bux, F., 2012. BODIPY staining, an alternative to the Nile Red fluorescence method for the evaluation of intracellular lipids in microalgae. Bioresour. Technol. 114, 507–511. https://doi.org/10.1016/j.biortech.2012.03.024

Günerken, E., D'Hondt, E., Eppink, M.H.M., Garcia-Gonzalez, L., Elst, K., Wijffels, R.H., 2015. Cell disruption for microalgae biorefineries. Biotechnol. Adv. 33, 243–260. https://doi.org/10.1016/j.biotechadv.2015.01.008

Halim, R., Danquah, M.K., Webley, P. a., 2012. Extraction of oil from microalgae for biodiesel production: A review. Biotechnol. Adv. 30, 709–732. https://doi.org/10.1016/j.biotechadv.2012.01.001

Halim, R., Rupasinghe, T.W.T., Tull, D.L., Webley, P. a., 2013. Mechanical cell disruption for lipid extraction from microalgal biomass. Bioresour. Technol. 140, 53–63. https://doi.org/10.1016/j.biortech.2013.04.067

Kim, D.Y., Vijayan, D., Praveenkumar, R., Han, J.I., Lee, K., Park, J.Y., Chang, W.S., Lee, J.S., Oh, Y.K., 2016. Cell-wall disruption and lipid/astaxanthin extraction from microalgae: Chlorella and Haematococcus. Bioresour. Technol. 199, 300–310. https://doi.org/10.1016/j.biortech.2015.08.107

Kim, J., Yoo, G., Lee, H., Lim, J., Kim, K., Kim, C.W., Park, M.S., Yang, J.W., 2013. Methods of downstream processing for the production of biodiesel from microalgae. Biotechnol. Adv. 31, 862–876. https://doi.org/10.1016/j.biotechadv.2013.04.006

Knight, J. a, Anderson, S., Rawle, J.M., 1972. ChemicalBasisof the Sulfo-phospho-vanillin Reactionfor Estimating Total Serum Lipids 199–202.

Kumar, S.P.J., Prasad, S.R., Banerjee, R., Agarwal, D.K., Kulkarni, K.S., Ramesh, K. V, 2017. Green solvents and technologies for oil extraction from oilseeds Green solvents and technologies for oil extraction from oilseeds. Chem. Cent. J. https://doi.org/10.1186/s13065-017-0238-8

Lai, Y.S., Parameswaran, P., Li, A., Baez, M., Rittmann, B.E., 2014. Effects of pulsed electric field treatment on enhancing lipid recovery from the microalga, Scenedesmus. Bioresour. Technol. 173, 457–461. https://doi.org/10.1016/j.biortech.2014.09.124

Lee, A.K., Lewis, D.M., Ashman, P.J., 2012. Disruption of microalgal cells for the extraction of lipids for biofuels: Processes and specific energy requirements. Biomass and Bioenergy 46, 89–101. https://doi.org/10.1016/j.biombioe.2012.06.034

Lee, S.Y., Cho, J.M., Chang, Y.K., Oh, Y.K., 2017. Cell disruption and lipid extraction for microalgal biorefineries: A review. Bioresour. Technol. 244, 1317–1328. https://doi.org/10.1016/j.biortech.2017.06.038

Miazek, K., Kratky, L., Sulc, R., Jirout, T., Aguedo, M., Richel, a., Goffin, D., 2017. Effect of organic solvents on microalgae growth, metabolism and industrial bioproduct extraction: A review. Int. J. Mol. Sci. 18. https://doi.org/10.3390/ijms18071429

Min, S.K., Yoon, G.H., Joo, J.H., Sim, S.J., Shin, H.S., 2014. Mechanosensitive physiology of chlamydomonas reinhardtii under direct membrane distortion. Sci. Rep. 4, 4675. https://doi.org/10.1038/srep04675

Minhas, A.K., Hodgson, P., Barrow, C.J., Adholeya, A., 2016. A review on the assessment of stress conditions for simultaneous production of microalgal lipids and carotenoids. Front. Microbiol. 7, 1–19. https://doi.org/10.3389/fmicb.2016.00546

Mishra, S.K., Suh, W.I., Farooq, W., Moon, M., Shrivastav, A., Park, M.S., Yang, J.W., 2014. Rapid quantification of microalgal lipids in aqueous medium by a simple colorimetric method. Bioresour. Technol. 155, 330–333. https://doi.org/10.1016/j.biortech.2013.12.077

Mojaat, M., Foucault, A., Pruvost, J., Legrand, J., 2008. Optimal selection of organic solvents for biocompatible extraction of ␣ -carotene from Dunaliella salina 133, 433–441. https://doi.org/10.1016/j.jbiotec.2007.11.003

Nezammahalleh, H., Nosrati, M., Ghanati, F., 2016. Exergy-based screening of biocompatible solvents for in situ lipid extraction from Chlorella vulgaris. J. Appl. Phycol. https://doi.org/10.1007/s10811-016-0921-5

Olmstead, I.L.D., Kentish, S.E., Scales, P.J., Martin, G.J.O., 2013. Low solvent, low temperature method for extracting biodiesel lipids from concentrated microalgal biomass. Bioresour. Technol. 148, 615–619. https://doi.org/10.1016/j.biortech.2013.09.022

P, J.K.S., Kumar, V., Dash, A., Scholz, P., Banerjee, R., 2017. Sustainable green solvents and techniques for lipid extraction from microalgae : A review. ALGAL 21, 138–147. https://doi.org/10.1016/j.algal.2016.11.014

Pataro, G., Goettel, M., Straessner, R., Gusbeth, C., Ferrari, G., Frey, W., 2017. Effect of PEF treatment on extraction of valuable compounds from microalgae C. Vulgaris. Chem. Eng. Trans. 57, 67–72. https://doi.org/10.3303/CET1757012

Postma, P.R., Miron, T.L., Olivieri, G., Barbosa, M.J., Wijffels, R.H., Eppink, M.H.M., 2015. Mild disintegration of the green microalgae Chlorella vulgaris using bead milling. Bioresour. Technol. 184, 297–304. https://doi.org/10.1016/j.biortech.2014.09.033

Qin, D., Xia, Y., Whitesides, G.M., 2010. Soft lithography for micro- and nanoscale patterning. Nat. Protoc. 5, 491–502. https://doi.org/10.1038/nprot.2009.234

Rakesh, S., Dhar, D.W., Prasanna, R., Saxena, A.K., Saha, S., Shukla, M., Sharma, K., 2015. Cell disruption methods for improving lipid extraction efficiency in unicellular microalgae. Eng. Life Sci. 15, 443–447. https://doi.org/10.1002/elsc.201400222

Ranjith Kumar, R., Hanumantha Rao, P., Arumugam, M., 2015. Lipid Extraction Methods from Microalgae: A Comprehensive Review. Front. Energy Res. 2, 1–9. https://doi.org/10.3389/fenrg.2014.00061

Roberts, K., Phillips, J.M., Hills, G.J., 1974. Structure, composition and morphogenesis of the cell wall of Chlamydomonas reinhardi. VI. The flagellar collar. Micron (1969) 5, 341–357. https://doi.org/10.1016/0047-7206(74)90021-1

Ryckebosch, E., Muylaert, K., Foubert, I., 2012. Optimization of an analytical procedure for extraction of lipids from microalgae. JAOCS, J. Am. Oil Chem. Soc. 89, 189–198. https://doi.org/10.1007/s11746-011-1903-z

Santana, a., Jesus, S., Larrayoz, M. a., Filho, R.M., 2012. Supercritical carbon dioxide extraction of algal lipids for the biodiesel production. Procedia Eng. 42, 1755–1761. https://doi.org/10.1016/j.proeng.2012.07.569

Slegers, P.M., Koetzier, B.J., Fasaei, F., Wijffels, R.H., van Straten, G., van Boxtel, a. J.B., 2014. A model-based combinatorial optimisation approach for energy-efficient processing of microalgae. Algal Res. 5, 140–157. https://doi.org/10.1016/j.algal.2014.07.004

Takeshita, T., 2011. Competitiveness, role, and impact of microalgal biodiesel in the global energy future. Appl. Energy 88, 3481–3491. https://doi.org/10.1016/j.apenergy.2011.02.009

Vanthoor-Koopmans, M., Wijffels, R.H., Barbosa, M.J., Eppink, M.H.M., 2013. Biorefinery of microalgae for food and fuel. Bioresour. Technol. 135, 142–149. https://doi.org/10.1016/j.biortech.2012.10.135

Velmurugan, N., Sung, M., Yim, S.S., Park, M.S., Yang, J.W., Jeong, K.J., 2013. Evaluation of intracellular lipid bodies in Chlamydomonas reinhardtii strains by flow cytometry. Bioresour. Technol. 138, 30–37. https://doi.org/10.1016/j.biortech.2013.03.078

Yap, B.H.J., Crawford, S.A., Dumsday, G.J., Scales, P.J., Martin, G.J.O., 2014. A mechanistic study of algal cell disruption and its effect on lipid recovery by solvent extraction. ALGAL 5, 112–120. https://doi.org/10.1016/j.algal.2014.07.001

Yap, B.H.J., Dumsday, G.J., Scales, P.J., Martin, G.J.O., 2015. Energy evaluation of algal cell disruption by high pressure homogenisation. Bioresour. Technol. 184, 280–285. https://doi.org/10.1016/j.biortech.2014.11.049

Zbinden, M.D.A., Sturm, B.S.M., Nord, R.D., Carey, W.J., Moore, D., Shinogle, H., Stagg-Williams, S.M., 2013. Pulsed electric field (PEF) as an intensification pretreatment for greener solvent lipid extraction from microalgae. Biotechnol. Bioeng. 110, 1605–1615. https://doi.org/10.1002/bit.24829

Complementary results

Impact of treatments on *Chlamydomonas reinhardtii* cells

Additional results concerning the effect of mechanical, electrical and chemical stress on Chlamydomonas cells (permeability, viability, lysis), wild type and mutant, are presented hereafter.

Effect of the order of the process on cell fragility

To study the potential of our chosen pretreatments as facilitators of lipid extraction, the impact of the different pretreatments and their order on cell permeability was assessed. The *Chlamydomonas reinhardtii* wild type cells were stained with Sytox Green and were analyzed using a flow cytometer as previously reported (see section 1.3.6). Part of these results were published in the article of Section 1; however, the following configuration was not discussed: mechanical compressions followed by PEFs.

Results demonstrated that the highest percentage of permeabilized cells was obtained for coupled pretreatments with PEFs as a first step followed by mechanical compressions. This also leads to a higher extraction efficiency when submitting the cells to lipid extraction using hexane. An increase of permeabilized cells from 4.2 % to 11.7 % was observed with mechanical compressions followed by PEFs.

These data clearly show that cell weakness is strongly dependent on the order of solicitations applied. The impact on the cell membrane is more significant when the cell is first submitted to the opening of pores through PEF and then to the mechanical compression that seems to mostly impact the cell wall (which was demonstrated in our previous and published results). These observations highlight the importance of studying the cell and specifically its morphological and structural responses to different pretreatments in order to improve lipid extraction from microalgae. This will be further be discussed in Chapter 4.

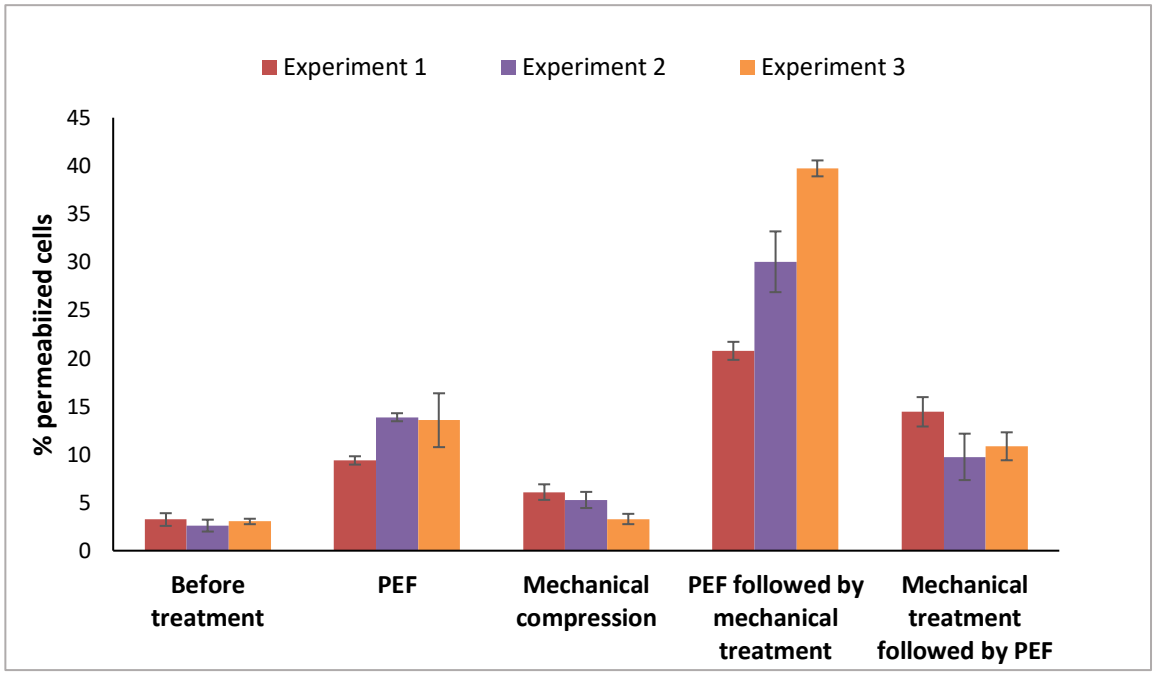

Figure 1 Percentage of permeabilized cells after undergoing different pretreatments. The experiment was conducted on three different cultures.

Screening of solvents for lipid extraction

In the following section, data on cell permeability, viability and lipid recovery for different tested conditions (type of solvent with different properties such as hydrophilicity, exposure time) are presented.

First, we focused on biocompatible solvents for lipid extraction. We therefore first tested the solvent decane (logP ≈ 6).

When submitting the microalgae cells to decane (ratio decane/cells: 2:1), no lysis was observed (extraction time: 120 min). The cell viability however started decreasing after 1 hour of extraction treatment, from 85 % to 47.4 % (Figure 2). These results are similar to the ones obtained in the case of the solvent duo decane-dichloromethane (1:1, logP dichloromethane ≈ 1.25; see hereafter). After 30 min, the cell viability was highly impacted when using this solvent duo.

No extraction was observed in the case of decane alone. In addition, no improvement was observed when cells were previously pretreated by PEFs followed by the mechanical compressions. Data clearly confirm the need to test other solvents.

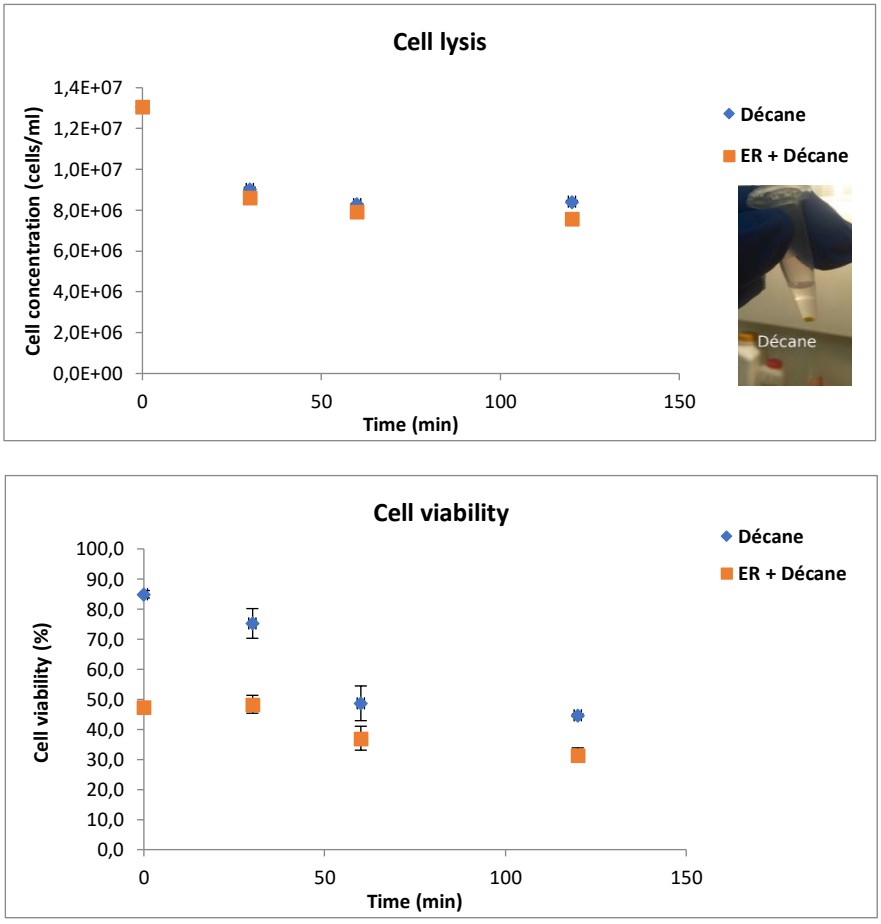

Figure 2 Flow cytometry analysis of the cell viability and cell concentration after decane extraction (control) and the pretreatment PEFs followed by mechanical compressions (ER).

Table 1 shows cell lysis, cell viability and lipid yield after an extraction using different solvents (ratio solvent:cells = 1:1 and extraction time = 30 min): dodecane (logP ≈ 7), decane (logP ≈ 6), hexane (logP ≈ 3.9), dichloromethane (logP ≈ 1.25), dodecane:dichloromethane (1:1), decane:dichloromethane (1:1) and hexane:ethanol (1:1).

	Before extraction	**Dodecane**	**Decane**	**Hexane**	**Dichloromethane**	**Dodecane-Dichloromethane (1:1)**	**Decane-Dichloromethane (1:1)**	**Hexane-Ethanol (1:1)**
Cell concentration (cells/ml)	8.8E+06	9.7E+06	9.7E+06	2.7E+06	7.2E+06	9.6E+06	9.4E+06	1.8E+05
% of cell lysis	0	0	0	69.6	17.7	0	0	97.9
Cell viaibilty (%)	95.5	85.2	86.9	2.3	0	0	0	0
Lipids extracted	/	-	-	+	+	-	-	+

Table 1 Analysis of the cell lysis and cell viability after different solvent extractions. Ratio solvent:cells = 1:1 and extraction time = 30 min.

Results show that cell lysis (cells disrupted entirely) occurred in the case of hexane (as it was previously discussed), dichloromethane and the mixture hexane:ethanol. The latter generated the highest cell lysis. For those conditions, lipids extraction was observed which is fully consistent with the fact that lysis must occur to induce extraction of lipids (already reported in Section 1.1).

In addition, lipid droplets structural changes seem to occur for cells submitted to dichloromethane and decane:dichloromethane unlike cells on decane (see Section 2, Figure 3). This may be related to the interaction between the solvent and the lipids when the solvent enters the cell.

Data also confirm the "biocompatibility" of dodecane and decane as the cell viability (remaining cells) only decreased from 95.5 % to 85.2 % with dodecane and 86.9 % with decane. All other solvents had a significant impact leading mostly to 0 % of viable cells.

Interestingly, the solvent mixtures dodecane:dichloromethane (1:1) and decane:dichloromethane (1:1) did not lead to any cell lysis (Figure 11) and, as expected, no lipids extraction was observed. However, when using dichloromethane alone, cells are disrupted, and lipids are extracted. There seems to be an interaction between decane or dodecane with the dichloromethane which inhibits its capability to extract the lipids.

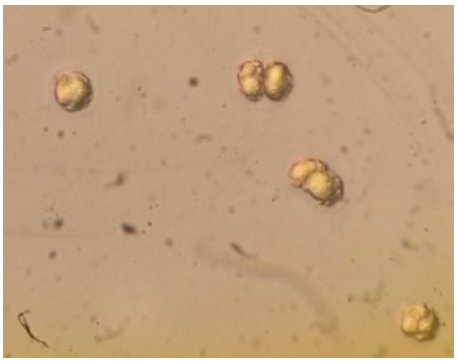

Figure 3 Cells after a solvent extraction of 30 min, using decane:dichloromethane (1:1)

To identify an optimal mixture of biocompatible-toxic solvent that extracts lipids from *Chlamydomonas reinhardtii* while minimizing cell lysis, solvent duo was investigated at different cells/toxic solvent/biocompatible solvent ratios: MethylEthylKetone (MEK; logP ≈ 0.29) and decane (logP ≈ 6).

	Sample composition (µl)			Total volume	Lipids extracted
	Experiment 1				
	Algae	MEK	Decane		
M	100	100	/		+++
D	30	/	170		-
MD1	50	75	75	200	++
MD2	50	50	100		++
Contrôle	200	/	/		
	Experiment 2				
	Algae	MEK	Decane		
DM1	50	50	150		+++
DM2	50	40	160	250	++
DM3	50	30	170		-
Contrôle	250	/	/		
	Experiment 3				
	Algae	MEK	Decane		
M	50	50	1000	1100	-
O	50	50	1400	1500	-
H	50	40	800	890	-
Z	50	40	1333	1423	+
Contrôle	1100	/	/	1100	

Figure 4 Analysis of lipid extractions using different solvent mixtures involving biocompatible solvents with toxic solvents

Results revealed two promising solvent duos that might generate less toxicity when in contact with the cells, cause less cell lysis: DM1 and DM2. The cell viability was however at 0 %.

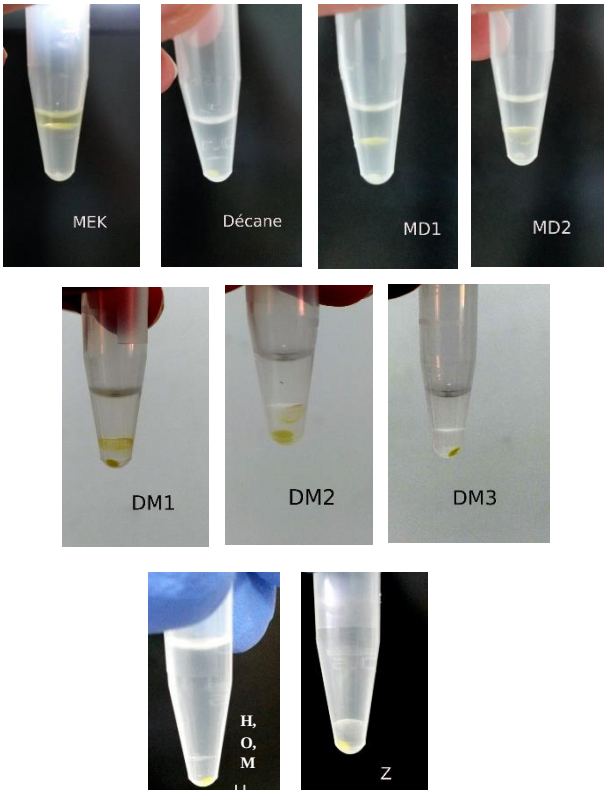

Figure 2 Observation of the cell sample after lipid extraction using different solvents

Effects of the pretreatments on the cell wall deficient *Chlamydomonas reinhardtii* (mutant)

The mutant strain of *C. reinhardtii*, deprived from a cell wall, was also submitted to the studied pretreatments (mechanical compressions and PEFs at 5.5 $kV \cdot cm^{-1}$) as an effort to further investigate the role of the cell wall. Microscopic observations were conducted after submitting the cells to a mechanical treatment and to pulsed electric fields. The experimental conditions were the same as those used in the case of the wild type strain of *C. reinhardtii* (see section 1.3.3).

Mechanical compressions

Mechanical compression had an important impact on the mutant microalga (Figure 6). Most of the cells disrupted after entering the device's constrictions (height/width of restriction: 5 µm). This observation highlights the role of the cell wall as a protection from cell disruption, the wild type being resistant to this mechanical compression (Figure 7).

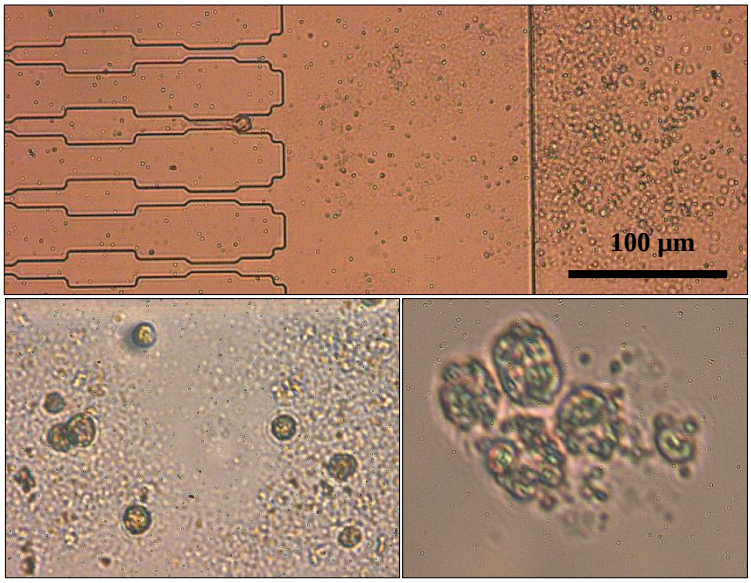

Figure 6 Microscopic observations of *C. reinhardtii*'s mutant strain after undergoing mechanical compressions (brightfield observations).

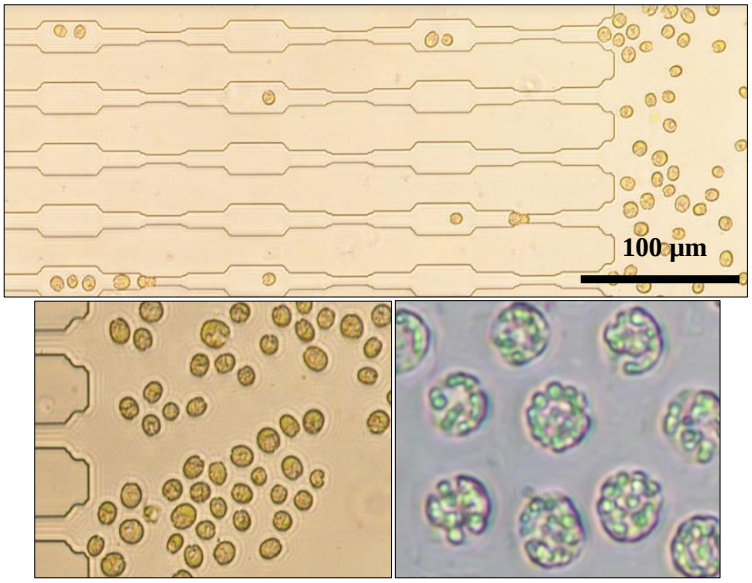

Figure 7 Microscopic observations of *C. reinhardtii*'s wild type strain after undergoing mechanical compressions (brightfield observations).

PEF treatment

No significant impact was observed after PEF treatment (reversible electroporation). The cells observed after being submitted to the PEF treatment showed no significant structural changes. The cells didn't disrupt either (Figure 8).

Before PEF treatment

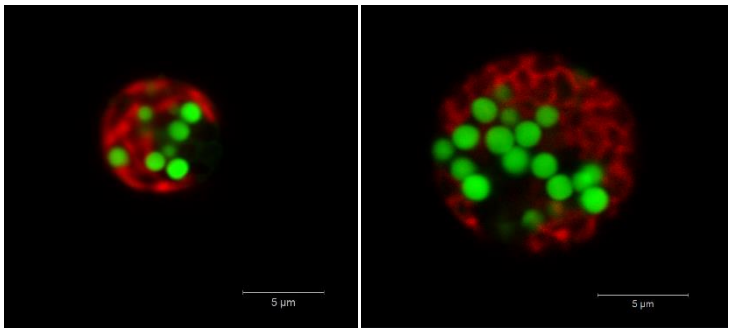

After PEF treatment

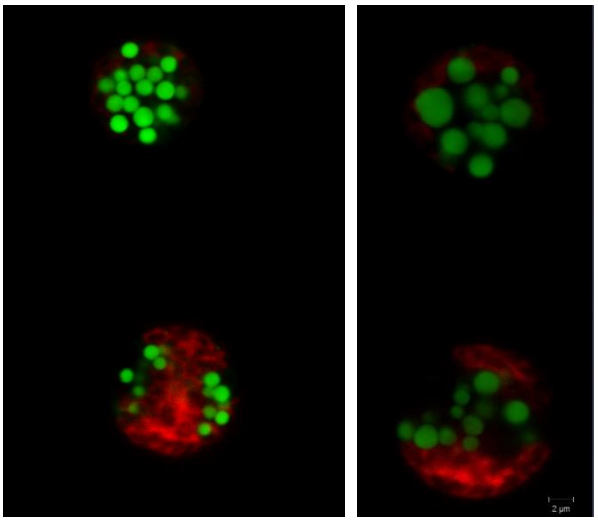

Figure 8 *C. reinhardtii*'s mutant strain before and after PEF treatment (Confocal microscopic observations).

To further investigate the impact of mechanical compressions and pulsed electric fields on the morphology and structure of the microalgae cells, Transmission Electron Microscopy (TEM) was used. This will be discussed in Chapter 4.

Effects of solvent extractions on the cell wall deficient *Chlamydomonas reinhardtii* (mutant)

To evaluate the impact of solvents on the cell wall deficient *Chlamydomonas reinhardtii* cells, several solvents were tested (the following solvent compositions were used: decane (100 %) and a mixture of decane and dichloromethane (ratio = 1:1)). The solvent:cells ratio was equal to 2:1).

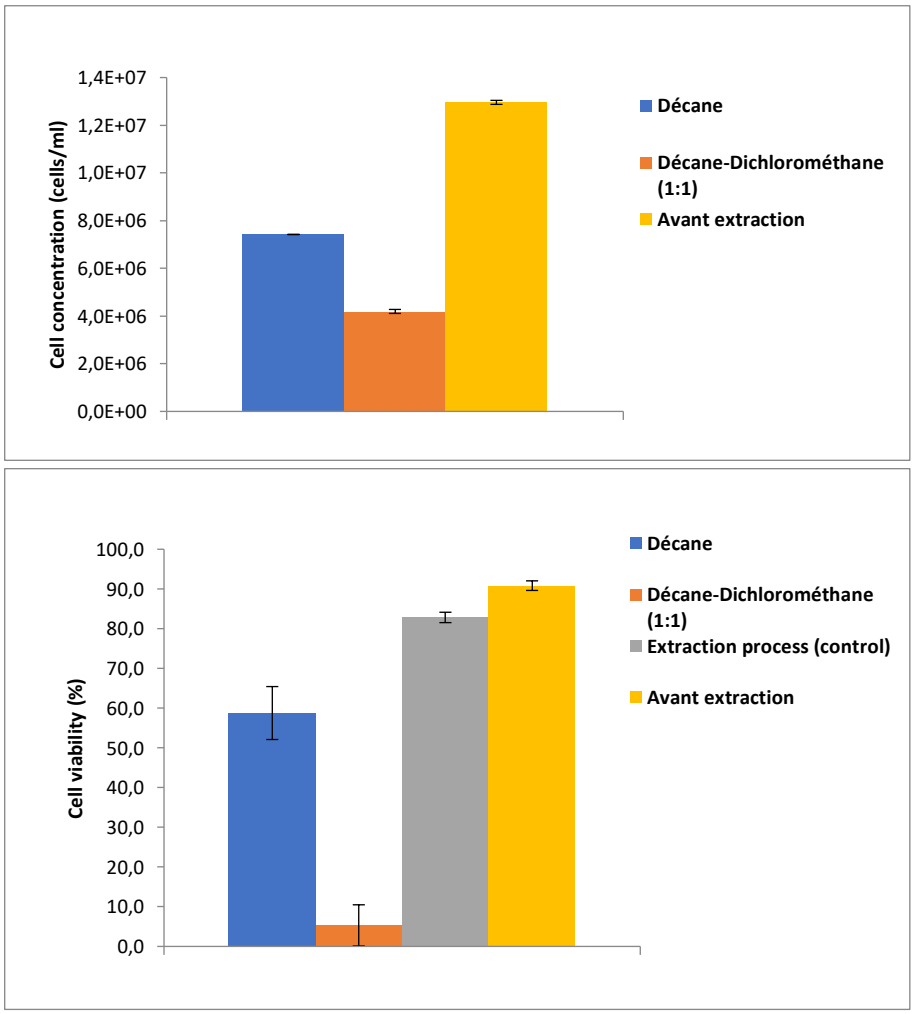

Figure 9 Solvent extractions on the mutant strain. Extraction process (control) corresponds to the application of the extraction protocol without using any solvent. Extraction time = 30 min.

According to Figure 9, cell lysis was higher in the presence of the solvent mixture decane-dichloromethane compared with the decane alone. The cell viability of the remaining cells after solvent extraction using decane-dichloromethane dropped dramatically after the 30 min of extraction (from 90 % to 5 %). In the case of decane alone, the decrease of cell viability in the remaining cells was less brutal, leading to 58.8 %.

In addition, mixing and centrifugation on cell viability is also highlighted.

The percentage of lipids extracted was equal to 3 % using decane and 54 % using decane and dichloromethane with an equivalent proportion.

Annex

Quantifying microalgae lipid content

In order to study the effect of treatments (mechanical, electrical, chemical) on lipids extraction from microalgae, accurate methods for lipid quantification are required. In addition, the use of microsystem devices to induce mechanical and electric stress in our study involve the use of very small sample volumes (in a range of 250-500 µl) which represent an additional constraint to consider.

Recently, bodipy staining has been used to detect and quantify neutral lipid in small volumes of microalgae suspensions (Wu et al. 2013; Xu et al. 2013).

While studying the effect of pretreatments on microalgae cells, our first approach was thus to use Bodipy 505/515 which stains neutral lipids; quantification was further carried out by flow cytometry analysis. Results however showed incoherent fluorescence intensities that demonstrated that this method is not appropriate for a quantitative analysis of the extracted lipids.

Figure 10 displays the average fluorescence intensity emitted by Bodipy 505/515 for cells submitted to the different treatments. From the data, a significant increase of the mean cell fluorescence after applying 7 $kV \cdot cm^{-1}$ is obtained while no significant differences were detected for the other tested conditions.

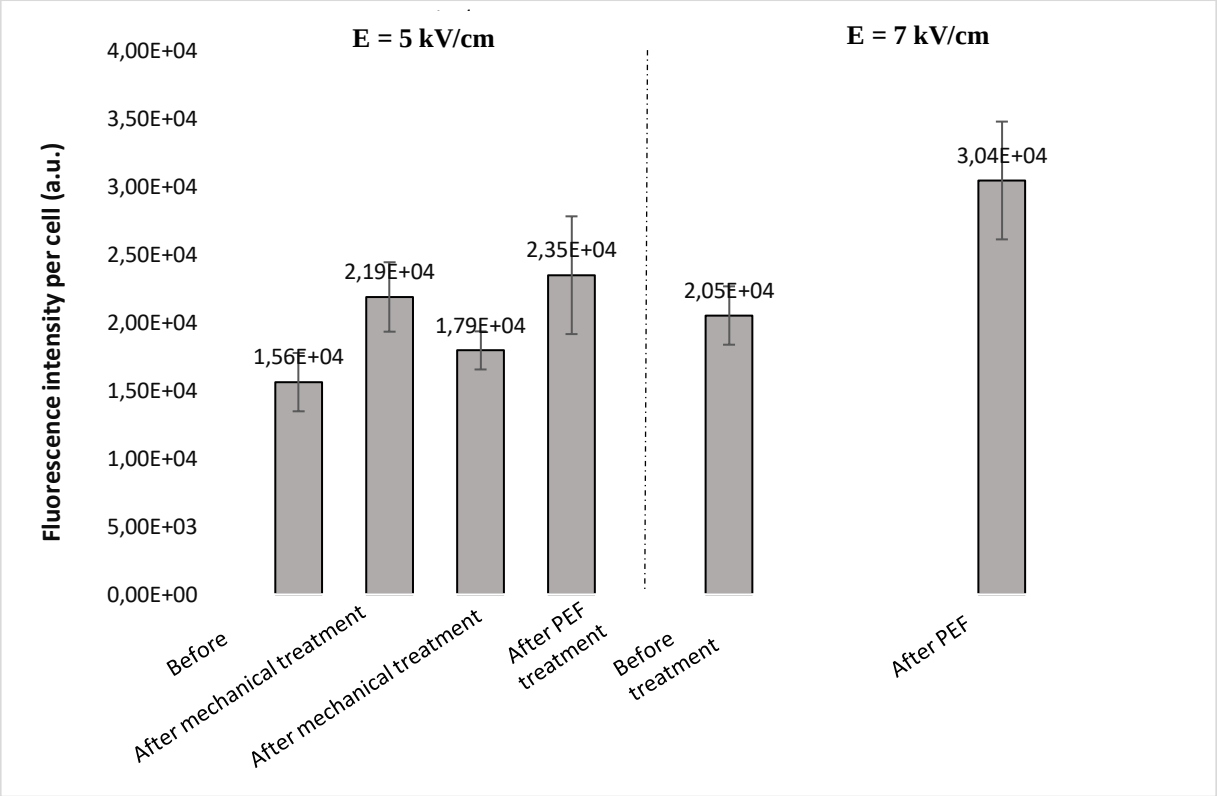

Figure 10 Representative cytometric results of the fluorescence intensity emitted by Bodipy 505/515 after the different conditions of treatments. (The cell suspensions were stained with bodipy after each treatment). Electroporation conditions: 10 unipolar pulses of 5 µs each, 10 Hz, 5,5 kV/cm for the left side of the graph and 7kV/cm for the right side of the graph.

Taking into account these unexpected data, additional assays were carried out to evaluate the feasibility of using lipid staining with bodipy for quantification purposes in our work.

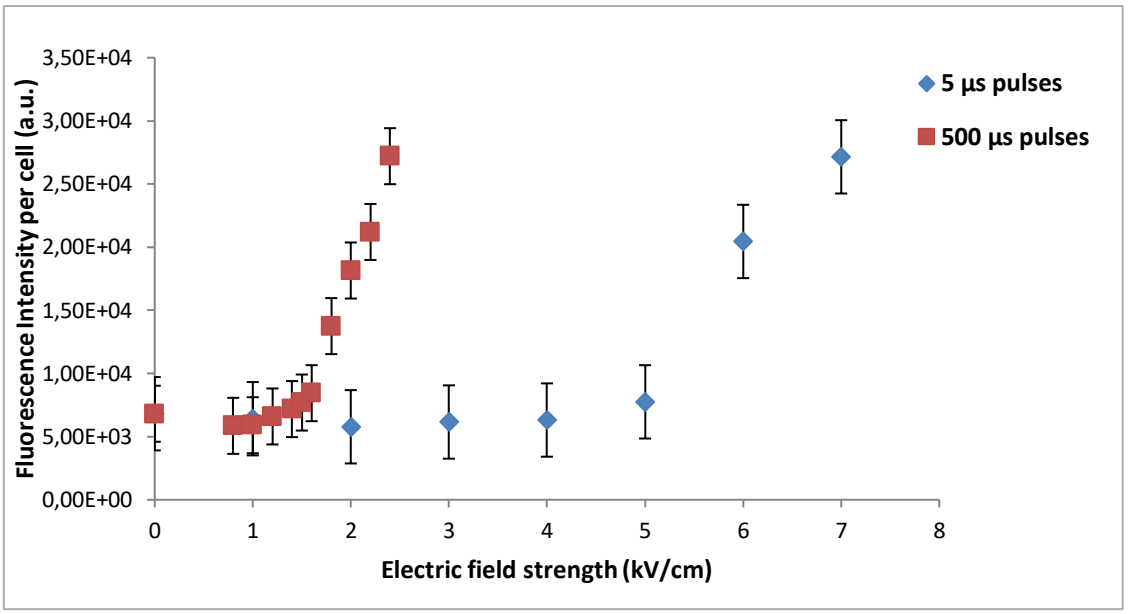

Figure 11 Evolution of the fluorescence intensity emitted by Bodipy with the electric field strength applied for two pulse durations. The experiment was held on *C. reinhardtii* wild type after being stressed for 7 days.

The effect of different PEF intensities on the mean bodipy fluorescence is presented in Figure 11.

An increase in the PEF strength clearly conducts to a rise in the mean fluorescence intensity (Figures 10 and 11). Pulse duration also affects bodipy mean fluorescence (Figure 11), fluorescence intensity increases even faster when the pulse duration is longer.

Data are in agreement with the fact that cell permeability is affected by PEF conditions, thus impacting lipid staining. Moreover, bodipy fluorescence intensity may also be affected by lipid droplets structure that clearly changes in PEF conditions (cf. Section 1 and Section Complementary results of Part 2).

To further confirm these data, an additional assay was carried out where the fluorescence intensity of cells previously stained with bodipy and flowing out of the microfluidic device inducing the mechanical stress was evaluated (Figure 12).

Results show that the fluorescence emitted by the Bodipy decreases dramatically after mechanical treatment compared to cells that did not undergo the treatment (control, Figure 12).

In addition, no release of the dye on the external medium was detected.

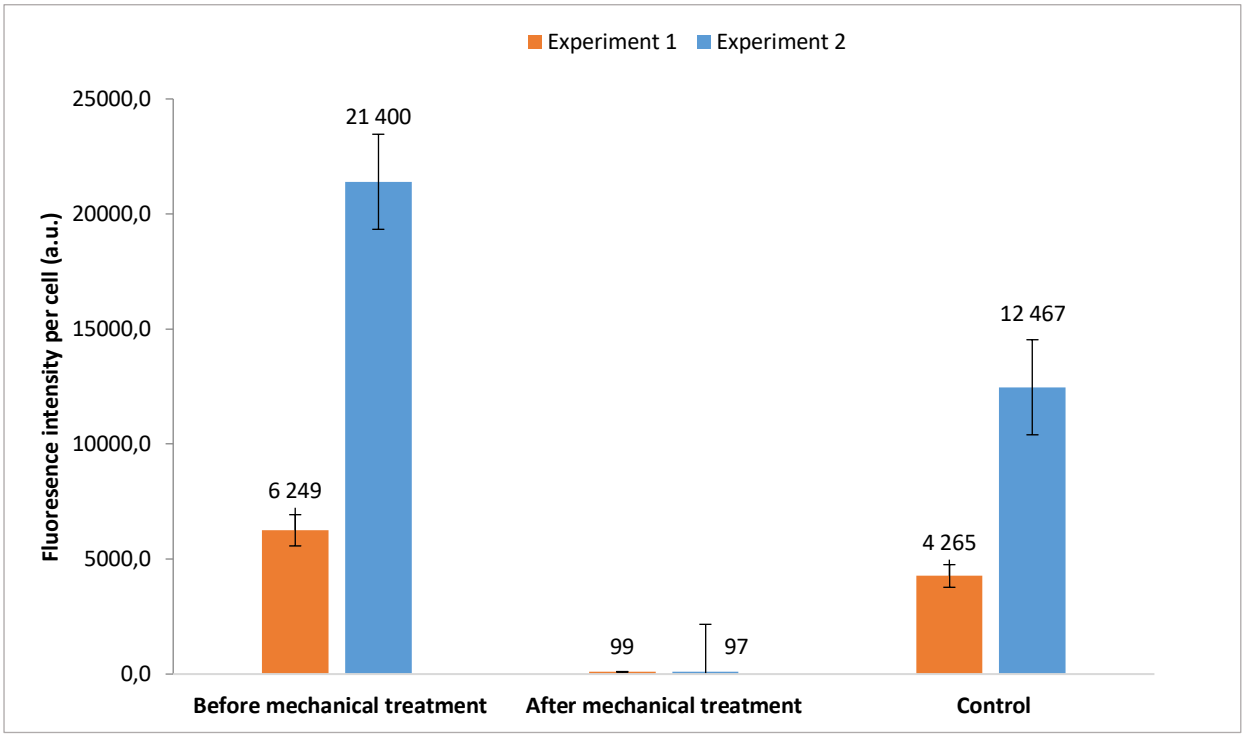

Figure 12 Effect of mechanical treatment on the staining of Bodpy 505/515. *Before mechanical treatment*: cells were stained with bodipy and analyzed before being pumped in the microfluidic constrictions; *After mechanical treatment*: cells were immediately analyzed after undergoing mechanical treatment (approximately 45min after entering the restrictions); *Control*: the cells were stained then analyzed at the same time as the cells that were submitted to mechanical treatment (after 45 min).

On the whole, our data largely support the fact that bodipy staining is not appropriate for quantifying microalgae lipid content in processes that affect membrane properties and lipid droplet structure.

A new protocol based on the sulfophosphovanillin method was therefore chosen four our study (described in Section 1.3.6).

Part 2 Relating the microalga's structure to the extraction of its lipids using solvents

2. Structural changes of *Chlamydomonas reinhardtii* cells during lipid enrichment and after solvent exposure

2.1 Abstract

Data are related to Confocal Laser Scanning Microscopy (CLSM) observations of lipid-enriched Chlamydomonas reinhardtii cells under different conditions. Firstly, the impact of stress conditions (nitrogen starvation) on the cell wall structure is assessed. Secondly is described the effect of solvents, in the context of lipid extraction, on the microalga's cell, particularly its lipid droplets, in the perspective of understanding the mechanisms behind solvent extraction of lipids. Furthermore, the role of the cell wall as a barrier to the solvent extraction action is highlighted.

2.2 Specifications Table

Subject area	Physics and biology
More specific subject area	Bioprocess engineering
Type of data	Confocal microscopy images
How data was acquired	Images were acquired by confocal microscope LSM 700 (Zeiss)
Data format	Raw
Experimental factors	*Chlamydomonas reinhardtii* cells were submitted to 7 days of nitrogen stress conditions in order to induce lipid accumulation
Experimental features	Fluorescent dyes were used to observe the microalga's lipid droplets and cell wall
Data source location	*Chlamydomonas reinhardtii* SAG-34.98 (Wild type) was obtained from the University of Goettingen (EPSAG, Germany). They were collected from a soil in the United States, MA.
Data accessibility	*Dataset is within this article*
Related research article	Understanding the mechanisms of lipid extraction from microalga *Chlamydomonas reinhardtii* after electrical field solicitations and mechanical stress within a microfluidic device (Bensalem et al.,

	2018) [1] (In revision)

2.3 Value of the Data

- The presented data provides information on the role of the cell wall as a barrier to molecules extraction; this information is of prime importance for lipid extraction from microalgae
- The data will be helpful to relate the microalga's cell wall structure and the ability of a given solvent to extract lipids
- The data gives significant information that might be crucial to highlight mechanisms of solvent extraction action, especially the role of the cell wall in the extraction efficiency
- The data presented here might lead to further investigations on microalgae cell wall during stress conditions and solvent extraction
- The data provides information to the scientific community on the effect of coupled solvents on the microalgae cells structure in the frame of the extraction of lipids from microalgae

2.4 Data

Three experiments using confocal microscopy imaging on 7 days-stressed *Chlamydomonas reinhardtii* are reported. Figure 1 shows the cytoplasm containing lipid droplets and the cell wall structure, while the microalgae are under nitrogen starvation, which induces lipid accumulation. Figure 2 and 3 describes the structural changes on lipid droplets on such stressed cells, when using solvents for lipid extraction purposes. The evolution of the 7 layers composing the cell wall of *Chlamydomonas reinhardtii*, during stress conditions, is shown for the first time in Figure 1. Figure 2 offers an original observation of the cell wall entrapping lipids after solvent contact, showing therefore the major role of the cell wall as a barrier to solvent extraction.

Figure 3 shows the structural changes on the cell, when submitted either to pure or mixtures of polar or nonpolar solvents.

2.5 Experimental Design, Materials, and Methods

2.5.1 Stress conditions

Lipid accumulation was induced by culturing the cells under the following conditions: nitrogen depleted TAP medium, light intensity of 150 $\mu mol \cdot m^{-2} \cdot s^{-1}$, 100 rpm agitation, a temperature of 24 °C ± 1 °C and 0.004 % CO_2.

2.5.2 Microscopic experiments

In order to visualize the cell wall and lipid droplets using confocal laser scanning microscope (CLSM 700, Carl Zeiss Microscopy GmbH, Germany) two fluorescent dyes were used: Concanavalin A conjugated with tetramethylrhodamine (ConA, yellow-orange fluorescence) for the cell wall and Bodipy 505/515 (green fluorescence) for the lipids. Chlorophyll was detected by red autofluorescence.

The stock solution of ConA (Molecular Probes, Lifetechnologies, C860) was prepared by dissolving it in 0.1 M sodium bicarbonate (pH ≈ 8.3) to a final concentration of 2 mg/ml. Fluorescence intensity was analyzed after 20 min of incubation time.

Bodipy 505/515 (green fluorescence) was prepared by dissolving it in DMSO to a concentration of 100 mg/L. The final concentration of bodipy in the cell sample was 1.5 µg/ml. Fluorescence intensity was analyzed after 10 min of incubation time.

2.5.3 Solvent extraction

Ethyl acetate

For this experiment, *Chlamydomonas reinhardtii* cells were mixed with ethyl acetate in a total volume of 100 µL during 10 min (7.5 µL of ethyl acetate was added to the algal solution).

Mixture of solvents

The following solvent mixture was used with a ratio of 1:1: dodecane as the biocompatible solvent with dichloromethane as the highly polar solvent. The solvent/cell ratio was 1:1 and the contact time was 30 min. The cell concentration of the sample was 1×10^7 cells·mL^{-1}.

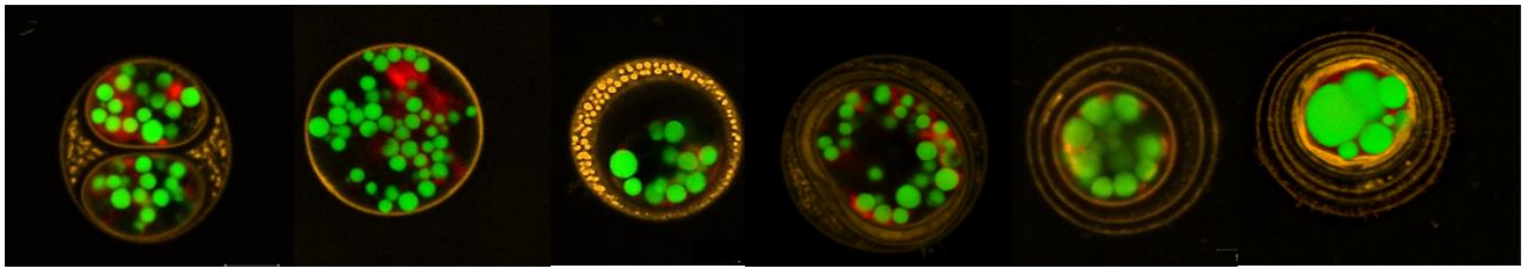

Fig. 1 *Chlamydomonas reinhardtii* observed under confocal microscopy during lipid accumulation. Cells evolve during stress conditions in terms of their cell wall. Different profiles could be observed: cells in division, cells with one thin layer of cell wall, cells with one very thick layer of cell wall, 2 to 3 layers of cell wall, and more than 3 layers, up to 7 layers. Lipid droplets were stained with Bodipy 505/515 (green), the cell wall with Concanavalin A (orange). Scale bar : 5 µm

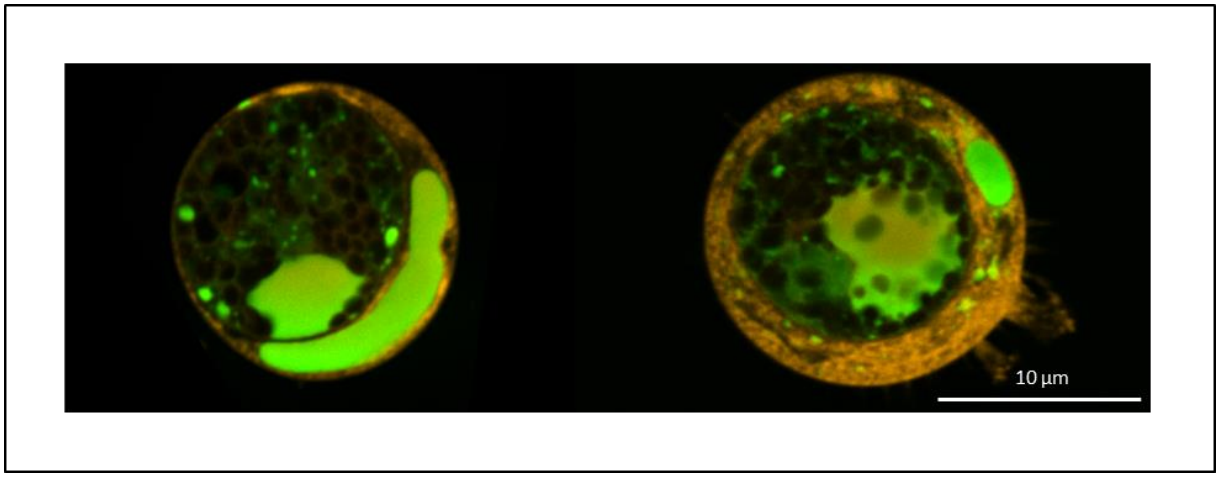

Fig. 2 Confocal microscopic observations of 7-days stressed *Chlamydomonas reinhardtii* cells after solvent contact with ethyl acetate. *Chlamydomonas reinhardtii* cells were mixed with ethyl acetate in a total volume of 100 µL during 10 min (7.5 µL of ethyl acetate was added to the algal solution). In green, lipid droplets stained by bodipy 505/515 and in orange the cell wall stained by concanavalin A. Images show the lipid droplets being trapped in the cell wall. Scale bar: 10 µm

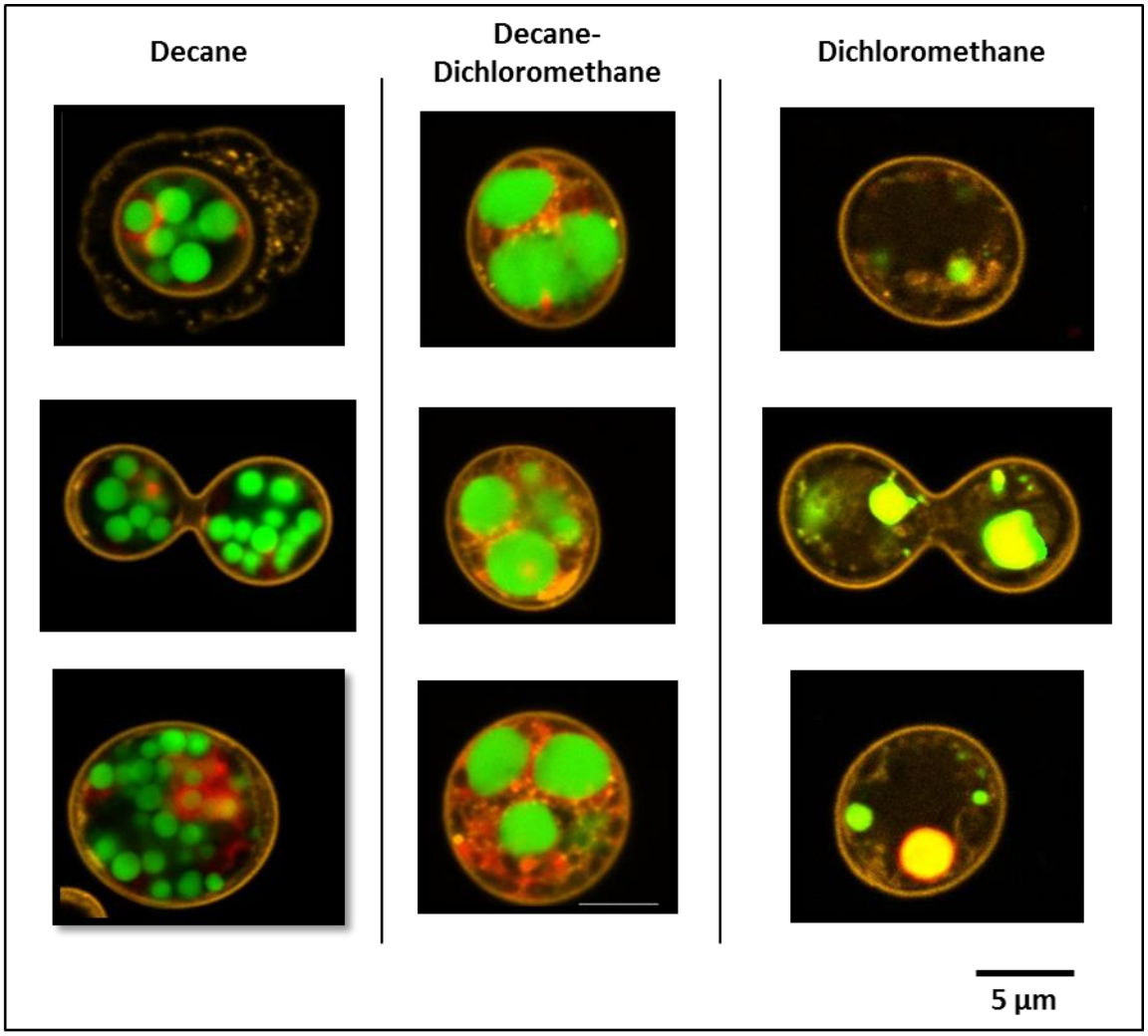

Fig. 3 Confocal microscopic observation of 7-days stressed *Chlamydomonas reinhardtii* cells after being in contact with different solvents. The solvent mixture was used with a ratio of 1:1; dodecane as the biocompatible solvent with dichloromethane as the toxic solvent. The solvent/cell ratio was 1:1 and the contact time was 30 min. Lipid droplets were stained with bodipy 505/515 (green), and the cell wall with concanavalin A (orange). Scale bar: 5 µm

2.6 Acknowledgments

This work was funded by the financial support of the LabeX LaSIPS (ANR-10-LABX-0040-LaSIPS) managed by the French National Research Agency under the "Investissements d'avenir" program (n°ANR-11-IDEX-0003-02).

2.7 References

[1] Bensalem, S., Bodénès, P., Pareau, D., Lopes, F., Français, O., Le Pioufle, B., 2018. Understanding the mechanisms of lipid extraction from microalga *Chlamydomonas reinhardtii* after electrical field solicitations and mechanical stress within a microfluidic device. Bioresour. Technol. (In revision)

Complementary results

Statistical analysis of the cell wall's structural changes

The variability of results encountered when analyzing the extraction efficiency or the cell permeability could be related to the variability of *C. reinhardtii*'s structure and morphology (particularly its cell wall) observed during our experiments (this was discussed in Section 2).

The experiments were held on three different cultures that were each stressed during 23 days. The results in terms of cell percentage are gathered in Table 1.

Experiment 1

	3 days	7 days	21 days
In division	27.3	25.0	0.0
1 thin layer	72.7	25.0	19.0
1 thick layer	0.0	25.0	0.0
2-3 layers	0.0	25.0	23.8
> 3 layers	0.0	0.0	57.1
Total	100	100	100

Experiment 2

	3 days	7 days	23 days
In division	11.5	5.8	0.0
1 thin layer	70.5	67.3	10.5
1 thick layer	13.1	1.9	7.9
2-3 layers	4.9	21.2	55.3
> 3 layers	0.0	3.8	26.3
Total	100	100	100

Experiment 3

	1 day	6 days	21 days
In division	19.3	6.1	0.0
1 thin layer	67.5	57.6	7.8
1 thick layer	9.6	13.6	13.0
2-3 layers	3.6	13.6	27.3
> 3 layers	0.0	9.1	51.9
Total	100	100	100

Mean of Exp 2 and 3

	3 days	7 days	21 days
In division	15.4±3.9	5.9 ±0.2	0.0
1 thin layer	69.0 ±1.5	62.4 ±4.9	9.2 ±1.3
1 thick layer	11.4 ±1.8	7.8 ±5.9	10.4 ±2.6
2-3 layers	4.3 ±0,7	17.4 ±3.8	41.3 ±14
> 3 layers	0.0	6.5 ±2.7	39.1 ±12,8
Total	100	100	100

Table 2 Statistical analysis of *C. reinhardtii*'s different morphological aspects depending on the stress duration. Each column displays the mean results in terms of cell percentage of three replicates.

Data shows that, other then the fact that cell division decreases with the nitrogen stress duration, the percentage of cells showing a larger cell wall increases as well (this was also discussed in Section 1.4.4 and shown in Section 2, Figure 1).

Additional images are presented below. The morphological aspect of the cells was analyzed by confocal microscopy at different steps of the stress conditions: 1-3 days; 6-7 days and 21-23 days (Figures 1, 2, and 3).

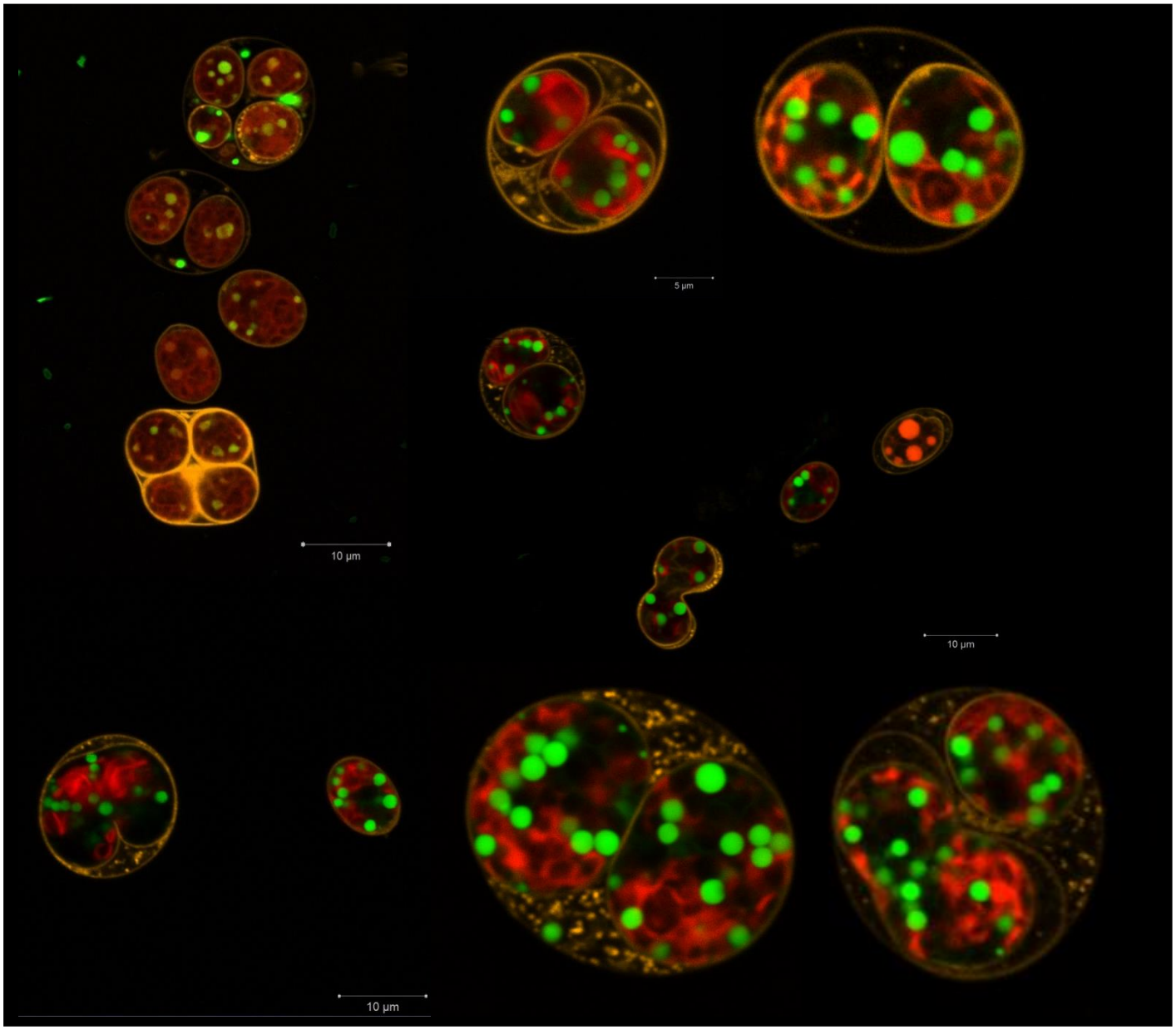

Figure 1 Confocal images of cells after 1-3 days of stress conditions.

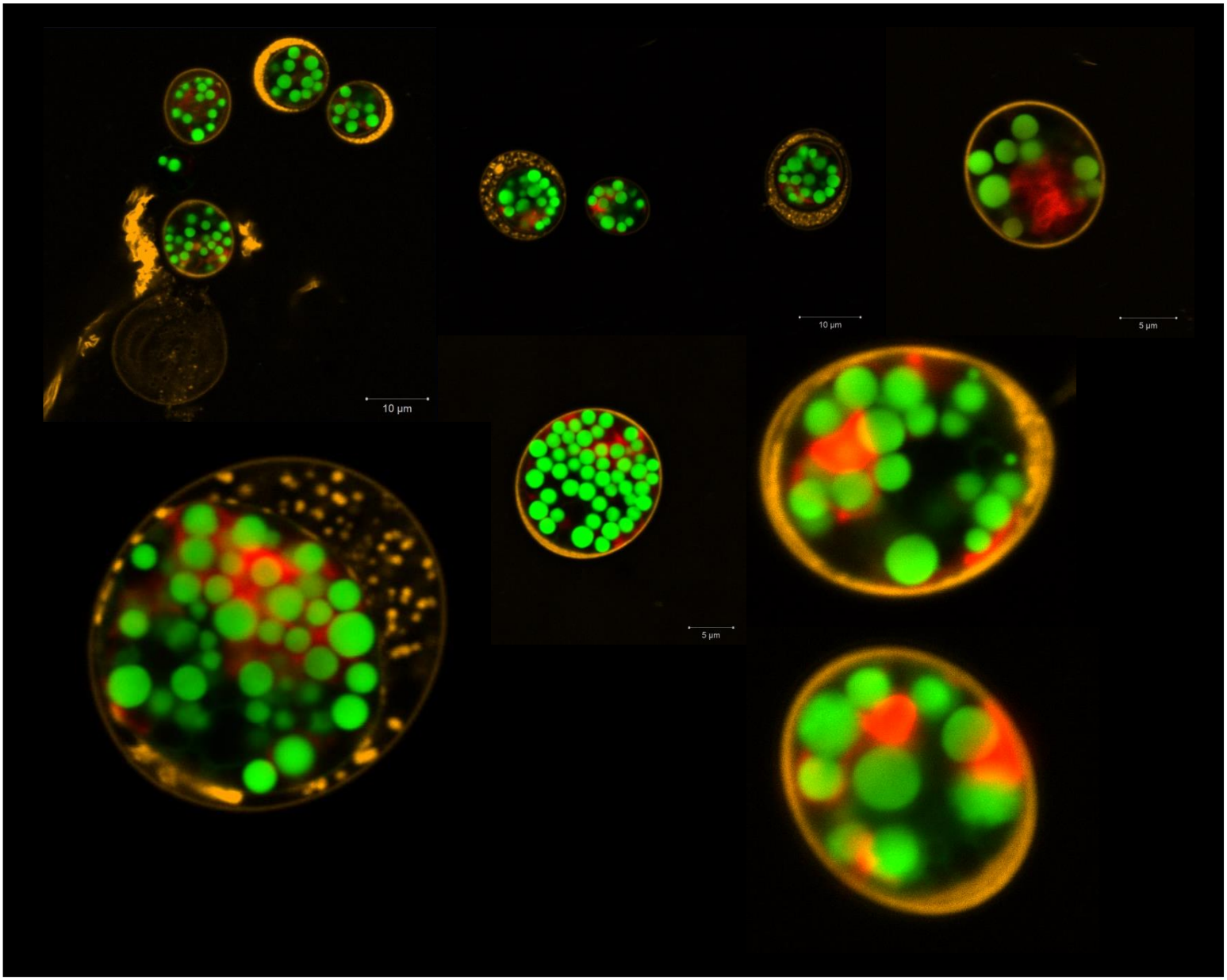

Figure 2 Confocal images of cells after 6-7 days of stress conditions.

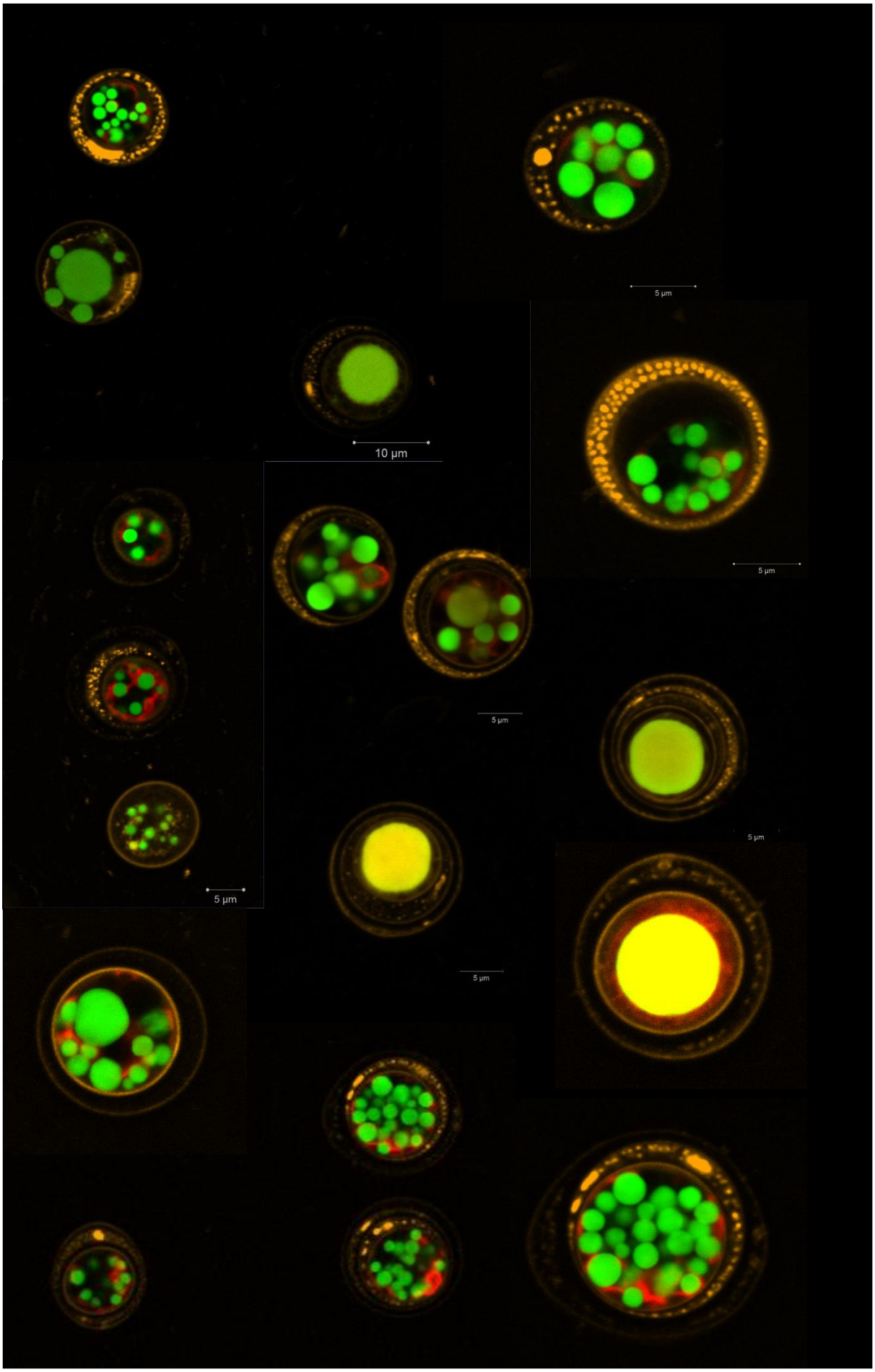

Figure 3 Confocal images of cells after 21-23 days of stress conditions.

As it was discussed previously (Section 1.4.4), lipid yield (after a solvent extraction using hexane) and cell lysis were higher for cells that have been submitted to more than 20 days of stress conditions (in comparison to cells after 1-3 days or 6-7 days of stress). Therefore, the longer the cell is stressed, the more the solvent's ability to extract the lipids is increased. This can be related to the morphology of the cell, and particularly, as it has been demonstrated in our case, its cell wall.

Annex

The following additional images show structural changes observed under the microscope during our experiments: cell lysis after solvent extraction using hexane (logP ≈ 3.9), lipid droplets fusion (Figures 5, 7 and 8), and structural changes after solvent extraction using other solvents (decane and dichloromethane, in addition to Section 2.5, Figure 3).

Bright field images showing *C. reinhardtii*'s cell lysis caused by solvent exposure

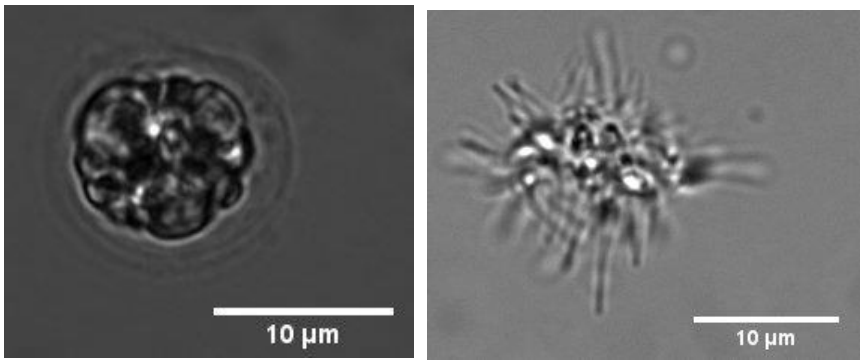

Figure 4 Brightfield images of *C. reinhardtii* before and after solvent exposure (hexane; 30 min).

Lipid droplets fusion under confocal microscopy

The fusion of droplets was observed when the cells were analyzed under the confocal laser scanning microscope, therefore when they were exposed to the laser.

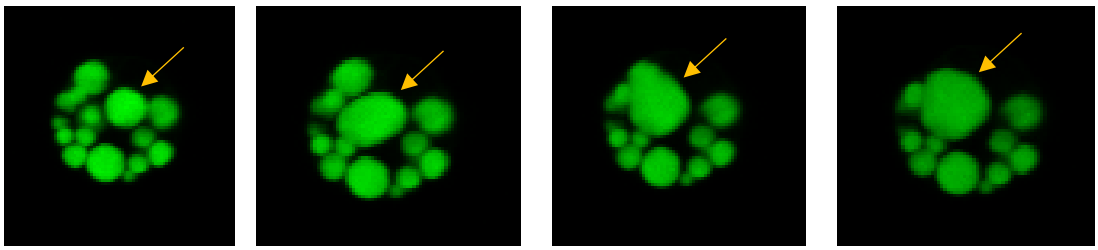

Figure 5 Evolution of the lipid droplet fusion under confocal microscopy.

Lipid droplets fusion after PEF treatment

Fusion of lipid droplets was induced by PEF treatment which agrees with previous data (Bodénès et al., 2016). Interestingly, lipid droplets structure or composition could be affected by a PEF treatment; the bodipy staining appears to be different (yellowish color instead of green).

Before

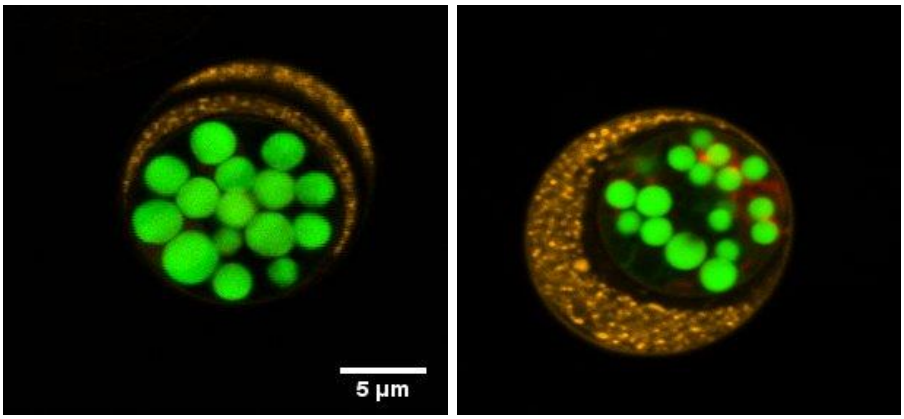

Figure 6 Confocal images of *C. reinhardtii* before being exposed to pulsed electric fields (PEFs)

After

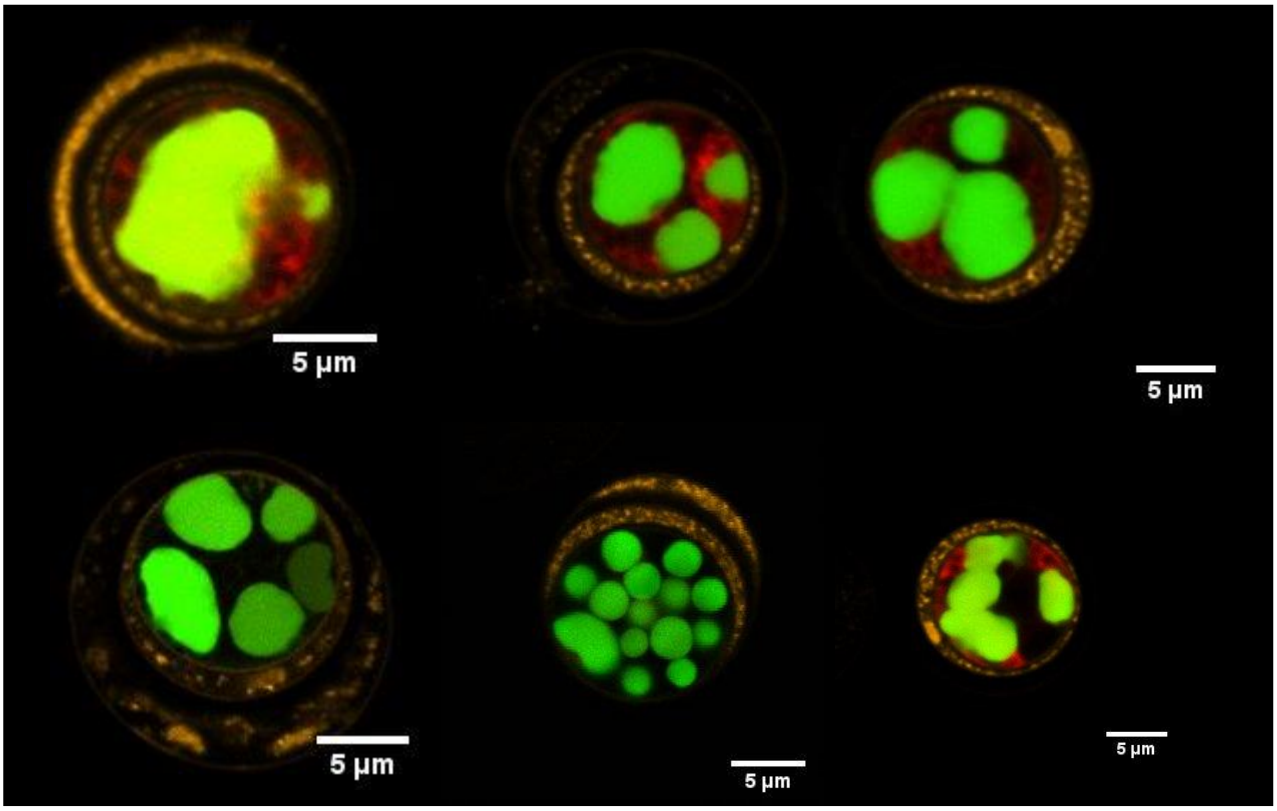

Figure 7 Confocal images of *C. reinhardtii* after being exposed to pulsed electric fields (PEFs)

Additional images of the cells after solvent exposure

Decane

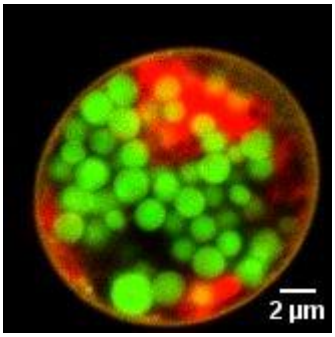

Dichloromethane

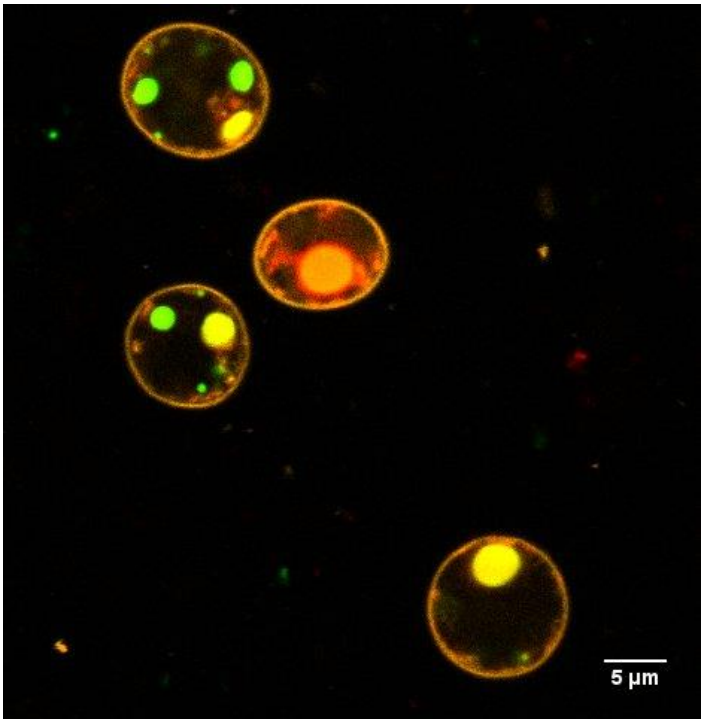

Decane-Dichloromethane

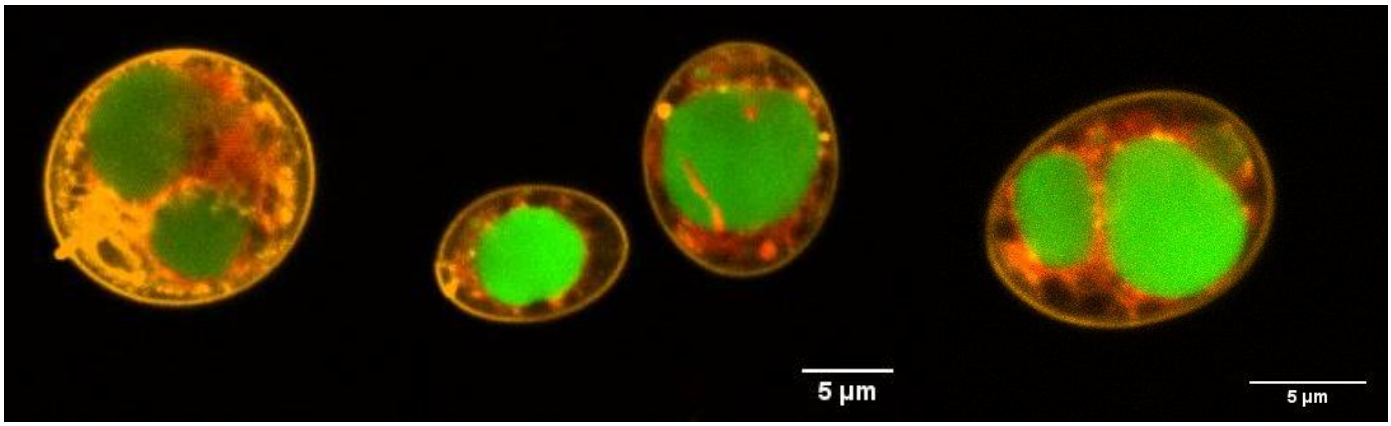

Figure 8 Confocal images of *C. reinhardtii* after being exposed to different solvents

Conclusions

In this chapter, **we have investigated the mechanisms behind a solvent lipid extraction and the impact of pretreatments and nitrogen stress conditions on the microalga *Chlamydomonas reinhardtii,* at the cellular scale**. The obtained results have highlighted significant effects of different conditions (pretreatments, solvent, stress conditions…) on the microalga such as an increase in cell permeability and cell lysis and morphological changes (intracellular components, cell membrane and cell wall).

The most significant increase in cell permeability and lipid yield, using hexane for the extraction, was obtained by submitting the cells to the following combination of pretreatments: pulsed electric fields followed by a cyclic mechanical compression. When this combination of pretreatments was used the other way around, meaning cyclic mechanical compressions followed by PEFs, the cell permeability wasn't influenced to the same extent.

Subsequently, we investigated on the mechanisms of action of the different pretreatments and solvent as an attempt to understand how this increase in lipid yield is obtained.

Results clearly confirmed that **PEF increases cell permeability and suggest that mechanical stress acts on the cell wall**. In addition, cell lysis has been shown to be required to extract lipids from *C. reinhardtii* with solvents including hexane. Data were further confirmed by microscopic observation that highlighted the important role of the cell wall as a barrier to lipid extraction, particularly to the solvent's ability (biocompatible and mixture of solvents) to access the lipid droplets inside the algal cell.

In addition, our search for an efficient solvent-duo using a biocompatible solvent combined with a highly polar solvent showed that the mixture of solvents can extract but, having a minimal impact on the cell lysis, it is limited to a certain efficiency of extraction. In any case, cell viability could not be preserved when using the solvents.

However, **when using the pretreatments only, viability was maintained** in the range of 46 % - 78.3 % depending on the configuration (PEFs alone, mechanical compression alone or the combination of both techniques). This is significant information, useful for the sequential extraction of different compounds. For example, a successful lipid extraction followed by a protein extraction requires that the treatments used preserve at a maximum extent, the cell's inner compounds or compartments that store these compounds.

Moreover, in the context of a biofuel production, there is naturally a stress phase imposed on the microalgal cells to trigger the accumulation of their lipids. It is therefore important to study the impact of this stress on the cells. Indeed, the applied stress conditions (including nitrogen depletion and a high light intensity) have an impact on the lipids produced and may affect other properties of the cell such as its morphology and structure, including the cell wall, thus probably impacting lipid extraction efficiency.

Our observations confirmed this hypothesis. Indeed, *Chlamydomonas reinhardtii*, known to have 7 layers of cell wall, showed interesting features when observed under the confocal microscope. Those 7 layers were not always visible. This was closely dependent on the

duration of the applied stress conditions. We therefore defined **different cell sorts**: cells in division, cells with one very thick layer of cell wall, cells with one thinner layer of cell wall, 2 to 3 layers of cell wall, and more than 3 layers. The three first sorts represented a majority in the first days of stress conditions. The two last aspects were major after at least 7 days of stress conditions. In addition, **the extraction efficiency was clearly related to differences in the cell structure** as a higher stress duration led to a higher lipid recovery from the solvent hexane. The cell walls that were submitted to a long duration of stress were therefore more susceptible to the solvent. These significant results confirmed that **an efficient lipid extraction must involve a thorough comprehension of the used alga** and specifically its cell wall's structure, and certainly the composition, to ensure a controlled and optimized cell disruption. This will further be discussed in Chapter 4, involving transmission electron microscopic analysis of the cell wall.

The study presented in this chapter has also raised questions on the existence or not of an impact on the cell wall due to the application of mechanical compressions, PEF treatment or the combination of both treatments. For instance, the PEF treatment only seems to impact the cell's membrane and not its cell wall and the mechanical compressions seem to impact the cell wall majorly. However, the sequential use of both pretreatments in a particular order generated the most promising results. Questions are therefore raised on the mechanisms behind these pretreatments. For example, why would this particular order where the cell membrane is first electroporated before submitting the cells to compressions lead to a better extraction efficiency from hexane? Are the pores created on the membrane maintained when the cells enter the restrictions? It is therefore important to clearly understand how the PEFs impact the membrane and most importantly, define which parameters are to be used to efficiently permeabilize the cell membrane for an optimal lipid or other compounds extraction. This study along with the study of the structural response of *Chlamydomonas reinhardtii* to the pretreatments (including the cell wall and other inner components) will be presented in the following chapter.

Chapter IV - Studying and characterizing the impact of preatreatments on *Chlamydomonas reinhardtii*'s structural properties and cell composition

Table of contents

Preamble - *Motivation and Objectives*

Pulsed Electric Fields and mechanical stress methods have both shown promising results as pretreatments to extract compounds (lipids, proteins, pigments…) from microalgae. In the context of large-scale biofuel or bioproduct productions from microalgae, this particularity is significantly attractive. However, in order to develop an efficient large-scale extraction process, the optimal pretreatment parameters need to be first determined at a lab scale.

Operating parameters such as electric field intensity, pulse duration in case of PEF or mechanical forces for the mechanical process must be optimized for a controlled cell permeabilization. Besides, the operating conditions for each pretreatment can significantly influence the cell's integrity and viability, which highlights the need for an optimization. In addition, understanding the effect of such parameters at cellular scale (structure, morphology) is also mandatory.

Furthermore, our previous study (see Chapter 3) revealed an improvement of lipid extraction efficiency from the microalga *C. reinhardtii* when combining the pretreatments PEFs followed by mechanical compressions. A preliminary study of the effect of PEF, mechanical compressions on cell structure (membrane, cell wall, intracellular compounds), permeability and viability were also established. In addition, nitrogen starvation stress on the cell wall, and its impact on lipid extraction by hexane were highlighted. Several questions were then raised such as: Is there an impact of PEF and mechanical stress on the cell wall? Does the membrane pore diameter increase when submitting the cells to the combined treatments (an increase in the percentage of permeable cells was obtained but no information on the pore size was measured)? How does the cell wall evolve with the nutritional stress?

The following chapter therefore focuses on the optimization of the PEF treatment and the impact of both pretreatments on the structural and morphological response of *C. reinhardtii*. The impact of the stress conditions to which the cells are submitted to accumulate lipids is also evaluated.

The study on the optimization and the effect of the PEF treatment is presented in the first section of this Chapter. It includes an investigation on the conditions inducing irreversibility and reversibility of the pores created on the microalgae's membrane. To do so, cell permeability was evaluated while varying the electric field (from 2 $kV \cdot cm^{-1}$ to 7 $kV \cdot cm^{-1}$) and the pulse durations (three pulse durations were tested: 5 µs, 50 µs and 500 µs). The other operating parameters, including the type of burst, the number of pulses and their repetition frequency were kept constant (monopolar, 10 bursts and 100ms respectively). The cell membrane's permeability was evaluated using Sytox Green; this molecule binds to the nucleic acid of the permeabilized cell forming a fluorescent complex (Ex/Em: 504/523) that was analyzed using a flow cytometer.

Furthermore, the pulse duration is also closely related to the energetic and thermic aspects of the applied PEF treatment. The lowest energy demand and temperature increase were found for the lowest pulse duration (5 µs) tested. This work therefore also presents an estimation of the total energy delivered and the temperature elevation in the medium during the treatment, depending on the applied electric field and pulse duration.

The impact of the duration of stress conditions and the cell concentration on the permeabilization was also investigated.

Finally, to characterize the pores created by the applied PEF treatment on the membrane, the kinetics of pore resealing was evaluated. In addition, a preliminary study of the pore size was assessed under reversible and irreversible conditions.

In the second section of this chapter, the size of the pores is further investigated using an original method specifically developed for this application.

The impact of the nutritional stress conditions (nitrogen starvation), the PEF treatment and the combination of both treatments (PEF followed by mechanical compressions) on the microalgae's morphology and structure was also evaluated in this part of the chapter through both confocal microscopy (CLSM) and transmission electron microscopy (TEM).

Overall, the first part of this Chapter relates to the study of the PEF treatment and its impact on *C. reinhardtii* cells. The work is presented through our published journal article in Algal Research (2018), "**Inducing reversible or irreversible pores in *Chlamydomonas reinhardtii* with electroporation: impact of treatment parameters**".

The second part of this Chapter relates to the structural response of *C. reinhardtii* cells to the treatments and the stress conditions leading to the intracellular accumulation of lipids. Here again, the work is presented through an article prepared for submission in Bioresource Technology (2018-2019): "***Chlamydomonas reinhardtii*'s morphological response to stress conditions, Pulsed Electric Fields and mechanical compressions for an efficient and controlled compound extraction**".

This second part includes further observations held during this study, either complementary to the results discussed in the article (permeability of the cell wall to dextran and entry of dextran in the cell after PEF application) or additional (TEM images showing for example the fusion of lipid droplets inside the cell, due to the stress or the PEF and mechanical treatment).

Acknowledgements

Section 1 of this chapter, in full, is a reprint of the material as it appears in Algal research 2018 (DOI: 10.1016/j.algal.2018.11.016). The dissertation author is the secondary investigator and author of this paper. The other authors on this paper are: Pierre Bodénès (primary author), Olivier Français, Dominique Pareau, Bruno Le Pioufle and Filipa Lopes.

Section 2 of this chapter, in full, is a reprint of the material as it has been prepared for a submission to Bioresource Technology 2018-2019. The dissertation author is the primary investigator and first author of this paper. The other authors on this paper are: Filipa Lopes, Dominique Pareau, Bertrand Cinquin, Olivier Français and Bruno Le Pioufle.

Part 1 Studying the pretreatement Pulsed Electric Fields on C. reinhardtii

1. Inducing reversible or irreversible pores in *Chlamydomonas reinhardtii* with electroporation: impact of treatment parameters

1.1 Abstract

Electroporation is investigated as a possible means to facilitate the extraction of valuable compounds from microalgae. In addition, reversible or irreversible pores on the cell membrane can be obtained by changing the PEF conditions. In this paper, we discuss the impact of PEF parameters (pulse duration, ranging from 5 to 500 µs, and electrical field amplitude, values up to 7 kV.cm^{-1}) and biomass characteristics (cell concentration, physiology) on the treatment efficiency and energy demand to induce reversible and irreversible permeabilization. Though similar levels of maximum reversible and irreversible permeabilization were obtained for all PEF conditions, the lowest energy demand and temperature increase were found for the lowest pulse duration (5 µs) tested. To better characterize microalgae electroporation, pore characterization (size and resealing time) was assessed. Pores with a maximum radius ranging from 0.8 to 0.9 nm reseal in few seconds, and do not affect cell division capability.

Keywords: *Chlamydomonas reinhardtii* – electroporation – viability – pore sizes

List of abbreviations

- PEF: Pulsed Electric Fields
- TAP: Tris-Acetate-Phosphate; medium for Chlamydomonas reinhardtii
- NP: Naturally permeabilized cells
- RP: Reversibly permeabilized cells
- IP: Irreversibly permeabilized cells
- NA: Non-affected cells
- SG: Sytox green
- SA: Staining 1h after treatment
- SB: Staining before treatment
- W: Energy delivered from the treatment (W)
- E: Electric Field (kV·cm-1)
- Δt_{pu}: Pulse duration (s)
- σ: Medium conductivity (S·m^{-1})
- C: Heat capacity (J·K^{-1})
- ρ: medium density
- CLSM: Confocal Laser Scanning Microscopy
- r_{crit}: critical pore radius leading to irreversible pores

1.2 Introduction

Pulsed Electric Fields (PEF), consists in delivering a transient electric stimulus to a biological sample. This treatment induces a large potential difference across cell membranes causing electropermeabilization [1,2]. Recently, PEF have been investigated as a downstream process for the extraction of valuable compounds from microalgae: proteins [3–5], pigments [6,7] or lipids [8,9]. . To develop an extraction process using PEF mechanisms at large-scale, it is highly important to determine optimal conditions of the process at small-scale. Indeed, parameters associated to PEF treatment (electric field intensity, pulse duration, frequency and shape), cell properties (radius, cytoplasm conductivity) and treatment conditions (cell concentration, medium conductivity) may affect membrane permeabilization efficiency. Additionally, PEF parameters strongly influence cell viability and can be optimized to induce reversible permeabilization [1,10].

Electric field amplitude and pulse duration have a tremendous impact on the pore size that are obtained [11–13], but also affect the energy spent and temperature of the medium [11,14] during the process. On the other hand, extraction of some intracellular targeted molecules is highly dependent on membrane pore size and solubility in water and/or organic solvents. The use of additional processes inducing cell wall partial or total rupture and solvent exposure may be combined with PEF in order to enhance molecule's extraction [15].

This paper deals with the impact of the treatment parameters (pulse duration and electric field amplitude) on microalgae permeabilization and cell viability. Reversibility or irreversibility of various PEF treatments is monitored through the penetration of a small molecule (Sytox Green, 600 Da) in *Chlamydomonas reinhardtii* cells. Energy consumption and heat generation during PEF treatment are estimated as they should be minimized for cost reasons. The capability of pore membrane to reseal as well as cell's ability to divide after PEF treatment are also examined. Because algae are usually concentrated [3,6,8,9,16] before PEF treatment, the impact of cell concentration on the permeabilization efficiency is also studied.

1.3 Materials and methods

1.3.1 Microalgae

Chlamydomonas reinhardtii SAG 34.89 (wild type) strain was obtained from the Culture Collection of Algae at the University of Goettingen (EPSAG, Nikolausberger Goettingen, Germany). Microalgae cells were cultivated in TAP Medium [17] to promote growth and in TAP nitrogen depleted medium for lipid accumulation (NH_4Cl removed from the TAP medium).

1.3.2 Culture conditions

Cells were cultivated photo-autotrophically under exponential growth conditions in 250 mL shake flasks with a culture volume of 50 mL (rotation speed 150 rpm, temperature 25 °C, enriched air 1.5 % CO_2, white light 20 µmol.m^{-2}.s^{-1} at the surface of the flask). In the exponential phase, microalgae concentrations ranged from $2{\cdot}10^5$ to $2{\cdot}10^7$ cells·mL^{-1}. Cell concentration was evaluated using a Guava easyCyte 5 flow cytometer (Millipore Corporation 25801 Industrial Blvd Hayward, CA 94545). To trigger the accumulation of neutral lipids, the algae cells were centrifuged (6000 g, 6 min) and resuspended at a concentration of $3{\cdot}10^6$ cells·mL^{-1} in 60 mL flasks under nutritional stress conditions (TAP nitrogen depleted medium). The following conditions were applied: light intensity of 150 µmol.m^{-2}.s^{-1}, agitation at 50 rpm, temperature set at 24±1 °C, 0.0035 % CO_2. Cell concentration and dry weight after 7 days of stress were respectively $1{\cdot}10^7$ cells·mL^{-1} and 1 g·L^{-1}. After 7 days of stress, the biomass contained 20 % dry weight of neutral fatty acids and 15 % dry weight of polar fatty acids. Cells at 7 days of nitrogen stress were submitted to PEF treatment.

1.3.3 Pulse Electric Field (PEF) conditions

The experiments were performed using a pulse generator Betatech Electrocell B10 HVLV which generates potential up to 1000 V and delivers monopolar or bipolar pulses. In this study, only monopolar pulses were used.

Assays were carried out in Gene Pulser®/Micropulser™ electroporation cuvettes with an electrode distance of 1 mm. PEF tested conditions were the following: potential applied U in the range of 0 to +700 V, pulse duration Δt_{pu} between 5 and 500 µs , pulse repetition frequency set at 100 ms, burst of 10 monopolar pulses. Using the stated electrode distance, a potential of 700 V corresponds to an electric field of 7 kV/cm (7 ± 0.36 kV/cm when considering cuvettes fabrication precision of 5% and generator precision of 0.1V). All PEF experiments were performed in TAP nitrogen depleted medium with a conductivity of 0.213 S/m [18].

1.3.4 Characterization of reversible and irreversible pores using Sytox Green

Cells membrane permeability was evaluated with Sytox Green (SG), a molecule of 600 Da which binds nucleic acid of permeabilized cells to form a fluorescent complex with excitation and emission peaks at 504 and 523 nm respectively.

Sytox green staining (% cells stained) was measured using a Guava easyCyte 5 flow cytometer (Millipore Corporation 25801 Industrial Blvd Hayward, CA 94545). SG was added to a final concentration of 0.5 µM to a sample with a concentration of $2.5{\cdot}10^5$ cells·mL^{-1}. Five minutes after SG staining, cells emitting a fluorescence above $2{\cdot}10^2$ a.u. at 583 nm were considered permeable to the molecule. The percentage of permeability to SG corresponds to the percentage of cells detected above this fluorescence value.

To evaluate reversible and irreversible permeability, 4 sorts of cells (% cells) could be distinguished: NP (Naturally Permeabilized cells), RP (Reversibly Permeabilized cells), IP (Irreversibly Permeabilized cells) and NA (Non-Affected cells). (NP), naturally permeabilized cells, corresponds to the control and refers to the cells whose membrane is permeable to SG before PEF treatment; (RP) reversibly permeabilized cells refers to cells permeable to SG during PEF treatment but not 1h after; (IP) irreversibly permeabilized cells refers to the cells whose membrane is permeable to SG during and 1h after PEF treatment; (NA) non-affected cells refers to cells impermeable to SG during and after PEF treatment.

The populations NP, RP, IP, NA were estimated after three treatment protocols:

NP cells were harvested, diluted with TAP N- medium to $2.5 \cdot 10^5$ cells·mL^{-1}, stained with SG and measured in the flow cytometer.

SA cells (SA – Staining after) were harvested, transferred to the electroporation cuvette, submitted to PEF treatment, diluted with TAP N- medium to $2.5 \cdot 10^5$ cells·mL^{-1}, stained with SG (0.5 µM) and their concentration measured in flow cytometry 1h after PEF treatment.

$$SA = NP + IP \qquad (1)$$

SB cells (SB – Staining before) were harvested, stained with SG, transferred to the electroporation cuvette, submitted to PEF treatment, and then immediately diluted with TAP N- medium to $2.5 \cdot 10^5$ cells·mL^{-1} for flow cytometry measurement.

$$SB = NP + IP + RP \qquad (2)$$

IP cells were estimated as following

$$IP = SA - NP \qquad (3)$$

RP cells were determined as

$$RP = SB - SA \qquad (4)$$

NA was estimated as

$$NA = 100 - NP - RP - IP \qquad (5)$$

Two independent assays were performed(N=2). SG permeability was measured in triplicate for each assay. Mean permeability values and the associated standard deviation were calculated from the average values of the two experiments.

1.3.5 Energetic and thermic aspects

The energy delivered during the PEF treatment W (expressed in $J \cdot m^{-3}$), was evaluated thanks to equation 6:

$$Wtreat = |E|^2 \, \Delta t_{pu} \, \sigma \, Np \qquad (6)$$

where σ is the medium conductivity (in $S \cdot m^{-1}$), E electrical field amplitude ($V \cdot m^{-1}$), Δt_{pu} pulse duration (s), Np number of pulses applied during treatment.

By neglecting thermal external exchanges (diffusion, convection), the temperature elevation (ΔT_{pu}) induced by a pulse, due to the Joule effect, can be over-estimated as shown in equation 7.

$$\Delta T_{pu} = \frac{W}{C \, \rho} \qquad (7)$$

where $C \cdot (J \cdot m^{-3} \cdot K^{-1})$ is the heat capacity of the medium, and ρ its density.

The minimal ΔT_{treat} estimation for the treatment considers cooling between each pulse. For the maximal ΔT_{treat}, an adiabatic process is presumed which led to over-estimated heat.

1.3.6 Impact of cell concentration on permeabilization

Cell cultures at 7 days nitrogen stress at $8 \cdot 10^6$ cells$\cdot mL^{-1}$ were either diluted or concentrated in the range of $4 \cdot 10^6$ cells$\cdot mL^{-1}$ up to $2 \cdot 10^8$ cells$\cdot mL^{-1}$ by consecutive centrifugation and re-suspension in TAP nitrogen depleted medium. These concentrations correspond to dry weights of 0.5 up to 25 $g \cdot L^{-1}$. Cells were stained with SG before treatment, in order to determine NP, and submitted to the following PEF conditions: 10 pulses of 5 µs at 7 $kV \cdot cm^{-1}$. Irreversible permeability was therefore determined as previously described (section 2.4). Two independent assays were performed(N=2). SG permeability was measured in triplicate for each assay. Mean permeability values and the associated standard deviation were calculated from the average values of the two experiments.

1.3.7 Impact of physiology on cell sensitivity to PEF

All PEF experiments of this work were performed on cells cultivated in depleted nitrogen conditions for 7 days to induce lipid accumulation (see section 2.2). In this specific section, cells at various stress durations, from 0 to 7 days, were submitted to reversible (4.5 $kV.cm^{-1}$, 5 µs) or irreversible (7 $kv.cm^{-1}$, 5 µs) PEF conditions to evaluate the impact of stress (and thus physiological modifications) on cell reversible and irreversible permeability. Measurements and calculations were carried out as previously described (section 2.4).

1.3.8 Cells division after PEF treatment

To evaluate cell division ability after reversible or irreversible PEF treatment, cells at 7 days of stress were PEF treated in sterile conditions and re-inoculated in TAP growth conditions (see section 2.2). Cell concentration was monitored over three days after treatment *via* flow cytometry as previously described (section 2.2). As a control, untreated cells at 7 days of stress were reinoculated in TAP growth conditions.

1.3.9 Characterization of reversible pores life duration

To evaluate pore resealing dynamics, SG penetration was evaluated by staining cells before treatment (SB), and at different time points after PEF treatment (SA). Staining before is used as a reference value (time after pulse equal to 0) were sytox green is already in contact with cells during treatment, indicating both irreversible and reversible permeabilization. SB and SA were performed as described in the section 2.4, except that SA was performed not 1h after PEF, but from 15 seconds to 3 minutes after treatment. SG permeability due to treatment was estimated by deducting the naturally permeabilized cells (NP) from the permeability measured over time. Experiment was performed at 20°C, on two independent essays (N=2); for each essay SG permeability was measured in triplicate. Mean values and the associated standard deviation were calculated from the average values of two experiments performed on different cell cultures.

1.3.10 Pores size

To characterize the pores induced by PEF in the cytoplasmic membrane of *Chlamydomonas reinhardtii* cells at 7 days of lipid stress, two molecules were used: Sytox Green (600 Da) and fluorescent Dextran FITC (490/520, 3000 Da). Sytox Green has a radius of approximately 0.5 - 0.7 nm [13]. Its penetration may thus require pores with a minimum 0.5 - 0.7 nm radius to enter and stain DNA. Whereas 3 kDa Dextran requires pores larger than 0.8 – 0.9 nm [13] to penetrate the cell. Dextran has no target in the cell and diffuses in the cytoplasm of permeable cells. Cells were incubated with Dextran 3 kDa at a final concentration of 5 µM before exposure to the PEF treatment. Few minutes later and until a maximum time of 1h, dextran fluorescence in exposed cells was monitored by Confocal Laser Scanning Microscopy (CLSM 700, Carl

Zeiss Microscopy GmbH, Germany) on approximately 50 to 100 cells per PEF condition. In addition, cell wall was stained with Concanavalin A (Molecular Probes, Lifetechnologies, C860) as described elsewhere [19], before PEF exposure.

1.4 Results

1.4.1 Reversible/irreversible permeabilization thresholds

Pulses with various durations (5 µs, 50 µs, 500 µs; applied as bursts of 10 monopolar square pulses; 10 Hz) led to either reversible or irreversible electroporation when varying the electric field applied (from 2 kV·cm^{-1} to 7 kV·cm^{-1}). The treatment was performed on *Chlamydomonas reinhardtii* after 7 days of nitrogen stress. The impact of short pulses (5 µs) on cell reversibility/irreversibility is shown in Figure 1. The percentage of non-affected (NA) and naturally-permeabilized cells (NP) are also presented in Figure 1. From 2.5 to 4.5 kV·cm^{-1}, the percentage of reversibly permeabilized cells (RP) increased. At these electric field intensities, pores created in the cell membrane enabled SG entrance within the cytoplasm during treatment. The maximum percentage of RP cells was observed at 4.5 kV·cm^{-1} (83.1 ± 3.1 %, Figure 1). When increasing the electric field above 4.5 kV·cm^{-1}, an increase of the percentage of irreversibly permeabilized cells (IP) was observed to the detriment of RP cells. Indeed, at 7 kV·cm^{-1}, 87.3 % of the cells were IP and 0.8 % RP. NP and NA represented 5.9 and 6.0 % of the cells, respectively.

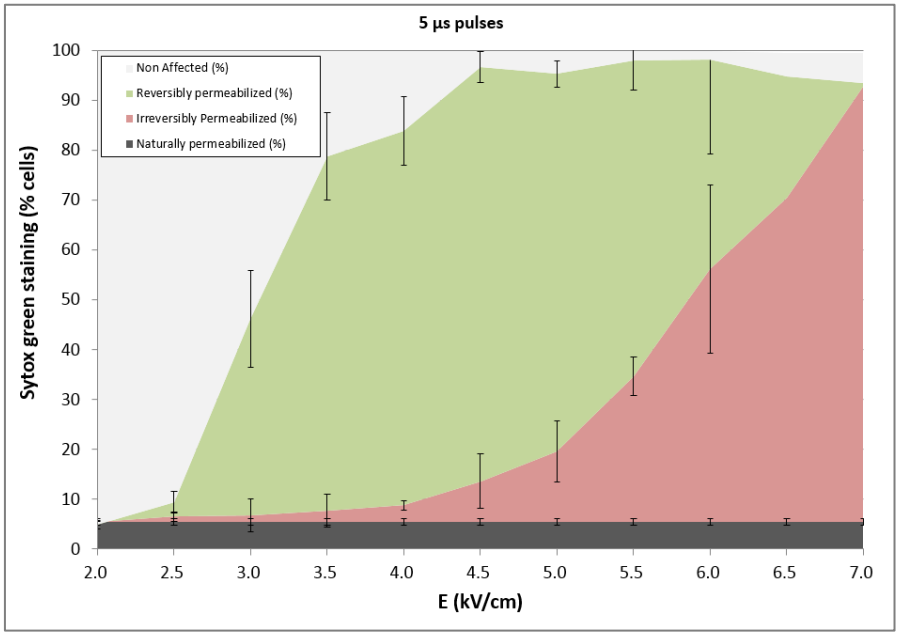

Figure 1: Impact of the electric field E on the distribution of reversibly (green) and irreversibly (red) permeabilization with a fixed pulse duration of 5 µs (burst 10 square pulses with 10 Hz frequency). Cells permeability before PEF treatment, corresponding to naturally permeabilization (NP), is displayed in black and non-affected cells (NA) are shown in grey. Experiments were performed on Chlamydomonas reinhardtii cells at 7 days of stress. Error bars corresponds to standard deviation (SD). Means and associated SD are obtained from two independent assays.

These experiments were also performed with 50 µs and 500 µs pulses, requiring in those cases lower electric fields to achieve reversible or irreversible pores (see supplementary data). Similar patterns were obtained for those conditions.

The distribution of RP and IP cells for an electric field varying from 0 $kV \cdot cm^{-1}$ to 7 $kV \cdot cm^{-1}$ are presented in Figure 2 and Figure 3, respectively.

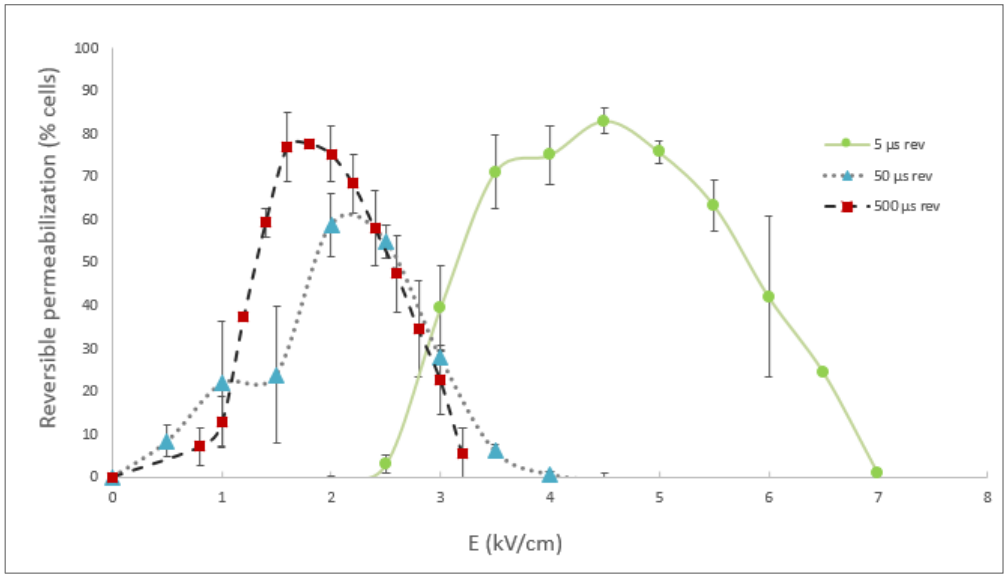

Figure 2: Impact of the electric field on the reversible permeabilization (RP cells) obtained using 5, 50 and 500 µs pulses respectively (burst 10 square pulses with 10 Hz frequency). Experiments were performed on Chlamydomonas reinhardtii cells at 7 days of stress. Error bars corresponds to standard deviation (SD). Error bars corresponds to standard deviation (SD). Means and associated SD are obtained from two independent assays.

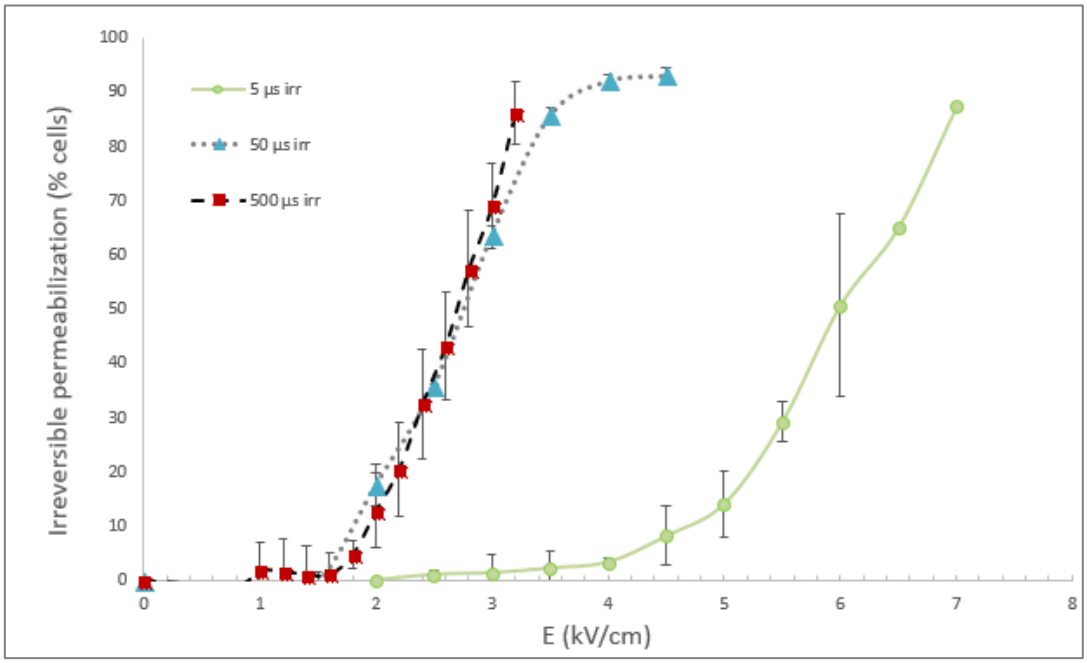

Figure 3: Impact of the electric field on the irreversible permeabilization (IP cells) obtained using 5, 50 and 500 µs pulses (burst 10 square pulses with 10 Hz frequency). Experiments were performed on Chlamydomonas reinhardtii cells at 7 days of stress. Error bars corresponds to standard deviation (SD). Means and associated SD are obtained from two independent assays.

The maximum percentage of reversible cells (RP) with 5, 50 and 500 µs pulses were obtained using 4.5, 2.2 and 1.7 kV·cm^{-1}, respectively (Figure 2). The electric fields required to obtain *a minimum* 85 % of IP are 7, 3.5 and 3.2 kV·cm^{-1} for 5, 50 and 500 µs pulses respectively (Figure 3).

In conclusion, similar values of the maximum percentage of reversible (RP) and irreversible (IP) cells were obtained with different PEF conditions. In addition, for longer pulse durations (50 and 500 µs), the transition from reversible to irreversible permeabilization was more sensitive to the electric field level, which makes it more difficult to control under those conditions.

1.4.2 Energy demand and heat production

The total energy of the treatment, Wt_{reat}, and the estimated temperature increase, ΔT_{treat}, calculated for the different conditions tested, are presented in Table 1.

E (kV/cm) ***Electric field required***	**W_{treat} (kJ/m^3)** **Total energy of the treatment**	**ΔT_{treat} (°C)** **Potential temperature increase of the treatment (min - max)**
	5 µs pulses	
Rev Perm: 4.5	$2.1 \cdot 10^3$	< 0.05 - 0.52
Irr Perm: 7	$5.2 \cdot 10^3$	< 0.12 - 1.24
	50 µs pulses	
Rev Perm: 2.2	$5.1 \cdot 10^3$	< 0.12 - 1.23
Irr Perm: 3.5	$13 \cdot 10^3$	< 0.31 – 3.12
	500 µs pulses	
Rev Perm: 1.7	$31 \cdot 10^3$	< 0.73 – 7.36
Irr Perm: 3.2	$110 \cdot 10^3$	< 2.61 – 26.08

Table 1: Electric fields E required to obtain maximal reversibly permeabilized cells and at least 85% of irreversible permeabilization with 5, 50 and 500 µs pulses and corresponding treatment energy W_{treat} and potential temperature increase ΔT_{treat}. Medium conductivity: 0.213 S·m^{-1}.

As shown in table 1, higher values of energy consumption and heat release were estimated for long pulses compared to those induced by short ones. Moreover, similar levels of permeabilization were obtained for all the conditions tested, suggesting that using short pulses is more energy efficient. Indeed, the application of 500 µs pulses is expected to require 10 to 20-fold more energy (and thus temperature increase) than 5 µs pulses. Furthermore, the

temperature increase may be critical (up to 20°C increase) when using 500 µs and irreversible pulses inducing conditions (3.2 $kV \cdot cm^{-1}$) while its increase was estimated to be negligible when using 50 and 5 µs pulses.

1.4.3 Effect of biomass concentration on the permeabilization sensitivity

The effect of cell concentration on irreversible permeabilization is presented in Figure 4. The biomass concentration did not seem to affect the percentage of IP cells except for the highest cell concentration where a statistical difference is observed ($p<0.05$). This slight increase at the highest cell concentration (10^8 $cells \cdot mL^{-1}$; corresponding to a volumetric fraction of 2 %) may be due to an increase of the medium conductivity after the concentration procedure (section 2.6).

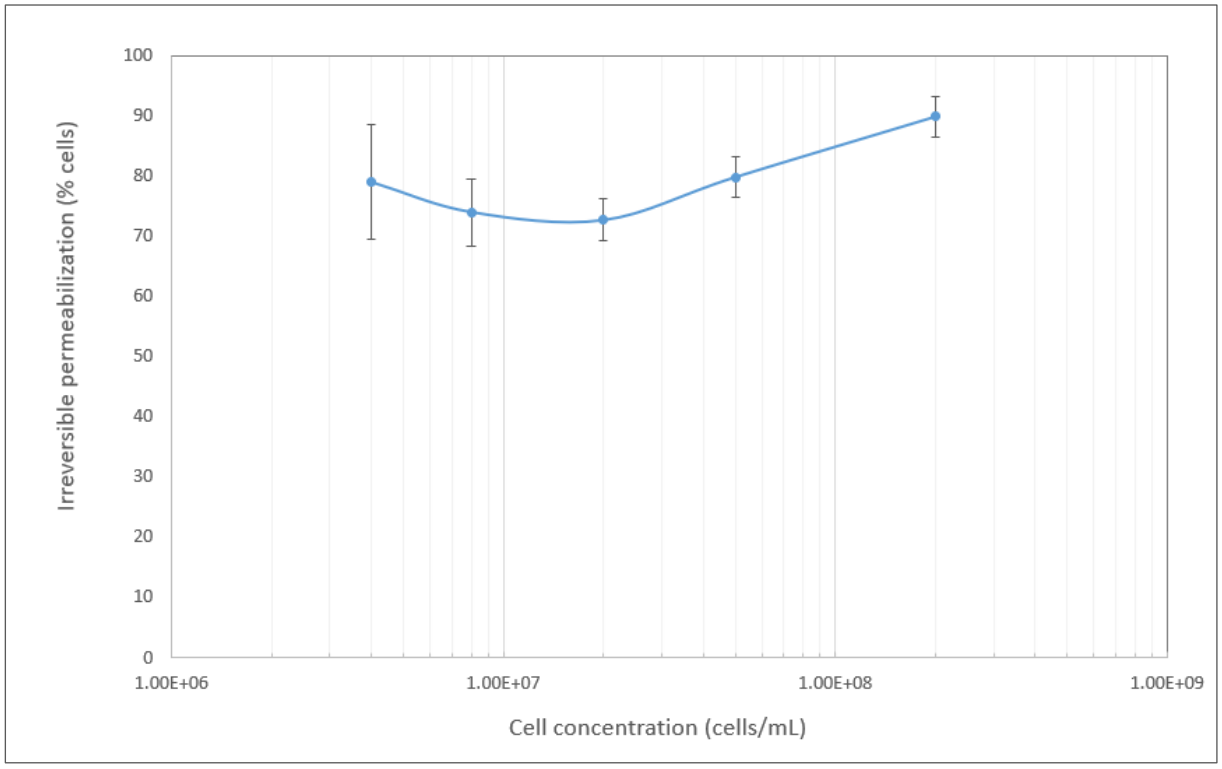

Figure 4: Effect of the cell concentration (from $4 \cdot 10^6$ to $2 \cdot 10^8$ $cells \cdot mL^{-1}$) on the irreversible permeabilization (IP cells) obtained after a treatment of 10 pulses of 5 µs and 7 kV/cm. Experiments were performed on Chlamydomonas reinhardtii cells at 7 days of stress. Error bars corresponds to standard deviation (SD). Means and associated SD are obtained from two independent assays.

1.4.4 Influence of physiology on cell sensitivity to PEF

Environmental stresses such as nitrogen depletion and high light intensity enhances lipid accumulation in *Chlamydomonas reinhardtii* cells [14]. This may change many cell features, such as cell size, membrane and cell wall properties [19], and cytoplasm conductivity (reduction by a factor 6 during lipid accumulation has been described [20]). A rise of the mean cell diameter from 7 µm up to 11 µm [14] and an increase of the cell wall thickness was observed over time in our conditions [21].

To evaluate the impact of physiology on cell permeability, cells at different stages of nitrogen stress were therefore submitted to PEF treatment. In our conditions, the observed physiological modifications did not seem to affect permeabilization, neither with reversible treatment (5 µs pulses, 4.5 kV·cm^{-1}) nor irreversible treatment (5 µs pulses, 7 kV·cm^{-1}), as shown in Figure 5.

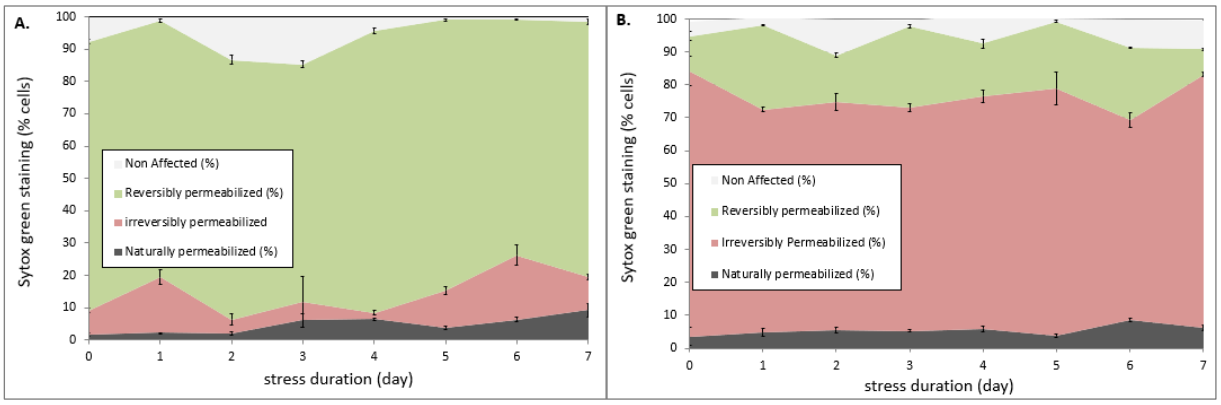

Figure 5: Effect of the stress duration on reversible (green) and irreversible (red) permeabilization obtained with 5 µs, 4.5 kV/cm pulses (treatment A) and 5 µs, 7 kV/cm (treatment B). Cells permeability before PEF treatment, NP, is displayed in black, non-affected cells, NA, are shown in grey. Experiments were performed on Chlamydomonas reinhardtii cells at 7 days of stress. Error bars corresponds to standard deviation (SD). Means and associated SD are obtained from two independent assays.

1.4.5 Cell growth after reversible and irreversible permeabilization conditions

The permeabilization impact on the cell's capability to divide was verified for the first time with algae cells. To do so, cells were inoculated in growth conditions after PEF treatment. Reversibly and irreversibly treated cells were compared with the control (no PEF treatment) in terms of growth for different PEF conditions (the cases of 5 and 500 µs pulses are respectively shown in Figure 6.A and Figure 6.B. Similar patterns were obtained for reversible and irreversible induced conditions at 50 µs (data not shown).

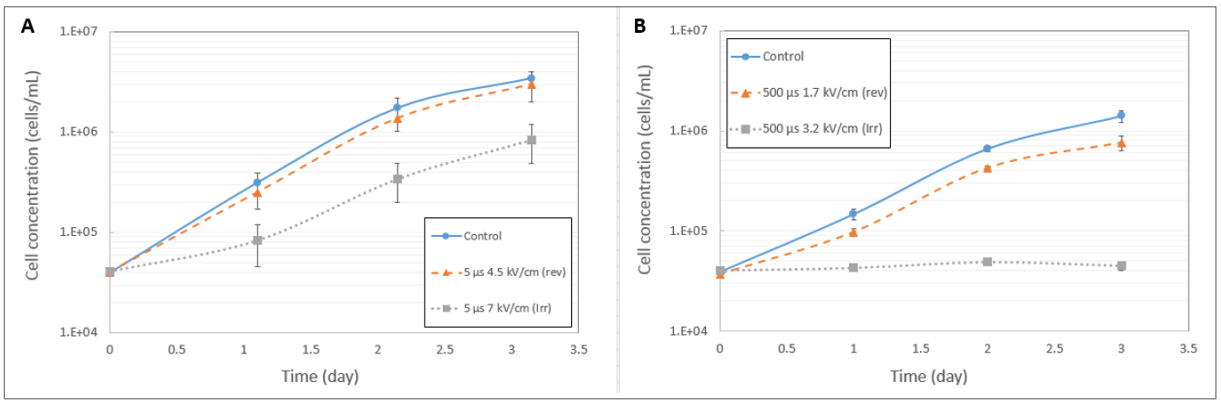

Figure 6: Cell concentration over time after PEF treatment. A) 5 µs pulses. B) 500 µs pulses (straight line round marks: no PEF; dashed line triangular marks: 500 µs, 1.7 kV/cm; dotted line square marks: 500 µs, 3.2 kV/cm). Error bars corresponds to standard deviation (SD). Means and associated SD are obtained from two independent assays.

Data from Figure 6 A (5 µs pulses) and B (500 µs pulses) show that cells submitted to reversible treatments could divide almost at the same rate than the control cells. Differences can be explained by the fact that the reversibility is achieved for 80-90 % of the cell population within the sample while only 8% of the cells are irreversibly permeabilized (see Figure 1). On the contrary, no growth was observed for cells subjected to irreversible conditions with 500 µs pulses (3.2kV/cm). Growth remained though possible when 5 µs pulses were applied in irreversible conditions (7 kV/cm, Figure 6A). Indeed, approximately 10 % of the cells (reversible, RP, and non-affected, NA) were able to grow after the treatment in these conditions (see Figure 1).

1.4.6 Life time of reversible pores with different treatments

To estimate the life time of reversible pores induced by PEF on *Chlamydomonas reinhardtii* cells, Sytox green penetration in the cell was measured over time (Figure 7).

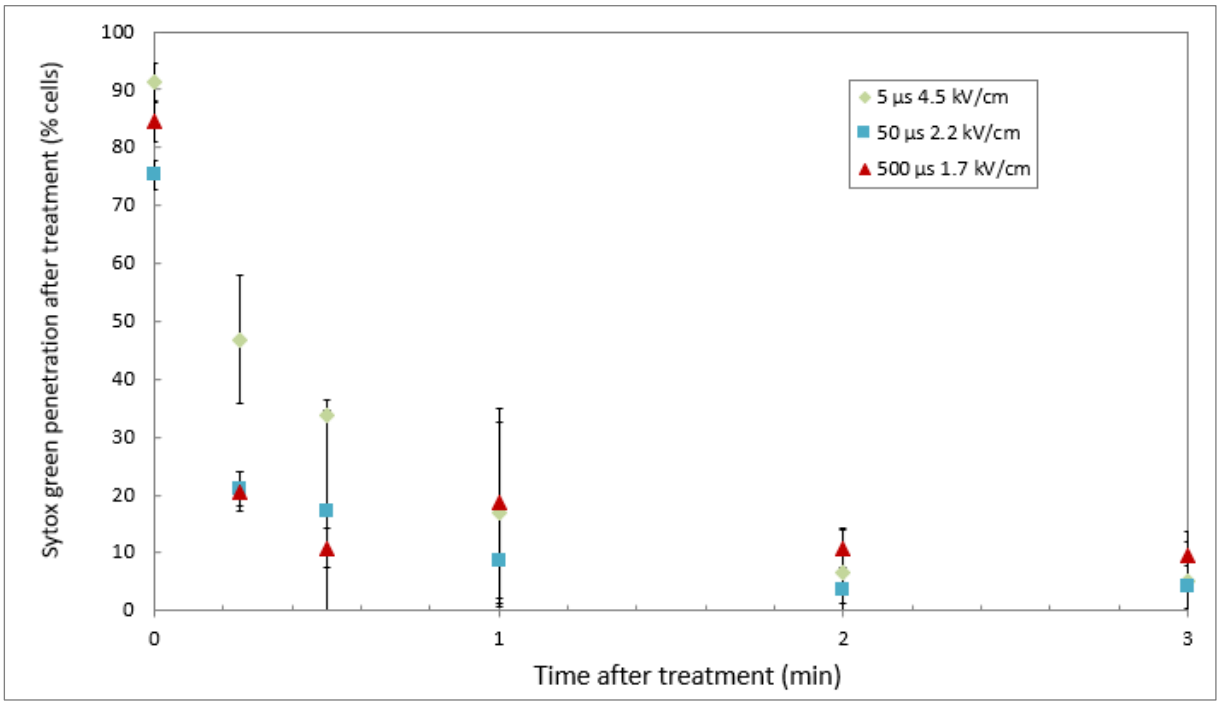

Figure 7: Sytox green penetration after reversible pulse treatment conditions measured from 0 to 3 minutes at 20°C. Experiments were performed on Chlamydomonas reinhardtii cells at 7 days of stress. Error bars corresponds to standard deviation (SD). Means and associated SD are obtained from two independent assays.

As it can be observed in Figure 7, the life time of reversible pores is characterized to be lower than 30 seconds in any condition. Only a significant difference ($p<0.01$) can be observed at 15 seconds after treatment for 5 µs, 4.5 kV/cm pulses were the number of reversibly permeabilized cell is slightly higher compared to other conditions.

1.4.7 Investigation towards pore size determination

Dextran FITC 3kDa molecules were used to investigate the pore formation with various PEF treatments. CLSM observations were used to assess the membrane permeability to Dextran: the fluorescent molecule diffused through the cell wall and the permeabilized membrane to exhibit a green fluorescence in the cytoplasm (Figure 8). Observations indicate the presence of Dextran FITC in the external medium and in the cell cytoplasm in the case of diffusion through the permeabilized membrane (green channel). The cell wall and chlorophyll are observed thanks to concanavalin A staining (yellow channel) and chlorophyll autofluorescence (red channel) respectively.

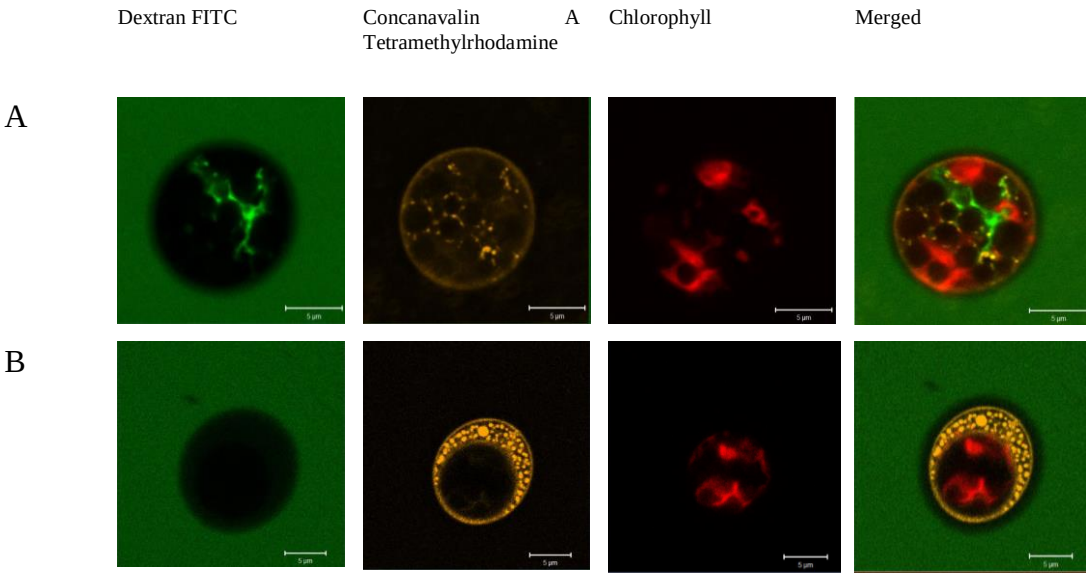

Figure 8: A) Cell after irreversible PEF treatment (E = 7 kV/cm and 5 µs pulse duration) and B) cell after reversible PEF treatment (4.5 kV/cm and 5 µs pulse duration). Dextran FITC (permeability) detected on the green channel, concanavalin A stained cell wall detected on the yellow channel, chlorophyll autofluorescence detected on the red channel. Scale bar: 5 µm.

Preliminary results showed that Dextran 3 kDa penetrated irreversibly permeabilized cells using either 5, 50 and 500 µs pulses. Our observations showed that Dextran 3 kDa was unable to penetrate reversibly permeabilized cells, but this result may be sensitive to cell culture conditions. Further investigations are currently undergone to determine the maximal pore radius obtained with reversible PEF treatment.

1.5 Discussion

1.5.1 Optimal parameters for PEF treatment

Our results showed similar permeabilization levels (reversible and irreversible) for all tested conditions though reduced energy demand is expected using short pulses associated with a high electric field. According to our calculations, heat released in the medium may be negligible in these conditions. This is in agreement with data from previous studies [10,14].

Cell growth after various reversible PEF treatments was observed, demonstrating that cell division can occur after inducing reversible pores. This observation demonstrated the absence of lethal side effects when using short pulses with moderate electric field intensities (5 µs with 4.5 $kV \cdot cm^{-1}$, 50 µs with 2.2 and 500 µs with 1.7 $kV \cdot cm^{-1}$).

If one aims at retaining cell viability, the use of pulse durations in the range of several micro-seconds seems therefore appropriate to avoid negative side effects in the cells while minimizing the energy demand of the treatment.

Additional experiments showed that physiological changes which occur in stressed cells (radius increase, increased cell wall thickness [20,21]) do not seem to impact significantly the permeabilization obtained (Figure 5). Interestingly, the treatment of diluted or highly concentrated cells (Figure 4) also showed negligible impact on the permeabilization obtained.

1.5.2 Pore characterization: pore sizes

To get a better insight into the mechanisms of microalgae electroporation, pores characteristics in terms of radius and resealing time were determined for our experimental conditions. Whereas such studies exist in the literature for mammal cells [11,13,22–25], as far as we know, no studies concerning algae cells are described in the literature.

During the application of the electric field, the electroporation process can be described in three separate stages (*i*) charging of the cell membrane, (*ii*) creation of pores, (*iii*) evolution of pores radius [23,25]. Pore formation is faster when increasing the field strength [26]. The application of electric field leads to the creation of thousands of pores of different sizes. In any conditions, most of the pores have a radius inferior to 1 nm [26]. In harsh conditions (long pulses or high electric field), a sub-population of larger pores may appear with a size up to 120 nm [23]. Pores with a radius inferior to a critical size r_{crit} will be able to reseal after the PEF treatment. If some pores appear with a radius superior to r_{crit} (corresponding to a critical voltage of resealing [27]), the membrane is unable to reseal and the permeabilization is irreversible. As discussed in the literature [27] [28], the case of irreversible permeabilization leads to unstable pores which size might increase after the treatment. We can assume that pore reversibility/irreversibility is associated with the maximum pore size induced by the treatment in the plasma membrane.

By using two molecules of specific sizes, we could investigate the critical radius r_{crit} to be in the range of 0.7 to 0.9 nm for *Chlamydomonas reinhardtii* in the conditions of our study. Indeed, Sytox green (SG, 600 Da ~ 0.5 – 0.7 nm radius) could penetrate reversibly permeabilized cells, while dextran (3000 Da ~ 0.8 – 0.9 nm radius) was retained out of the cells, suggesting that reversible pores were smaller than Dextran molecules in our preliminary experiment. In addition, pores corresponding to irreversible permeabilization conditions led to the penetration of 3kDa Dextran. Thus, cells submitted to irreversible conditions (7KV/cm and 5µs) had a pore radius higher than 0.8 – 0.9 nm. Tuning the amplitude and duration of pulses altogether, one can control the maximum aperture of membrane pores, leading to reversible or irreversible permeabilization. Further investigations on the determination of the critical radius (corresponding to the maximum pore size for which plasma membrane can reseal) is currently held.

1.5.3 Pore characterization: dynamics of pore resealing

Our study shows that the pores created by the applied electric field (see Table1) can reseal after only a few seconds (Figure 7). According to literature, the resealing time ranges from a few milliseconds to a couple of hours depending on the experimental conditions such as the size of the molecule used to determine it [22]. In the first seconds after the application of the electric field (in reversible conditions), a rapid decrease of pore size happens. The complete pore resealing and membrane conductance relaxation might take several hours and the membrane may remain permeable to small ions during this healing process [13,22]. The healing process is thus dependent on the pore size considered. Temperature also highly impacts the membrane fluidity and its resealing kinetics. The understanding of resealing process is therefore important in the choice of pulse frequency and the envisaged applications. Considering Figure 7, the time between each consecutive pulse (100 ms) is lower than the measured resealing time of the pores.

1.5.4 Potential applications of reversible or irreversible electropermeabilization of microalgae

PEF have been recently studied as a pre-treatment for the extraction of valuable compounds from microalgae. Our results show that reversible electropermeabilization of microalgae opens small transient pores (max radius: 0.8 – 0.9 nm), which limits permeability to small molecules (Figure 7). This can be achieved with a low energy demand. Our study also demonstrates that the opening of large pores (above 0.8 – 0.9 nm radius) is inevitably associated with irreversible permeabilization and therefore cell death. Thus, algae milking (compounds extraction while maintaining cell viability and thus enabling cells to be reused) could only be possible for small hydro soluble molecules of size similar or lower than that of sytox green (less than 0.7 nm radius). Anyway, according to our work, and as mentioned in several studies, in the perspective of large molecules extraction, irreversible electropermeabilization seems to be required. However, it should be kept in mind that the recovery of those molecules is still limited by the presence of the microalgal cell wall [21]. Thus, in this context, treatments aiming at weakening the cell wall may be required before PEF treatment [15].

1.6 Conclusions

Electric fields conditions leading to reversible or irreversible electroporation of C*hlamydomonas reinhardtii* cells were determined in this work. For both conditions of reversible and irreversible permeabilization, PEF energy demand can be optimized by changing the electric field conditions (amplitude and pulse duration). Indeed, at similar permeabilization levels (and thus pore sizes), the lowest energy demand was obtained for the shortest pulse duration and the highest field amplitude tested (4.5 and 7 $kV \cdot cm^{-1}$, 5 µs, for reversible and irreversible conditions respectively).

Preliminary experiments for the determination of the mean radius of membrane pores, for cells submitted to PEF reversible conditions, were achieved using either Sytox green (SG, 600 Da ~ 0.5 – 0.7 nm radius) or dextran (3000 Da ~ 0.8 – 0.9 nm radius). Further investigations are needed to determine precisely the critical radius. The pore resealing time was determined to be approximately 30 sec. On the other hand, cells subjected to irreversible conditions presented pores larger than the radius of dextran (0.8 – 0.9 nm).

In the context of compounds extraction, reversible conditions associated with low energy demand and maintenance of cell viability can be considered for the recovery of small hydro-soluble molecules. This will be studied in future work.

1.7 Acknowledgements

This work has benefited from the financial support of the LabeX LaSIPS project MES-ALG and ALGUIMPACT (ANR-10-LABX-0040-LaSIPS) managed by the French National Research Agency under the "Investissements d'avenir" program (no. ANR-11-IDEX-0003-02). The authors acknowledge project supports: ENS Paris Saclay, CentraleSupélec, Institut d'Alembert, and CNRS.

1.8 Authors contributions

All authors have contributed significantly to the conception and design of the work, methodology development, data analysis and writing. PB and SB collected the data.

1.9 Conflict of interest statement

The authors confirm that there are no known conflicts of interest associated with this publication and there has been no significant financial support for this work that could have influenced its outcome.

1.10 Statement of informed consent, human/animal rights

No conflicts, informed consent, human or animal rights applicable.

1.11 Declaration of authors agreement to authorship and submission of the manuscript

All authors have agreed to be so listed and approved the manuscript submission to the journal.

1.12 References

[1] T. Kotnik, W. Frey, M. Sack, S. Haberl Meglič, M. Peterka, D. Miklavčič, Electroporation-based applications in biotechnology, Trends Biotechnol. 33 (2015) 480–488. doi:10.1016/j.tibtech.2015.06.002.

[2] J. Teissie, M. Golzio, M.P. Rols, Mechanisms of cell membrane electropermeabilization: A minireview of our present (lack of ?) knowledge, Biochim. Biophys. Acta - Gen. Subj. 1724 (2005) 270–280. doi:10.1016/j.bbagen.2005.05.006.

[3] M. Goettel, C. Eing, C. Gusbeth, R. Straessner, W. Frey, Pulsed electric field assisted extraction of intracellular valuables from microalgae, Algal Res. 2 (2013) 401–408. doi:10.1016/j.algal.2013.07.004.

[4] M. Coustets, N. Al-Karablieh, C. Thomsen, J. Teissié, Flow process for electroextraction of total proteins from microalgae, J. Membr. Biol. 246 (2013) 751–760. doi:10.1007/s00232-013-9542-y.

[5] G.P. 't Lam, P.R. Postma, D.A. Fernandes, R.A.H. Timmermans, M.H. Vermuë, M.J. Barbosa, M.H.M. Eppink, R.H. Wijffels, G. Olivieri, Pulsed Electric Field for protein release of the microalgae Chlorella vulgaris and Neochloris oleoabundans, Algal Res. 24 (2017) 181–187. doi:10.1016/j.algal.2017.03.024.

[6] E. Luengo, S. Condón-Abanto, I. Alvarez, J. Raso, Effect of Pulsed Electric Field Treatments on Permeabilization and Extraction of Pigments from Chlorella vulgaris., J. Membr. Biol. 247 (2014) 1269–77. doi:10.1007/s00232-014-9688-2.

[7] O. Parniakov, F.J. Barba, N. Grimi, L. Marchal, S. Jubeau, N. Lebovka, E. Vorobiev, Pulsed electric field and pH assisted selective extraction of intracellular components from microalgae nannochloropsis, Algal Res. 8 (2015) 128–134. doi:10.1016/j.algal.2015.01.014.

[8] M.D.A. Zbinden, B.S.M. Sturm, R.D. Nord, W.J. Carey, D. Moore, H. Shinogle, S.M. Stagg-Williams, Pulsed electric field (PEF) as an intensification pretreatment for greener solvent lipid extraction from microalgae, Biotechnol. Bioeng. 110 (2013) 1605–1615. doi:10.1002/bit.24829.

[9] K. Flisar, S.H. Meglic, J. Morelj, J. Golob, D. Miklavcic, Testing a prototype pulse generator for a continuous flow system and its use for E. coli inactivation and microalgae lipid extraction, Bioelectrochemistry. 100 (2014) 44–51. doi:10.1016/j.bioelechem.2014.03.008.

[10] M.C. Vernhes, P.A. Cabanes, J. Teissie, Chinese hamster ovary cells sensitivity to localized electrical stresses, Bioelectrochemistry Bioenerg. 48 (1999) 17–25. doi:10.1016/S0302-4598(98)00239-6.

[11] K.C. Smith, R.S. Son, T.R. Gowrishankar, J.C. Weaver, Emergence of a large pore subpopulation during electroporating pulses, Bioelectrochemistry. 100 (2014) 3–10. doi:10.1016/j.bioelechem.2013.10.009.

[12] Y.U.N.Z. Hou, R.O.E.K. Umon, J.I.C. Ui, C.H.X.D. Eng, THE SIZE OF SONOPORATION PORES ON THE CELL MEMBRANE, 35 (2009) 1756–1760. doi:10.1016/j.ultrasmedbio.2009.05.012.

[13] G. Saulis, R. Saule, Size of the pores created by an electric pulse: Microsecond vs

millisecond pulses, Biochim. Biophys. Acta - Biomembr. 1818 (2012) 3032–3039. doi:10.1016/j.bbamem.2012.06.018.

[14] P. Bodénès, F. Lopes, D. Pareau, O. Français, B. Le Pioufle, Microdevice for studying the in situ permeabilization and characterization of Chlamydomonas reinhardtii in lipid accumulation phase, Algal Res. 16 (2016) 357–367. doi:10.1016/j.algal.2016.03.023.

[15] G.P. Lam, J.A. Van Der Kolk, A. Chordia, M.H. Vermue, G. Olivieri, M.H.M. Eppink, R.H. Wij, V. Tecchio, Mild and Selective Protein Release of Cell Wall De fi cient Microalgae with Pulsed Electric Field, (2017). doi:10.1021/acssuschemeng.7b00892.

[16] C. Safi, L. Cabas Rodriguez, W.J. Mulder, N. Engelen-Smit, W. Spekking, L.A.M. van den Broek, G. Olivieri, L. Sijtsma, Energy consumption and water-soluble protein release by cell wall disruption of Nannochloropsis gaditana, Bioresour. Technol. (2017). doi:10.1016/j.biortech.2017.05.012.

[17] No Title, Https://Www.Auburn.Edu/~mossant/Chlamydomonasmedia.Pdf. (n.d.).

[18] P. Bodénès, F. Lopes, D. Pareau, O. Français, B. Le Pioufle, Microdevice for studying the in situ permeabilization and characterization of Chlamydomonas reinhardtii in lipid accumulation phase, Algal Res. 16 (2016) 357–367. doi:10.1016/j.algal.2016.03.023.

[19] S. Bensalem, F. Lopes, P. Bodénès, D. Pareau, O. Français, B. Le Pioufle, Structural changes of Chlamydomonas reinhardtii cells during lipid enrichment and after solvent exposure, Data Br. 17 (2018). doi:10.1016/j.dib.2018.02.042.

[20] M.S. Bono, B.A. Ahner, B.J. Kirby, Detection of algal lipid accumulation due to nitrogen limitation via dielectric spectroscopy of Chlamydomonas reinhardtii suspensions in a coaxial transmission line sample cell, Bioresour. Technol. 143 (2013) 623–631. doi:10.1016/j.biortech.2013.06.040.

[21] S. Bensalem, F. Lopes, P. Bodénès, D. Pareau, O. Français, B. Le Pioufle, Understanding the mechanisms of lipid extraction from microalga Chlamydomonas reinhardtii after electrical field solicitations and mechanical stress within a microfluidic device, Bioresour. Technol. 257 (2018). doi:10.1016/j.biortech.2018.01.139.

[22] G. Saulis, M.S. Venslauskas, J. Naktinis, Kinetics of pore resealing in cell-membranes after electroporation, Bioelectrochemistry Bioenerg. 26 (1991) 1–13.

[23] W. Krassowska, P.D. Filev, Modeling electroporation in a single cell, Biophys. J. 92 (2007) 404–417. doi:10.1529/biophysj.106.094235.

[24] A. Winter, Impact of Pulsed Electric Fields (PEF) on post- permeabilization processes in plant cells, (2011) 76. doi:10.1016/j.ifset.2011.02.003.

[25] W. Sung, P.J. Park, Dynamics of pore growth in membranes and membrane stability, Biophys. J. 73 (1997) 1797–1804. doi:10.1016/S0006-3495(97)78210-9.

[26] A. Angersbach, V. Heinz, D. Knorr, Effects of pulsed electric fields on cell membranes in real food systems, Innov. Food Sci. Emerg. Technol. 1 (2000) 135–149. doi:10.1016/S1466-8564(00)00010-2.

[27] B. Chemistry, T. Helmholtz, B. Chemistry, 1. Introduction, 19 (1984) 211–225.

[28] E. Puértolas, O. Cregenzán, E. Luengo, I. Álvarez, J. Raso, Pulsed-electric-field-assisted extraction of anthocyanins from purple-fleshed potato, Food Chem. 136 (2013) 1330–1336. doi:10.1016/j.foodchem.2012.09.080.

1.13 Supplementary material

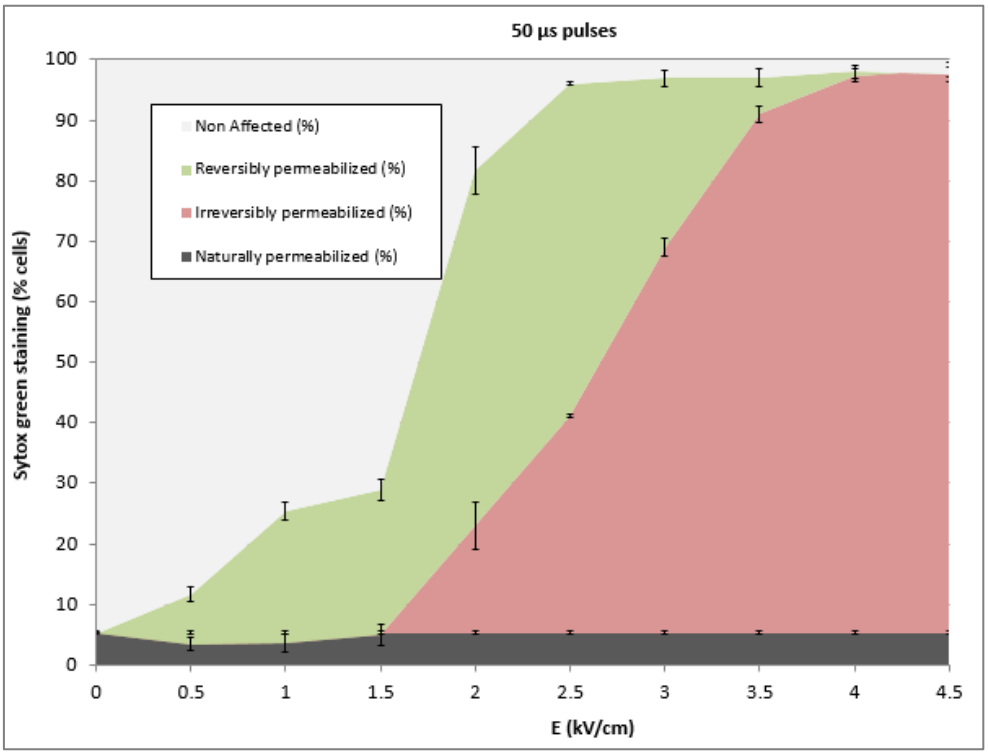

Figure: Impact of the electric field E on the distribution of reversibly and irreversibly permeabilization with a fixed pulse duration of 50 µs (burst 10 square pulses with 10 Hz frequency). Experiments performed on Chlamydomonas reinhardtii cells at 7 days of stress.

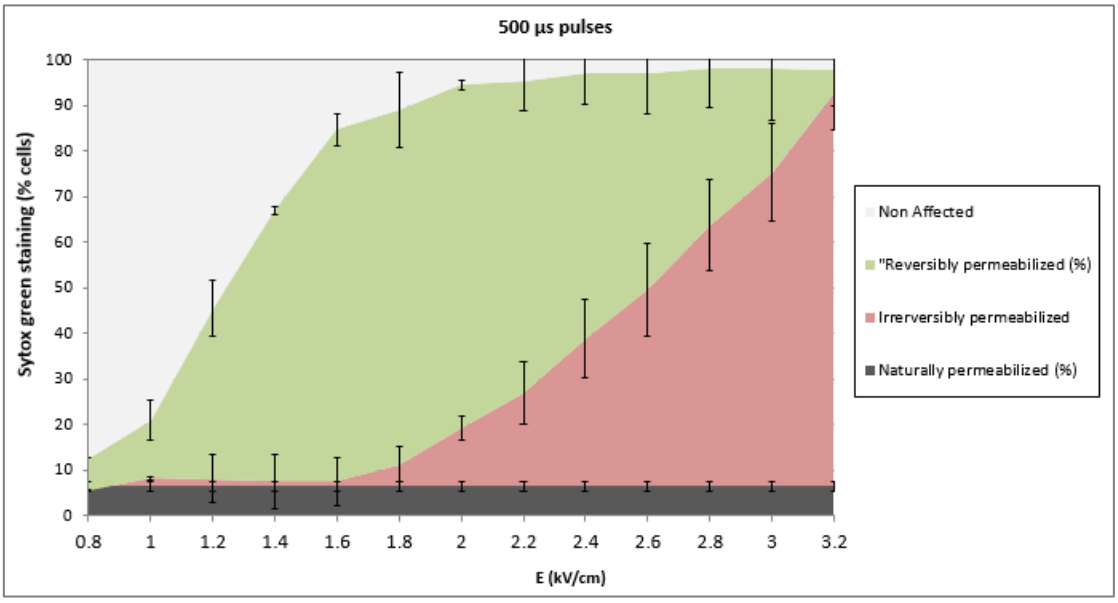

Figure: Impact of the electric field E on the distribution of reversibly and irreversibly permeabilization with a fixed pulse duration of 500 µs (burst 10 square pulses with 10 Hz frequency). Experiments performed on Chlamydomonas reinhardtii cells at 7 days of stress.

Part 2 *C. reinhardtii*'s morphological response to pretreatments and stress conditions

2. *Chlamydomonas reinhardtii*'s structural response to stress conditions, Pulsed Electric Fields and mechanical compressions for an efficient and controlled compound extraction

2.1 Abstract

Current research findings from the domain of microalgal biorefinery clearly reveal the role of the cell wall as a key obstacle to an efficient and optimal compound extraction such as lipids, proteins and pigments. The most widely accepted strategy focuses on the use of cell disruption methods as pretreatments to the extraction of compounds. The efficiency of a cell disruption process is closely related to the microalga used as a source for compound production, specifically its cell structure and physiology. Furthermore, microalgae have thick and multilayered cell walls that are specific to each species. To ultimately develop and control an efficient microalgal extraction, the characterization of the algal cell wall, in terms of physiology, composition, morphology and structure is therefore mandatory.

This work focuses on studying *C. reinhardtii*'s structural response to the nutritional stress conditions that are required to induce lipid accumulation in the cell as well as to pretreatments commonly used to improve their extraction, Pulsed Electric Fields (PEFs) and mechanical stress. The impact of such mechanical and electrical solicitations and culture conditions is investigated by characterizing the size of pores created on the cell membrane, and structural features using confocal laser scanning and transmission electron microscopy, and protein analysis based on electrophoresis. Regarding the impact of the PEF pretreatment, results revealed that both reversible (5 $kV \cdot cm^{-1}$) and irreversible (7 $kV \cdot cm^{-1}$) PEF conditions with a pulse duration of 5 µs could generate pores with a radius between 0.77 and 1.59 nm (respectively corresponding to the dextran molecules with a size between 3kDa and 10 kDa). Moreover, longer pulse durations led to the formation of larger pores on the cell membrane. The cell wall also showed a sensitivity to the nutritional stress conditions, and the combination of both pretreatments, leading to the penetration of larger dextran molecules in *C. reinhardtii*'s cells.

Highlights

- Pore size characterization on *C.reinhardtii*'s cell membrane after PEF and mechanical compression.
- Pretreatments such as PEF and mechanical solicitations have an impact on the cell wall's structure.
- Under specific conditions, *C. reinhardtii*'s cell wall becomes permeable to a certain size of compounds.

Key words: Microalgae – Mechanical stress - Pulsed Electric Fields (PEFs) - Cell wall - Compound extraction

2.2 Introduction

Microalgal compounds are currently recognized as potential renewable sources for the commercial production of biodiesel, in the case of lipids, and for bioproducts such as proteins and pigments (Khanra *et al.*, 2018). However, various bottlenecks have been reported for the past few years at different stages of the production; they must be overcome before producing at a large scale. The main steps that need optimization to become less costly economically and environmentally are cultivation, harvesting and extraction step (Singh, Nigam and Murphy, 2011; Kim *et al.*, 2013; Leite, Abdelaziz and Hallenbeck, 2013; Khanra *et al.*, 2018).

In the case of extraction, a pretreatment consisting of a disruption process before placing the cells in contact with a solvent is commonly used; this step is of utmost influence on the quantity and quality of compounds obtained from the microalgae. Therefore, choosing the most efficient disruption method, well adapted to the microalgal strain used, is significantly important to improve extraction. Besides, lipid extraction includes the use of organic solvents, highly toxic to human health and the environment (Cho *et al.*, 2009; Miazek *et al.*, 2017). Finally, both steps of cell disruption and lipid extraction are currently highly expensive (Lee *et al.*, 2017). They represent therefore key obstacles to the development of an economical microalgal biodiesel production process (Lee, Lewis and Ashman, 2012; Kim *et al.*, 2016).

Several studies of cell disruption pretreatments were published in the past few years. It is widely accepted today that the major obstacle to an optimal extraction is the cell wall of microalgae. The most common components of the cell wall are proteins, glycoproteins and polysaccharides (Work *et al.*, 2013). But microalgae present a wide cell wall variety, depending on the species and on the environment in which they grow. Each microalga has therefore its own, specific cell wall in terms of thickness and composition. The latter includes the molecular composition as well as the intra- and intermolecular interactions, that ultimately define the overall structure of the cell wall.

Several microalgal species (*Chlorella sp.*, *Chlamydomonas sp.*, *Nannochloropsis sp.* and *Haematococcus sp*….), known to have a significant potential as renewable sources for biofuel production, are surrounded by a thick, sometimes multilayered, cell wall that needs to be disrupted before proceeding with the extraction step (Arnold *et al.*, 2015; Kim *et al.*, 2016). Specifically, in the case of lipid extraction, it has been demonstrated that the solvent's extraction efficiency is enhanced when the cell wall is weakened (Gerken, Donohoe and Knoshaug, 2013; Mubarak, Shaija and Suchithra, 2015; Bensalem *et al.*, 2018; Kröger, Klemm and Nelles, 2018). There are various techniques of cell disruption that are either non-mechanical, such as physical (e.g. microwaves and pulsed electric fields), chemical (supercritical CO_2) and biological methods (enzymatic degradation) or mechanical such as bead milling or high-pressure homogenization (Lee, Lewis and Ashman, 2012; Günerken *et al.*, 2015). Combinations of

pretreatments, such as sonication and homogenization, have also shown promising results for an improved lipid extraction (Park *et al.*, 2015).

Furthermore, to enhance extraction and lower the environmental impact of biofuel production, the currently used organic solvents are highly investigated, either for improving their protocol of extraction, for example by adding a water treatment (Ren *et al.*, 2017), or for replacing them by greener solvents, such as ionic liquids (Praveenkumar *et al.*, 2014). But to compete with toxic organic solvents, exhibiting very high extraction efficiencies, green or low-toxicity solvents need to be accompanied by pretreatments, such as pulsed electric fields, which have shown promising results in terms of extraction (Sheng, Vannela and Rittmann, 2011; Zbinden *et al.*, 2013).

In all cases, it is clear that the microalgal cell wall disruption is a primordial step for an improved and efficient extraction. Besides, the efficiency of the chosen cell disruption pretreatment is closely related to the microalga, which has its own physiological characteristics, including cell wall's composition and morphology as previously stated. A thorough comprehension of the microalga's wall and cell structures is therefore highly required in the research of an optimal extraction including the most adequate pretreatment. Comprehensive studies of the microalgae's cell wall structure in the context of an extraction process using pretreatments are currently limited.

Two different pretreatments (PEFs and mechanical compressions), were investigated in this work as they have shown a great potential in the improvement of lipid extraction. Their impact on the physiology and cell wall morphology of *C. reinhardtii* cells was studied, as well as the one of the culture stress conditions leading to lipid accumulation.

C. reinhardtii is a well-known microalga that has been studied for many years in biological research (Harris, 2001; Harris, 2009), most recently as a potential biofuel and bioproduct renewable source (Dubini, 2011; Scranton *et al.*, 2015; Sierra, Dixon and Wilken, 2017). *C. reinhardtii* is a unicellular, biflagellate green alga, with a 7-layered cell wall structure, composed of hydroxyproline-rich glycoproteins. This structure intrigued many scientists and was a subject of debate due to divergencies of opinion on the composition of each layer (Miller, Mellman and Lamport, 1974; Roberts, Phillips and Hills, 1974; Goodenough and Heuser, 1985). In the case of an optimization of compound extraction efficiencies from *C. reinhardtii*, it is significantly important to take into consideration this cell wall structural complexity.

Therefore, in this study, Transmission Electron Microscopy (TEM) was used to analyze the effect of PEFs, mechanical compressions and lipid accumulation duration on the alga's cell structure, inner components, cell membrane and most importantly its cell wall morphology. Furthermore, a dedicated experiment was held using Confocal Laser Scanning Microscopy (CLSM) and fluorescent labelled molecules (FITC-Dextrans) as references for determining the size of pores created on the cell membrane after submitting the microalgae to the different pretreatments. Finally, the relation between lipid accumulation and *C. reinhardtii*'s physiological was investigated using gas chromatography with flame ionization detector (GC-FID) for the total lipid analysis and SDS PAGE gel electrophoresis for the total protein analysis.

2.3 Materials and Methods

2.3.1 Microalgae strain

This study was held on the green, unicellular microalga *Chlamydomonas reinhardtii*. The wild type strain (SAG 34.89) and the cell wall deficient mutant strain (SAG 83.81) were both acquired from the Culture Collection of Algae at the University of Göttingen, Germany (SAG).

2.3.2 Microalgae cultivation

The algae strains were cultured in 250 mL flasks.

Growth conditions

For the growth of both microalgae strains (wild type and mutant), the following conditions were applied: a constant temperature of 25 ± 0.5 °C, continuous agitation at 100 rpm, atmospheric CO_2 (0.004 %), and mean light intensity of 20 µmol·m^{-2}·s^{-1}. The algae were cultivated in TAP medium (Gorman and Levine, 1965) for an optimal growth (with a conductivity of 0.184 ± 0.001 S·m^{-1} and a pH around 8.55), at a concentration ranging from 2×10^5 to 1×10^7 cells·mL^{-1} and in a total volume of 50 mL. The culture's conductivity was 0.089 ± 0.001 S·m^{-1}.

Stress conditions

After growing in the previous conditions, the cells were centrifuged at a rate of 6000 g for 5 min and, to induce lipid accumulation, cultured, with the same agitation and temperature as above, under stress conditions: nitrogen depleted TAP medium (TAP N-: removal of NH_4Cl, conductivity of 0.119 ± 0.001 S·m^{-1} and pH around 8.8) and higher light intensity (150 µmol·m^{-2}·s^{-1}). The culture conductivity in this case was of 0.081 ± 0.001 S·m^{-1}. The cells were immersed in a total volume of 60 mL (TAP N-) at a concentration of 3×10^6 cells·mL^{-1}. For all experiments, the cell sample was concentrated to a final value of $6x10^6$ cells·mL^{-1} before treatment.

2.3.3 Pretreatments

Pulsed Electric Field (PEF) treatment

Chlamydomonas reinhardtii cells were submitted to a PEF treatment using a bipolar pulse generator (Betatech Electrocell B10 HVLV, potential range of –1000 V to +1000 V), in plastic electroporation cuvettes (Bio-Rad) with an electrode distance of 1 mm. The cell samples, with a total volume of 130 µL, were electroporated using only monopolar pulses at various pulse durations ranging from 5 to 500 µs and potentials ranging from 0 to 1000 V, depending on the applied electric field. For all PEF treatments, the following parameters were kept constant:

pulse repetition frequency of 100ms and a burst of 10 monopolar pulses. The PEF parameters leading to reversible and irreversible electroporation were determined previously on *C. reinhardtii* cells (Bodénès *et al.*, 2018): with a pulse duration of 5 µs, 5 $kV \cdot cm^{-1}$ lead to reversible pores and 7 $kV \cdot cm^{-1}$ to irreversible pores. It was also determined that the life time of reversible pores was lower than 30 seconds.

A combination of PEFs with mechanical compressions

In the case of this pretreatment, PEFs were combined with a cyclic mechanical compression of the cells through microfluidic constrictions. The detailed description of the microfluidic system was included in our previous work (Bensalem *et al.*, 2018).

In brief, soft lithography standard protocol (Qin, Xia and Whitesides, 2010) was used to fabricate the microfluidic device. The design includes 8 analysis frames containing 24 parallel microchannels. The cells flow through the restrictions included in these microchannels. The dimensions of each restriction, generating a compression on the cell, is 5 µm in width and in height.

The algal cells were first submitted to a PEF treatment before flowing through the microfluidic constrictions for a cyclic mechanical compression. The resulting cell sample was then analyzed for a pore size characterization and a microscopic observation.

2.3.4 Pore size characterization

The characterization of the pore size induced by different pretreatments was held using a Confocal Laser Scanning Microscope (CLSM, Confocal Leica SP8), FITC-Dextrans for estimating the membrane permeability and a fluorescent dye (Concanavalin A) for the observation of the cell wall. Chlorophyll was observed by autofluorescence.

FITC-Dextrans

For this experiment, various fluorescein-labeled (Excitation/Emission (nm): 488/495 - 540) and dextran molecules were tested; they differ by their molecular weight: 3, 10, 40 and 70 kDa. All dextran molecules were purchased from Thermo Fisher Scientific (Invitrogen).

Aqueous solutions of the 4 different dextran molecules were prepared in an aqueous buffer with a final concentration, depending on their maximal solubility which decreases as the molecular weight increases. The final concentration for each dextran was therefore 500 µM for 3 kDa dextran, 500 µM for 10 kDa dextran, 250 µM for 40 kDa dextran, and 100 µM for 70 kDa dextran.

The dextran solution was then added to the cell sample (volume: 100 µL; cell concentration in the range of $6x10^6$ – $1x10^7$ $cells \cdot mL^{-1}$) to obtain a final concentration of 50 µM for 3 kDa

dextran, 37.5 µM for 10 kDa dextran, 10 µM for 40 kDa dextran and 2.5 µM for 70 kDa dextran. The incubation time before confocal analysis was 20 min; this value was chosen after a short kinetic study performed between 10 and 30 min.

Dextrans are hydrophilic polysaccharides, composed of glucose molecules that are linked by α-1,6 glycosidic linkages. These glucose polymers can be defined by their equivalent coil radius, that was calculated by the method described below.

To determine the size of a polymer, different properties must be taken into consideration such as its structure, its composition and the way it behaves in the chosen fluid. A polymer is a large, macromolecule composed of small sub-units (monomers) that are covalently bonded together thereby forming a chain. There exists a large variety of forms (linear, branch chain or cross-linked polymers) and sizes. Their flexibility depends on the size and chemical structure of the monomers (they could be composed of identical or chemically different monomers) and the bonds linking the monomers together. In our work, they are dissolved in a liquid solution (solvent) where they naturally form random coils thanks to the flexibility of the polymer's backbone. The size of a polymer should therefore correspond to the size of the coil that is formed. To simplify the calculations, linear polymers with chemically identical monomers are chosen as the model for our study.

P. J. Flory considered a polymer as a long and ideal polymeric chain (which represents a simple and first approximate model for a specific polymer chain). This means that it is composed of monomers with very few interactions between them and that are bonded to each other by highly flexible linkages (Flory, 1953). In the case of a "good solvent", in which the polymer is soluble, as water for hydrophilic polymers, the polymer chain is much expanded and its interactions with the solvent molecules favored. In contrast, in a "bad solvent", the polymer is less soluble and the chain stays very condensed as the monomer-monomer interactions are favored over the monomer-solvent interactions. The radius will therefore depend on the nature of the solvent in which the molecule is diluted. Flory defined a radius of gyration for the polymer molecule:

$$R_g = \frac{R_0}{\sqrt{6}} ,$$

where $R_0 = aN^{\nu}$, with a, the monomer size, N, the degree of polymerization (number of bond segments), and ν, the Flory exponent. For a good solvent, ν is equal to 3/5. The monomer size is estimated at approximately 0.36 nm (it corresponds for example to the size of polyethylene glycol (PEG)).

In our case, the dextran molecules were diluted in DMSO which is considered a good solvent and after in water (a good solvent for hydrophilic molecules).

An equivalent coil size was then calculated for each dextran molecule (Table 1).

Dextran MW (Da)	**R_g (nm)** ***Coil radius***	**N** ***Degree of polymerization***

3000	0.77	16.7
10000	1.59	55.5
40000	3.66	222
70000	5.11	388.6

Table 1 Determination of the equivalent coil size for each dextran molecule

Cell wall staining

The lectin Concanavalin A (ConA), conjugated with tetramethylrhodamine, was used to visualize *C. reinhardtii*'s cell wall as it binds to α-mannopyranosyl and α-glucopyranosyl residues (C860, Molecular Probes, Inc., Invitrogen). When bound to its targets, the tetramethylrhodamine conjugate emits an orange-red fluorescence (Excitation/Emission (nm): 561/571 – 620). A stock solution was prepared by dissolving the reagent in sodium bicarbonate (0.1 M, pH ≈ 8.3), at a final concentration of 2 $mg \cdot mL^{-1}$. Finally, 20 µL of the ConA stock solution was added to the cell sample and incubated during 20 min before microscopic observation.

Analytical method

The different fluorescein-labeled dextran molecules were used to determine the minimal size of pores formed on the algae's cell membrane after the different pretreatments.

A specific method was developed to automatically assess the size of the pore created in the membrane. The first step was to acquire confocal images of the microalgal cells right after they have been submitted to the pretreatment and stained with ConA for the observation of their cell wall. Then two additional images were acquired: one corresponding to chlorophyll autofluorescence (Excitation/Emission (nm): 405/550 – 650) and the other on light transmission. These two last images were mostly used for quality control and for testing the remaining "viability" of the cells; to be considered "viable", the cells should indeed still contain chloroplasts and their structure must not be disrupted.

This method was written in ImageJ Macro language (option Bio-Formats). It can be described as follows: an automatic segmentation of the microalgal cell image is performed using the "cell wall" channel (ConA) to determine the limit between the extracellular and intracellular media. A mask is then created and applied to the dextran channel to determine the presence or absence of dextran fluorescence inside the cell. The cells, chosen of approximately equal diameters, are automatically divided into 10 zones of equal area: nine concentric rings (from ring 1 corresponding to the cell wall to ring 9) and one inner circle (Fig. 1). The segmentation of the cell into several zones is necessary to compare the fluorescence intensities in the different parts of the cell. Finally, the mean dextran fluorescence intensity emitted by each zone is measured.

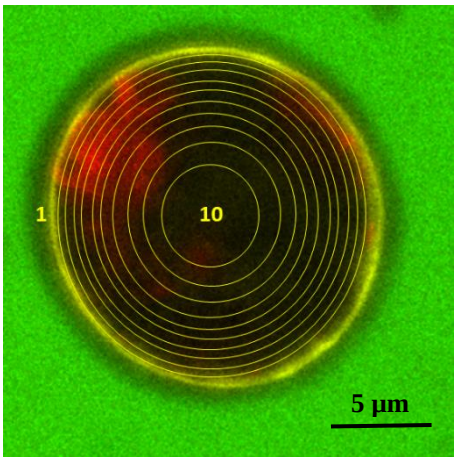

Figure 7 CLSM image of *C. reinhardtii* after a PEF treatment (4.5 kV/cm, 5 µs, 10 pulses). The cell is electroporated in a medium containing 3 kDa Dextran-FITC. It is segmented into 9 concentric rings: from ring n°1, that includes the cell wall, to ring n°9) and 1 inner circle (n°10), all equal in terms of area. Scale bar: 5 µm

Exclusion size filters were also used to sort out cell debris or exceptional individuals (gigantic microalgae, multibodies…). From the individual intensity profiles acquired for about 10 to 20 microalgal cells, an average profile and standard deviations can be deduced for the different applied conditions.

2.3.5 *C. reinhardtii* – Cell structure and functional morphology

The impact of PEF treatments and mechanical compressions on *C. reinhardtii*'s cell structure and morphology was monitored using a JEOL JEM-1400 transmission electron microscope operating at 120 kV (experiments held at the Institute for Integrative Biology of the Cell (I2BC), Paris-Sud University/CNRS/CEA). Images were acquired using a postcolumn high-resolution (11 megapixels) high-speed camera (SC1000 Orius; Gatan) and processed with Digital Micrograph (Gatan) and ImageJ. To preserve the state of the algal cells during analysis, the medium solution was previously removed by centrifugation (6000 g for 5 min) and the cells were incubated over night at 4°C with 4% glutaraldehyde in 0.1 M cacodylate buffer at pH 6.8. The cells were then washed with cacodylate 0.1 M, pH 6.8.

The solid algal samples were then cut into semithin (250 nm) or ultrathin sections (80 nm) with an ultramicrotome EM UC6 (Leica Microsystems) and respectively collected on glass slides or on Formvar carbon-coated copper grids (Agar Scientific) before observation. Semithin sections were stained with methyleneblue-azur II and observed with a Leica DM750 microscope for the

screening of the blocks. Ultra-thin sections were stained with 2% uranyl acetate (Merck) and lead citrate (Agar Sientific).

2.3.6 *C. reinhardtii* – Cell protein composition

Experiments were also held to analyze the total protein profile (content and size) of *C. reinhardtii* cells under lipid accumulation conditions: cells in exponential growth (control) and cells after 4, 7, 15 and 20 days of stress conditions (lipid accumulation).

The algal cell samples were first prepared using an extraction buffer. The extracted proteins were then separated by SDS-Polyacrylamide Gel Electrophoresis (SDS-PAGE) and compared to a prestained protein ladder (PageRuler Plus Prestained Protein Ladder, Thermo Scientific) of protein size standards (in the range of 10 kDa to 250 kDa).

2.4 Results and discussion

2.4.1 Impact of pretreatments on *C. reinhardtii*

C. reinhardtii cells were submitted to three different pretreatments: PEFs, a combination of PEFs with cyclic mechanical compressions and a combination of PEFs with an increased mechanical compression (by increasing the number of compressions applied on the algal cell). As explained in the previous paragraph, the impact of these pretreatments was then assessed by estimating the size of the pores created on the cell membrane and by analyzing through microscopic observations the morphology of the cell and its wall structure.

Cell membrane: pore size characterization

The size of the pores created on the membrane, after the cell was submitted to different pretreatments, was determined according to the method described before (see section 2.4.3.), using various sizes of fluorescein-labeled molecules: 3kDa, 10 kDa, 40 kDa and 70 kDa dextrans.
Single PEF treatments were applied on samples containing algal cells (7 days stressed) and a dextran molecule. The impact of PEF parameters was tested for two electric field intensities, 5.5 $kV \cdot cm^{-1}$ and 7 $kV \cdot cm^{-1}$ (respectively corresponding to reversible and irreversible electroporations; (Bodénès *et al.*, 2018)), with a pulse duration varying from 5 µs to 500 µs. The combined pretreatments included this first step of PEF, followed by mechanical compressions where the cells are forced through microfluidic constrictions of 5 µm.
The control corresponds to 7 days stressed cells that weren't submitted to any pretreatment. The cells mean diameter was around 10 µm.

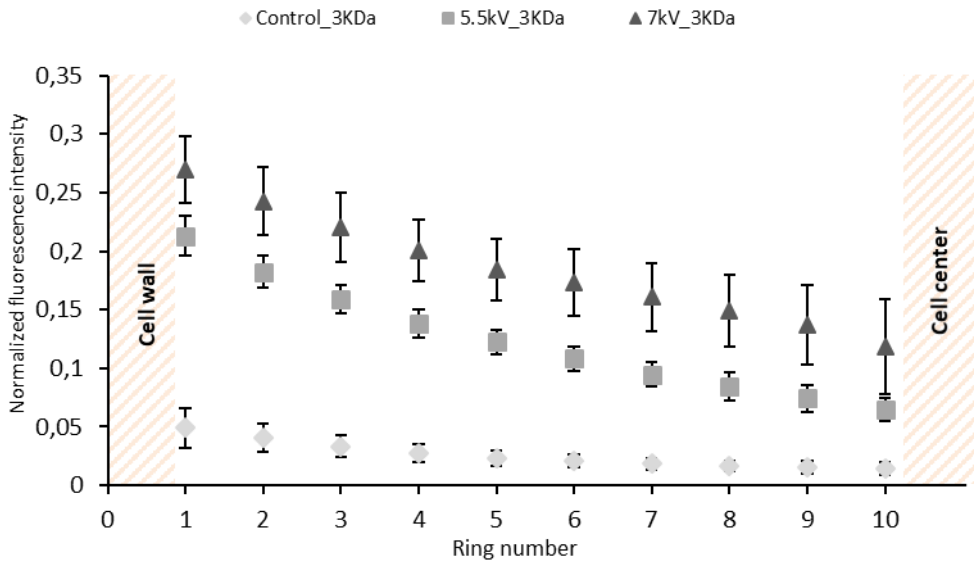

Figure 2 Fluorescence intensity emitted by 3 kDa dextran in algal cells previously submitted to reversible electroporation (5.5 kV·cm^{-1}) and irreversible electroporation (7 kV·cm^{-1}); ratio of the fluorescence intensity of 3 kDa dextran emitted in each zone by the fluorescence intensity emitted in the medium. The other PEF parameters were kept constant: burst of 10 pulses, repetition frequency of 10 Hz and pulse duration of 5 µs. The control corresponds to 7 days stressed cells that weren't submitted to any pretreatment.

Figure 2 shows the mean fluorescence intensity of the 3 kDa dextran in the 10 zones of the cell. In the case of the control, the mean fluorescence intensity stays quite stable from the outer cell wall to the cytoplasm, indicating reduced penetration. It should be noted that 3 kDa dextran enters the cell, in the same way for both reversible (5.5 kV·cm^{-1}) and irreversible (7 kV·cm^{-1}) PEF conditions, with a pulse duration of 5 µs.

A significant decrease of the mean fluorescence intensity of the dextran from the outer ring to the center of the cell for both PEF treatments is observed. The distribution of the molecule inside the cell is then inhomogeneous, which could be explained by the rather slow diffusion of dextran from the wall to the center of the cell; the presence of inner components, especially lipid droplets, in the cytoplasm could enhance the resistance to dextran diffusion. Indeed, after 7 days of stress conditions the algal cells used in these experiments were highly rich in lipid droplets (Ball *et al.*, 1990; Balls, 2009; Wang *et al.*, 2009; Bodénès *et al.*, 2016; Bensalem *et al.*, 2018).

These results also indicate that the minimal pore radius, created in these conditions, is 0.77 nm (table 1). To determine the maximum pore size, 10, 40 and 70 kDa dextran molecules were also tested in the same conditions. The obtained results showed no entry for neither 10 kDa, 40 kDa nor 70 kDa dextran. We thus concluded that none of them entered the cell. Therefore, both reversible and irreversible PEF conditions with a pulse duration of 5 µs lead to the formation of pores with radiuses between 0.77 and 1.59 nm (table 1).

A further experiment was held to determine the electric field intensity and pulse duration necessary to create pores of a radius equal or greater than 1.59 nm, 3.66 nm and 5.11 nm, corresponding respectively to the 10, 40 and 70 kDa dextran molecules (data not shown). The results showed that higher pulse durations, in the range of 10 – 500 µs, could lead to the entry of the tested dextran molecules. This increase in pulse duration therefore resulted in larger pores, permitting the entry of molecules of a maximal size of 70 kDa. Consequently, the minimal pore radius created in these conditions is 5.11 nm.
This result is consistent with previous publications, showing that higher pulse durations lead to larger pores on the membrane of different types of cells (Saulis, 2010; Smith *et al.*, 2014).

In addition, the microscopic observations acquired during these experiments showed that 3 kDa dextran could penetrate the cell wall of 7 days stressed *C. reinhardtii* without using any pretreatment (data not shown). This was also observed in the case of cells under growth conditions. The cell wall of the algal cells is therefore naturally permeable to molecules of a radius corresponding to the 3 kDa dextran (0.77 nm). Interestingly, all tested dextran molecules penetrated the 7-days stressed mutant cells (deficient in cell wall) without any pretreatment, in contrast with the wild type cells. The latter were penetrated by dextran molecules from 10 to 70 kDa size when submitted to time pulses in the range of 10 to 500 µs. This may suggest differences in membrane composition between mutant and wild type cells.
The impact of the combination of PEFs with mechanical compressions was also investigated in this work and is shown on figure 3, where the normalized intensity of each zone from ring 1 to circle 10 (vs control) is plotted.

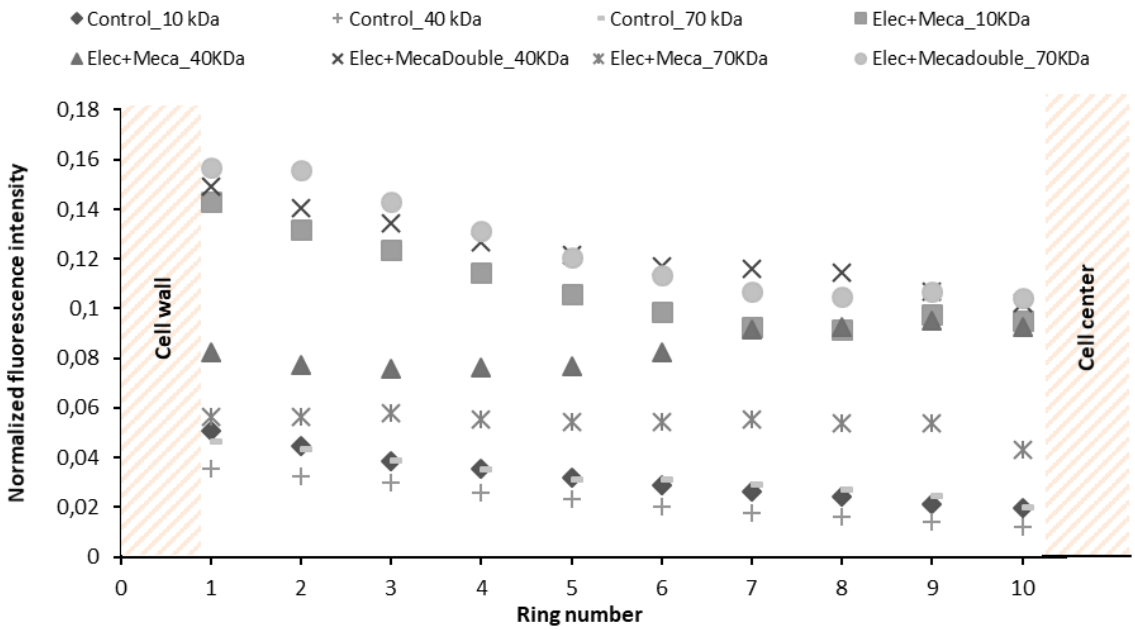

Figure 3 Impact of pretreatments on *C. reinhardtii*'s permeability to different sizes of dextran-FITC molecules (7 kV·cm^{-1}, 5 µs); ratio of the fluorescence intensities of zones 1 to 10 by the fluorescence intensity emitted in the medium. The control corresponds to 7 days stressed cells that were not submitted to any pretreatment, "Elec" to an electroporation under the following conditions: 10 unipolar pulses, 7 kV·cm^{-1}, 5 µs pulse duration and a repetition frequency of 10 Hz, "Elec + Meca" to the combination of

the electroporation with mechanical compressions and "Elec + Mecadouble" to the same combination of pretreatments with a higher amount of mechanical compressions (two-fold).

For this experiment, the electric field intensity was equal to 7 $kV \cdot cm^{-1}$, therefore corresponding to irreversible conditions, and the pulse duration to 5 µs.
In the case of the 10 kDa dextran, the results clearly show that these PEF conditions combined with a mechanical solicitation lead to the formation of pores large enough to permit the entry of the molecule, which is not possible when the PEF conditions are used without the mechanical treatment, as stated previously. Under these conditions, the mechanical compression therefore enlarged the pores from a radius compatible with the entry of the 3kDa dextran (0.77 nm) to a radius compatible with the entry of 10 kDa dextran (1.59 nm).
In the case of the 40 kDa and 70 kDa dextran, the increase in mean fluorescence intensity after the cells were pretreated with a combination of PEF and mechanical compression was very low, indicating a very reduced penetration. However, when the cells were submitted to a combination of PEF and a higher number of mechanical compressions, a slight intensity increase was observed for the 70 kDa dextran and a significant one for the 40 kDa: this latter molecule then significantly penetrated the cell in contrast with the other.
This result highlights the impact of mechanical compressions on the permeability of 7 days stressed *C. reinhardtii* to the dextran molecules. An increase in the number of compressions applied on the algal cell leads to the enlargement of the pores created by the combination of PEFs and mechanical compressions from 1.59 nm to at least 3.66 nm. This result is significant when aiming at developing a selective extraction process of compounds from microalgae: one can recover molecules of different sizes by controlling the intensity of the mechanical forces.
Overall, the pretreatments have a clear impact on the cell membrane and its permeability. Additional experiments were then held to analyze their impact on *C. reinhardtii*'s cell morphology and cell wall structure.

Cell morphology and cell wall structure

C. reinhardtii cells at 7 days of stress were characterized by TEM. Figure 4 shows the acquired images, demonstrating a clear impact of the pretreatments, PEF and mechanical compression, on the cell's membrane and wall. Three different conditions were tested in this experiment: reversible PEF treatment, irreversible PEF treatment and a combination of reversible PEF treatment with mechanical compressions.

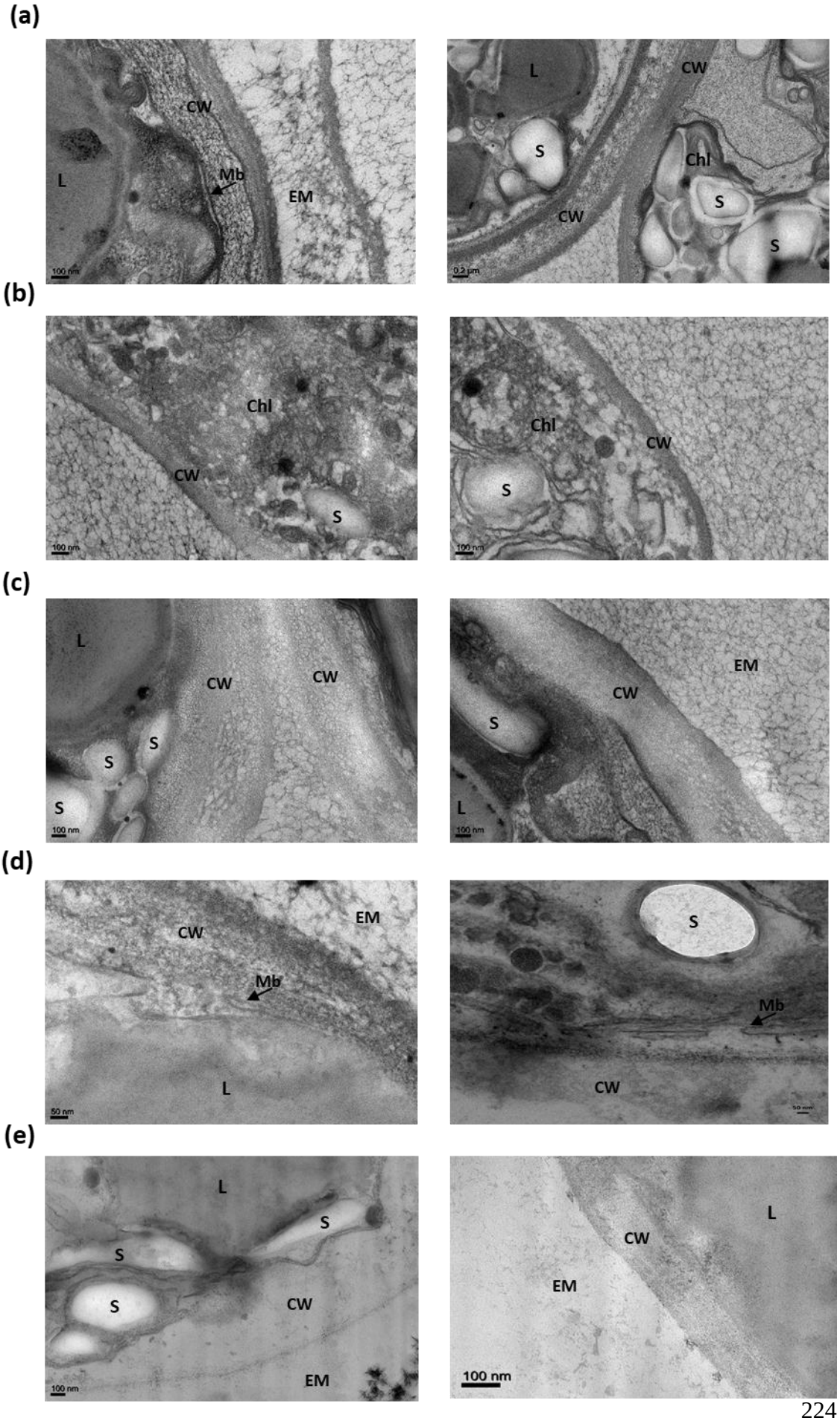
(a)
CW
L
Mb
EM
100 nm
L
CW
S
Chl
S
CW
S
0.2 µm
(b)
Chl
CW
S
100 nm
Chl
CW
S
100 nm
(c)
L
CW
CW
S
S
S
100 nm
EM
CW
S
L
100 nm
(d)
CW
EM
Mb
L
50 nm
S
Mb
CW
(e)
L
S
S
S
CW
EM
100 nm
L
CW
EM
100 nm

Figure 4 TEM observations showing the impact of PEF and mechanical compressions on 7 days stressed *C. reinhardtii* cells. **(a)** Control, **(b)** cells submitted to a reversible electroporation (5.5 kV·cm^{-1}, 5µs), **(c)** cells submitted to reversible (left image) and irreversible (right image) electroporation (7kV·cm^{-1}, 5µs), **(d)** cells submitted to an irreversible electroporation, **(e)** cells submitted to the pretreatment combining reversible electroporation and mechanical compressions. **CW**: Cell wall; **L**: lipid droplets; **S**: Starch; **Chl**: Chloroplast; **Mb**: Plasma membrane; **EM**: Extracellular Medium.

First, these microscopic observations show the impact of electroporation on chloroplast that is, compared to the control (section (a), Figure 4, cells at 0 days, Figure 6), much less organized after the pretreatment and, even in reversible conditions, and dispersed into smaller fragments in the cytoplasm (Fig. 4, section (b)). The TEM images in the case of an irreversible electroporation (Section (d), Figure 4) show its impact on the cell membrane, where pores were created after the treatment.

Finally, in the case of both reversible and irreversible electroporation, the cell wall was less structured, its complex structure did not appear as clearly as it was in the case of the control (Fig. 4, section (c)). Besides, when the cell was pretreated by the combination of both PEF and mechanical compressions, the cell wall seems even less structured, sometimes inexistent or uneasy to perceive as the different layers and limits between the cell membrane and cell wall were very hard to distinguish (section (e), figure 4). Overall, the PEF treatment influenced both the cell membrane and wall, and the mechanical compressions seemed to increase the effect on the cell wall. In addition, we show, for the first time, an effect of PEF on microalgae cell wall. These observations can be related to previous results showing that the extraction of lipids from *C. reinhardtii* is increased with the pretreatments, the cell wall and membrane being weakened and therefore their permeability increased (Bensalem *et al.*, 2018).

2.4.2 Impact of stress conditions on *C. reinhardtii* physiology and structure

The impact of stress conditions was also investigated in this study through three different experiments: CLSM observations of the dextran penetration in the cell, a protein characterization and TEM analysis of the cells at different stages of the stress conditions.

Impact of the duration of stress conditions on the permeability of cells

The 40 kDa dextran was used to evaluate the permeability of the cell wall and cell membrane under stress conditions. After the cells were submitted to 7 days of stress conditions, the 40 kDa dextran molecule could not penetrate the cell. However, the same cells, submitted to 20 days of stress conditions, were permeable to the tested dextran. This result could be related to either the increase in permeability of the cell membrane and/or the weakening of the cell wall after a longer duration of stress conditions. This issue should be studied in a further work.

Effect of the stress conditions on the algae protein content

Figure 5 presents the profile of total proteins of *C. reinhardtii* with nitrogen stress duration. In response to the stress conditions a degradation of cell proteins seems to occur after 4 days of treatment. Indeed, a decrease in the proteins size is observed from day zero to day 7. We may also conclude from the SDS-Page protein profile that there are very few changes when cells are in stress conditions for 7, 15 or 20 days.

Besides, the resulting proteins from cells at day zero have a molecular weight of about 50 and 37 kDa. This could correspond to the enzyme RuBisco, known for its important role in photosynthesis and which size is around 50 kDa, and the LHCII proteins (photosynthetic light harvesting complex proteins) of about 30 kDa, as it has been demonstrated in previous studies (Ferreira and Teixeira, 1992; Giordano, Pezzoni and Hell, 2000; Zhang, Happe and Melis, 2002; Sierra, Dixon and Wilken, 2017). The decrease in protein size after 7 days may be explained by the nitrogen starvation that is known to inhibit photosynthesis in microalgal cells. S. Sierra et al. also showed that after, 4 days of stress conditions, *C. reinhardtii* shows a gradual decrease in high MW proteins and an increase in low MW proteins of about 6 kDa. The increase in low MW proteins is not visible as the minimal size of the protein standards used here is 10 kDa. Overall, our results confirm the decrease in high MW proteins after 4 days of stress, along with significant lipid accumulation (Bensalem *et al.*, 2018) and an increase in low MW proteins (below or equal to 10 kDa) after stress conditions. Moreover, stable profile in low MW proteins from 4 to 20 days of stress was determined.

This is an interesting result since our pretreatments have led to the permeabilization of the cell membrane, by creating pores corresponding to a size around 10 kDa (1.59 nm). These pretreatments could therefore be used in the case of a successive and selective extraction of compounds from *C. reinhardtii*: first proteins or peptides and later lipids (as demonstrated in our previous work, (Bensalem *et al.*, 2018)) as already reported by other authors (Ansari *et al.*, 2017; Hayes *et al.*, 2017; Ventura *et al.*, 2017).

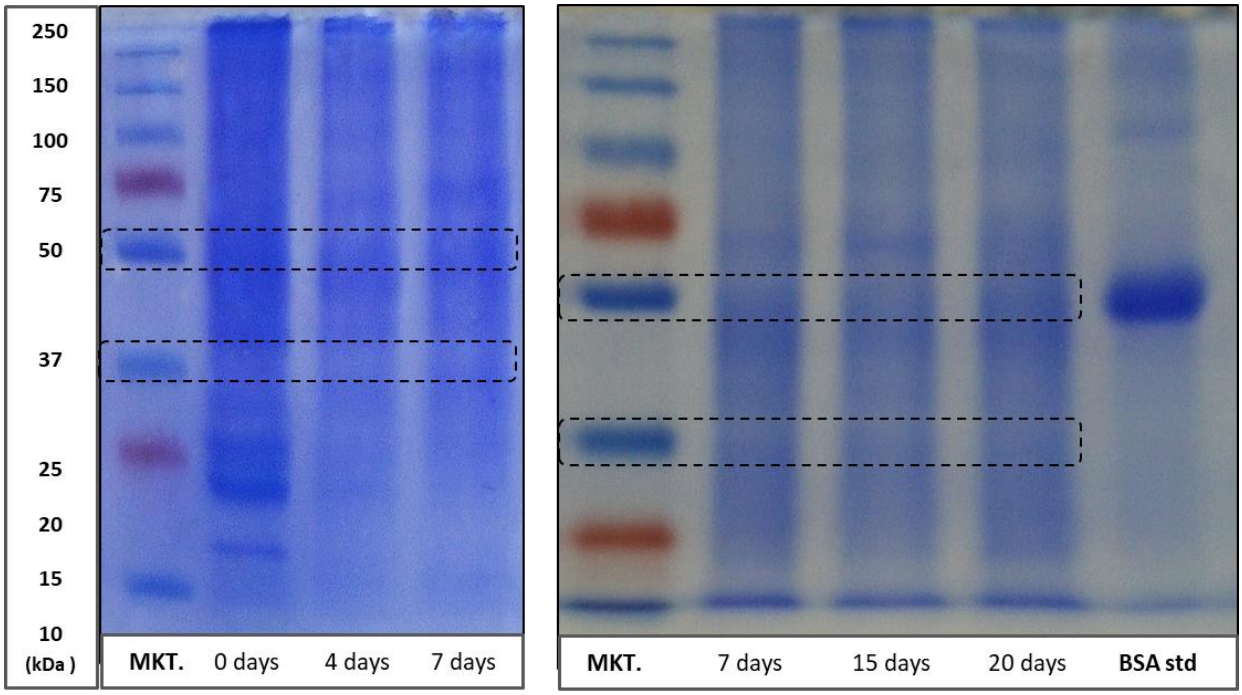

Figure 5 SDS-PAGE analysis of the protein content in *C. reinhardtii* cells after different stress durations: 4, 7, 15 and 20 days. The control corresponds to cells that haven't been submitted to stress conditions (0 day). MKT. corresponds to protein size standards and BSA std to a Bovine Serum Albumin standard.

In order to better understand the impact of stress duration on cell physiology and structure, it would be interesting to analyze the proteins' profile, and in general, the full composition of the isolated cell wall of *C. reinhardtii* in a further work. This is significant when developing an optimized compound extraction process, as the cell wall represents a key bottleneck to the extraction efficiency.

Microscopic observations

The impact of stress duration on *C. reinhardtii* cells was assessed by TEM. Images are shown in figure 6 including cells in growth conditions, cells after 7 days of stress and cells after 15 days of stress. These images reveal a gradual effect of the stress on the algal cells.
C. reinhardtii is known to have a multilayered cell wall, and during stress conditions, these layers differ in their structural complexity. The cells under optimal growth conditions show a thin but very dense cell wall, protecting the cells (Fig. 6, section (a)). After 7 days of stress, the cell wall's morphology is clearly different. It shows larger layers, therefore a thicker cell wall, and in other cases, specifically after a longer time of stress duration (i.e. 15 days), a much less dense, sometimes absent, network, displaying very few linkages amongst the different layers (Fig. 6). This may justify the penetration of 40 kDa dextran on cells at 20 days of nitrogen stress, as reported previously (see section 3.2.1.).

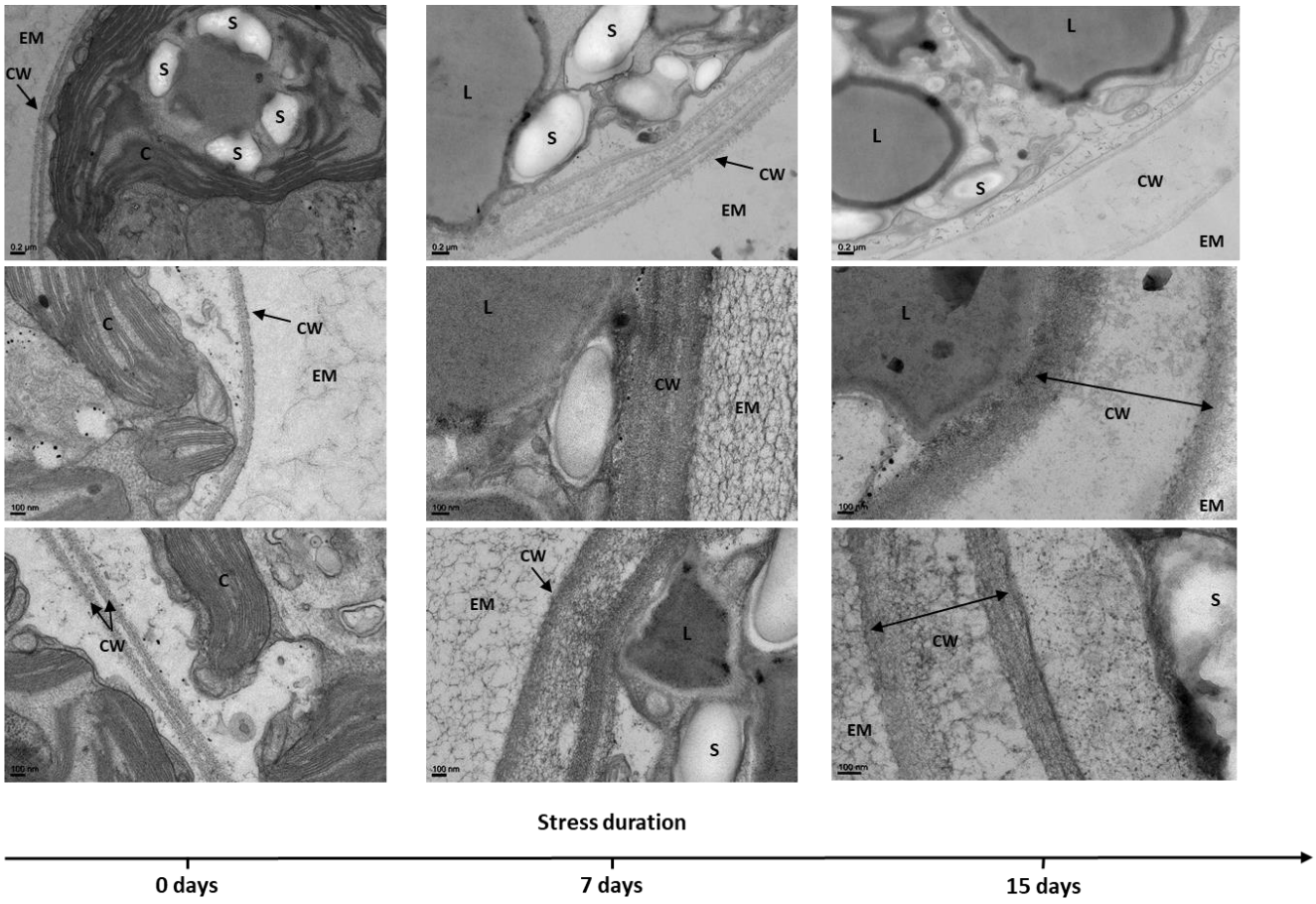

Figure 6 Impact of the duration of stress conditions on the cell's morphological properties observed using TEM, evolution of the cell wall's morphology. CW: Cell wall; L: lipid droplets; S: Starch; c: Chloroplast; EM: Extracellular Medium.

2.5 Conclusions

This work investigated the effect of stress conditions and of the pretreatments PEF and mechanical compressions on the structure morphological properties of *C. reinhardtii*. A clear impact was assessed in all cases on the cell wall. In addition, membrane pore size was determined depending on the PEF conditions, leading to an additional knowledge on the size of molecules that could be extracted from the algae. The obtained results, along with the microscopic observations, could be used in the development of adequate pretreatments for an efficient microalgal lipid extraction or a selective sequential compound extraction of bio compounds from microalgae.

2.6 Acknowledgements

This work was funded by the financial support of the LabeX LaSIPS (ANR-10-LABX-0040-LaSIPS) managed by the French National Research Agency under the "Investissements d'avenir" program (n°ANR-11-IDEX-0003-02).

The authors thank the Institute of Integrative Biology of the Cell (I2BC) for their contribution to the experiments through their platform of electronic microscopy and Iuliana Popa and the Faculty of pharmacy of the University Paris-XI for their contribution to the experiments of protein characterization (SDS-PAGE analysis).

2.7 References

Ball S. G., Deschamps P. 2009. Starch metabolism, p. 1–40 InStern D., editor. (ed.), The Chlamydomonas sourcebook, 2nd ed. Organellar and metabolic processes, vol. 2. Academic Press, Oxford, United Kingdom

Ansari, F. A. *et al.* (2017) 'Exploration of Microalgae Biorefinery by Optimizing Sequential Extraction of Major Metabolites from Scenedesmus obliquus', *Industrial and Engineering Chemistry Research*, 56(12), pp. 3407–3412. doi: 10.1021/acs.iecr.6b04814.

Arnold, A. A. *et al.* (2015) 'Identification of lipid and saccharide constituents of whole microalgal cells by13C solid-state NMR', *Biochimica et Biophysica Acta - Biomembranes*. Elsevier B.V., 1848(1), pp. 369–377. doi: 10.1016/j.bbamem.2014.07.017.

Ball, S. G. *et al.* (1990) 'Physiology of starch storage in the monocellular alga Chlamydomonas reinhardtii', *Plant Science*, pp. 1–9. doi: 10.1016/0168-9452(90)90162-H.

Ball S. G., Deschamps P. (2009), 'The Chlamydomonas sourcebook', 2nd ed. *Organellar and metabolic processes*, vol. 2. Academic Press, Oxford, United Kingdom

Bensalem, S. *et al.* (2018) 'Understanding the mechanisms of lipid extraction from microalga Chlamydomonas reinhardtii after electrical field solicitations and mechanical stress within a microfluidic device', *Bioresource Technology*, 257. doi: 10.1016/j.biortech.2018.01.139.

Bodénès, P. *et al.* (2016) 'Microdevice for studying the in situ permeabilization and characterization of Chlamydomonas reinhardtii in lipid accumulation phase', *Algal Research*, 16(October), pp. 357–367. doi: 10.1016/j.algal.2016.03.023.

Bodénès, P. *et al.* (2018) 'Inducing reversible or irreversible pores in Chlamydomonas reinhardtii with electroporation: Impact of treatment parameters', *Algal Research*. Elsevier, 37(December), pp. 124–132. doi: S2211926418301036.

Cho, C. W. *et al.* (2009) 'Toxicity assessment of common organic solvents using a biosensor based on algal photosynthetic activity measurement', *Journal of Applied Phycology*, 21(6), pp. 683–689. doi: 10.1007/s10811-009-9401-5.

Dubini, A. (2011) 'Green energy: Biofuel production from Chlamydomonas reinhardtii', *The Biochemical Society*. doi: 10.1007/978-1-84882-647-2.

Ferreira, R. M. B. and Teixeira, A. R. N. (1992) 'Sulfur starvation in Lemna leads to degradation of ribulose-bisphosphate carboxylase without plant death', *Journal of Biological Chemistry*, 267(11), pp. 7253–7257.

Flory, P. J. (1953) *Principles of Polymer Chemistry*. Cornell University Press.

Gerken, H. G., Donohoe, B. and Knoshaug, E. P. (2013) 'Enzymatic cell wall degradation of Chlorella vulgaris and other microalgae for biofuels production', *Planta*, 237(1), pp. 239–253. doi: 10.1007/s00425-012-1765-0.

Giordano, M., Pezzoni, V. and Hell, R. (2000) 'Strategies for the Allocation of Resources under Sulfur Limitation in the Green Alga *Dunaliella salina*', *Plant Physiology*, 124(2), pp. 857–864. doi: 10.1104/pp.124.2.857.

Goodenough, U. W. and Heuser, J. E. (1985) 'The Chlamydomonas Cell Wall Glycoproteins Analyzed by the Technique and Its Constituent Quick-Freeze, Deep-Etch', 101(October).

Günerken, E. *et al.* (2015) 'Cell disruption for microalgae biorefineries', *Biotechnology Advances*, 33(2), pp. 243–260. doi: 10.1016/j.biotechadv.2015.01.008.

Harris, (2001) 'Chlamydomoans as a model organism', *Annual Review of Plant Physiology and Plant Molecular Biology*, 52(1), pp. 363–406. doi: 10.1146/annurev.arplant.52.1.363.

Harris, E. H., Stern, David B. and Witman, George B. (2009), The Chlamydomonas Sourcebook, 2nd Edition

Hayes, M. *et al.* (2017) 'Microalgal proteins for feed, food and health', *Microalgae-Based Biofuels and Bioproducts: From Feedstock Cultivation to End-Products*, pp. 347–368. doi: 10.1016/B978-0-08-101023-5.00015-7.

Khanra, S. *et al.* (2018) 'Downstream processing of microalgae for pigments, protein and carbohydrate in industrial application: A review', *Food and Bioproducts Processing*. Institution of Chemical Engineers, 110, pp. 60–84. doi: 10.1016/j.fbp.2018.02.002.

Kim, D. Y. *et al.* (2016) 'Cell-wall disruption and lipid/astaxanthin extraction from microalgae: Chlorella and Haematococcus', *Bioresource Technology*. Elsevier Ltd, 199, pp. 300–310. doi: 10.1016/j.biortech.2015.08.107.

Kim, J. *et al.* (2013) 'Methods of downstream processing for the production of biodiesel from microalgae', *Biotechnology Advances*. Elsevier Inc., 31(6), pp. 862–876. doi: 10.1016/j.biotechadv.2013.04.006.

Kröger, M., Klemm, M. and Nelles, M. (2018) 'Hydrothermal disintegration and extraction of different microalgae species', *Energies*, 11(2), pp. 1–13. doi: 10.3390/en11020450.

Lee, A. K., Lewis, D. M. and Ashman, P. J. (2012) 'Disruption of microalgal cells for the extraction of lipids for biofuels: Processes and specific energy requirements', *Biomass and Bioenergy*. Elsevier Ltd, 46, pp. 89–101. doi: 10.1016/j.biombioe.2012.06.034.

Lee, S. Y. *et al.* (2017) 'Cell disruption and lipid extraction for microalgal biorefineries: A review', *Bioresource Technology*. Elsevier Ltd, 244, pp. 1317–1328. doi: 10.1016/j.biortech.2017.06.038.

Leite, G. B., Abdelaziz, A. E. M. and Hallenbeck, P. C. (2013) 'Algal biofuels: Challenges and opportunities', *Bioresource Technology*, 145, pp. 134–141. doi: 10.1016/j.biortech.2013.02.007.

Miazek, K. *et al.* (2017) 'Effect of organic solvents on microalgae growth, metabolism and

industrial bioproduct extraction: A review', *International Journal of Molecular Sciences*, 18(7). doi: 10.3390/ijms18071429.

Miller, D. H., Mellman, I. R. A. S. and Lamport, D. T. A. (1974) 'The chemical composition of the cell wall of Chlamydomonas Gymnogama and the concept of a plant cell wall protein', 63, pp. 420–429.

Mubarak, M., Shaija, a. and Suchithra, T. V. (2015) 'A review on the extraction of lipid from microalgae for biodiesel production', *Algal Research*. Elsevier B.V., 7, pp. 117–123. doi: 10.1016/j.algal.2014.10.008.

Park, J. Y. *et al.* (2015) 'Sonication-assisted homogenization system for improved lipid extraction from Chlorella vulgaris', *Renewable Energy*. Elsevier Ltd, 79(1), pp. 3–8. doi: 10.1016/j.renene.2014.10.001.

Praveenkumar, R. *et al.* (2014) 'Breaking Dormancy: An energy-efficient means of recovering astaxanthin from microalgae', *ARPN Journal of Engineering and Applied Sciences*. doi: 10.1039/b000000x.

Qin, D., Xia, Y. and Whitesides, G. M. (2010) 'Soft lithography for micro- and nanoscale patterning', *Nature Protocols*. Nature Publishing Group, 5(3), pp. 491–502. doi: 10.1038/nprot.2009.234.

Ren, X. *et al.* (2017) 'Current lipid extraction methods are significantly enhanced adding a water treatment step in Chlorella protothecoides', *Microbial Cell Factories*. BioMed Central, 16(1), pp. 1–13. doi: 10.1186/s12934-017-0633-9.

Roberts, K., Phillips, J. M. and Hills, G. J. (1974) 'Structure, composition and morphogenesis of the cell wall of Chlamydomonas reinhardi. VI. The flagellar collar', *Micron (1969)*, 5(4), pp. 341–357. doi: 10.1016/0047-7206(74)90021-1.

Saulis, G. (2010) 'Electroporation of cell membranes: The fundamental effects of pulsed

electric fields in food processing', *Food Engineering Reviews*, 2(2), pp. 52–73. doi: 10.1007/s12393-010-9023-3.

Scranton, M. A. *et al.* (2015) 'Chlamydomonas as a model for biofuels and bio-products production', *Plant Journal*, 82(3), pp. 523–531. doi: 10.1111/tpj.12780.Chlamydomonas.

Sheng, J., Vannela, R. and Rittmann, B. E. (2011) 'Evaluation of cell-disruption effects of pulsed-electric-field treatment of Synechocystis PCC 6803', *Environmental Science and Technology*, 45(8), pp. 3795–3802. doi: 10.1021/es103339x.

Sierra, L. S., Dixon, C. K. and Wilken, L. R. (2017) 'Enzymatic cell disruption of the microalgae Chlamydomonas reinhardtii for lipid and protein extraction', *Algal Research*. Elsevier, 25(April), pp. 149–159. doi: 10.1016/j.algal.2017.04.004.

Singh, A., Nigam, P. S. and Murphy, J. D. (2011) 'Mechanism and challenges in commercialisation of algal biofuels', *Bioresource Technology*. Elsevier Ltd, 102(1), pp. 26–34. doi: 10.1016/j.biortech.2010.06.057.

Smith, K. C. *et al.* (2014) 'Emergence of a large pore subpopulation during electroporating pulses', *Bioelectrochemistry*. Elsevier B.V., 100, pp. 3–10. doi: 10.1016/j.bioelechem.2013.10.009.

Ventura, S. P. M. *et al.* (2017) 'Extraction of value-added compounds from microalgae', *Microalgae-Based Biofuels and Bioproducts: From Feedstock Cultivation to End-Products*, (December), pp. 461–483. doi: 10.1016/B978-0-08-101023-5.00019-4.

Wang, Z. T. *et al.* (2009) 'Algal lipid bodies: Stress induction, purification, and biochemical characterization in wild-type and starchless chlamydomonas reinhardtit', *Eukaryotic Cell*, 8(12), pp. 1856–1868. doi: 10.1128/EC.00272-09.

Work, V. H. *et al.* (2013) 'Biocommodities From Photosynthetic Microorganisms', *Joint Commission Journal on Quality and Patient Safety*, 39(7), pp. 319–323. doi: 10.1002/ep.

Zbinden, M. D. A. *et al.* (2013) 'Pulsed electric field (PEF) as an intensification pretreatment for greener solvent lipid extraction from microalgae', *Biotechnology and Bioengineering*, 110(6), pp. 1605–1615. doi: 10.1002/bit.24829.

Zhang, L., Happe, T. and Melis, A. (2002) 'Biochemical and morphological characterization of sulfur-deprived and H2-producing Chlamydomonas reinhardtii (green alga)', *Planta*, 214(4), pp. 552–561. doi: 10.1007/s004250100660.

Complementary results

Complementary microscopic observations of *C. reinhardtii* under different conditions

The following section presents additional images acquired under confocal and transmission electron microscopy during the different experiments. The images show observations of the microalga's cell wall permeability and membrane permeability to the dextran molecule, and the structure of intracellular components (lipids, pyrenoid…).

C. reinhardtii's intake of the 3 kDa dextran after reversible or irreversible electroporation

When exposed to a reversible (5.5 $kV \cdot cm^{-1}$) or an irreversible electroporation (7$kV \cdot cm^{-1}$), with a pulse duration of 5 µs, the microalgae cells were permeable to the 3 kDa dextran, which corresponds to a radius of 0.77 nm. Figure 1-b shows *C. reinhardtii*, after being submitted to such PEF treatment. The cell is surrounded by the 3kDa dextran molecule. As it can be observed, the dextran molecule was able to enter the cell. Figure 1-a corresponds to the control, meaning a 7-days stressed cell that has not been submitted to the PEF treatment. As we can see, the dextran molecule couldn't enter the cell in these conditions.

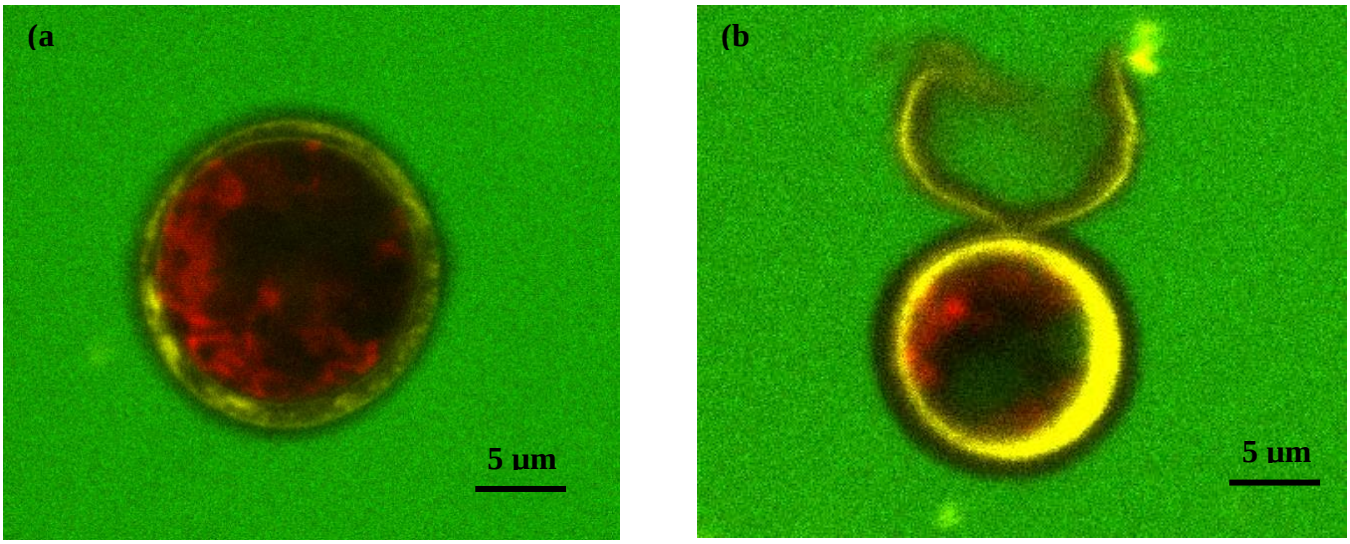

Figure 8 7-days stressed C. reinhardtii before and after PEF treatment observed under confocal microscopy. The green fluorescence corresponds to the 3 kDa dextran.

Natural permeability of *C. reinhardtti*'s cell wall to the 3 kDa dextran molecule

This figure shows *C. reinhardtii* cells under growth conditions (the cells were not submitted to any stress conditions), surrounded by the 3 kDa dextran. As we can see, the dextran molecule penetrates the cell wall. This was also observed when the cells were submitted to 7 days of stress conditions. The cell therefore is naturally permeable to a molecule with a size corresponding to a radius of 0.77 nm. Interestingly, the same behavior is observed in Figure 2 for cells in division.

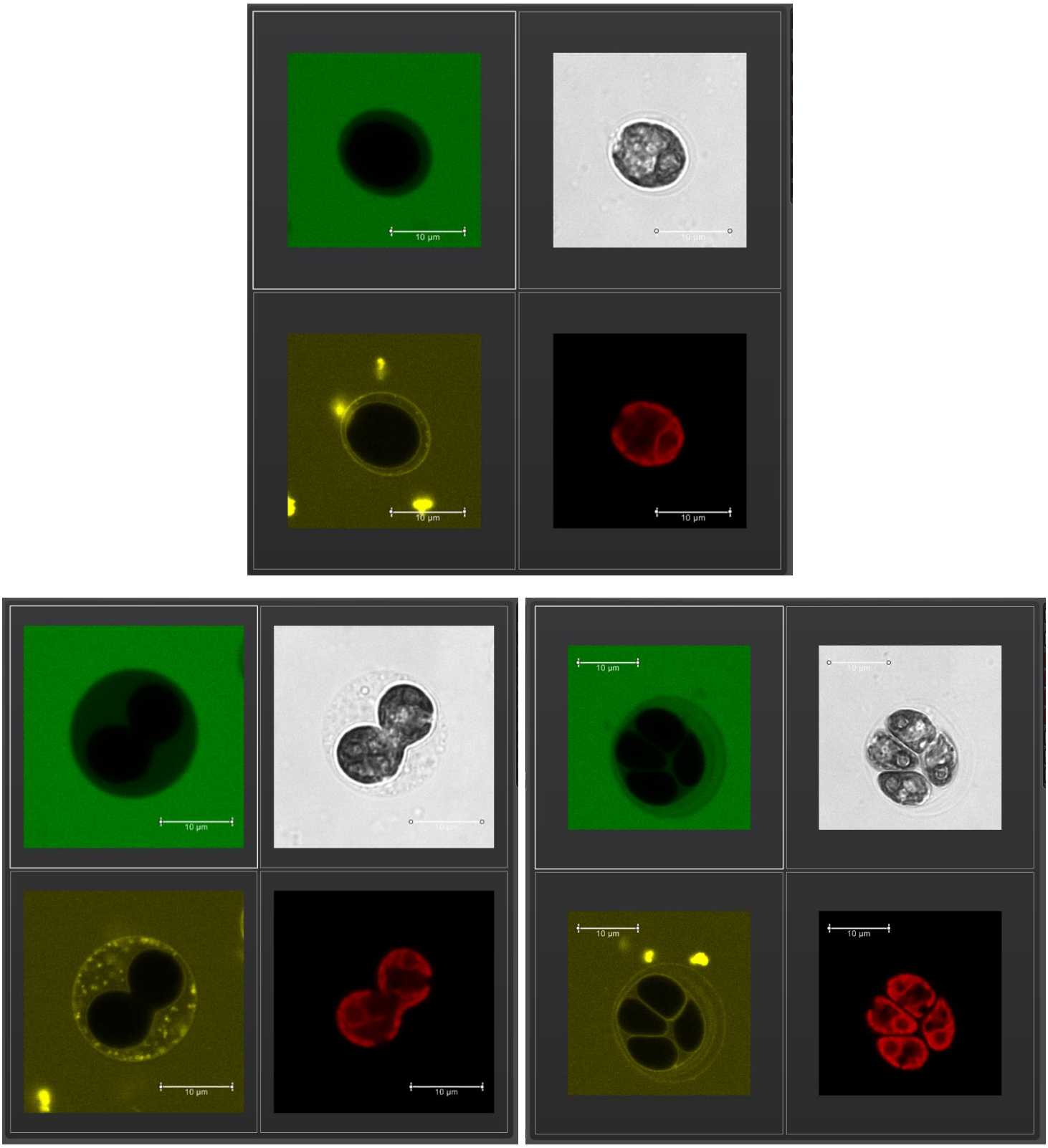

Figure 9 Confocal images showing C. reinhardtii's cell wall's natural permeability to the 3 kDa dextran molecule. The cells were under growth conditions and have not been submitted to any stress conditions. Scale bar: 10 µm

TEM analysis of *C. reinhardtii*'s inner components

Fusion of lipids

The following figure shows the coalescence of lipids under TEM observation: due to stress or PEF (as already described using Confocal Laser Scanning Microscopy, Bodénès et al., 2016) and mechanical compression. The lipid droplets seem to form a sort of network where they are all linked with each other.

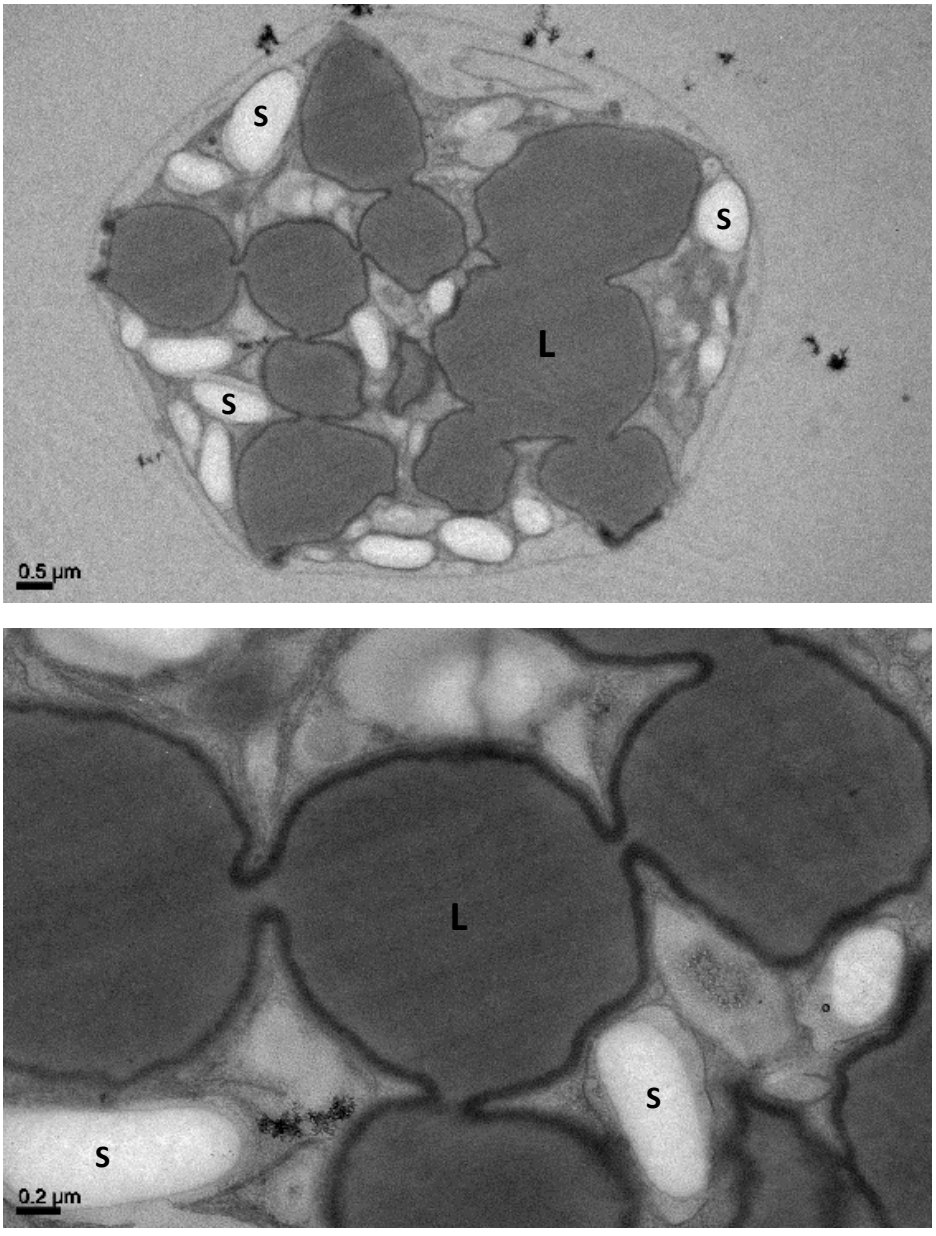

Figure 10 TEM observations showing the fusion of C. reinhardtii's lipid droplets. L: lipid droplet; S: starch.

Various aspects of the pyrenoids

While observing *C. reinhardtii* cells under growth conditions through TEM microscopy, it was also possible to visualize its pyrenoid. In the case of green algae, this component is often surrounded by pyrenoidal starch (Chan, 1972) that is believed to originate from the fact that the CO_2 switches from a high to a low level (Steven G. Ball and Philippe Deschamps, in The Chlamydomonas Sourcebook 2nd edition, Chapter 1, 2009). The following figure shows the morphological evolution of the pyrenoid through three different aspects. The surrounding pyrenoidal starch grows along with the pyrenoid.

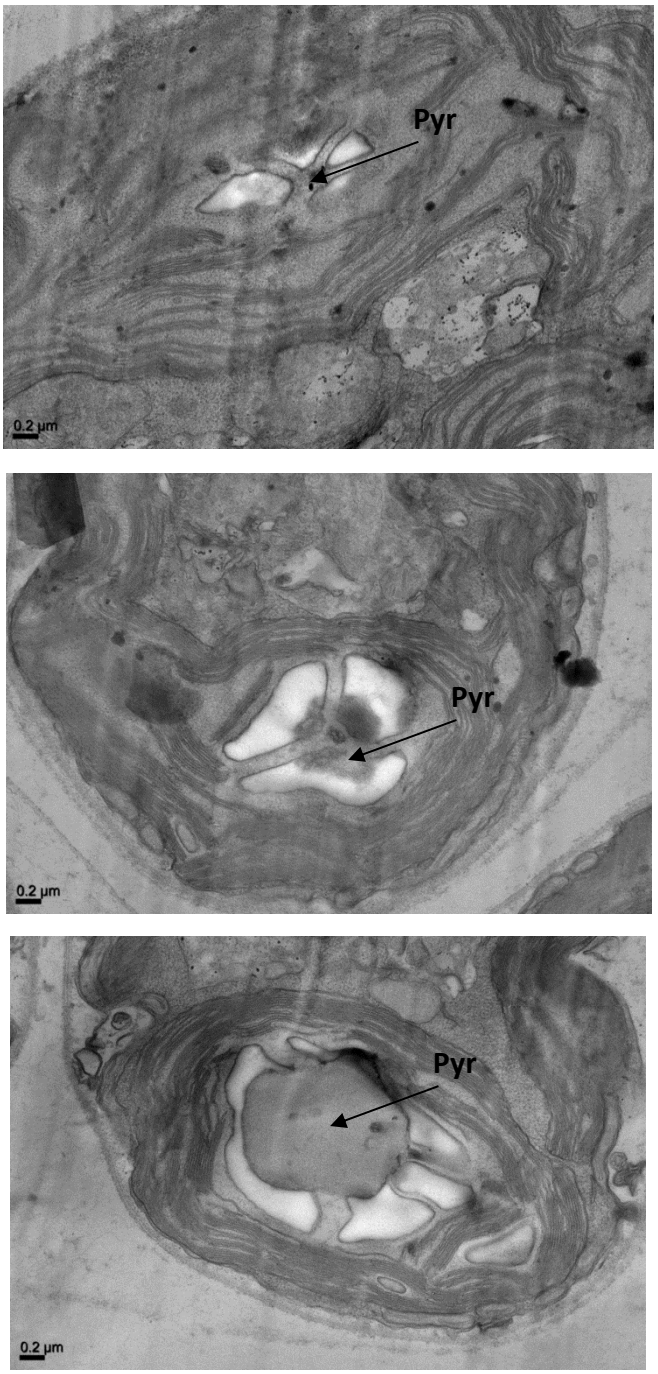

Figure 11 Different aspects of the pyrenoid (Pyr) and its surrounding starch, observed under TEM microscopy.

It has been reported that the pyrenoid is mostly, if not only, composed of aggregated rubisco molecules and that its formation is related to the intrinsic properties of Rubisco (Steven G. Ball and Philippe Deschamps, in The Chlamydomonas Sourcebook 2nd edition, Chapter 1, 2009; Morita et al., 1997; Borkhsenious et al., 1998; Nozaki et al., 2002).

During this study, we have also observed a merging of what seems to be the thylakoid membrane with the pyrenoid (Figure 5).

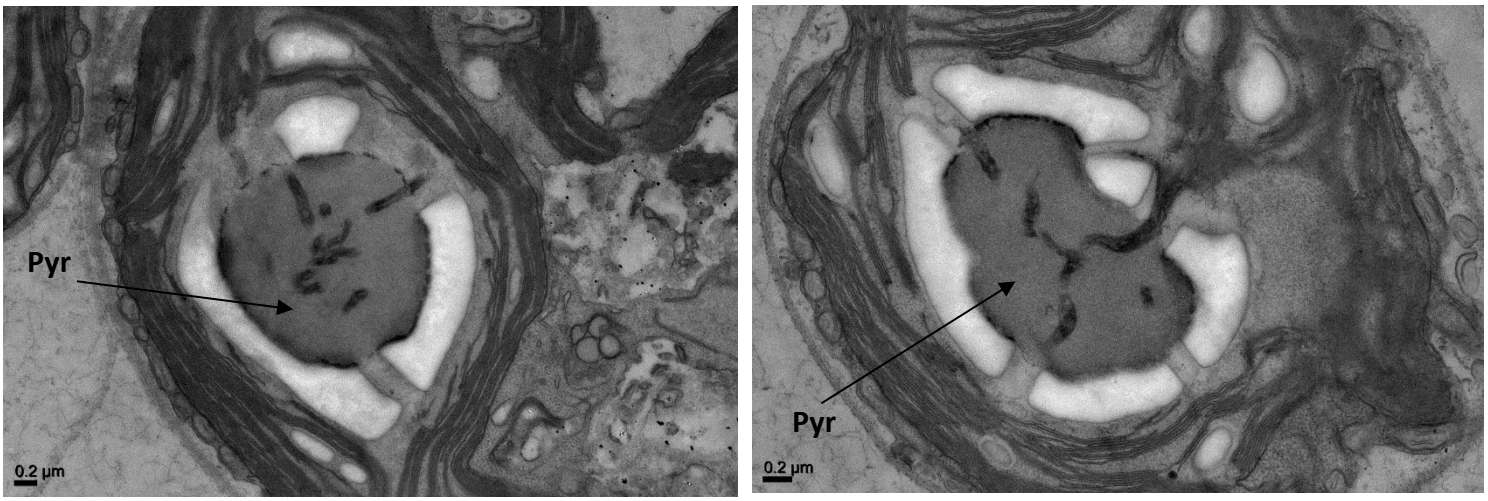

Figure 12 C. reinhardtii's under TEM observation showing thylakoid membrane merging inside its pyrenoid (Pyr).

Annex: Additional images of *C. reinhardtii*'s components

The following section presents additional images of the other components of *C. reinhardtii* that were observed during the experiments.

Chl: chloroplast; **GA**: Golgi apparatus; **S**: starch; **L**: lipid droplets; **Pyr**: pyrenoid; **Thy**: Thylakoid; **Fb**: Flagella base; **N**: nucleus; **EM**: Extracellular Medium.

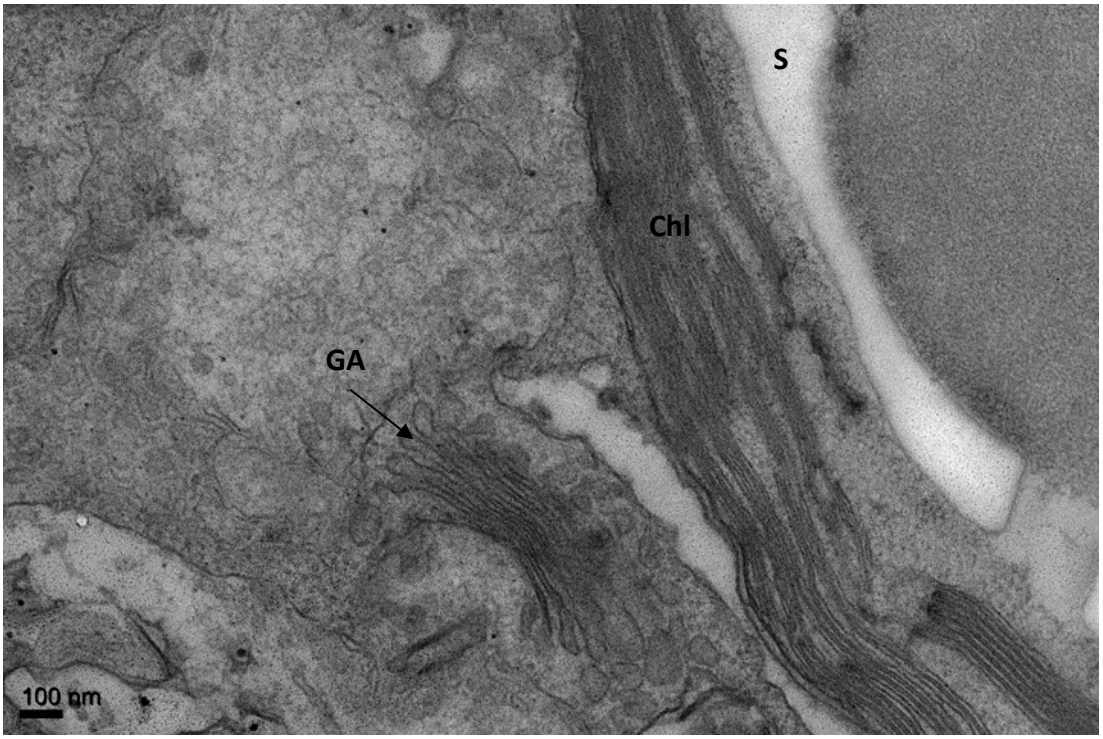

Golgi apparatus

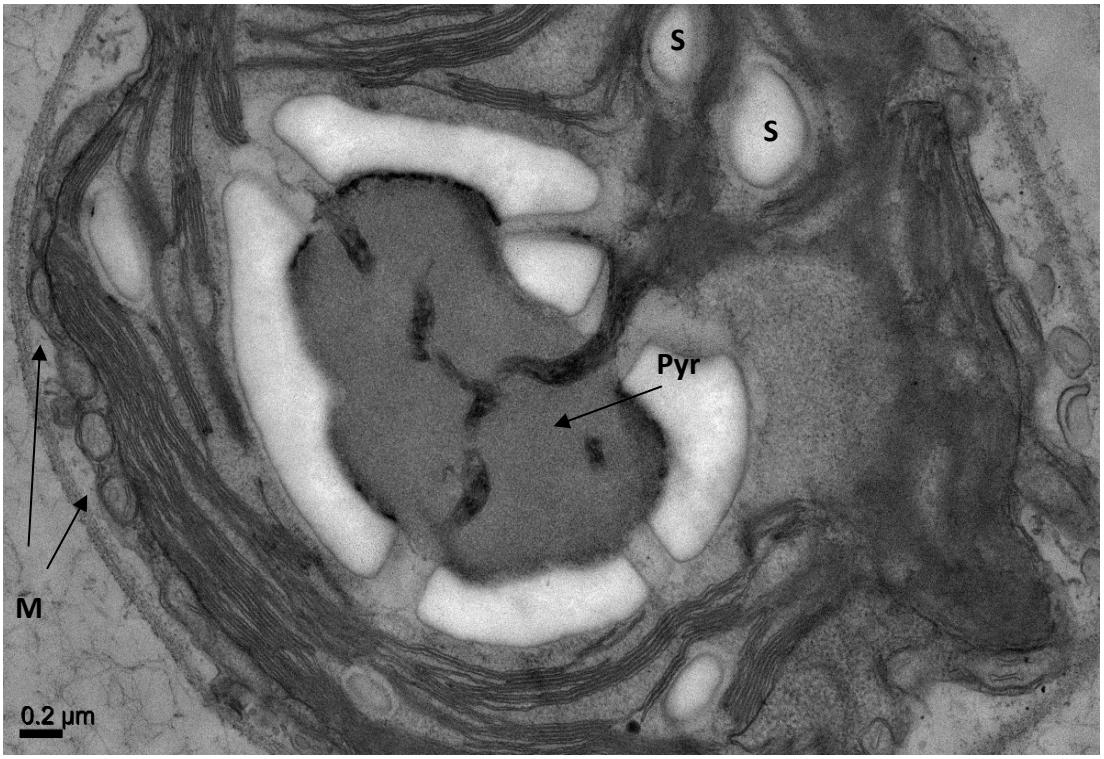

Mitochondria

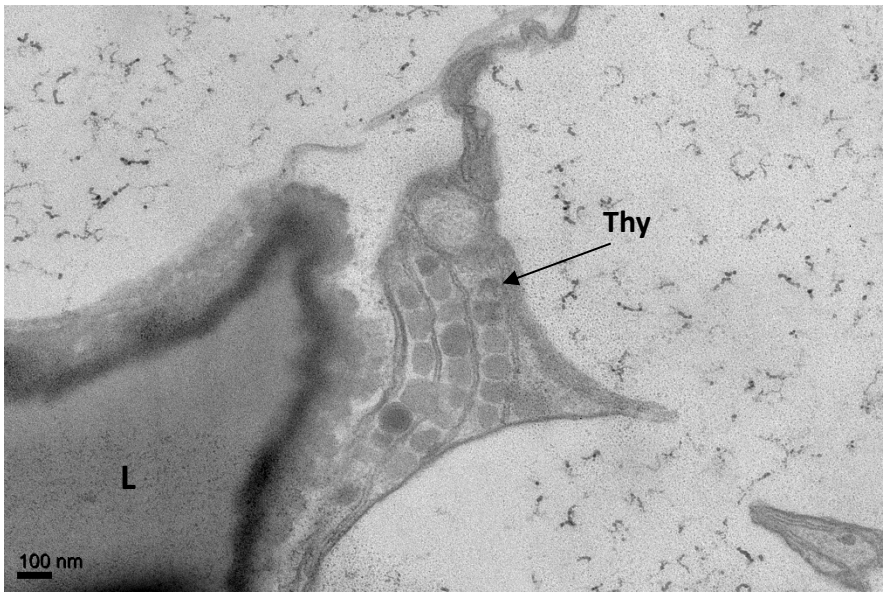

Thylakoids (and its grana) where photosynthesis takes place

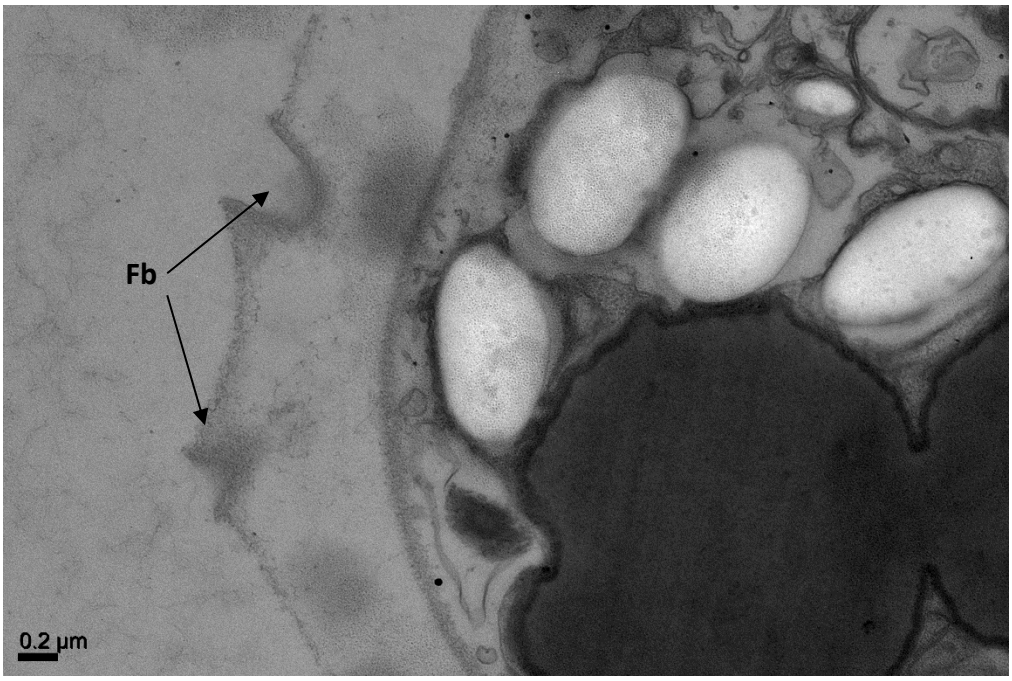

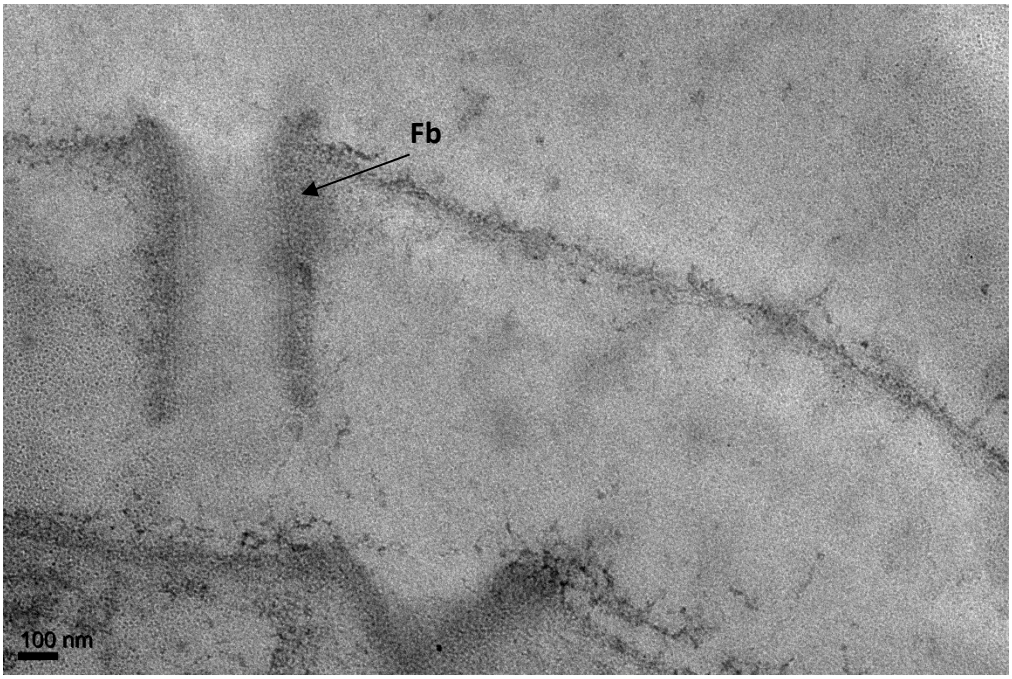

Flagella base

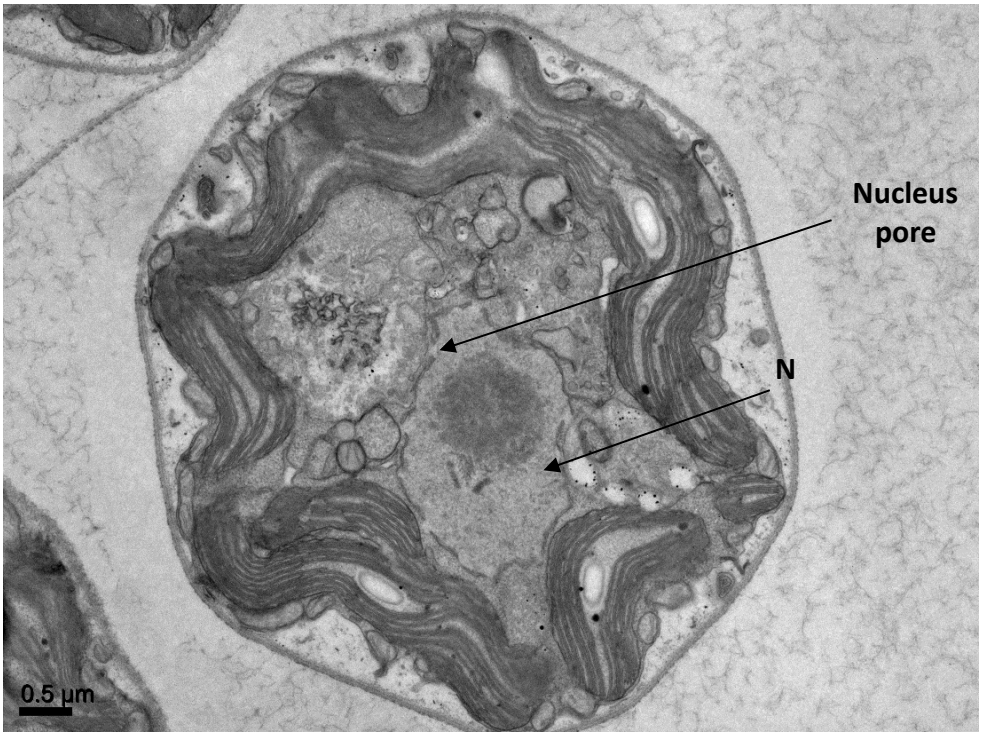

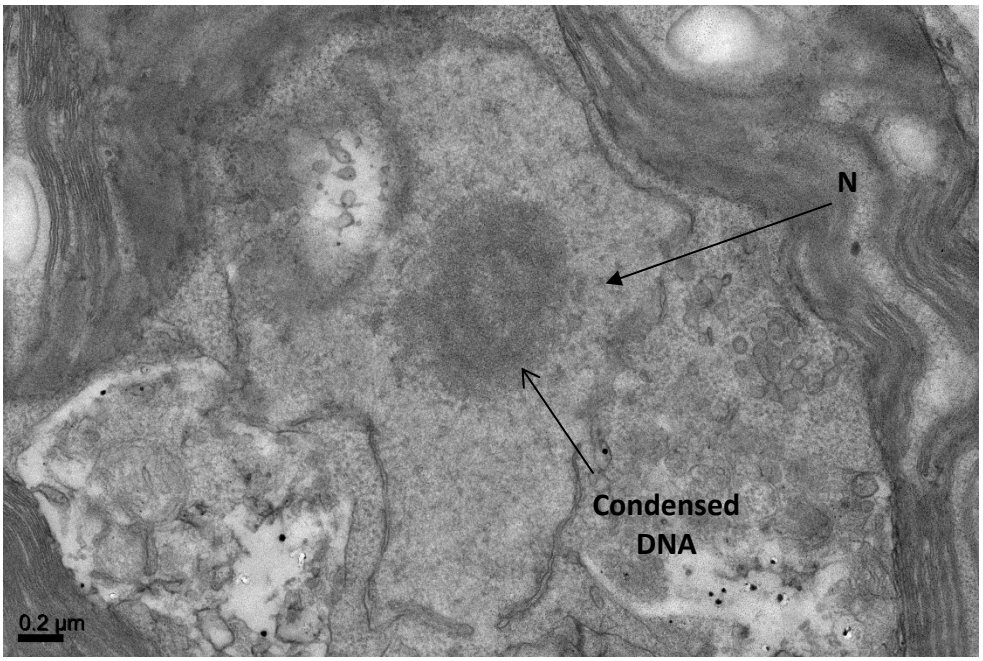

Nucleus (pores and condensed DNA)

Conclusions

This chapter presented the study focusing on the pretreatments (PEFs and mechanical compressions) as well as their impact on the structure and morphology of *C. reinhardtii*. This is carried out in the context of developing an extraction process for a large-scale biofuel production using microalgae as a source.

Therefore, in the case of the PEF treatment, conditions inducing irreversible or reversible pores, the energy demand or the temperature increase of the process were estimated. Results showed that they were at their lowest level when the highest electric field amplitude was tested (4.5 $kV \cdot cm^{-1}$ for a reversible electroporation and 7 $kV \cdot cm^{-1}$ for an irreversible electroporation) with a pulse duration of 5 µs.

Furthermore, the pores created after a reversible electroporation (a condition in which the cells' division and growth capacity are maintained) were first characterized in terms of size and resealing time; their radius was found between 0.7 and 0.9 nm and they reseal in a few seconds (maximum 30 s).

Irreversible (7 $kV \cdot cm^{-1}$) and reversible (5.5 $kV \cdot cm^{-1}$) electroporation, with a pulse duration of 5 µs, led to the formation of pores in the range of 0.77 (size corresponding to the 3 kDa dextran molecule) to 1.59 nm (10 kDa dextran molecule). Moreover, longer pulse durations (i.e. 10 µs) generated larger pores, permeable to the 10, 40 and 70 kDa dextran molecules. To determine the maximum size of pores created in these conditions, further investigations using for example larger dextran molecules are needed. This could also be related to the types of molecules that could be extracted from *C. reinhardtii* in these specific conditions.

In addition to this investigation, the impact of the pretreatments and the stress conditions was evaluated through microscopic analysis (CLSM and TEM). Amongst the primary observations, the morphology of the cell wall, known as a strong and significant barrier to the extraction of compounds, showed a significant variation (under TEM observation) depending on the stress duration and on the pretreatments. Overall, an enlargement of the cell wall was observed when the stress duration was increased above 7 days, as previously observed by CLSM (Chapter 3, Part 2). The 7 layers of *C. reinhardtii*'s cell wall appeared to distance from each other, leaving intermediary zones much less dense than the ones observed for 7 days of stress conditions.

The permeability of the cell wall showed a variability depending on its morphology and should therefore be thoroughly examined with the long-term objective of optimizing a large-scale bio compound production process. Further investigations concerning the microalgal cell wall are therefore needed. For example, the detailed composition of the cell wall could be analyzed, depending on the conditions in order to determine a cell wall profile that could enable an easy extraction of the compounds from the cell.

Conclusions and outlook

In the context of developing sustainable and economically feasible algae-based biofuel productions, several key challenges must be addressed.
In the case of the extraction of neutral lipids for the production of biodiesel, few information is available on the mechanisms behind lipid extraction using organic solvents (chemical treatment). Moreover, to improve lipid recovery, numerous studies have emerged in the past few years on the use of mechanical or non-mechanical solicitations as pretreatments to improve the extraction step. However, information is lacking on the mechanisms behind such solicitations and their impact on the cell's morphology and structure. Yet, this is a significant issue that must be considered when aiming at developing and optimizing innovative processes for the recovery of high-value compounds from microalgae with industrial exploitability.

During this PhD thesis, we firstly investigated the potential of pulsed electric fields and mechanical compressions (through microfluidic channels) as pretreatments to enhance the lipid recovery from the microalga *Chlamydomonas reinhardtii* using hexane as the organic solvent for the extraction; the efficiency of lipid extraction was quantified. The goal here was to investigate the mechanisms behind this extraction and the impact of each treatment (physical, mechanical and chemical) on the microalga's morphology and structure (plasma membrane, cell wall and inner components (e.g. lipid droplets generated as a response to nitrogen starvation stress)).

Moreover, the morphological response of C. *reinhardtii* to the nitrogen starvation stress (for the accumulation of lipids) was also examined.

The cell's properties such as its viability, membrane permeability and lysis were evaluated throughout this study using flow cytometry analysis while microscopic techniques (Confocal Laser Scanning Microscopy and Transmission Electron Microscopy) were used to assess the effects on the microalga's cell morphology and structure.
Also, a dedicated microsystem was developed and coupled to microscopic observations for the application of successive mechanical compressions on the cells. This made it possible to evaluate *in situ* and in real time the response of the cells to the applied mechanical compressions.

The major results of this study are presented below:

- The use of **PEFs combined with mechanical compressions increases lipid recovery** using organic solvents such as hexane. The highest lipid yield was obtained when using the pretreatments in a specific order: PEFs followed by the mechanical compressions (**25% increase of the lipids extracted** compared to the solvent alone).

- Cell lysis, specifically the **disruption of the cell wall, is necessary to extract lipids** with organic solvents such as hexane. Cell viability however cannot be maintained in these extraction conditions.

- The investigated **pretreatments affect the microalga's structure in different ways**. PEFs impact both the cell wall and the membrane's permeability (and the lipid droplets' structure, causing them to merge) while mechanical compressions mainly affect the cell wall.

- The nitrogen stress conditions showed an impact on the cell's structure, specifically its **cell wall, that changes in appearance depending on the stress duration**. The lipid extraction efficiency of the organic solvent is certainly dependent on these different aspects of *C. reinhardtii*'s cell wall.

- The PEF treatment parameters that could lead to a **reversible or irreversible electroporation while minimizing the energy consumption** were determined (2 $MJ \cdot kg^{-1}$ for a reversible electroporation and 5 $MJ \cdot kg^{-1}$ for an irreversible electroporation).

- **Irreversible (7 $kV \cdot cm^{-1}$) and reversible (5.5 $kV \cdot cm^{-1}$) electroporation, with a pulse duration of 5 µs, led to the formation of pores in the range of 0.77 to 1.59 nm**. Longer pulse durations generated larger pores.

The results of this study have therefore helped further understand the phenomena involved in an extraction of lipids from microalgae cells, which could be considered in an application at a larger scale (industrial production).

Besides, in the context of developing innovative processes for the extraction of microalgal compounds of interest, our dedicated microfluidic device, coupled with microscopic analysis could be an interesting tool for the screening of different microalgae species under stress conditions.

The combination of pulsed electric fields and mechanical compressions was investigated through a successive application. To further evaluate their potential as facilitators to the extraction of lipids, it could be interesting to evaluate their use with a simultaneous application.
In addition, with the aim of developing biocompatible extraction processes, these pretreatments could be further investigated with an extraction of lipids using "green solvents".

Finally, the studied pretreatments could be investigated for the extraction of other valuable compounds from microalgae (such as carbohydrates, proteins and pigments) in a single step or in a sequential extraction with a lipid extraction step.

université PARIS-SACLAY | ÉCOLE DOCTORALE Physique et ingénierie : électrons, photons, sciences du vivant (EOBE)

Titre : Extraction de composés énergétiques à partir de microalgues par application conjuguée d'impulsions de champs électriques et de sollicitations mécaniques dans un système microfluidique.

Mots clés : microalgues, molécules d'intérêt, extraction, champs électriques pulsés, compressions mécaniques, microsystèmes

Résumé : Les microalgues présentent un vrai potentiel d'innovation dans les principaux secteurs industriels tel que l'énergie, l'agroalimentaire, la cosmétique et la santé. Elles sont considérées comme étant la solution privilégiée pour répondre aux besoins énergétiques futurs et ainsi permettre une transition des énergies fossiles vers les énergies renouvelables. Néanmoins, les systèmes de production à grande échelle à partir de microalgues nécessitent encore des améliorations afin de les rendre économiquement compétitifs et durables tout en préservant l'environnement.
Ainsi, l'objectif de cette thèse consiste à évaluer de nouvelles voies pour l'extraction de composés d'intérêt à partir de microalgues et à caractériser leurs performances en termes d'efficacité d'extraction. L'utilisation combinée de champs électriques pulsés, et de compressions mécaniques (à travers un système microfluidique dédié) en tant que prétraitements à l'extraction de composés lipidiques, riches en énergie, produits par la microalgue *Chlamydomonas reinhardtii*, a donc été étudiée. Les mécanismes mis en jeu, à l'échelle de la cellule, ont été mis en évidence.
Les résultats obtenus ont permis de confirmer le potentiel des technologies étudiées dans l'amélioration du rendement d'extraction de l'huile algale. Un des apports importants de cette étude est la mise en évidence des mécanismes mis en jeu à l'échelle de la cellule. Une étude approfondie de la réponse physiologique de l'algue aux prétraitements et aux conditions de stress est proposée ; elle démontre notamment le rôle important de la paroi cellulaire de l'algue en tant qu'obstacle à une extraction optimale.

Title: Extraction of energetic molecules from microalgae, combining the use of electrical field solicitations and mechanical stress within a microfluidic device.

Keywords: microalgae, compounds of interest, extraction, pulsed electric fields, mechanical compression, microsystems

Abstract: Microalgae have a real potential in the innovation of the main industrial sectors such as energy, food, cosmetics and health. They are considered as a promising solution to meet future energy needs and thus enable a transition from fossil to renewable energies. Nevertheless, large scale production systems using microalgae still need improvements to become economically competitive and sustainable while preserving the environment.
Thus, the aim of this thesis is to evaluate an innovative approach for the extraction of compounds of interest from microalgae and characterize their performance in terms of extraction efficiency. The effect of combining pulsed electric fields and mechanical compressions (through a dedicated microfluidic system) as pretreatments for the extraction of lipids, energy-rich compounds produced by the microalga *Chlamydomonas reinhardtii*, was therefore studied. The mechanisms involved, at the cellular scale, were highlighted.
The obtained results have confirmed the potential of the technologies studied to improve the algal oil extraction. For the first time, mechanisms involved at the cell level were highlighted. A comprehensive study of the microalgae's physiological response to pretreatments and stress conditions is proposed, demonstrating in particular the important role of the algae's cell wall as an obstacle to an optimal extraction.